The Catalytic Asymmetric Intermolecular Prins Reaction

Inaugural-Dissertation

zur

Erlangung des Doktorgrades

der Mathematisch-Naturwissenschaftlichen Fakultät

der Universität zu Köln

vorgelegt von

Christian David Díaz-Oviedo

aus Fusagasugá (Kolumbien)

Köln 2022

Berichterstatter: Prof. Dr. Benjamin List

Prof. Dr. Hans-Günther Schmalz

Tag der mündlichen Prüfung: 26.01.2022

“For the great doesn’t happen through impulse alone,

and is a succession of little things that are brought together.

(…) And the great isn’t something accidental; it must be *willed*.”

Vincent Van Gogh

Page left intentionally blank

Acknowledgements

Coming to Germany to pursue my doctoral studies at one of the most renowned institutes of chemistry once felt like a dream, something unreachable. But it did come true, and I am deeply grateful to each and every single person with whom I shared this life-changing experience.

Special thanks to my *Doktorvater*, Prof. Dr. Benjamin List, for giving me the chance to join his awesome research group. The freedom I got from him to pursue my own ideas, combined with his philosophy of going after the big problems in science, showed me how capable I am of doing things I would have otherwise considered “out of my league”. Thank you for inspiring me to do the things I am truly passionate about, because that passion is the key to overcome the many obstacles that the pathway of scientific research is paved with.

I would also like to thank Prof. Dr. Hans-Günther Schmalz for accepting to review this thesis, and Prof. Dr. Axel Klein and Dr. Monika Lindner for serving on my defense committee.

A special thank you goes to the people who helped me proofreading this thesis: Benjamin Mitschke, Manuel Scharf, Mathias Turberg, Luc Debie, Sebastian Brunen, Dr. Sebastian Schwengers, Dr. Oleg Grossmann, Wencke Leinung, Dr. Miles Aukland and Dr. Gabriela Gerosa. Thanks for keeping those eyes open, I owe you all.

Next, I would like to thank those with whom I collaborated during my studies, including Dr. Rajat Maji and Dr. Sensheng Liu, and although only for a short time, to Marian Guillén. Meine liebe Joyce Grimm, my *i*IDP “partner-in-crime”, thank you so much for always sharing your catalysts, especially when things got “decomposed” and you rescued me from that dark hole. The PhD students of my “generation”: Dr. Jenni Kennemur, Dr. Oleg Grossmann and Dr. Sebastian Schwengers, it was very nice how we stood together for each other, especially for this last part of our PhD roads. Box 1 and Office 901 were my new home, thanks to you all for your patience with my loud music and my witty comments.

Keeping a group of this size under control can be challenging, and German bureaucracy certainly does not make it any easier. That is why I want to thank Dr. Monika Lindner, Dr. Chandra Kanta De and Alexandra Kaltsidis, as well as the student assistants we had in these years (Franziska Scheel, Laura Fröhlich and Max Jansen), for keeping this boat floating. On the same line, the great amount of excellent work we can achieve in the List laboratory depends greatly on the hard work from our technicians, providing us with key catalyst building

blocks and keeping all our machines running, and also from the amazing analytical departments (MS, GC/HPLC, X-ray and NMR: special thanks to Dr. Markus Leutzsch for the help with those kinetic profiles). Special mention to Stefanie Dehn, *la chica caliente*, for all the nice conversations and for always looking after me.

All work and no play makes Jack a dull boy.
This was my first experience in such a big research group, and also in one as multicultural as the List group. I really enjoyed meeting people from so many places in all these years. Thanks to all the current and previous members that I had the fortune to meet in the last five years. Every party, every pizza/Döner we shared, every International Dinner and Boat Trip, every Cocktail Tour/MPI Tour, and even the madness of organizing a party to celebrate a Nobel Prize in just a few hours. We are really an *awesome* group!

Thanks to the “Bored in Mülheim”, “Fish Friday”, “Falafel Wednesday/Dönerstag” and whichever other groups we created to not lose our minds while the world was going through a pandemic. These have been weird times and none of us would have imagined what the last “Corona years” have been like, but here we are! Carla, Luc, Bruni, Wencke, Marian, Mathias, Manuel, Benni, Miles, Jenni, Robi, Gabyta, Joyce, Oleg, Schwengers, Steffi, Alex Z., Vikas, Yihang, and everyone else I might have forgotten to mention: thank you all!

I want to thank my beloved *Spanish Mafia*: Dr. Gabriela Gerosa, Dr. Carla Obradors, Dr. Diane Bécart, and the newest member, “la *Prins*esa” Marian Guillén. Here I also want to thank my dear Colombian friend, Cristian Escobar, for sharing with me the intricacies of this “German dream”. Muchas gracias por siempre haber estado ahí, escuchándome con mis tonterías y mis dramas. Ustedes me hicieron sentir siempre casi como si estuviese en casa.

At this point I would also like to thank Stephan Reppel for all the support in the last years! Thanks for having been there, for supporting me with great amounts of patience, for listening to me on the good and not-so-good days, and letting me play (sometimes a bit too aggressively) with Mats and Noah. Ich danke dir von ganzem Herzen.

Last but not least, I would like to thank my family for the unconditional support and for their genuine love. These years were not easy, and the pandemic gave us some hard time and kept us apart even longer, but we were/are/will be there for each other. A toda mi familia, especialmente a mis padres y mi hermano, ¡muchas gracias por el apoyo incondicional todos estos años desde la distancia! Este logro va para ustedes también, porque esta experiencia en Alemania no hubiese ocurrido si no hubiera tenido su apoyo desde el primer momento.

Table of Contents

Abstract

The development of strategies for the transformation of olefins represents a highly rewarding challenge in chemical synthesis, due to the versatile reactivity and widespread accessibility of this functionality. The reactions of olefins with heteroatom-containing electrophiles result both in carbon–carbon bond formation and introduction of heteroatoms in the molecular skeleton, thus allowing to convert the relative structural simplicity of olefins into complex structures.

The following work describes the catalytic, asymmetric, intermolecular reaction between aryl olefins and paraformaldehyde, known as the *Prins reaction*, enabled by the development of sterically-confined imino-imidodiphosphate (*i*IDP) Brønsted acid catalysts. By careful fine-tuning the catalyst structure, a great number of aryl olefins could be transformed, covering a broad range of electron density on the alkene moiety. In this way, enantiomerically-enriched 1,3-dioxanes were efficiently prepared from inexpensive and commercially available reagents. The obtained enantioenriched 1,3-dioxane rings could also be transformed to the corresponding optically-active 1,3-diols. These compounds constitute valued intermediates for the synthesis of multiple pharmaceutically-relevant molecules, such as Fluoxetine®, Dapoxetine® and Tomoxetine®, among others. Additionally, the developed catalytic, asymmetric Prins reaction was successfully utilized for the synthesis of several deuterium-containing enantioenriched 1,3-dioxanes, where the position and degree of deuteration could be controlled by proper choice of the starting materials.

Mechanistic studies (isotope-labeling experiments and computations) showed that the reaction using the confined *i*IDP as catalyst proceeds by a highly asynchronous, concerted pathway, whereas a catalyst with a more open active site, such as *p*-toluenesulfonic acid, shifts the reaction to take place by a stepwise mechanism.

Taken together, the work described in this thesis represents a new tool in synthetic chemistry for the streamlined formation of structural complexity from rather simple, highly available starting materials. It also opens up the field for further contributions toward a more general intermolecular reaction of olefins and aldehydes.

Kurzzusammenfassung

Die Entwicklung von Strategien zur Umwandlung von Olefinen stellt aufgrund der vielseitigen Reaktivität und der weitverbreiteten Zugänglichkeit ihrer Funktionalität eine äußerst vielversprechende Herausforderung in der chemischen Synthese dar. Die Reaktionen von Olefinen mit heteroatomhaltigen Elektrophilen führen sowohl zur Bildung von Kohlenstoff-Kohlenstoff-Bindungen als auch zur Einführung von Heteroatomen in das Molekülgerüst, wodurch die relative strukturelle Einfachheit von Olefinen in komplexe Strukturen umgewandelt werden kann.

Die folgende Arbeit beschreibt die katalytische, asymmetrische, intermolekulare Reaktion zwischen Arylolefinen und Paraformaldehyd, bekannt als Prins-Reaktion, die durch die Entwicklung von sterisch begrenzten Imino-imidodiphosphat (*i*IDP) Brønsted-Säure-Katalysatoren ermöglicht wird. Durch sorgfältige Optimierung der Katalysatorstruktur konnte eine große Zahl von Arylolefinen umgewandelt werden, die einen weiten Bereich unterschiedlicher Elektronendichte der Alkeneinheit abdecken. Auf diese Weise wurden enantiomerenangereicherte 1,3-Dioxane aus kostengünstigen und kommerziell erhältlichen Reagenzien effizient hergestellt.

Die erhaltenen enantiomerenangereicherten 1,3-Dioxanringe konnten außerdem in die entsprechenden optisch aktiven 1,3-Diole umgewandelt werden. Diese Verbindungen stellen wertvolle Zwischenprodukte für die Synthese mehrerer pharmazeutisch relevanter Moleküle dar, wie unter anderem Fluoxetine®, Dapoxetine® und Tomoxetine®. Darüber hinaus wurde die entwickelte katalytische, asymmetrische Prins-Reaktion erfolgreich für die Synthese mehrerer deuteriumhaltiger enantiomerenangereicherter 1,3-Dioxane genutzt, bei denen Position und Grad der Deuterierung durch geeignete Wahl der Ausgangsmaterialien gesteuert werden können.

Mechanistische Studien (Experimente zur Isotopenmarkierung und theoretische Berechnungen) zeigten, dass die Reaktion mit dem sterisch eingeschränkten *i*IDP als Katalysator über einen hoch asynchronen, konzertierten Weg verläuft, während mit einem Katalysator mit einem offeneren aktiven Zentrum, wie *p*-Toluolsulfonsäure, die Reaktion über einen schrittweisen Mechanismus verläuft.

Zusammengefasst stellt die in dieser Dissertation beschriebene Arbeit ein neues Werkzeug in der Synthesechemie für die Bildung von komplexen Molekülstrukturen aus relativ einfachen, leicht verfügbaren Ausgangsmaterialien bereit. Sie öffnet auch das Feld für weitere Beiträge zu einer allgemeineren intermolekularen Reaktion von Olefinen und Aldehyden.

List of Abbreviations

Ac	acetyl
AcO	acetate
Alk	alkyl
anh.	anhydrous
Ar	aryl, aromatic
aq.	aqueous
BALT	binaphthyl-allyl tetrasulfone
BINOL	1,1'-bi-2-naphthol
Bn	benzyl
Boc	*tert*-butyloxycarbonyl
Bu	butyl
CAN	cerium ammonium nitrate
cat.	catalyst/catalytic
conv.	conversion
CPA	chiral phosphoric acid
Cy	cyclohexyl
d	doublet
d	day(s)
dba	dibenzylideneacetone
DCE	1,2-dichloroethane
DIPEA	diisopropylethylamine, Hünig's base
DKR	dynamic kinetic resolution
DMF	dimethylformamide
DMSO	dimethylsulfoxide
DPP	diphenyl phosphoric acid
DSI	disulfonimide
dr	diastereomeric ratio
E	electrophile
EI	electron impact
equiv.	equivalent(s)
er	enantiomeric ratio
Et	ethyl
ESI	electrospray ionization
EDG	electron-donating group

EWG	electron-withdrawing group
GC (GC-MS)	gas chromatography (gas chromatography coupled with mass detection)
h	hour(s)
HMDS	hexamethyldisilazane
HOMO	highest occupied molecular orbital
HPLC	high performance liquid chromatography
HRMS	high resolution mass spectrometry
i	iso
IDP	imidodiphosphate
*i*IDP	imino-imidodiphosphate
IDPi	imidodiphosphorimidate
KIE	kinetic isotope effect
LA	Lewis acid
LDA	lithium diisopropylamide
LHMDS	lithium hexamethyldisilazane
Lit.	literature
LUMO	lowest unoccupied molecular orbital
m	*meta*
m	multiplet
M	molar (Concentration)
Me	methyl
Mes	mesityl (2,4,6-trimethylphenyl)
MOM	methoxymethyl
MS	mass spectrometry, molecular sieves
Ms	methylsulfonyl
MTBE	methyl *tert*-butyl ether
m/z	atomic mass units per charge
n	normal
n.d.	not determined
NMR	nuclear magnetic resonance spectroscopy
NTPA	*N*-triflylphosphoramide
Nu-H/Nu	nucleophile
o	*ortho*
p	*para*
Ph	phenyl
pin	pinacolato

Pr	propyl
p-TsOH	*para*-toluenesulfonic acid
py	pyridine
quint	quintet
rac.	racemic
RB	round-bottom
rt	room temperature
satd.	saturated
sept	septet
sext	sextet
SPhos	dicyclohexyl(2′,6′-dimethoxy[1,1′-biphenyl]-2-yl)phosphane
SPINOL	1,1’-spirobiindane-7,7’-diol
t, *tert*	tertiary
t	triplet
Tf	trifluoromethylsulfonyl, triflyl
TFA	trifluoroacetic acid
THF	tetrahydrofuran
TLC	thin layer chromatography
TMS	trimethylsilyl
TRIP	3,3’-bis(2,4,6-triisopropylphenyl)-1,1’-binaphthyl-2,2’-diyl hydrogen phosphate
Ts	*para*-toluenesulfonyl, tosyl
TTP	tetra(triflyl)propene
%w/w	percentage by weight

Page left intentionally blank

1 Introduction

Olefins are among the most fundamental functionalities in chemical synthesis because of their versatile reactivity and their widespread accessibility.[1] Many large-scale industrial processes use olefins as starting materials or yield olefins as products, with notable examples including polymerization reactions and steam cracking from crude oil. The research that has been conducted on the utilization and functionalization of olefins, particularly in the last century, has provided the synthetic community with highly useful chemical transformations (Scheme 1.1), such as the *Heck reaction*,[2] the *Diels–Alder cycloaddition*,[3] *olefin hydroformylation*,[4] and *olefin metathesis*,[5] to just name a few C–C bond-forming methods. Also redox transformations on olefins have become available, including asymmetric variants for some of them, to change the game rules of chemical synthesis, such as the *asymmetric epoxidation* and *dihydroxylation* developed by Sharpless,[6] the *Wacker oxidation*,[7] or *asymmetric hydrogenations* developed by Knowles and Noyori.[8] Given the importance of these transformations, it is not surprising to find out that many of their developers have been awarded with the Nobel Prize.

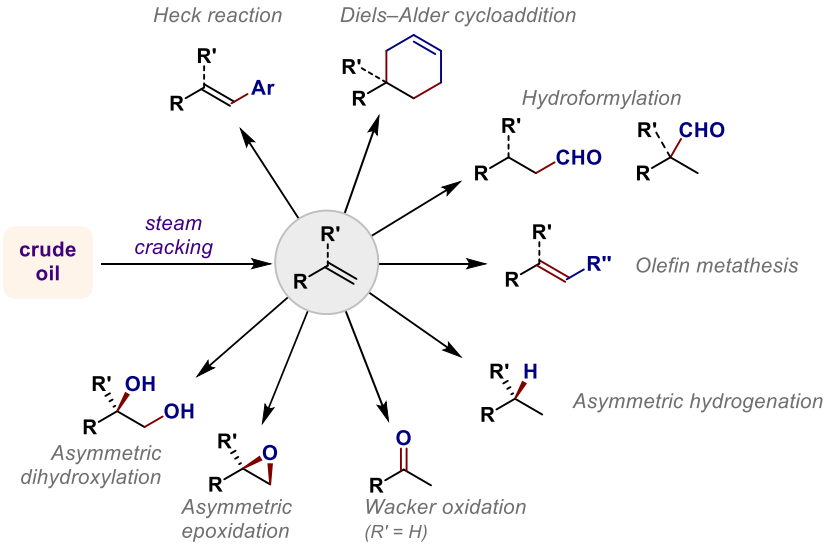

Scheme 1.1. An overview of fundamental organic transformations from olefins.

If chemists were to choose another functionality with such level of versatility and accessibility, probably the carbonyl group would be the first in line. Aldehydes and ketones can be easily accessed either from alcohols or from carboxylic acids, and also from olefins by methods like the already mentioned Wacker oxidation and hydroformylation strategies. Aldehydes and ketones also represent outstanding starting points to perform C–C bond-forming events. Transformations like the *aldol reaction* or the *Mannich reaction* have been key to the growth of synthetic organic chemistry as a field.

On one side, olefins behave as nucleophiles, with the π-electrons occupying the HOMO; on the other side, and as a consequence of the electronegativity of the oxygen atom, carbonyl

compounds present an electrophilic character on the carbonyl carbon atom, which has a significant contribution to the LUMO. Therefore, the reaction between olefins and carbonyl compounds seems like a legitimate way of forming C–C bonds, which explains the great interest that this type of transformation has caused in the organic chemistry community for decades. The pathway by which the reaction between an olefin (aliphatic or aromatic) and a carbonyl compound (aldehyde/ketone) takes place will depend on the structural and electronic properties of the substrates, as well as the reaction conditions (catalyst, solvent, temperature, concentration, additives, irradiation with light, etc.). Some possible transformations that can take place in this general scenario include the *Prins reaction*, the *carbonyl-ene reaction*, *carbonyl-olefin metathesis*, and, for more specific types of olefins or aldehydes/ketones, the *hetero-Diels–Alder cycloaddition*, among others (Scheme 1.2).

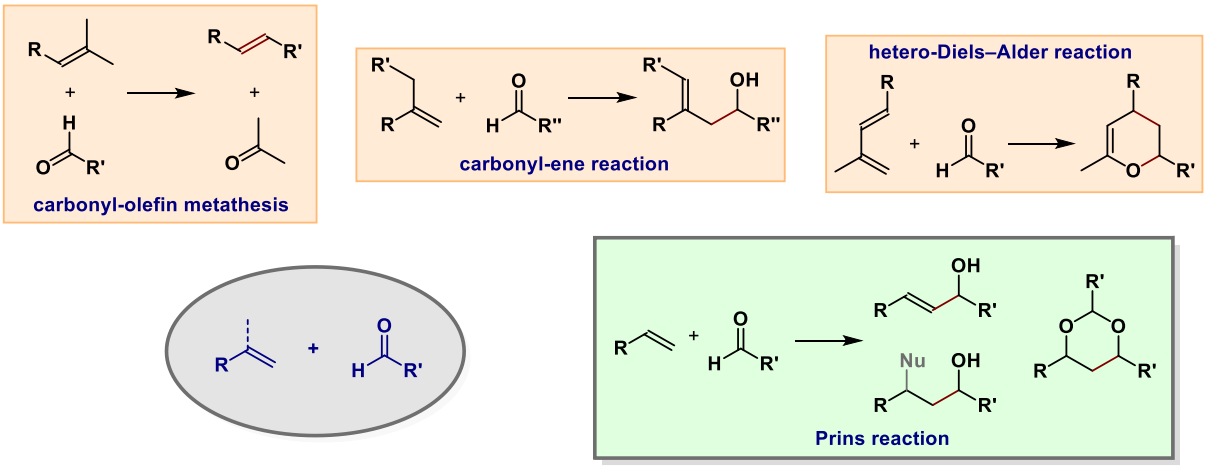

Scheme 1.2. Olefin + Aldehyde: Which route to take?

The Prins reaction consists in the addition of an olefin to an acid-activated aldehyde/ketone and commonly results in products such as 1,3-diols or esters thereof, 1,3-dioxanes or unsaturated alcohols.[9] Mechanistically, it is generally accepted to proceed by initial activation of the carbonyl compound forming a carbonylonium ion, to which the olefin adds to generate a γ-hydroxycarbenium ion, and the fate of this carbocation determines the outcome of the reaction.[9] The 1,3-dioxygenation pattern that is obtained is a valuable building block for the synthesis of fragrances and pharmaceutically-active compounds.[10] However, despite the great application potential that such a synthetic tool might entail, at the beginning of this doctoral work there were no reported methodologies for a catalytic, asymmetric, intermolecular Prins reaction.

2 Background

2.1 Asymmetric Brønsted Acid Catalysis

Centuries ago, alchemists sought the Philosopher's Stone that would transform base materials into noble ones. This is one example of how mankind has constantly wanted to unlock the power lying latent in nature and to utilize it to transform matter.[11] Catalysis can be considered the closest to the realization of this long-lasting dream, and this answer has been there all the time, connected to life itself, which depends on many vital enzyme-catalyzed biochemical transformations. Catalytic processes have also played a key role in the development of the multi-billion euro business of chemical processing to such an extent, that it would be nearly impossible to imagine those industries without the aid of catalysts.[12]

The notion of a *catalyst* as a substance that participates in a chemical reaction without being consumed, yet increasing the reaction rate, as impressive as it might sound, relies on the principles of thermodynamics and chemical kinetics. The catalyst does not modify the energy of reactants or products, and therefore it leaves the equilibrium of the reaction unchanged, but it does interact with some of the reactants/intermediates to form activated complexes, thus enabling the reaction to occur via a different, less energetically-demanding pathway (Figure 2.1).

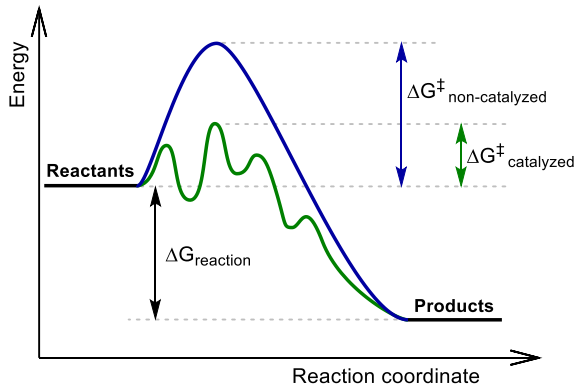

Figure 2.1. Effect of a catalyst on the energetics of a chemical reaction.

Accessing chiral substances in enantiopure form is an important aim for applications in biological systems, as well as to modulate properties of optical and electronic materials.[13] For the preparation of enantiomerically pure substances, one class of catalysis, *asymmetric catalysis*, stands out in comparison to other approaches. For example, separating racemates (resolution) is limited to a maximum yield of 50%, unless a dynamic kinetic resolution can be performed; and the use of "chiral pool" materials (either as reactants or as auxiliaries), although effective and widespread, is not generally applicable. On the other side, the use of catalysts to induce asymmetry represents a broader strategy, since ideally there are no constraints in terms of either the substrate structure or the type of reaction to be performed.[14] Because of the

advantages that it represents, the efforts on asymmetric catalysis have been acknowledged with the Nobel Prize in Chemistry not once but twice: first in 2001, awarded to W. Knowles and R. Noyori "for their work on chirally catalysed hydrogenation reactions", and to K. B. Sharpless "for his work on chirally catalysed oxidation reactions",[6, 8] and also with the 2021 Prize, which was recently announced to go to B. List and D. W. MacMillan "for the development of asymmetric organocatalysis".[15]

Throughout history, the development of science has repeatedly occurred by taking inspiration from nature. For example, chemists continuously aim to convert relatively simple building blocks into highly complex molecules in a selective fashion, in the same way that many enzymatic processes take place. This motivation has served as the driving force in many areas of science, and also in the development of asymmetric catalysis. Until the beginning of the 21st century, the many contributions from scientists all over the world to this field could be classified in two groups, namely *transition metal catalysts* and *biocatalysts*. Later on, *organocatalysis* became the third pillar to complement the field of asymmetric catalysis as we know it today.

Organocatalysis is defined as the use of small organic molecules, where a metal is not part of the active principle, to catalyze organic transformations. One of the earliest known examples of an organocatalytic reaction is the addition of HCN to aldehydes, catalyzed by cinchona alkaloids, and was published in 1912 by Bredig and Fiske.[16] In the 1970s, Hajos and Parrish at Hoffmann La Roche reported the use of (*S*)-proline (**2.1**) as the catalyst for intramolecular aldol reactions of triketones that, after subsequent acid-mediated dehydration, furnished the corresponding bicyclic enones **2.2** and **2.3**, commonly called "Hajos–Parrish ketone" and "Wieland–Miescher ketone", respectively (Scheme 2.1).[17] This work resembled the report from Eder, Sauer and Wiechert at Schering, who obtained directly the condensation products by the reaction of the triketones using (*S*)-proline and an acid cocatalyst.[18] It is worth mentioning that the enantioenriched enones obtained in the so-called *Hajos–Parrish–Eder–Sauer–Wiechert reaction* (a proline-catalyzed intramolecular aldol reaction) could have direct application in the synthesis of steroids and other natural products.[19] However, the actual mechanism and rational of this transformation remained a mystery for a long time. Following several proposals that eventually were refuted, the accepted mechanistic and stereochemical model for this transformation (Scheme 2.1) relies on quantum mechanical calculations reported by Houk,[20] with additional experimental evidence provided by List.[21]

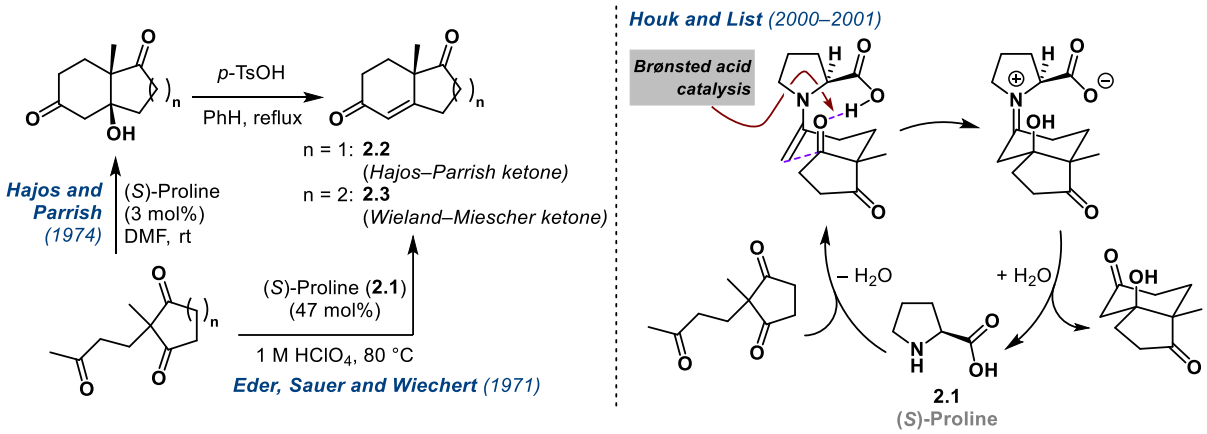

Scheme 2.1. The Hajos–Parrish–Eder–Sauer–Wiechert reaction, and the mechanism proposed by Houk and List.

Nonetheless, the use of proline as general asymmetric organocatalyst became possible thanks to that understanding, when List, in 2000, reported a direct asymmetric intermolecular proline-catalyzed aldol reaction of acetone with several aldehydes, via the proline-derived acetone enamine (Scheme 2.2).[22] Inspired by this groundbreaking development, this work was quickly followed by other reports on the use of enantiopure proline as the catalyst for α-functionalizations of enolizable compounds (Mannich, amination, aminoxylation).[23]

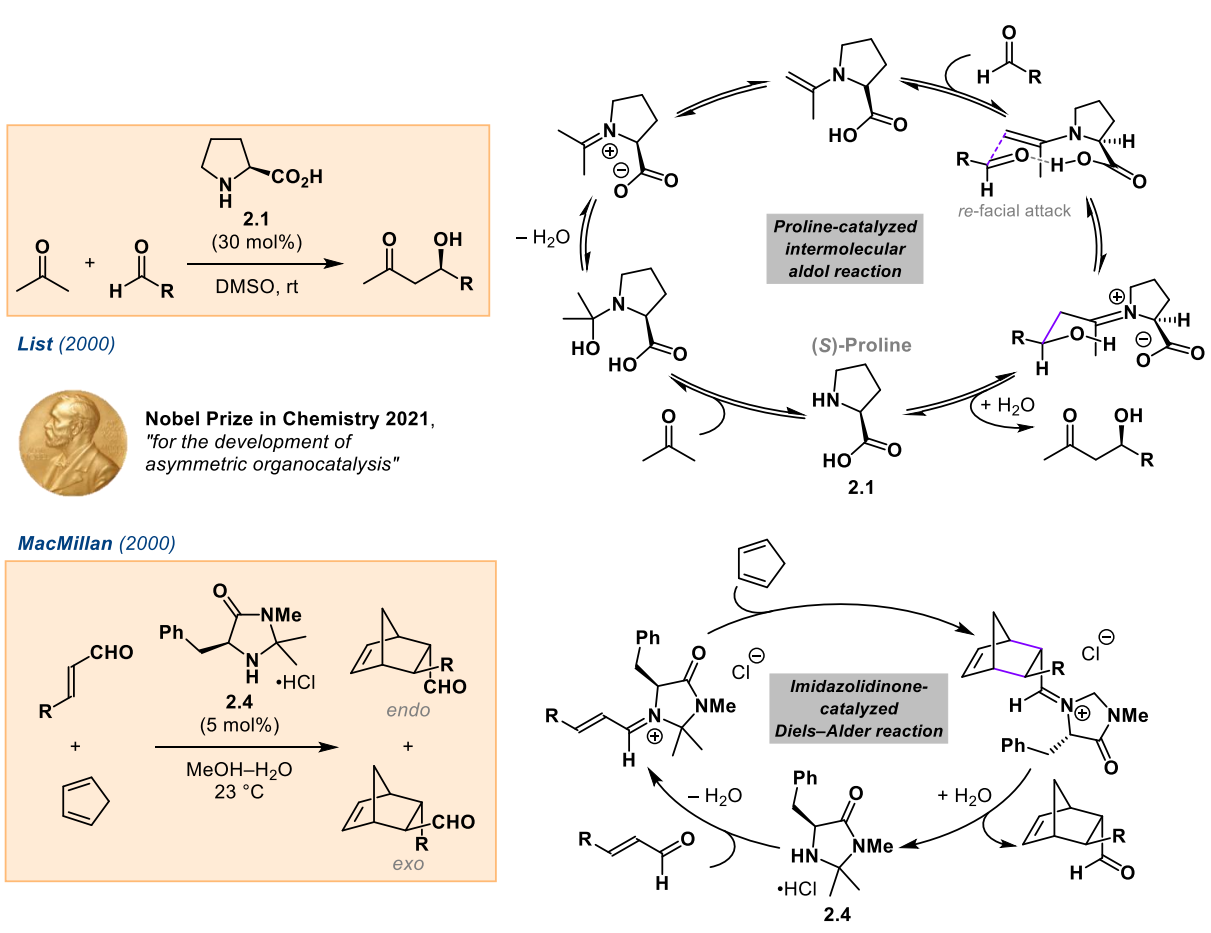

Scheme 2.2. Proline-catalyzed intermolecular aldol reaction (List) and imidazolidinone-catalyzed Diels–Alder reaction (MacMillan).

Independently, in 2000 MacMillan reported the application of amino acid-derived imidazolidinones (**2.4**) as organocatalysts for the Diels–Alder reaction of cyclopentadiene and α,β-unsaturated aldehydes, via the imidazolidinone-derived iminium ion of the enal (Scheme 2.2).[24] Ever since, these two pioneering examples have been considered the starting point of organocatalysis as a field in chemistry, with a remarkable increase in publications regarding the use of small organic molecules as catalysts.

The growing interest from the chemical community on organocatalysis translated into a large number of new catalysts being reported in just a few years, and the scope limitations of these initial activation modes (*enamine catalysis* and *imine catalysis*) were quickly recognized. Further exploration led to organocatalysts acting under other types of substrate activation, and pushing the boundaries with even more challenging substrates. The great number of reports on organocatalysis revealed the need for some classification system. For example, the one proposed by List uses the fundamental concepts of Brønsted/Lewis acid/base to present four classes of organocatalysis, depending on the type of catalyst: *Brønsted acid catalysis*, *Lewis acid catalysis*, *Brønsted base catalysis*, and *Lewis base catalysis* (Scheme 2.3).[25]

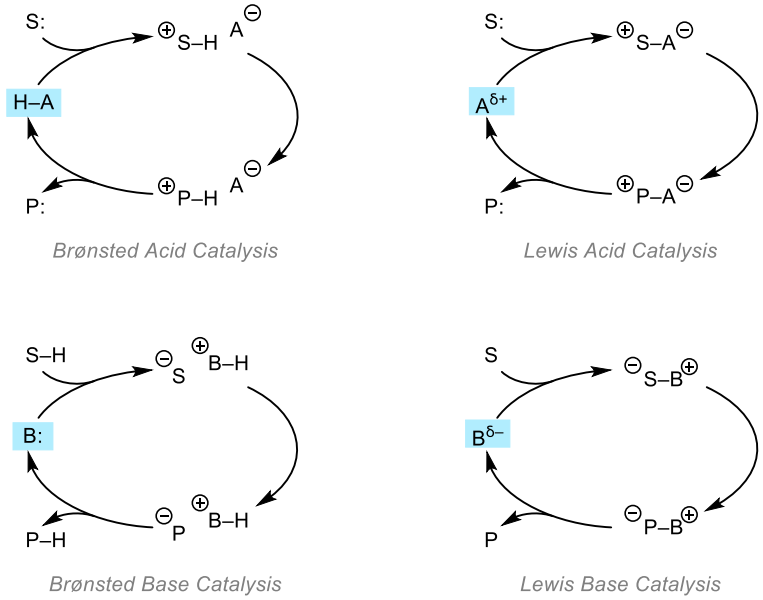

Scheme 2.3. Systematic classification of the main reaction modes on organocatalysis. S: substrate, P: product.

It is necessary to mention, however, that, as with every attempt of classification, this one does not fully cover all reports on organocatalysis, and also that several catalysts possess bifunctional structures, containing both acidic and basic sites. An example of this can be found in the very same proline, where the carboxyl group and the secondary amine moiety are a Brønsted acidic and a Lewis/Brønsted basic site, respectively (see Figure 2.2). In fact, both sites play crucial roles in the substrate activation during a catalytic process.

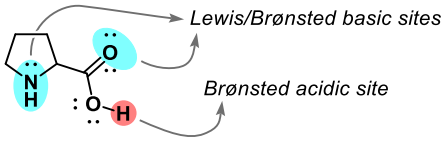

Figure 2.2. Proline as an example of a bifunctional organocatalyst.

The reactions that are catalyzed by proline/imidazolidinones involve the formation of reactive intermediates (enamine/imine, respectively) via covalent bonding of the substrate and catalyst, modulating the electronic properties of the substrate. However, substrates with low reactivity or that cannot form imines/enamines at all were excluded from these approaches. Taking into account that many organic reactions proceed via cationic intermediates and can be catalyzed by acids, it seems logical to use chiral, enantiopure organic proton donors as catalysts. After substrate protonation, a contact ion pair would originate with the activated cationic reaction intermediate in close proximity to the chiral, enantiopure anion. It is worth to mention that removing the covalent bonding between substrate and catalyst is expected to make the enantioinduction process more challenging, since it will rely solely on non-covalent interactions. Careful catalyst design must be performed to maximize the chances of chirality transfer, so that in the formed contact ion pair, the chiral anion may exert influence on the stereoselectivity of the subsequent reaction steps. Conceptually, this scenario was defined by List as *asymmetric counteranion-directed catalysis* (ACDC),[26] which is "*[…] the induction of enantioselectivity in a reaction proceeding through a cationic intermediate by means of ion pairing with a chiral, enantiomerically pure anion provided by the catalyst*".[27]

Historically, acids have been divided in two major groups: *Brønsted acids* and *Lewis acids*. IUPAC defines a Lewis acid as "a molecular entity (and the corresponding chemical species) that is an electron-pair acceptor and therefore able to react with a Lewis base to form a Lewis adduct", and a Brønsted acid as "a molecular entity capable of donating a hydron (proton) to a base (i.e., a 'hydron donor') or the corresponding chemical species"[28]: the proton itself (H^+) can then be understood as the simplest Lewis acid. The acid-base interactions mentioned in these definitions have been used as a strategy for the use of acids as catalysts of organic reactions: when a Lewis basic moiety of the substrate interacts with the acidic catalyst, it leads to a LUMO lowering of the substrate and, therefore, to an increase in its electrophilic character. Depending on the strength of such acid-base interaction (in part related to the acidity of the catalyst), acid catalysis can be divided in two subclasses (Figure 2.3):

- *General Brønsted acid catalysis:* relatively weak acid-base interaction, commonly in the form of hydrogen bonds. Several chiral structures belong to this subclass, such as thioureas,[29] squaramides,[30] and diols (e.g., TADDOL and BINOL).[31]

- *Specific Brønsted acid catalysis:* strong acid-base interaction, resulting in substrate protonation. Commonly used strong Brønsted acids fall into this subclass, such as arylsulfonic acids (e.g., *p*-TsOH), TfOH, Tf_2NH, HBF_4, or HPF_6.

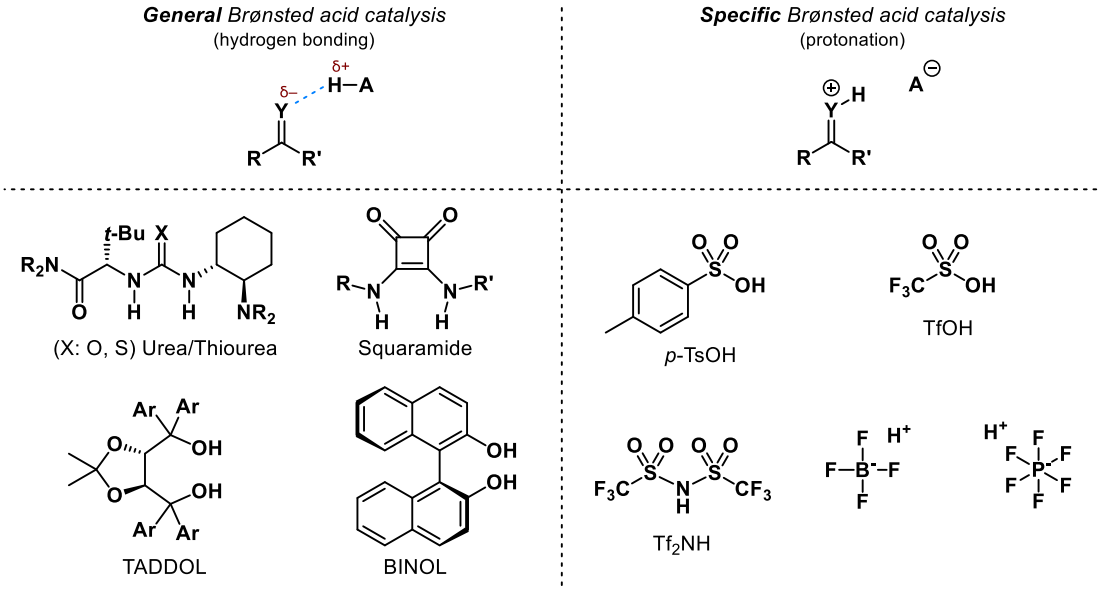

Figure 2.3. General and specific Brønsted acid catalysis.

Despite the success of chiral small-molecule H-bond donors as asymmetric organocatalysts in recent years, this strategy presents an inherent limitation on the type of substrates that can be activated, being these mostly imines and some carbonyl compounds. Therefore, to achieve better activation of less Lewis basic substrates, a stronger acid-base interaction is required, which translates into a need for *stronger chiral acids*.

2.1.1 Strong Asymmetric Brønsted Acid Catalysts

In comparison to the relatively established examples of catalysts for *general asymmetric acid catalysis*, the use of strong chiral Brønsted acids as catalysts has remained underexplored. Partly due to their unavailability, only recently have strong organic acids started to become more accessible.[32] In 2004, Akiyama and Terada independently reported the preparation of chiral phosphoric acids (CPAs) derived from enantiopure BINOL (1,1'-binaphthalene-2,2'-diol), as well as their use as catalysts for enantioselective Mannich reactions between aromatic imines and carbon nucleophiles.[33] Noteworthy, some years later it was revealed that the catalyst prepared by Terada was actually the corresponding calcium salt of the phosphoric acid, but it was demonstrated that the reaction still proceeds with the free Brønsted acid, although with inversion of the stereoselectivity.[34] Nevertheless, these reports represent the starting point for the rapid development of strong chiral Brønsted acids, with innumerous reports of different CPAs, most of them based on BINOL backbones or similar chiral biphenols,

such as H_8-BINOL, SPINOL, SPHENOL, VANOL, VAPOL, TADDOL, and planar chiral diols (ferrocene-based or cyclophane-based), among others (Figure 2.4).[35]

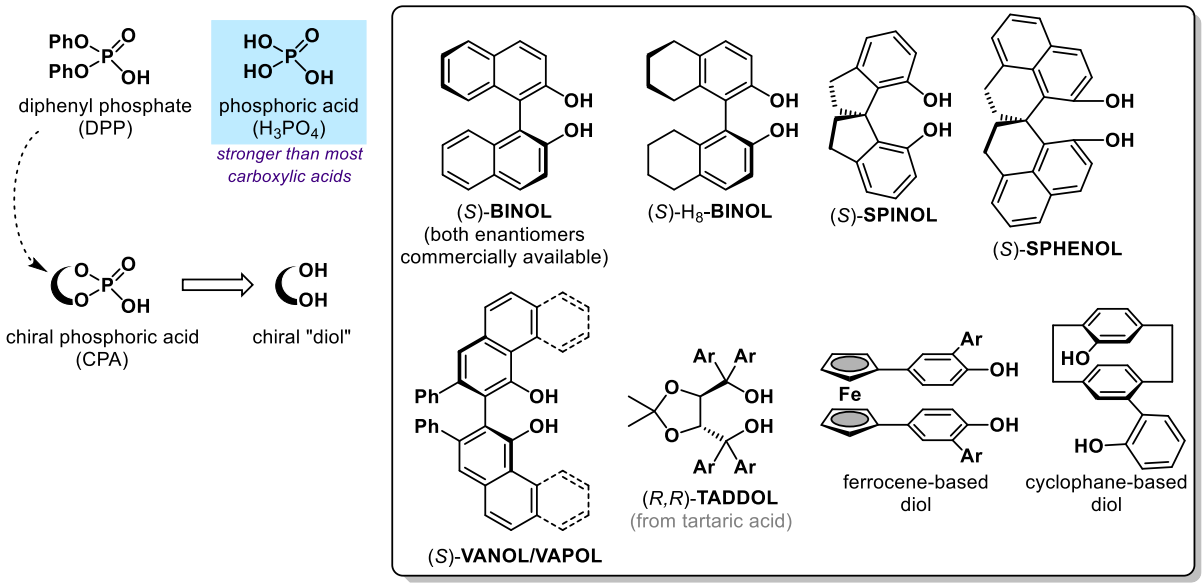

Figure 2.4. Development of the concept of chiral phosphoric acids (CPAs), and different chiral diol backbones used in asymmetric catalysis.

In general, CPAs perform very well in transfer hydrogenations as well as in addition reactions to aldimines/ketimines. However, the moderate acidity of these catalysts (pK_a ~12–14, in MeCN)[36] is normally not enough for the more demanding activation of less basic carbonyl electrophiles, which motivated several groups to develop more acidic chiral organocatalysts. The conceptual exchange of oxygen atoms by N-(EWG) groups, an idea originally described by Yagupolskii in 2002,[37] proved beneficial to further increase the acidity of the phosphate-based catalysts. In this way, when an oxygen atom of the phosphoric acid moiety was replaced with an N-SO_2CF_3 (*N*-triflyl) group, more acidic catalysts were obtained. For example, in 2006 Yamamoto reported *N*-triflyl-phosphoramides (NTPAs, Figure 2.5) and their application in asymmetric Diels–Alder reactions,[38] where the increased acidity (average pK_a values of NTPAs (in MeCN) are ~6–7)[36] was reflected in the observed reactivity, outperforming CPA catalysts. A similar approach toward stronger acids consisted in replacing the acidic hydroxyl group of the CPA structure for a phosphinylamino unit, as in the *N*-phosphinyl-phosphoramides (NPPAs) reported by List, which performed better than the corresponding phosphoric acids in an *N*,*O*-acetalization of aldehydes.[39] Also the replacement of oxygen atoms with sulfur/selenium translates into stronger acids, as can be seen from examples with dithiophosphoric acids,[40] and *N*-triflyl-substituted thio/selenophosphoramides.[41] A second "Yagupolskii substitution" leads to phosphoramidimidates (PADis, Figure 2.5), introduced by the List group in 2015, and their superior acidity was evident by enabling more challenging reactions, such as the Friedel–Crafts alkylation of isophytol and hydroquinone to produce α-tocopherol; however, only with moderate stereodifferentiation.[42]

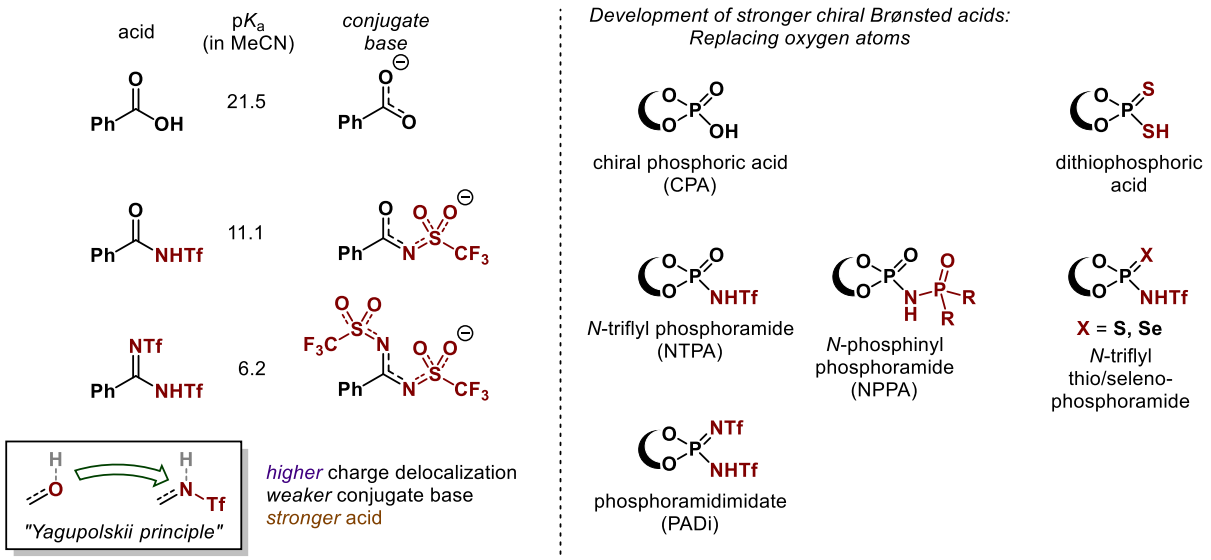

Figure 2.5. Development of stronger (chiral) Brønsted acids by replacement of oxygen atoms with more electron-withdrawing units. Tf = SO_2CF_3.

However, not only phosphoric acid has served as scaffold for the construction of chiral acid catalysts. Moving to sulfur as central element, several chiral sulfonic acids and derivatives thereof have been developed, displaying excellent reactivity and outstanding enantioinduction (Figure 2.6). In 2008, List and Ishihara independently reported the synthesis of enantiopure BINOL-derived bis(sulfonic acids) (BINSAs),[43] which have been used as catalysts (mostly as mono-pyridinium salts) in several nucleophilic additions to imines (Mannich-type, aza-Friedel–Crafts, Strecker, aminal synthesis).[44] One year later, reports from List and from Giernoth introduced BINOL-derived disulfonimides (DSIs),[45] a privileged catalyst motif for multiple C–C bond-forming reactions, such as *Mukaiyama aldol*, *Mukaiyama–Mannich*, *hetero-Diels–Alder*, *(aza-)Hosomi–Sakurai*, and *cyanosilylation of aldehydes*, to just name a few.[46] Several strategies were applied to further increase the acidity of DSIs and/or to achieve more organized catalyst/substrate arrangements, such as introducing electron-withdrawing groups on the BINOL backbone,[47] or introducing hydroxyl groups near to the acidic proton (HYDRAs).[48] It is worth to mention that DSIs display excellent reactivity as Brønsted acids, but also as Lewis acids upon hydrogen-silicon exchange with silyl group donors. Finally, Berkessel reported the development of a family of sulfuric acid-derived acids (bis(sulfuryl)imides, also called JINGLEs).[49] Although they are more acidic than DSIs (pK_a, in MeCN: 5.2 and 8.4, respectively),[36, 50] they have only been reported as catalysts a few times.[51]

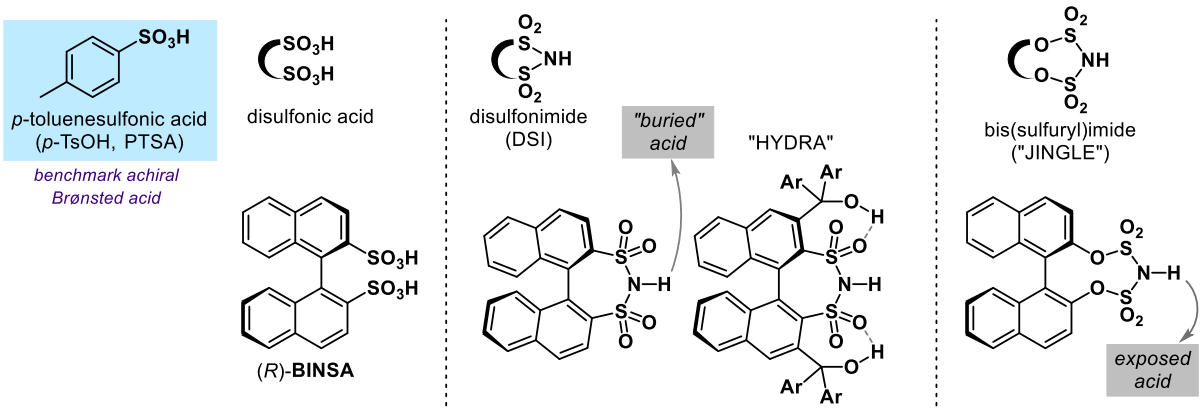

Figure 2.6. Brief overview of sulfur(VI)-based chiral acids used in organocatalysis.

Another possible structural scaffold for designing strong acids can be found in C–H acids, such as tris(trifluoromethanesulfonyl)methane (Tf_3CH). In 2016, the List group introduced binaphthyl-allyl tetrasulfones (BALT) as a new class of chiral C–H acids that, upon *in situ* silylation with a substoichiometric amount of a silyl ketene acetal, efficiently catalyzed asymmetric Diels–Alder reactions of cyclopentadiene and 9-fluorenylmethyl cinnamates (Figure 2.7).[52] In the same year, they also presented the synthesis of tetratriflylpropene (TTP), a strong, allylic C–H acid that has displayed outstanding reactivity, outperforming common strong acids, such as trifluoromethanesulfonic acid (TfOH) and bis(trifluoromethane)sulfonamide (Tf_2NH). Another type of strong chiral C–H acids, pentacarboxycyclopentadienes (PCCPs), based on the high stability of the aromatic cyclopentadienyl anion, was reported also in 2016 by Lambert. They have been applied as acid catalysts for *Mukaiyama–Mannich* and *Mukaiyama acetal-aldol reactions*.[53]

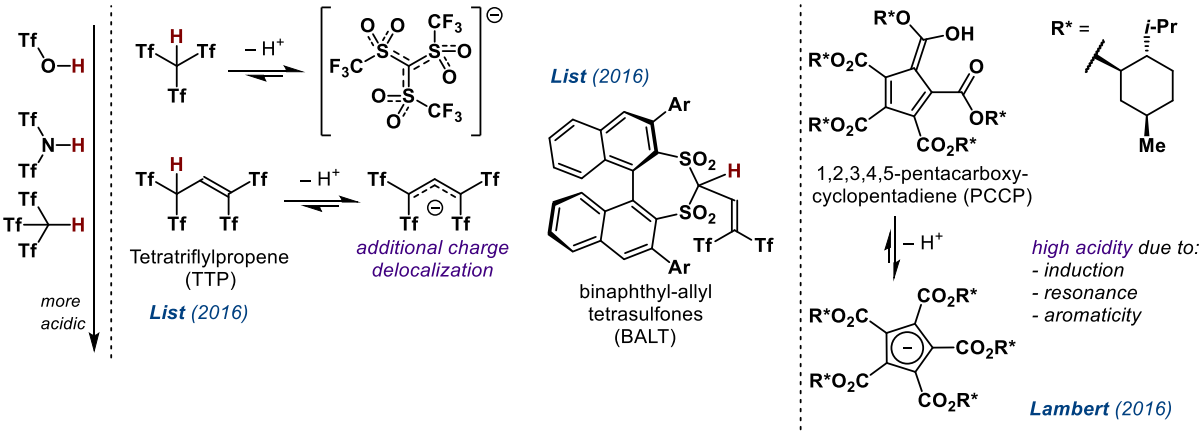

Figure 2.7. Strong C–H acids used in organocatalysis.

2.1.2 The Next Generation of Asymmetric Brønsted Acid Catalysts: Strong *and* Confined

Whereas all the previously mentioned chiral acids performed very well in reactions involving structurally-biased substances, such as substrates containing aromatic rings and/or sterically-demanding substituents, enantioselective conversions of small, structurally-unbiased substrates within the frame of ACDC has remained elusive, due to insufficient catalyst-induced stereofacial bias. This trend has been attributed to the relative "open" character of the acids, for which the hypothesis that a more structurally encumbered, yet strongly acidic catalyst could improve the enantioinduction gained strength. It was thought that a blocked catalytic pocket can limit the conformational freedom of transition states arising from small substrates, thus increasing the selectivity. This is probably one of the reasons behind the success of TRIP: a chiral phosphoric acid substituted in the 3,3'-positions with bulky 2,4,6-triisopropylphenyl groups, which was introduced by the List group[54] and has been applied ever since for a good number of asymmetric transformations, such as *reductive aminations*, *allylations*, and *Friedel–Crafts alkylations*.[35] To further constrain the active site, the List group later developed C_2-symmetric BINOL-derived imidodiphosphoric acids (IDPs). The active site of the IDP is shielded by the four substituents on the 3,3'-positions of the BINOL backbone, resulting in a well-defined, very tight chiral microenvironment, but still displaying a bifunctional character because of the presence of one acidic (P–OH) and one basic site (P=O), as can be seen on Figure 2.8. This combination of features was reflected in the excellent enantiocontrol of carbonylonium ions for the spiroacetalization of unbiased, aliphatic substrates.[55] For example, the more open (*S*)-TRIP acid was also able to catalyze spiroacetalizations, although requiring substrates with significant structural bias.[56] Due to their *confined* character, IDPs also delivered successful results when applied as catalysts for a number of reactions, such as *intermolecular acetalizations*, *oxidation of sulfides* and *vinylogous Prins cyclizations*, among others.[57]

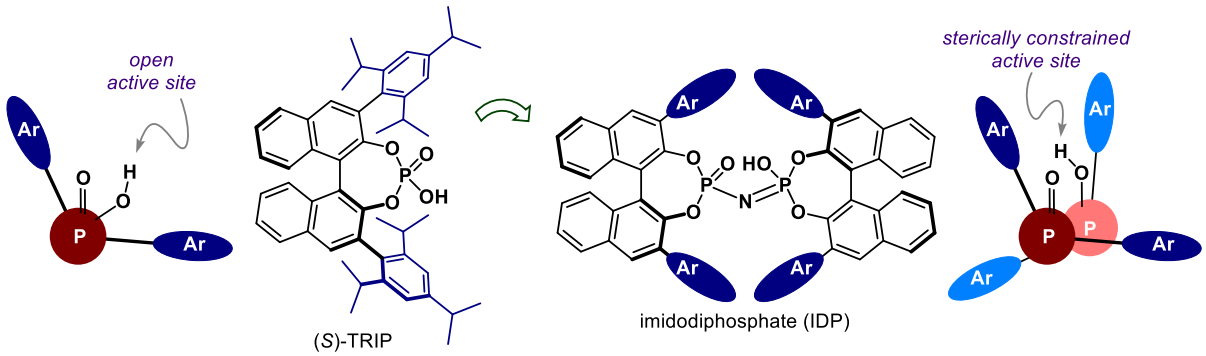

Figure 2.8. Toward chiral, confined Brønsted acids: imidodiphosphates with sterically constrained active sites.

However, the highly confined IDPs were not particularly acidic (pK_a ~11, in MeCN), which limited the type of substrates that could be activated with them. To increase their acidity,

electron-withdrawing groups were installed on the BINOL backbone (Scheme 2.4), and thus a nitrated IDP was able to provide the required reactivity as well as to control the enantioselectivity for the cyclization of carbonylonium ions tethered to electron-rich aromatic rings: the *oxa-Pictet–Spengler reaction*.[58] By applying the so-called "Yagupolskii principle" (replacement of =O with =NTf) on one of the P=O moieties from the active site, a new family of confined, stronger acids was obtained, namely the C_1-symmetric imino-imidodiphosphates (*i*IDPs, pK_a ~9, in MeCN, Scheme 2.4). These catalysts allowed to further develop intramolecular reactions of carbonylonium ions, now tethered with even less nucleophilic alkene moieties, which were formed in situ by condensation of homoallylic alcohols and aldehydes (*Prins cyclization*).[59]

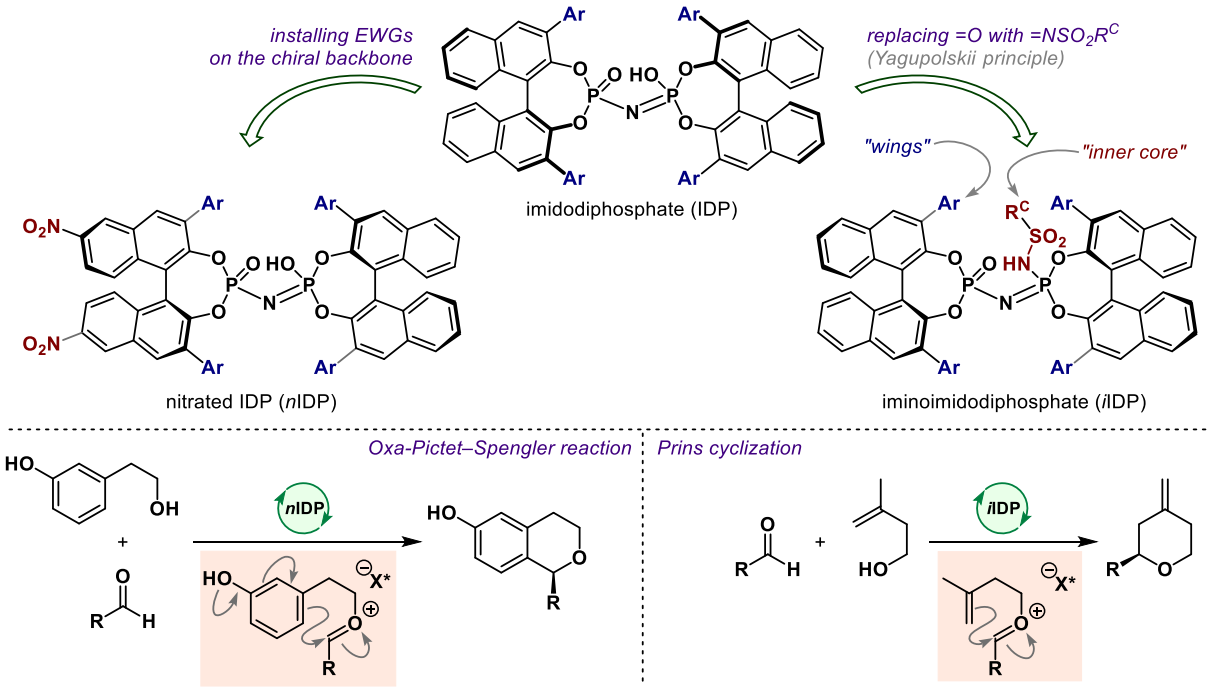

Scheme 2.4. Strategies toward more acidic, highly confined imidodiphosphate-based catalysts.

Considering the significant increase in acidity observed after the first P=O → P=NTf exchange in the IDP structure, the next logical step was to effect a second replacement. In doing so, the even stronger imidodiphosphorimidates (IDPis) were obtained, proving successful in combining acidity and confinement.[60] In recent years, reports from our group have shown how IDPis can act not only as powerful Brønsted acids (pK_a from approx. 4 to ≤2, in MeCN), but also as precursors for chiral, strong "silylium" Lewis acid catalysts. As evidence of their superb performance as asymmetric catalysts, IDPis have been able to protonate inherently less basic (and therefore more challenging) olefins for *intramolecular hydroalkoxylations* and *hydroarylations*.[61] These acids can also perform challenging Mukaiyama aldol reactions under sub-ppm catalyst loadings,[50] displaying an enzyme-like behavior. One example of this can be found in the selective recognition of small acetaldehyde-derived silyl enol ethers to perform *only one* aldol addition without forming polymeric products.[62]

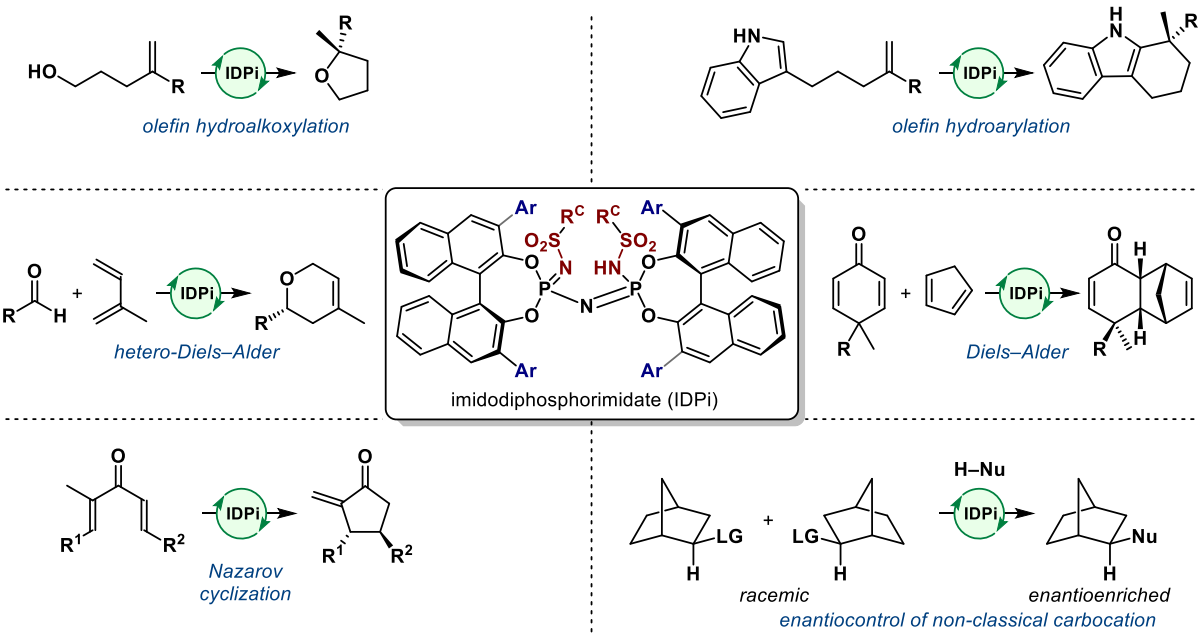

Scheme 2.5. Imidodiphosphorimidates (IDPis) as strong, confined, chiral Brønsted acids.

However, despite the impressive and highly promising activity of the confined imidodiphosphate-type catalysts (IDPs, *i*IDPs and IDPis), their reported syntheses from 3,3'-disubstituted BINOLs were not straightforward, requiring multiple reaction steps and isolation of intermediates; also, these routes worked poorly –or not at all– in the presence of bulky substituents in the 3,3'-positions of the BINOL backbone, due to steric repulsions in the late-stage dimerization step to build the P=N–P skeleton. Addressing these limitations, the List group developed an improved procedure for the single-flask synthesis of these confined acids via consecutive chloride substitutions of hexachlorobisphosphazonium salts, providing a simplified route to imidodiphosphate-type catalysts with high structural confinement (Scheme 2.6).[63]

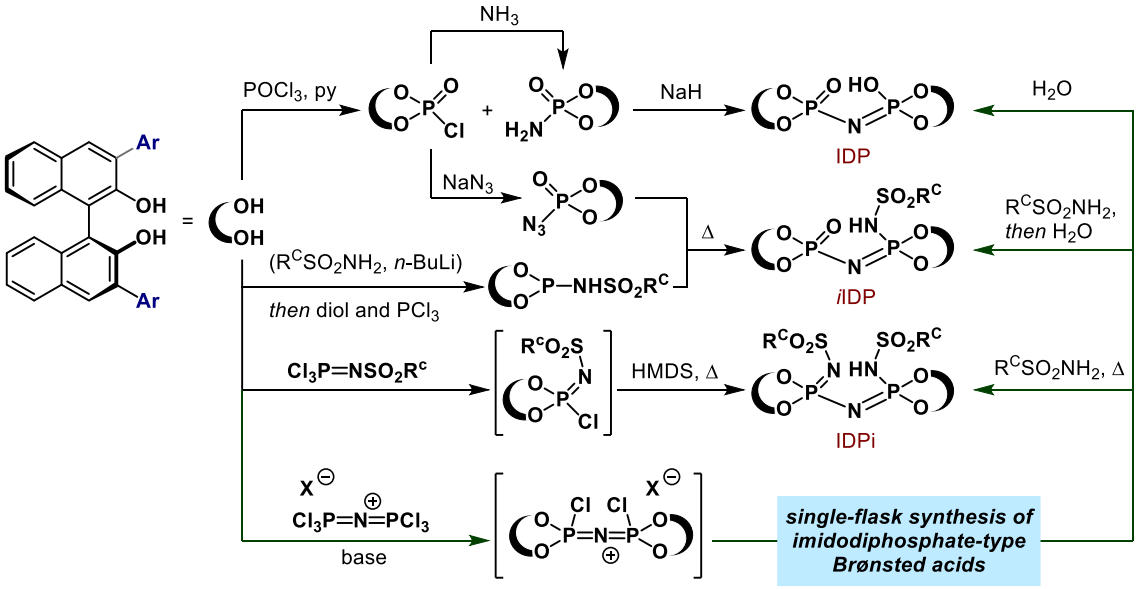

Scheme 2.6. Synthesis of imidodiphosphate-type Brønsted acids: improved single-flask procedure.

2.2 Nucleophile Meets Electrophile: Olefins and Heteroatom-Stabilized Carbocations in C–C Bond-Forming Reactions

The reaction of aldehydes/ketones/imines (or their vinylogous derivatives) with olefins can be of great interest for the synthetic chemist. On one side, the carbon chain is extended by the formation of C–C bonds; on the other side, heteroatoms (nitrogen or oxygen, respectively) are introduced to the molecular skeleton of the starting olefin.

Mechanistically, this type of transformation can be described in a stepwise fashion, where the olefin reacts with the electrophile (carbonylonium or iminium ion) to produce a cationic intermediate. Depending on the reaction conditions, the cationic intermediate can either cyclize (determined by the strain of the formed ring), undergo deprotonation giving an unsaturated product, or be trapped by a nucleophile to increase the functionalization degree of the product (Scheme 2.7).

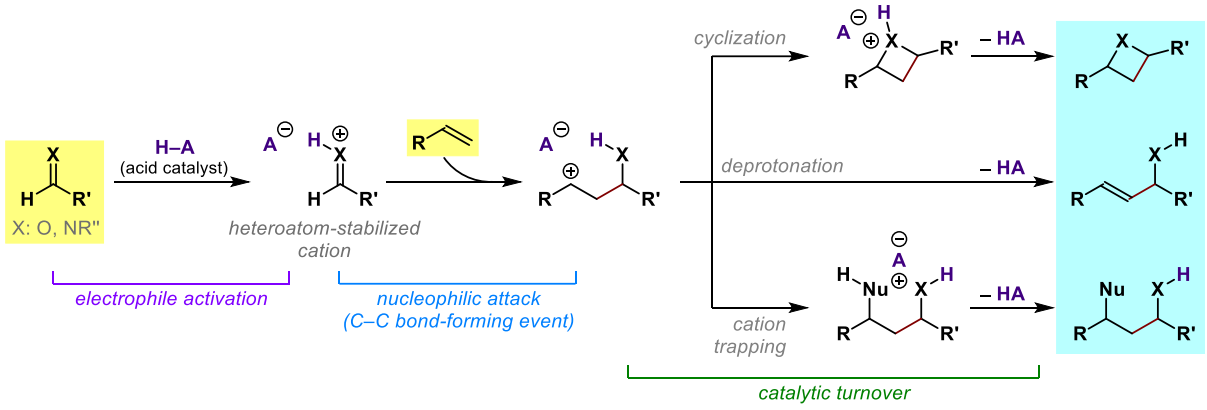

Scheme 2.7. General reactivity pathways for the reaction of olefins and heteroatom-stabilized cations.

2.2.1 On the Electrophile: Heteroatom-Stabilized Carbocations

Due to the polarity of C=O and C=N bonds, respectively, carbonyl compounds (aldehydes and ketones) and imines behave as electrophiles and undergo nucleophilic addition. This process starts with the activation of the substrate using an acid catalyst, thus forming more electrophilic, cationic intermediates, to which the nucleophile readily adds. The activation of a carbonyl group involves the interaction of free electron pairs on the oxygen atom with the acid (either H^+ or another Lewis acid), forming a *carbonylonium ion*[64] (unambiguous, more accurate name for the species that has commonly been called *oxocarbenium ion* in the past). Similarly, the acid activation of an imine results in the formation of an iminium ion. These two cationic species (carbonylonium and iminium ions) are more stable than the non-heteroatom-containing counterparts, mostly due to resonance stabilization, as shown in Scheme 2.8, for which they can be regarded as *heteroatom-stabilized carbocations*.

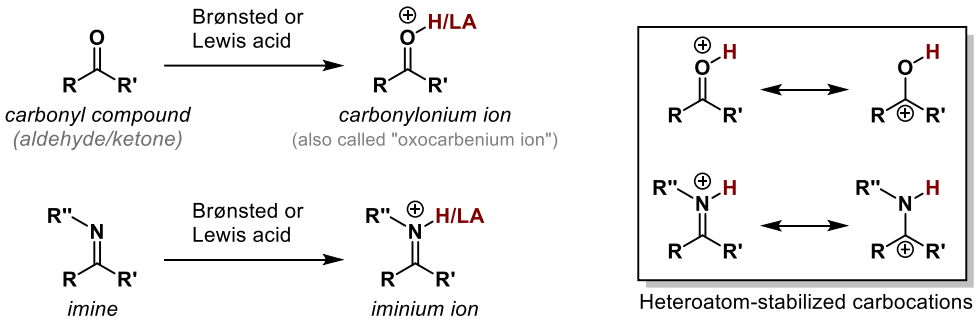

Scheme 2.8. Activation of carbonyls and imines with acids: heteroatom-stabilized cations (carbonylonium and iminium ions).

C=X systems (X: C, N, O) can be ordered according to their relative Lewis basicity as follows: imines > carbonyls > olefins. This basicity trend can be confirmed by comparing the pK_{BHX} values, as can be seen in Figure 2.9.[65] Therefore, it is not surprising that many reports of asymmetric additions to imines successfully utilize chiral phosphoric acids as catalysts, which, in contrast, perform badly when similar transformations are attempted with carbonyl compounds. Needless to say, the protonation of unbiased olefins requires even stronger acids, explaining the challenge behind asymmetric olefin hydrofunctionalizations. Particularly, when comparing imines and carbonyls, the substrate can be activated (LUMO lowering) by hydrogen bonding or rather be protonated, and determining which scenario takes place will depend both on the basicity of the substrate and the acidity of the catalyst.

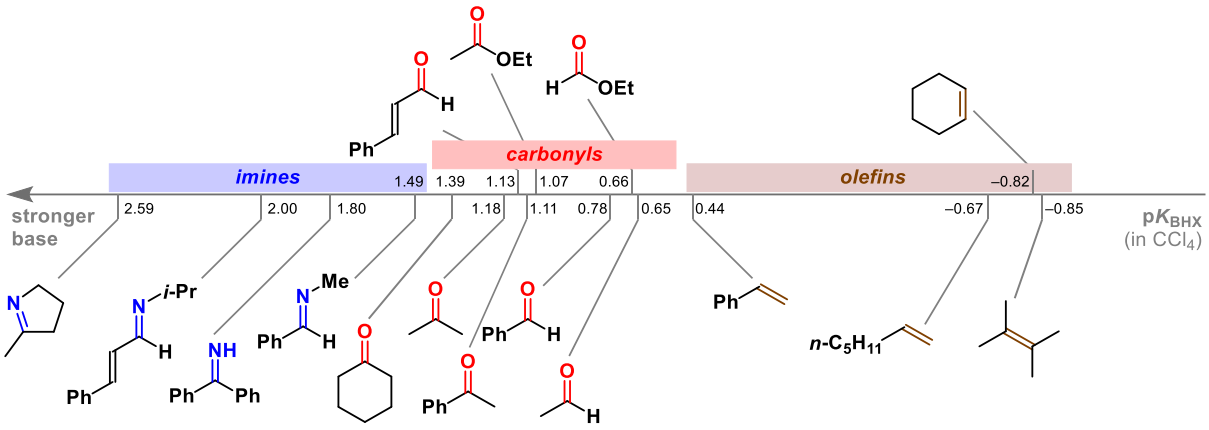

Figure 2.9. Basicity of imines, carbonyls and olefins, based on their pK_{BHX} values.

While the acid catalyst indeed performs a lowering of the LUMO of the electrophile, a suitable nucleophile should also have an appropriate HOMO to facilitate the addition step to take place. It is then clear that, to utilize relatively weak nucleophiles, a stronger activation of the electrophile must occur, which translates into the requirement of a stronger acid catalyst. This explains why most of the currently available asymmetric additions to iminium/carbonylonium ions have been developed either in an intramolecular fashion and/or using highly activated nucleophiles.

2.2.2 On the Nucleophile: Olefins

If a carbon nucleophile subsequently adds to an activated carbonyl/imine group, the transformation results in the formation of a C–C bond. Frequently utilized *C*-nucleophiles, such as enol derivatives (e.g., silyl enol ethers, silyl ketene acetals, metal enolates) and organometallic reagents (RMgX, RLi, etc.), disclose an excellent nucleophilic character and their use represents a fundamental strategy in the synthesis of organic compounds. However, they are not generally stable, requiring them to be freshly made before every use and to be handled under strictly inert reaction conditions. Other types of *C*-nucleophiles, namely C(sp^2) nucleophiles, are *alkenes* and *arenes*. These functionalities possess a high potential as useful building blocks, since they are found in the structures of many organic compounds, both simple oil-derived substances and complex natural products. However, they also have a lower average nucleophilicity than the aforementioned enol derivatives, which makes them challenging partners for the development of reactions with electrophiles, requiring in turn stronger acids as catalysts.

Using the nucleophilicity scale developed by Mayr,[66] the disadvantageous position of unbiased olefins as *C*-nucleophiles in comparison to the previously mentioned nucleophiles becomes more clear (Figure 2.10). Keeping in mind that the Mayr equation implies a logarithmic relationship between the *N* value and the rate constant, it is evident that activated dienes, such as Danishefsky's diene (*N* = 8.57), are by several orders of magnitude much more nucleophilic than the less biased 1,3-butadiene (*N* = –0.87). Similarly, silyl ketene acetals (*N* ≈ 12 to 8) and silyl enol ethers (*N* ≈ 7 to 3) are much more nucleophilic than allylsilanes (e.g., allyl-TMS: *N* = 1.68), or aryl olefins, such as styrene (*N* = 0.78). Not surprisingly, alkyl olefins are in the lowest part of the scale (e.g., 1-hexene, *N* = –2.77), only accompanied by the even less nucleophilic alkane C(sp^3)–H bonds.

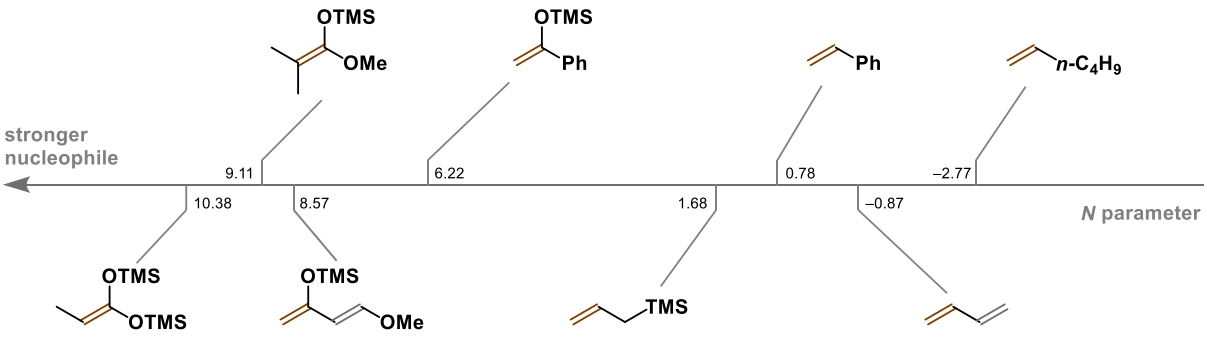

Figure 2.10. Nucleophilicity of several C=C bond-containing compounds, based on their *N* values.

This pro/contra balance of C(sp^2)-nucleophiles explains the growing interest in the last decades in methods for their functionalization, also in an asymmetric fashion.

2.2.3 Organocatalytic Reactions of C(sp^2)-Nucleophiles and Heteroatom-Stabilized Carbocations: A Quick Overview

When considering the reactions of non-activated C(sp^2)-nucleophiles (olefins) and heteroatom-stabilized carbocations (iminium or carbonylonium ions), several reactions come immediately in mind, which will be shortly mentioned and discussed below (Scheme 2.9).

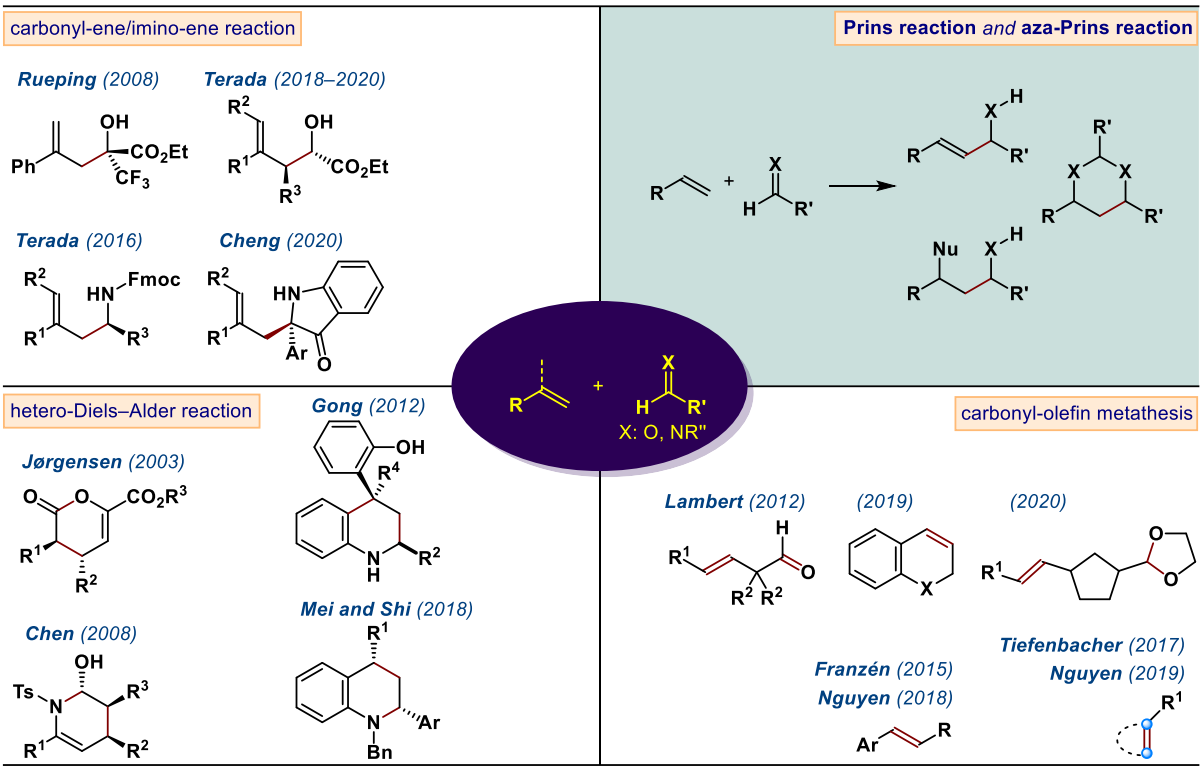

Scheme 2.9. Quick overview of some intermolecular C–C bond-forming reactions between C(sp^2)-nucleophiles and aldehydes/ketones/imines.

It is important to mention though that, whereas catalytic, non-asymmetric versions of all these reactions have been developed and optimized in the last century, their asymmetric counterparts remain underdeveloped, with most reports dealing with intramolecular approaches and/or requiring highly activated substrates. Although many of these reactions have interesting applications, a deep discussion about them exceeds the interest of this doctoral thesis; therefore, the following discussion is just a short overview of the organocatalytic, asymmetric methodologies available in literature for these transformations.

OXA-DIELS–ALDER AND AZA-DIELS–ALDER CYCLOADDITION: INVERSE-ELECTRON-DEMAND

The Diels–Alder cycloaddition is one of the most well-known organic transformations worldwide, and this success is likely due to its high efficiency to construct six-membered rings with good regio- and stereoselectivity in one single step. The “classical” Diels–Alder reaction (normal-electron-demand) involves an electron-abundant diene (HOMO raising) and an

electron-deficient dienophile (LUMO lowering). However, an unbiased olefin acts rather as a moderately electron-rich dienophile, and requires then an electron-poor diene to react: this type of [4+2] cycloaddition with "switched polarity" is known as the "inverse-electron-demand Diels–Alder reaction" (IEDDAR).[67]

Examples of organocatalytic, asymmetric IEDDAR with α,β-unsaturated carbonyl compounds as dienes, for the construction of oxygen-containing heterocycles, include the works from Jørgensen,[68] and Shi.[69] In a similar fashion to the previous examples, α,β-unsaturated imines can also act as dienes and undergo aza-IEDDAR with suitable electron-rich olefins,[70] as demonstrated in the work of Chen[71] and Xu.[72] *Ortho*-quinone methide imines have also proven to be suitable dienes, reacting under Brønsted acid catalysis even with less activated olefins, such as styrenes, as reported by Mei and Shi,[73] and Rueping.[74] A particular case of aza-IEDDAR is when aniline-derived imines are used as dienes, and the corresponding [4+2] cycloaddition, known as the *Povarov reaction*,[75] affords tetrahydroquinoline-type products. The reports from Masson[76] and Gong[77] are interesting examples of three-component, organocatalytic, asymmetric Povarov reactions.

CARBONYL-ENE REACTION AND IMINE-ENE REACTION

The ene reaction is probably one of the most useful, atom-economic methods for the formation of C–C bonds, where an olefin with allylic hydrogens ("*ene*") reacts with a double bond (X=Y, "*enophile*") (Scheme 2.10). It belongs to the family of pericyclic reactions, having some resemblance with sigmatropic rearrangements (migration of σ bond) and also with cycloadditions (a π bond is converted into a σ bond). If the enophile is a carbonyl or an imine group, the reaction (carbonyl-ene or imine-ene, respectively) affords useful building blocks for synthesis (homoallylic alcohols or amines, respectively). Given the relatively low nucleophilicity of simple olefins, the reports on these reactions commonly resort either to highly electrophilic enophiles, such as trifluoropyruvates, glyoxylates or trihalomethyl-ketones, or to designing substrates for the reaction to occur in an intramolecular fashion.[78]

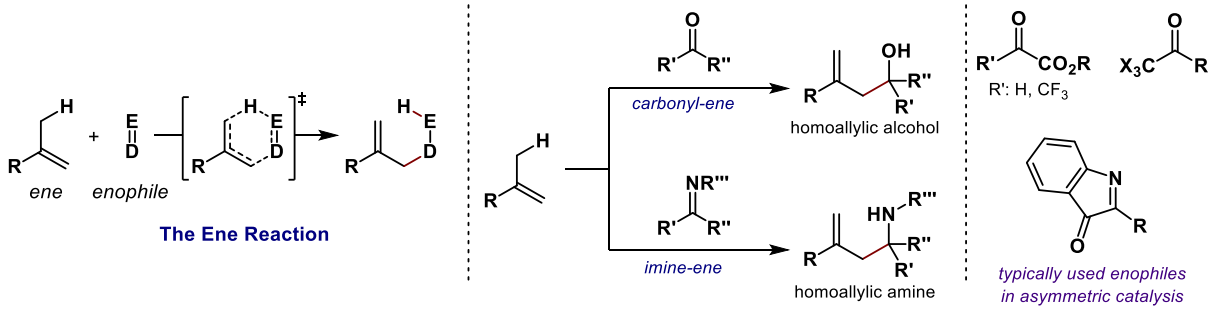

Scheme 2.10. The ene reaction and variants: carbonyl-ene and imine-ene

The first publication of an organocatalytic intermolecular carbonyl-ene reaction dates back to 2007, by Clarke, which used ethyl trifluoropyruvate as the enophile,[79] and was later improved

by Rueping.[80] Terada developed a series of Brønsted acids with the electron-deficient chiral backbone F_{10}BINOL, which allowed the use of slightly less activated enophiles, namely glyoxylates[81].

When imines are used as enophiles (imine-ene reaction), the majority of reports use highly activated ene-carbamates as ene-component, whereas the more challenging, less biased olefins remain underexplored. In 2016, Terada reported a three-component reaction of aldehydes, Fmoc-NH_2 and styrenes, using an F_{10}BINOL-based phosphoric acid as catalyst.[82] Cheng recently reported an asymmetric example of the even more challenging ketimine-ene reaction.[83]

CARBONYL-OLEFIN METATHESIS

Olefin metathesis is among the most powerful carbon–carbon bond-forming reactions due to the availability of simple olefins and the versatility of the more complex alkenes obtained from this reaction. In a similar fashion, the exchange between an olefin and a carbonyl compound also enables the formation of carbon–carbon bonds from readily available materials, although such a reaction remained underdeveloped until recently. In addition to significant progress from the area of Lewis acid catalysis, like the work of the Schindler group with iron(III) salts as catalysts,[84] there have also been some contributions from the organocatalytic world to further improve the development of the carbonyl-olefin metathesis (COM).[85] Lambert has published a series of reports using bicyclic hydrazine salts as catalysts for COM[86], in addition to other contributions from Franzén,[87] Nguyen,[88] and Tiefenbacher.[89] Even though it does not classify as an organocatalyst, iodine was reported by Nguyen to be a metal-free catalyst for the COM reaction.[90]

The reader might wonder at this point about one transformation involving olefins and carbonyls that is missing: *the Prins reaction*. Before introducing this transformation in Section 2.4, the following subchapter (Section 2.3) will provide a brief overview of the components of that transformation, which are *olefins* and aldehydes (commonly *formaldehyde*).

2.3 Olefins and Formaldehyde

2.3.1 The Importance of Olefin Functionalization

Simple olefins, such as ethylene and propylene, along with some aromatics (benzene, toluene and xylenes) represent some of the most important building blocks for the petrochemical industry. Worldwide, approximately 10^9 tons of hydrocarbon feedstock is transformed into over $4x10^8$ tons of light olefins per year, while the remaining $6x10^8$ tons is composed of higher hydrocarbons (mostly gasoline fractions).[1] For decades, the most widely established approach to obtain these substances has relied on the thermal steam cracking of different materials from oilfields, such as naphtha (C_5–C_{12}) and ethane (C_2). Typical products from a steam cracking process include ethylene, propylene, butadiene; modulating the reaction temperature also allows benzene to be obtained.[91]

Styrene is another industrially relevant olefin, used as precursor of plastics, elastomers and surfactants. It is commonly obtained by dehydrogenation of ethylbenzene, which is in turn formed by a Friedel–Crafts reaction between benzene and ethylene.[92] Some recent research has described single-step approaches based on oxidative arene vinylation (Scheme 2.11).[93]

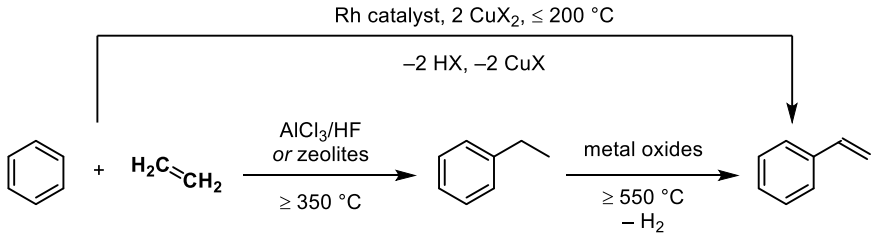

Scheme 2.11. Industrial routes for the preparation of styrene from benzene and ethylene.

Considering the abundant availability of olefins, there are currently huge efforts toward the expansion of upgrading strategies for these hydrocarbon sources into high-value substances (Scheme 2.12), such as pharmaceuticals, scents and other fine chemicals. In fact, some recently developed transformations involving unsaturated hydrocarbons (alkenes, alkynes and dienes), such as the *Heck reaction*, *Diels–Alder cycloaddition*, *olefin metathesis*, *Ziegler–Natta polymerization*, *Sharpless dihydroxylation* and *epoxidation*, and the *asymmetric hydrogenation*, have had an enormous impact in the chemical community. Because of this, their developers have been awarded with the Nobel Prize, further emphasizing the importance and relevance of C–C π bonds for the construction of complex molecular structures.[94]

The versatility of olefins as starting materials is also made evident by the broad realm of hitherto available hydrofunctionalizations, due to their conceptual simplicity and their perfect atom economy, in addition to the increased value of the resulting products. Many of the reports on this type of transformation involves Brønsted acid- or transition metal-catalysis.

Nevertheless, asymmetric variants thereof have remained elusive, with only few examples on catalytic asymmetric olefin hydroaminations[95] and on hydrofunctionalization of dienes/allenes.[40b, 96] In recent years, after recognizing the potential of the newly developed, strong and confined IDPi catalysts, the List group addressed the complex task of expanding the toolset of asymmetric olefin hydrofunctionalizations. Thus, intramolecular variants of olefin hydroalkoxylation[61a] and hydroarylation[61b] reactions were developed, as well as the intermolecular hydroarylation of norbornene via the non-classical 2-norbornyl cation.[97] In all cases, these reactions take advantage of the confined, highly acidic IDPi catalyst class, allowing the activation of inherently weakly Lewis basic substrates and the efficient stabilization of highly reactive intermediates by the enantiopure IDPi counteranion, controlling the selectivity of the subsequent reaction with the nucleophile.

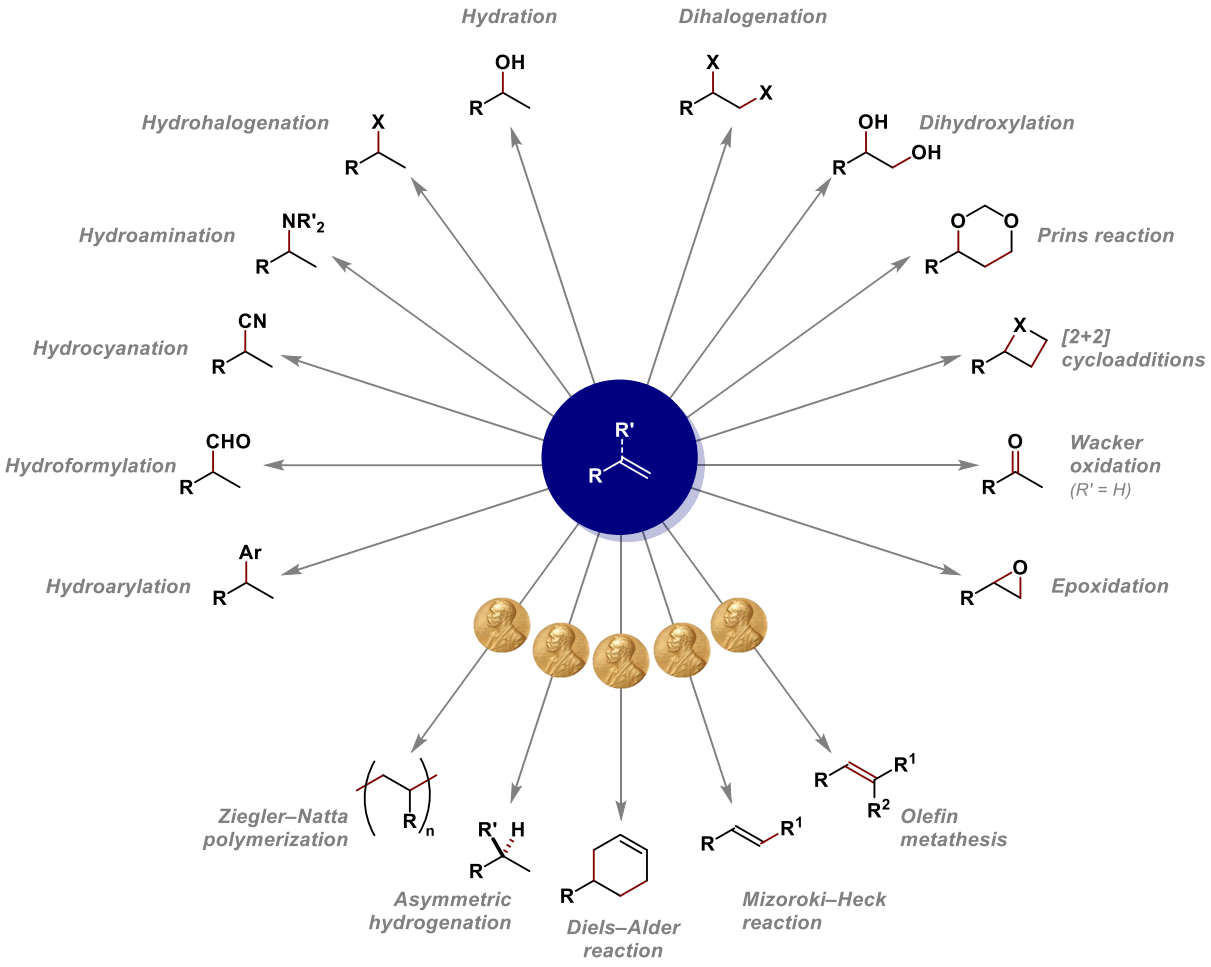

Scheme 2.12. Olefins as versatile starting materials for multiple organic transformations.

2.3.2 Formaldehyde: A Challenging, Small, Unbiased Electrophile

Formaldehyde, first identified in 1855 by the Russian scientist Alexander Butlerow, is the simplest of the aldehydes, and probably the most useful one-carbon (C_1) electrophile in organic synthesis.[98] However, the symmetric structure of formaldehyde and its high reactivity make it also one of the most challenging aldehydes to control in asymmetric catalysis.[99] It has been detected in interstellar space[100] and it is also considered to have played a key role in the origin and evolution of life on our planet.[101] Formaldehyde also represents one of the most important raw materials in chemical industry, mostly for the production of resins (phenol-formaldehyde, urea-formaldehyde, and melamine-formaldehyde), and is produced industrially from methanol (generally using a silver catalyst, air as the oxidant, and at high reaction temperatures).[102] From a structural point of view, similarly to all the other carbonyl compounds, the difference in electronegativity causes the C=O bond in formaldehyde to be polarized, which translates into the carbon atom acting as a Lewis acid and the oxygen atom acting as a Lewis base (Figure 2.11). In addition, the absence of substituents attached to the carbonyl group renders formaldehyde particularly electrophilic.

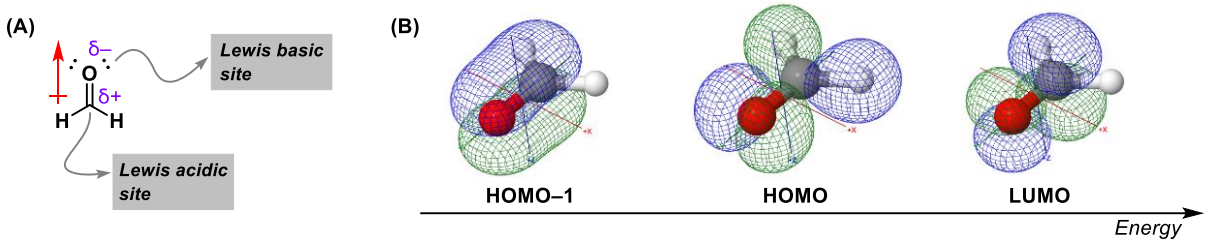

Figure 2.11. (A) Structural features of formaldehyde, (B) frontier molecular orbitals of formaldehyde.[103]

HIGH REACTIVITY OF FORMALDEHYDE: UTILITY *AND* TOXICITY

Because of its special structural features, it is not surprising that a plethora of nucleophiles readily add to formaldehyde, such as enolizable aldehydes/ketones, enolate equivalents, amines, water/alcohols, aromatic rings, and alkenes, to just name a few. Formaldehyde is then frequently used as a C1 electrophile in several C–C bond-forming transformations, such as the *Mannich reaction* and the *Eschenmoser methylenation*, *aldol reaction*, *Biginelli reaction*,[104] *Ugi reaction*,[105] *Blanc chloromethylation*,[106] and the *Prins reaction*, among others (Scheme 2.13).[107]

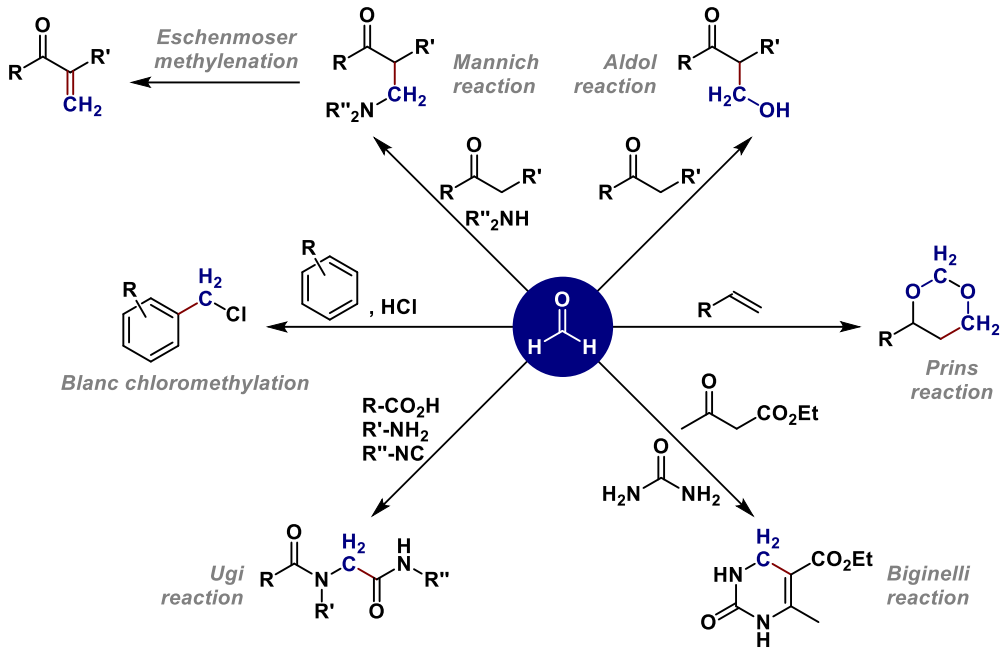

Scheme 2.13. Some C–C bond-forming reactions using formaldehyde.

This reactive versatility accounts not only for the widespread use of formaldehyde in synthesis, but also for its toxicity, known since the beginning of the 20th century[108] and for which it has been classified by several health organizations as "*known to be a human carcinogen*".[109] Living organisms possess several pathways for the metabolism of formaldehyde (also called "formaldehyde detoxification"), such as: *(i)* the glutathione pathway, and *(ii)* the tetrahydrofolate pathway (Scheme 2.14). The glutathione pathway involves the reaction of a thiol group from glutathione (GSH) with formaldehyde to produce the corresponding hemithioformal (*S*-hydroxymethylglutathione, HMG), followed by alcohol dehydrogenase-catalyzed oxidation to form *S*-formylglutathione, which releases formate upon hydrolysis.[110] The tetrahydrofolate pathway consists of the capture of formaldehyde by two secondary amino groups from tetrahydrofolate (H_4F) to produce the corresponding aminal (5,10-CH_2-H_4F), which then reacts with glycine to produce serine, thus entering the so-called *serine cycle*.[111]

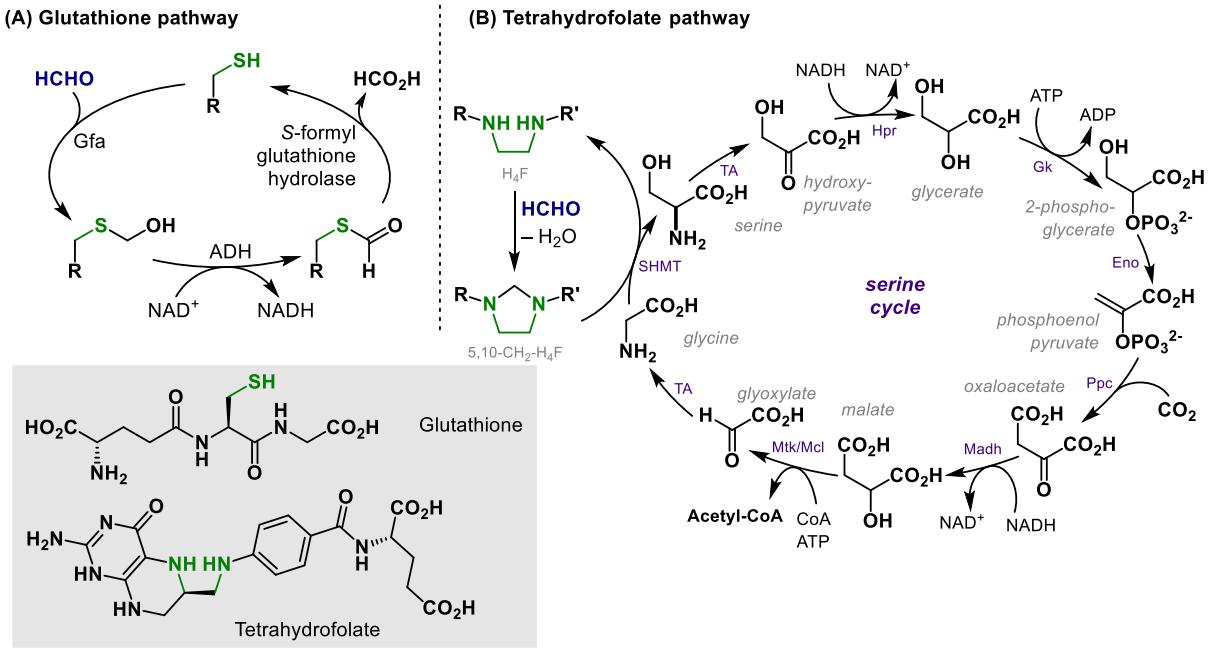

Scheme 2.14. Main pathways for the detoxification of formaldehyde: (A) Glutathione pathway, (B) Tetrahydrofolate pathway.

SMHT: serine hydroxymethyltransferase, TA: transaminase, Hpr: hydroxypyruvate reductase, Gk: glycerate kinase, Eno: enolase, Ppc: phosphoenolpyruvate carboxylase, Madh: malate dehydrogenase, Mtk: malate thiokinase, Mcl: malyl-CoA lyase.

TRIMER, OLIGOMERS AND THE MONOMER: THE MANY FACES OF FORMALDEHYDE

Another consequence of the high reactivity of formaldehyde can be evidenced in the fact that the "monomeric HCHO" tends to react with itself forming oligomers. As a liquid or a gas (boiling point = –19 °C), formaldehyde readily polymerizes at low and ambient temperatures below 80 °C), so formaldehyde gas must be stored at 100–150 °C to prevent polymerization. Therefore, formaldehyde is commonly sold in several oligomeric/polymeric forms (Figure 2.12), such as:

Formalin: aqueous solution of HCHO (~ 37% *w/w*), normally with methanol (up to 10–12%) as an additive to prevent oxidation and polymerization. In aqueous formaldehyde solutions, the main species present is usually methylene glycol ($CH_2(OH)_2$, formaldehyde monohydrate), coexisting with oligomers.[112]

1,3,5-Trioxane: also called *sym*-trioxane, is a stable cyclic trimer of formaldehyde, used as a precursor in the preparation of polyoxymethylene plastics. Like most acetals, trioxane can be hydrolyzed under acidic conditions to generate monomeric formaldehyde, which readily polymerizes and produces high-molecular-weight poly(oxymethylenes). Trioxane is prepared by the trimerization of formaldehyde (world production in 2015: 1.4 x 10^6 ton/year): previous methods involved heating paraformaldehyde/polyoxymethylenes with acid, whereas the

currently used production method is based on the acid-catalyzed trimerization from highly concentrated aqueous formaldehyde solutions (60–65 % *w/w*) and subsequent extraction with CH_2Cl_2.[102]

Paraformaldehyde: a polymeric, crystalline solid, consisting of a mixture of poly(oxymethylene)glycols HO–$(CH_2O)_n$–H with n = 8–100. It is considered the smallest linear polyoxymethylene due to the relatively low degree of polymerization.[102] Paraformaldehyde tends to precipitate out of highly concentrated aqueous formaldehyde solutions, especially at low temperatures; therefore, this polymer is ordinarily prepared by evaporating aqueous solutions of formaldehyde under vacuum to the point at which precipitation of the polymer occurs upon cooling.[113] Paraformaldehyde-d_2 is also commercially available, which is prepared from methylene dihalides (CH_2Br_2 or CH_2I_2) by base-mediated exchange with D_2O to give the deuterated dihalides (CD_2X_2), followed by formation of the deuterated diacetate ($CD_2(OAc)_2$) and subsequent acidic hydrolysis/polymerization.[114] Paraformaldehyde, as well as its deuterated analogue, is poorly soluble in water and in organic solvents, and only moderately soluble in hot water. Conversely, it dissolves very well in alkaline solutions, and this property has been utilized greatly to prepare methanol-free formaldehyde solutions, particularly useful for studies with biological samples and microscopy applications.

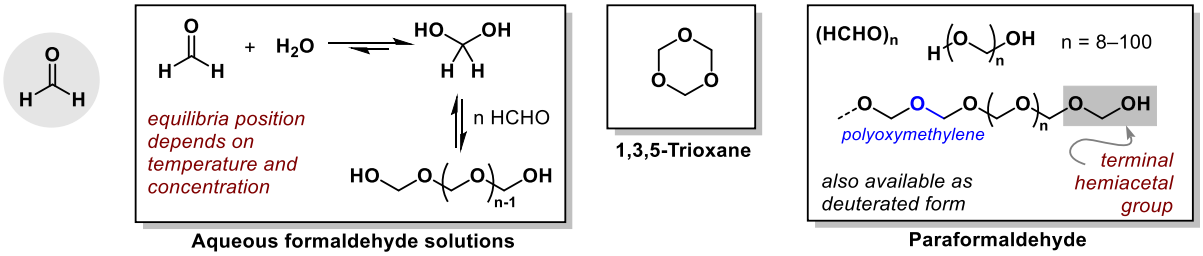

Figure 2.12. Commercial presentations of formaldehyde.

Polyoxymethylenes (POM): Since the 1920s, several studies on the physical properties of polymeric formaldehyde chains with higher degrees of polymerization indicated their potential as useful plastics; however, these polyoxymethylenes were not stable enough at common plastic processing temperatures (Scheme 2.15).[115] In 1956, a team from DuPont reported the improved stability when the terminal hemiacetal groups (–OH) are “capped” as acetates (–OAc), which led to the construction of a production plant (capacity: 7000 ton/year) of the polymer introduced as “Delrin”.[116] The introduction of this homopolymer in the market was followed by the development of a thermally stable acetal copolymer, formed from trioxane and cyclic ethers/acetals. The homopolymers (POM-H) are produced by anionic polymerization of formaldehyde, for which a monomeric starting material with high purity is required. The

monomeric formaldehyde undergoes anionic polymerization with the aid of a nucleophilic additive: amines, alkoxides, phosphines and arsines, among others, have proven to be suitable initiators for this process.[117]

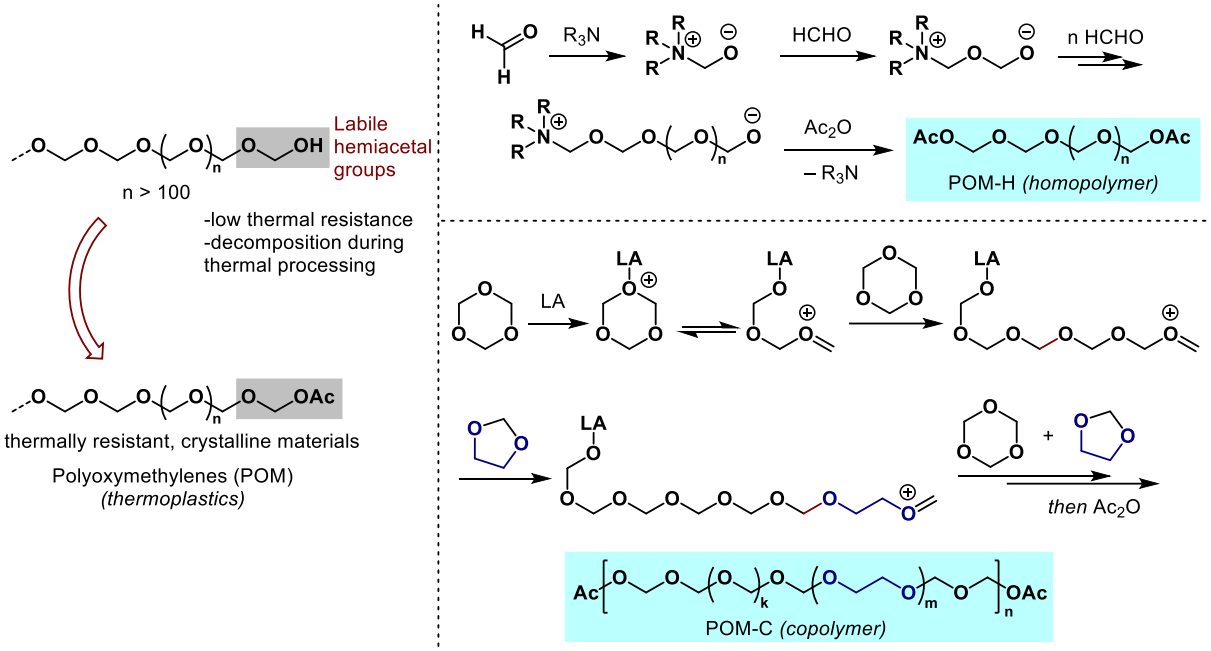

Scheme 2.15. Polyoxymethylenes: anionic homopolymerization and cationic copolymerization.

For the copolymer (POM-C), trioxane is used as starting material and the polymerization takes place using an acid catalyst (commonly $BF_3{\cdot}OEt_2$) and adding a comonomer, such as dioxolane or ethylene oxide, to replace some $–OCH_2–$ groups for $–OCH_2CH_2–$ groups.[118] Following on the idea of capping the terminal hemiacetal groups of polyoxymethylene chains, in the last decades there has been an increasing interest in oligomeric polyoxymethylene dimethyl ethers (PODEs, DMMs or POMDMEs), with formula $MeO–(CH_2O)_n–Me$, $n \geq 2$.[119] Particularly, the POMDMEs within n = 2–4 have been studied as potential diesel substitutes.[120]

Monomeric formaldehyde: Monomeric formaldehyde can be obtained by thermal cracking of paraformaldehyde, as the method reported by Schlosser, where paraformaldehyde is treated with a Lewis acid ($BF_3{\cdot}OEt_2$ or Ts_2O) in THF and, with gentle heating, formaldehyde is co-distilled.[121] Yamamoto[122] and Onaka[123] have reported the stabilization of monomeric formaldehyde using sterically constrained aluminum complexes or zeolites, respectively, where the complexed monomer readily engages in carbonyl-ene reactions with olefins. Monomeric formaldehyde of high purity is obtained via the cyclohexanol hemiformal (absorption in CyOH, separation and thermal cracking).

2.4 The Prins Reaction

The addition of olefins to aldehydes or ketones in the presence of Brønsted acids is usually called the *Prins reaction*. A simplified reaction mechanism includes the nucleophilic attack of the olefin (**2.M1**) to the activated carbonyl compound (carbonylonium ion, **2.M2**) to produce a γ-hydroxycarbenium ion (**2.M3**), whose fate determines the type of product that will be obtained (Scheme 2.16). This cation can *(i)* cyclize to produce an oxetane (**2.M4**), *(ii)* react with a second molecule of carbonyl compound to produce a cationic hemiacetal, which readily cyclizes to produce a 1,3-dioxane derivative (**2.M5**), *(iii)* be trapped by a molecule of water to produce a 1,3-glycol (**2.M6**), *(iv)* be trapped by another nucleophile to produce a γ-functionalized alcohol (**2.M7**), or *(v)* undergo deprotonation to produce an allylic or homoallylic alcohol (**2.M8** and **2.M9**) The homoallylic alcohol can further react with the carbonyl compound to produce another carbonylonium ion (**2.M10**), which undergoes an intramolecular Prins reaction (known as the *Prins cyclization*) to generate a carbenium ion (**2.M11**), which can undergo a similar fate to the γ-hydroxycarbenium ion **2.M3** (trapping with water or a nucleophile, or deprotonation), producing dihydropyrans and tetrahydropyrans.

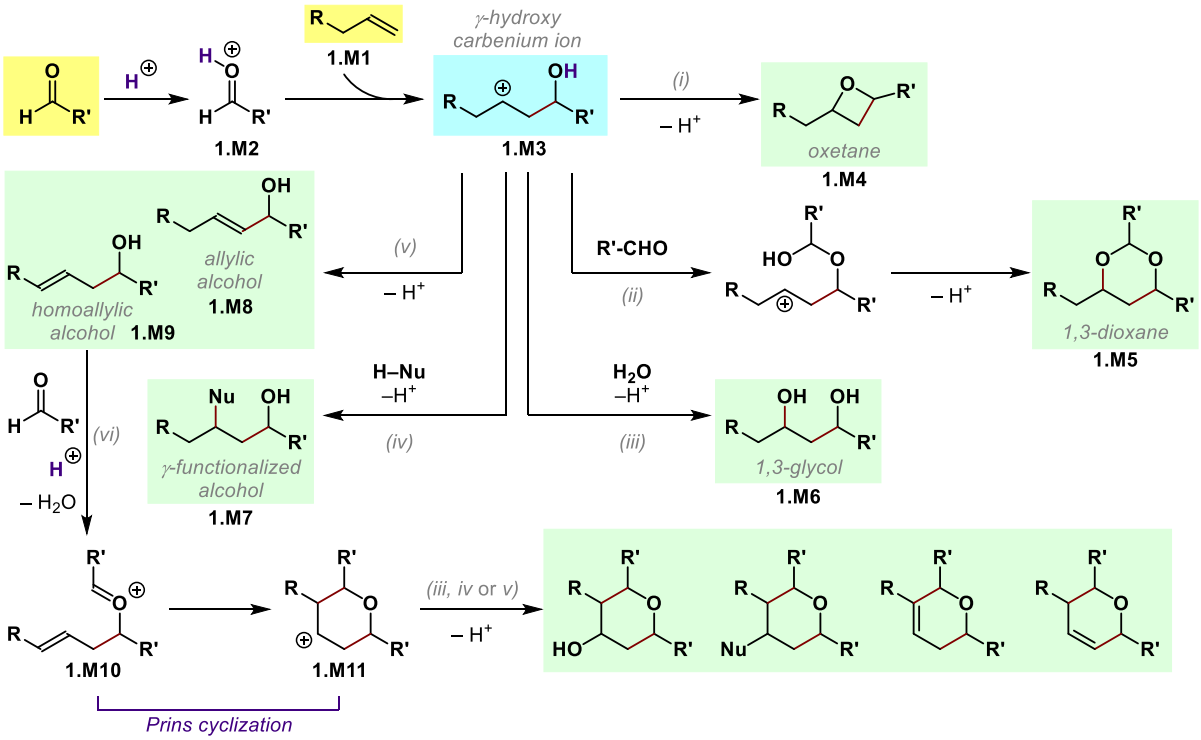

Scheme 2.16. The Prins reaction: one reaction, many possible products.

It is worth to mention that the potential formation of homoallylic alcohols resembles a carbonyl-ene reaction, with the difference between both reactions depending on whether the reaction mechanism is concerted (*carbonyl-ene*) or rather stepwise (*Prins*). It is therefore not unusual to find reports in literature muddling the names of these two transformations.

The complexity of the reaction mixtures that are commonly obtained in the acid-catalyzed reactions of carbonyl compounds and olefins can be evidenced with the outcome of the reaction between cyclohexene (**2.5**) and paraformaldehyde, in acetic acid, in the presence of sulfuric acid (Scheme 2.17).[124] These studies were conducted in the 1940s and 1960s, and the structure elucidation techniques were not as advanced as the currently available ones, so there were different proposed structures for the isolated products, but one thing was clear: the reaction mixtures were quite complex. Additionally, other side reactions may complicate the outcome of the reaction, such as the polymerization of the olefin in the presence of the acidic catalyst.

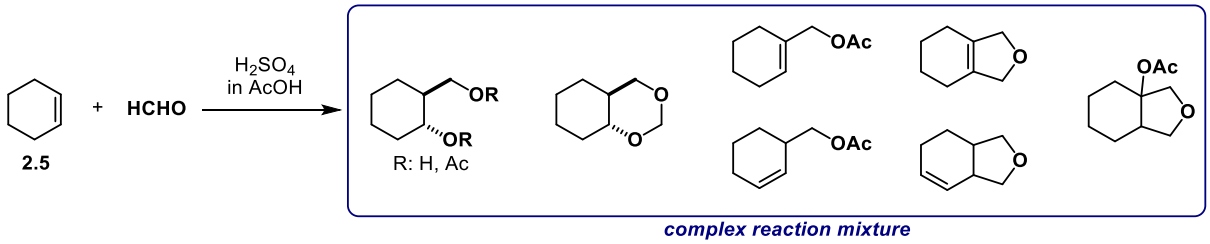

Scheme 2.17. Reported products for the acid-catalyzed reaction of cyclohexene and paraformaldehyde.

2.4.1 Historical Development

In 1899, Kriewitz reported the formation of unsaturated alcohols when a mixture of pinene and paraformaldehyde was heated, although without any explanation of the observations nor any structural formula of the obtained products (now we know that the product formed is nopol, a fragrance material).[125] It was not until the time between 1917 and 1919 that the Dutch chemist H. J. Prins performed a comprehensive study of this type of transformation, which led to a series of reports on the reaction of several olefins (styrene, anethole, isosafrol, α-pinene, D-limonene, and camphene) with formaldehyde in the presence of sulfuric acid.[126] Despite the lack of current analytical techniques, Prins could determine that formation of new C–C bonds took place in all cases. However, depending on the reaction conditions, especially on the solvent (either water or acetic acid), 1,3-glycols (or their acetates) and the corresponding formals, as well as unsaturated alcohols could be obtained. Interestingly, Prins proposed two isomeric structures for each glycol/formal, depending on the regioselectivity of the nucleophilic attack of the olefin to the aldehyde; however, for the reaction with styrene, he claimed that the products should be derivatives of 2-phenylpropane-1,3-diol. In 1930, Fourneau, Benoit and Firmenich proved though that those products presented a different connectivity, namely as derivatives of the isomeric 1-phenylpropane-1,3-diol (Scheme 2.18).[127]

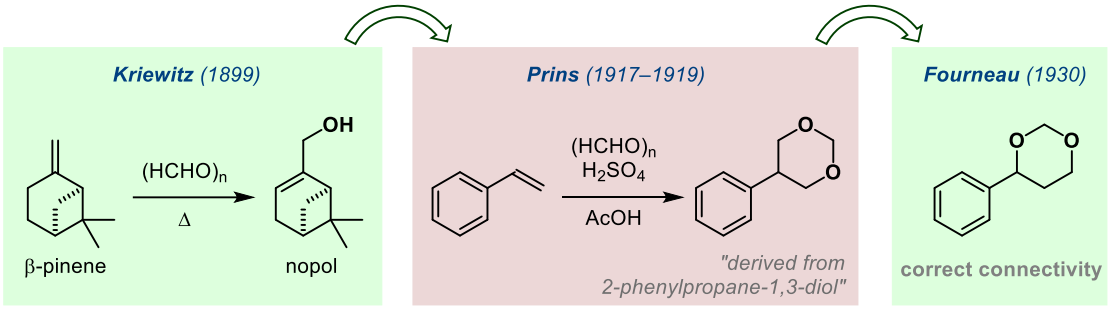

Scheme 2.18. From Kriewitz to Prins: historical development of the Prins reaction.

From the early years of the transformation, it was clear that many products could be formed, and that fine-tuning of the reaction conditions was necessary to control this product selectivity. In the following decades, great efforts were made to optimize the reaction conditions (solvent, temperature, catalyst type and concentration, stoichiometry, among others) for many types of olefins in order to favor the formation of one product.[128]

Particularly in the 1960s there were also a good amount of reports on mechanistic studies for the Prins reaction.[129] The main strategy to gather information relied on the determination of the relative configuration of the obtained products from the sulfuric acid-catalyzed reaction of internal olefins (both alkyl- and aryl olefins) with formaldehyde in protic solvents (water or acetic acid). However, in many cases the results proved to be very sensitive to the utilized reaction conditions, and the presence of side reactions (olefin hydration or polymerization) also generated reproducibility issues between different researchers. Nevertheless, a general trend settled in for the addition of formaldehyde and water to olefins: alkyl olefins seemed to undergo a *trans*-addition, whereas the Prins products from aryl olefins indicated rather a *cis*-addition. Several possible explanations were proposed (Scheme 2.19): *(i)* the intermediacy of a cyclic carbonium ion (in equilibrium with a protonated oxetane), forcing water to effect the nucleophilic attack from the opposite face (*trans*-addition, toward 1,3-glycol),[129c, 129e] or *(ii)* the intermediacy of a formaldehyde dimer, where two formaldehyde units add to the same face of the olefin (*cis*-addition, toward 1,3-dioxane).[129f]

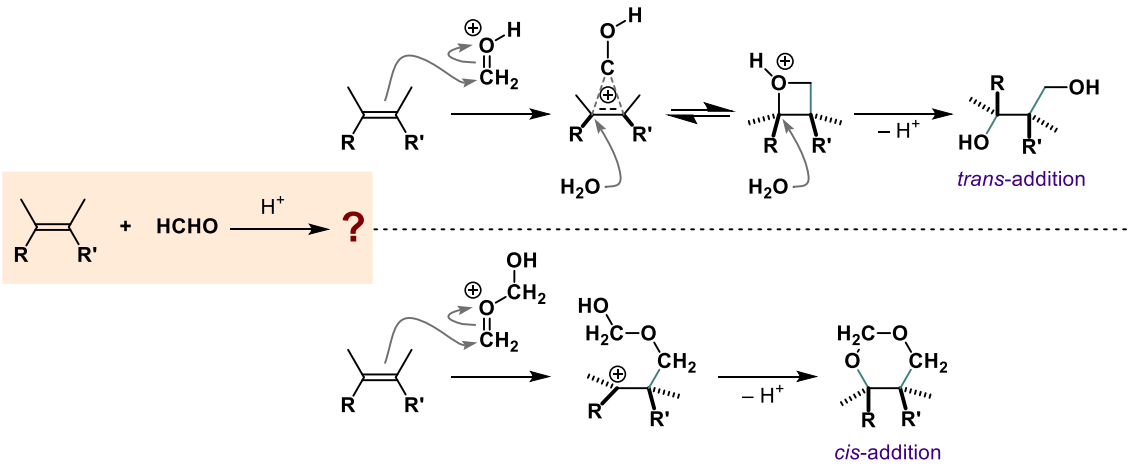

Scheme 2.19. Proposed operating pathways (from the 1960s) for the Prins reaction of internal olefins with formaldehyde: *cis*- or *trans*-addition?

Considering all these studies, it is therefore not surprising that a great amount of information is now available for this reaction, and it has been summarized in several reviews.[9, 128, 130] Further work on the reaction of olefins and carbonylonium ions has been conducted, mostly from two approaches: *(i)* as the intermolecular reaction of olefins and aldehydes, or *(ii)* as the intramolecular reaction of olefin-tethered carbonylonium ions, originated from alkenols and aldehydes (the so-called *Prins cyclization*). These two classes of Prins reactions have also been extended to other subclasses, such as the Prins-pinacol rearrangement[131] or the Prins–Ritter reaction,[132] among others. Although these variants of the "Prins chemistry" have also proven to be synthetically useful, the next part will focus the discussion on the *intermolecular Prins reaction*.

2.4.2 The Intermolecular Prins Reaction

Due to the low nucleophilicity of olefins, most of the work on intermolecular Prins reactions has involved highly electrophilic carbonyl compounds, with the majority of reports using formaldehyde as electrophile. Some few examples of Prins reactions using less activated aldehydes will also be presented.

FORMALDEHYDE

The reaction of simple olefins react with formaldehyde usually affords 1,3-glycols and 1,3-dioxanes as major products, with minor amounts of monoalcohols. In addition to the reports from the first half of the 20th century using H_2SO_4, a variety of acids have been employed as catalysts, like hydrochloric acid, phosphoric acid, *p*-toluenesulfonic acid, and aqueous solutions of BF_3 or $ZnCl_2$,[133] although dilute sulfuric acid was in most cases the most efficient catalyst for the synthesis of 1,3-dioxanes. Also the reaction temperature seemed to play a

critical role for the dioxane/glycol selectivity.[134] The Prins products could also be further transformed to produce conjugated dienes. For example, the Prins reaction/pyrolysis sequence depicted in Scheme 2.20 transforms isobutylene (**2.6**) into isoprene (**2.7**), an important starting material for the rubber industry.[135]

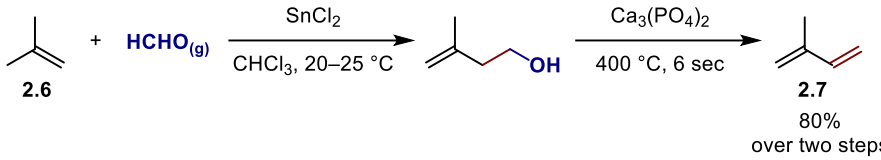

Scheme 2.20. From isobutylene to isoprene: Prins reaction and dehydrative pyrolysis.

As can be seen in Scheme 2.21, the use of Brønsted acids reveals a striking difference in the behavior of aryl and alkyl olefins. Du reported the use of trifluoromethanesulfonic acid (TfOH) as catalyst for the Prins reaction of styrenes with aqueous formaldehyde, with a scope including terminal styrenes both with EDG and EWG, and also the more challenging β-substituted and β,β-disubstituted styrenes; α-methylstyrene resulted in sluggish mixtures due to side reactions.[136] Yang found a similar trend when utilizing dodecylbenzenesulfonic acid (DBSA) as catalyst for the reaction in aqueous media, although in that case α-substituted styrenes provided the desired 1,3-dioxanes in good yield.[137] In the presence of stoichiometric amounts of hydrogen halides, terminal alkyl olefins react with formaldehyde (as paraformaldehyde or formalin) to produce 3-alkyl-4-halotetrahydropyrans **2.8**,[138] and a similar type of product was found when trifluoroacetic acid was used both as solvent and also to replace the hydrogen halide;[139] however, if dilute sulfuric acid and formalin are used, the main product are 3-alkyltetrahydropyran-4-ols **2.9** and 4-alkyl-1,3-dioxanes **2.10**.[140] Also Wells–Dawson-type molybdovanadophosphoric heteropolyacids could catalyze the reaction of both aryl and terminal alkyl olefins with paraformaldehyde, affording with good product selectivity the corresponding 1,3-dioxanes **2.11**.[141]

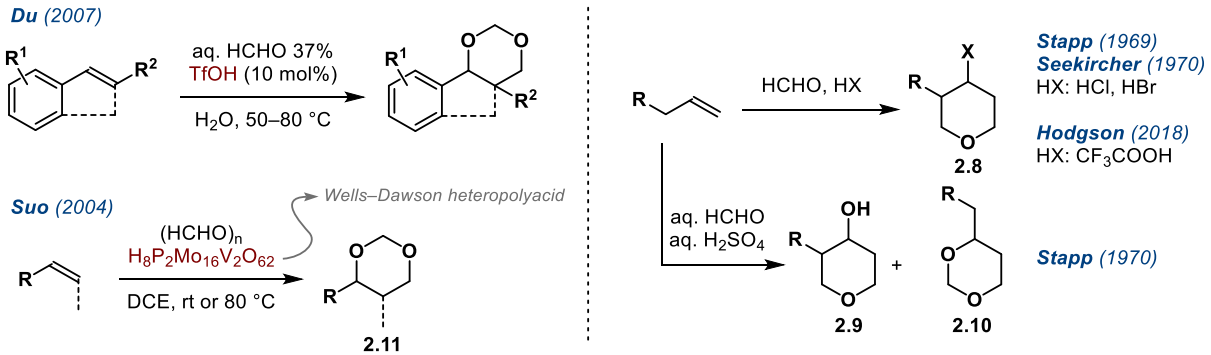

Scheme 2.21. Prins reaction: olefins and formaldehyde in the presence of Brønsted acids.

Lewis acids have also been introduced as suitable catalysts for Prins reactions (Scheme 2.22). For example, in 2002 Bach reported a sterically-hindered aryloxy-difluoroborane **2.12** as highly selective catalyst for the synthesis of 1,3-dioxanes from aryl olefins and paraformaldehyde.[142]

As reported by Yadav, the combination of $InBr_3$ as catalyst and an ionic liquid as solvent allowed not only the conversion of styrenes under mild conditions (room temperature), but also terminal alkyl olefins reacted at 90 °C.[143] Other Lewis acids, such as $Bi(OTf)_3$ or the highly fluorous $Hf(N(n\text{-}C_8F_{17})_2)_4$, have also proven to efficiently convert aryl olefins and formaldehyde to 1,3-dioxanes; given the high fluorine content of the latter Lewis acid, the reaction could be performed in a fluorous biphasic system, facilitating the purification of the products and catalyst recovery (solvent mixture: DCE and GALDEN® SV 135, which is a mixture of perfluoropolyethers).[144] According to the report of Yadav, stoichiometric amounts of iodine (I_2) can also accelerate Prins reactions of both aryl and terminal alkyl olefins with paraformaldehyde.[145]

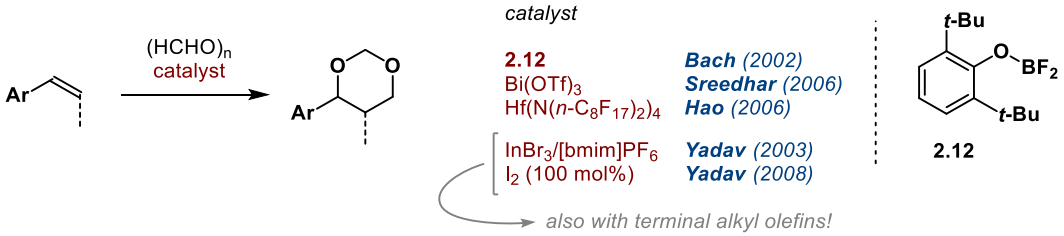

Scheme 2.22. Prins reaction: olefins and formaldehyde in the presence of Lewis acids.

In the last years there has been an increasing interest in the application of ionic liquids in catalysis, and this trend has also had some contributions to the development of the intermolecular Prins reaction (Scheme 2.23). Several ionic liquids containing Brønsted acidic moieties have shown satisfactory performance accelerating Prins reactions of aryl olefins and formaldehyde.[146] Also several heterogeneous catalysts have been applied to the Prins reaction.[147] In this regard, along with the reported catalytic activity from solid-supported acids, such as acidic ion exchange resins,[148] silica-supported Lewis acids[149] or silica-supported Brønsted acids,[150] there are also several reports on zeolite-catalyzed Prins reactions.[151]

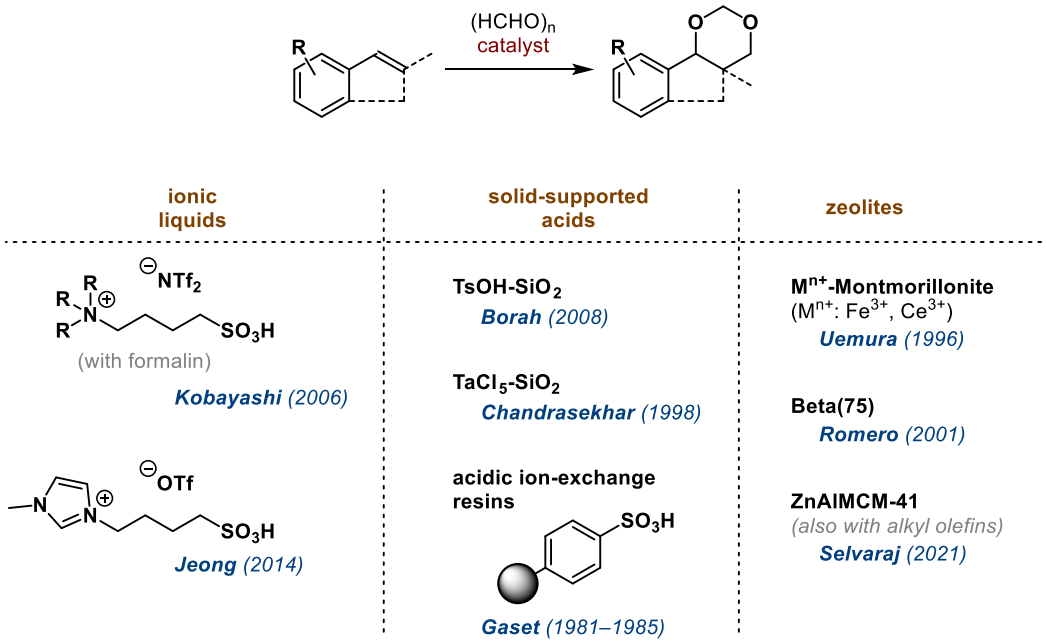

Scheme 2.23. Prins reaction: ionic liquids, solid-supported acids or zeolites as catalysts.

In the 1970s, the Prins reaction proved to be an efficient approach toward the synthesis of bicyclic lactones, which could act as precursors for the Corey synthesis of natural prostaglandins and analogues thereof (Scheme 2.24).[152] Peel and Sutherland studied the Prins reaction of norbornadiene **2.13** in formic acid, producing the nortricyclene diformate **2.14**, which was readily transformed into bicyclic lactone **2.15**.[153] A couple of years later, Kovács reported the regiospecific Prins reaction of unsaturated bicyclic lactone **2.16** with paraformaldehyde in H_2SO_4/AcOH, which led to the *trans*-diacetate **2.17**,[154] and further studies on this type of reactivity were later published.[155]

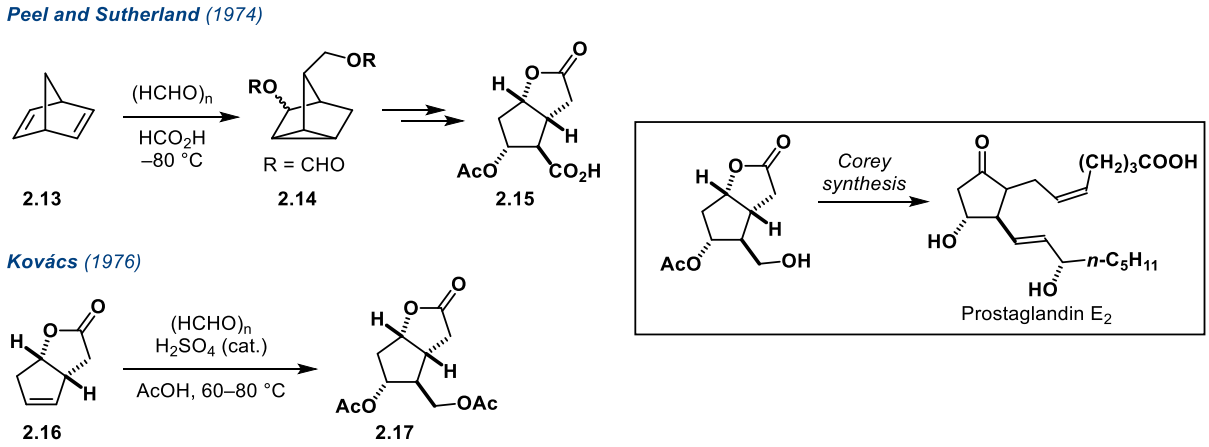

Scheme 2.24. Application of Brønsted acid-catalyzed Prins reactions as entry point for prostaglandin syntheses.

Regarding asymmetric olefin-formaldehyde reactions, Yamamoto reported in 2000 a BINOL-derived formal complexed with $SnCl_4$ (**2.18**), as chiral alkoxymethylating reagent in the acetal-ene reaction with internal alkyl olefins (Scheme 2.25), affording the enantioenriched

homoallylic alcohols.[156] Needless to say, the use of a chiral reagent diminishes the beauty of this approach.

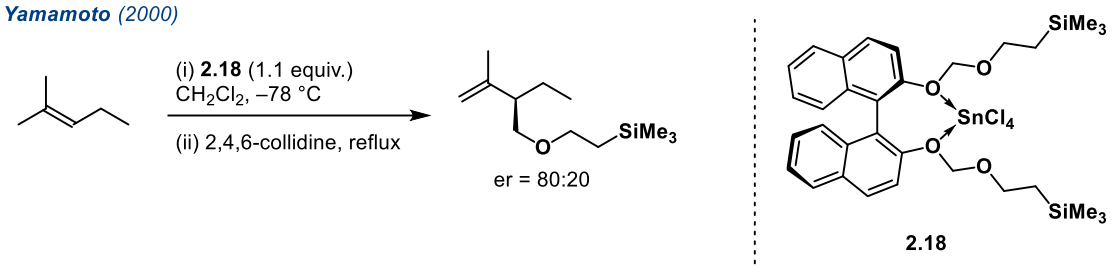

Scheme 2.25. Asymmetric olefin alkoxymethylation using chiral reagent **2.18**.

Remarkably, despite the utility that such a methodology could have in synthesis, no *catalytic*, *asymmetric* version of an *intermolecular* Prins reaction between an olefin and formaldehyde is available so far in literature.

ELECTRON-DEFICIENT ALDEHYDES

Aldehydes containing electron-withdrawing groups attached to the carbonyl functionality are particularly electrophilic, such as trihaloacetaldehydes (fluoral, chloral) and glyoxylates. These aldehydes react with several olefins (both terminal and internal) in a carbonyl-ene fashion to produce the corresponding homoallylic alcohols, as can be seen from the many reports available in literature of thermal or Lewis acid-catalyzed processes.[130a] Unlike formaldehyde, these aldehydes possess enantiotopic faces (*re*/*si*), so that the addition of the olefin (or any nucleophile) results in the creation of (at least) one stereogenic center, and several chiral Lewis acids (metal complexes with chiral ligands, like BOX or BINOL derivatives) have been utilized for the development of asymmetric carbonyl-ene reactions with these highly activated aldehydes.[130b] As previously mentioned, whether these transformations are “true” carbonyl-ene reactions or they rather proceed via a more “Prins-like” pathway, depends on the choice of Lewis acid and the utilized reaction conditions.

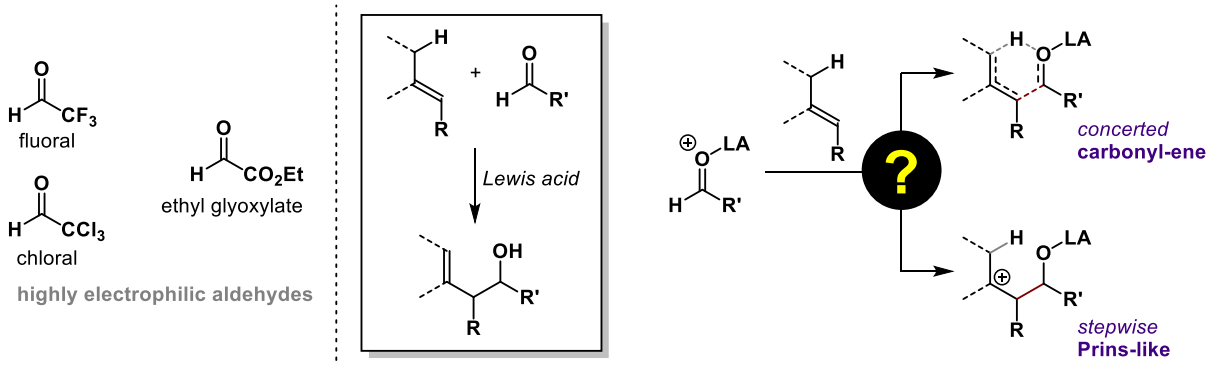

Scheme 2.26. Highly electrophilic aldehydes and their reaction with olefins: carbonyl-ene or Prins-like?

In any case, the presence of allylic hydrogens seems to be a requirement for these activated aldehydes to react with olefins, since there are so far no reports on reactions with olefins without allylic hydrogens, such as styrenes.

OTHER ALDEHYDES

Whereas the formation of 1,3-dioxanes from formaldehyde can give rise to up to two stereocenters, a similar reaction with other aldehydes creates two additional stereocenters, increasing the number of possible diastereomers. As expected, normal aliphatic/aromatic aldehydes are less reactive than formaldehyde, which renders their reaction with olefins more challenging. In the previously mentioned report from Yadav using I_2 in stoichiometric quantities for the Prins reaction of aryl olefins, also some examples with aliphatic aldehydes (acetaldehyde, propionaldehyde and cyclohexanecarbaldehyde) were included, as well as the reaction of 1-octene and acetaldehyde; there is however no comment on the diastereoselectivity of the process.[145] In 2017, Berkessel reported a *catalytic* approach for the Prins reaction of styrenes with acetaldehyde, using molecular iodine in the presence of bis(trifluoromethanesulfonyl)imide salts **2.19**, in addition to some examples with other aliphatic aldehydes; in this case, the reaction occurred with moderate diastereoselectivity.[157] The Prins reaction of α-methylstyrene and acetaldehyde is particularly interesting for the fragrance industry, since the product displays "fruity rhubarb undertones" and is commercialized as racemic mixtures of two diastereomers (**2.20** and **2.21**) under the names *Floropal* (**2.20**: 64%, **2.21**: 34%) and *Vertacetal* (**2.20**: 54%, **2.21**: 44%).[158]

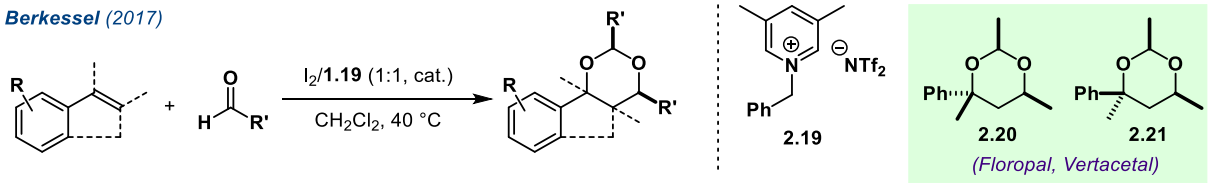

Scheme 2.27. Prins reaction of styrenes and aliphatic aldehydes, and application to the synthesis of Floropal/Vertacetal.

3 Objectives

The goal of this doctoral work is to develop catalytic, enantioselective, intermolecular reactions between simple olefins and carbonyl compounds. The main focus was put on the highly fundamental, yet challenging enantioselective, intermolecular Prins reaction between olefins and formaldehyde, since such a transformation thus far has remained elusive.

Asymmetric additions of strong, activated *C*-nucleophiles to carbonyl compounds (aldehydes or ketones) are now established synthetic methods, either using chiral reagents, chiral auxiliaries, or asymmetric catalysis. Contrarily, *C*-nucleophiles such as olefins or arenes, which are less activated but also much more available, stable and accessible than the above-mentioned activated ones, have remained relatively underexplored in their reactivity toward carbonyl compounds (Scheme 3.1), especially from the point of view of asymmetric variants of these transformations.

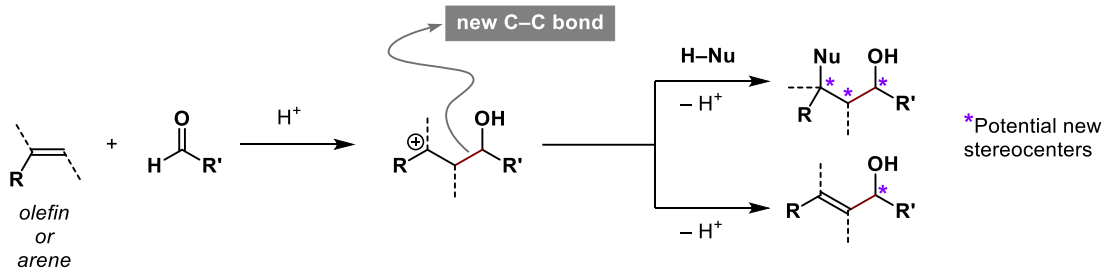

Scheme 3.1. Acid-catalyzed addition of *C*-nucleophiles to carbonyl compounds.

The Prins reaction presents a great synthetic potential due to the utility of the products, since 1,3-dioxygenated patterns are useful building blocks in the pharmaceutical industry and for the preparation of fragrances. In contrast to the significant progress in the development of asymmetric variants for the intramolecular version (Prins cyclization), such advancement for the intermolecular reaction of olefins and aldehydes has remained an unmet challenge. We decided then to embark on this adventure, envisioning that the strong, highly confined Brønsted acids, designed in the last years in the List group, can catalyze and control both the product selectivity and the enantioselectivity on the reaction of olefins and aldehydes (Scheme 3.2), involving small substrates such as formaldehyde.

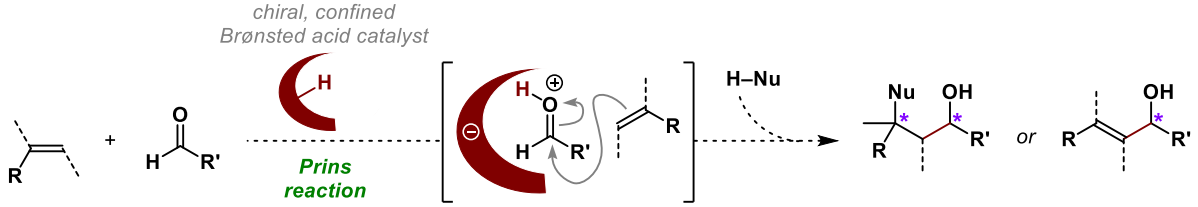

Scheme 3.2. Envisioned asymmetric, intermolecular Prins reaction using a chiral Brønsted acid catalyst.

Page left intentionally blank

4 Results and Discussion

4.1 Reaction Design and Optimization Studies

4.1.1 Preliminary Screenings

We initiated our study on the intermolecular Prins reaction by using styrene **4.1a** and paraformaldehyde **4.2a** as substrates, producing the corresponding 1,3-dioxane **4.3a**. Neither CPA **4.4a**, DSI **4.4b**, nor the more confined IDP **4.4c** showed any conversion (24 h, rt, in CH_2Cl_2), probably because their acidity is not enough to activate **4.2a** sufficiently for the later reaction with **4.1a** (Scheme 4.1).

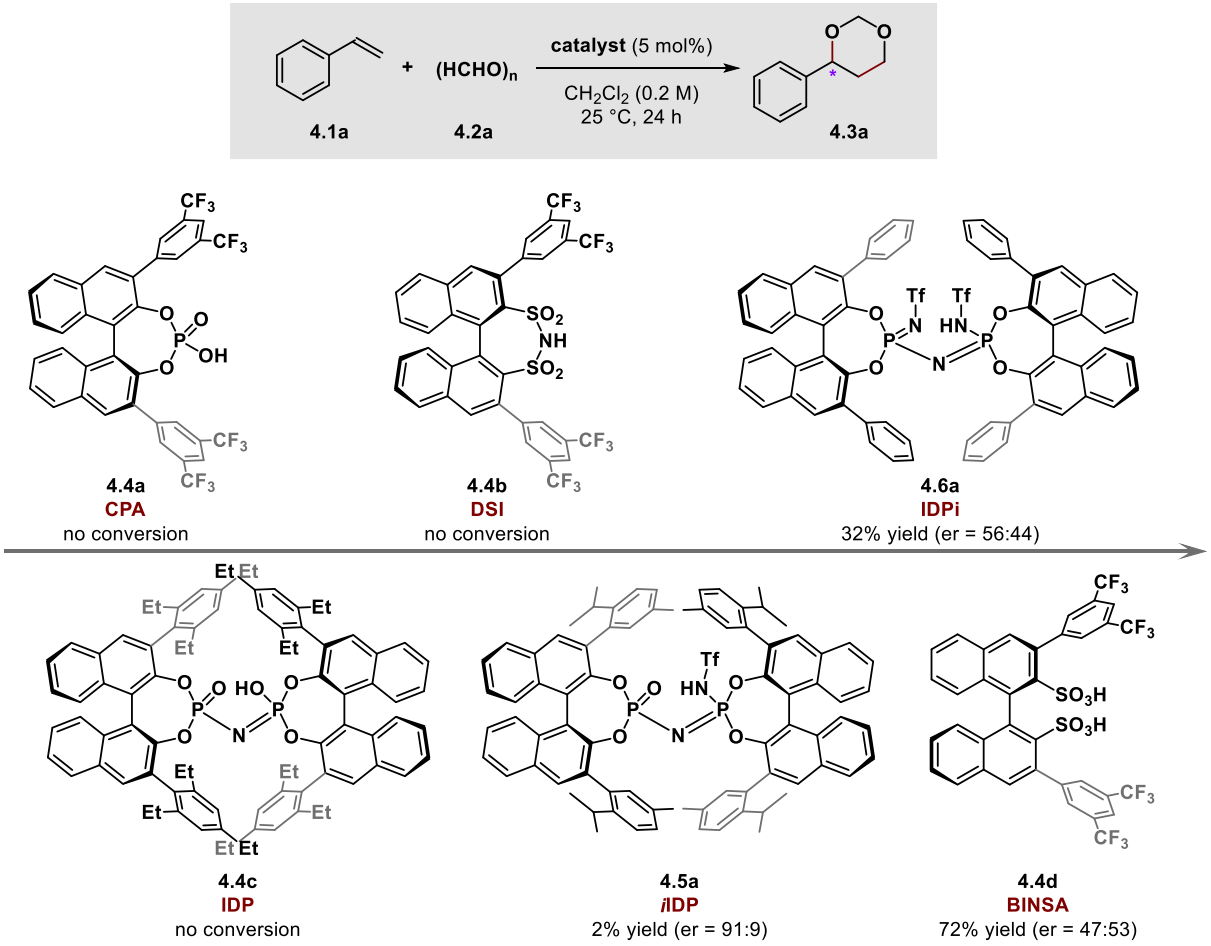

Scheme 4.1. Initial catalyst screening for the Prins reaction of styrene and paraformaldehyde.

The *i*IDP **4.5a** afforded the corresponding 1,3-dioxane product **4.3a** in trace amounts, but with a promising enantiomeric ratio of 91:9. Unfortunately, screening different reaction conditions did not lead to any improved reactivity. Gratifyingly, IDPi **4.6a** afforded **4.3a** with better yield (32%), but with decreased enantioselectivity (er = 56:44, 12% ee).

(*R*)-BINOL-derived disulfonic acid (BINSA) **4.4d** proved to be highly reactive (72% yield), although the product was obtained almost as a racemate (er = 47:53, 6% ee).

Based on these initial promising results, we decided to further explore the IDPi catalyst class, which we considered more tunable, using the 3,3'-positions ("wings", R^W) and the inner sulfonyl group ("core", R^C).

4.1.2 IDPis and Formaldehyde: An Interesting Combination

Using IDPi **4.6a**, a screening of reaction conditions revealed higher enantioinduction with $CHCl_3$ as solvent (21%, 57.5:42.5 er). More striking was the effect of higher temperatures: *changing from 25 °C to 50 °C resulted in* higher yield (from 21% to 71%), but surprisingly also in *a much higher enantiomeric ratio* (79.5:20.5 er). We hypothesized that the higher temperature might crack the polymeric chain of paraformaldehyde, releasing some species that the catalyst can accommodate better in the active site, which could translate into the observed increased enantioselectivity. With these improved reaction conditions ($CHCl_3$, 50 °C), we carried out an extensive screening with the catalysts available at that moment in our laboratory. Switching to aromatic inner cores proved beneficial in terms of enantioselectivity, which led us to IDPi **4.6b**, with an extended aromatic inner core. Using this IDPi, **4.3a** was obtained with high enantioselectivity (92.5:7.5 er) and moderate yield (38%) after 48 h (Scheme 4.2).

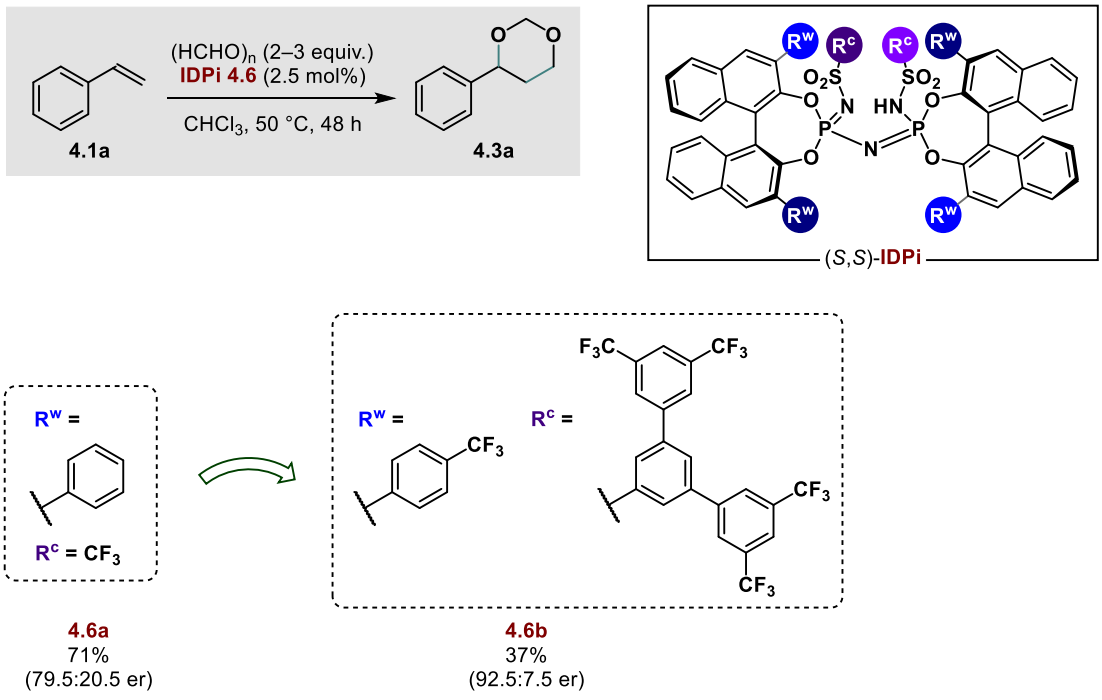

Scheme 4.2. Using IDPis for the model Prins reaction.

We observed nevertheless that full conversion was not achieved and longer reaction times did not result in increased yields. As observed by a kinetic ^{1}H NMR monitoring, the reaction seemed to stop leaving unreacted **4.1a** (Figure 4.1).

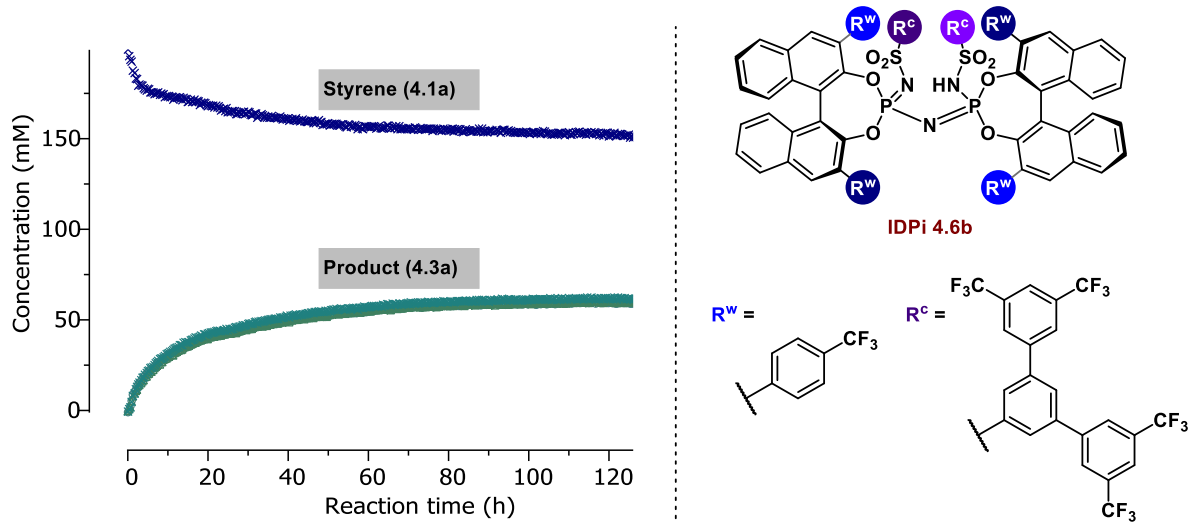

Figure 4.1. ^{1}H NMR monitoring of the model Prins reaction with catalyst **4.6b** (in $CDCl_3$, 50 °C).

Intrigued by these observations, we decided to gain more information about the reaction progress. Reaction mixtures (styrene, paraformaldehyde and **4.6b**, in $CDCl_3$ at 50 °C) were monitored by NMR (^{1}H and ^{31}P) and by MS (ESI) over time, which allowed us to gather the following observations (Figure 4.2 and Figure 4.3):

(a) over time, the intensity of the IDPi ^{31}P NMR signal (singlet at –10 ppm) becomes less intense and, after 24 h, is no longer visible;

(b) along with the mentioned decrease of the IDPi signal, the ^{31}P spectra show the appearance of new signals, namely at –7 ppm (dd) and at 0.5 ppm (singlet);

(c) when the new ^{31}P NMR signals show up, the signals of the 1,3-dioxane product **4.3a** start being visible on ^{1}H NMR;

(d) when the new ^{31}P NMR signals appear, the MS analyses of the crude reaction mixture no longer show signals for the anion of the IDPi (*m/z* 2379.2), but rather two intense signals at lower *m/z* values: 1815.2 and 1252.2.

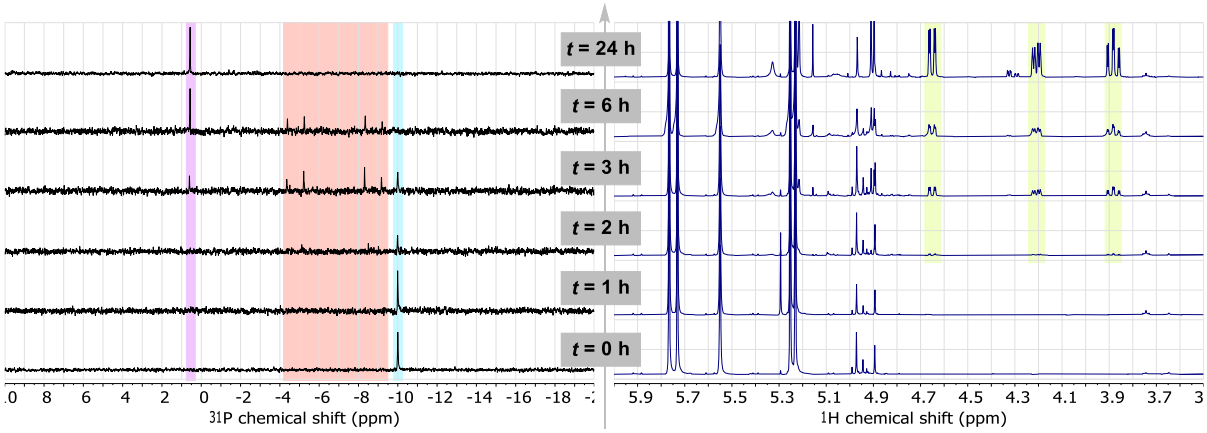

Figure 4.2. NMR monitoring (^{31}P and ^{1}H) of the model Prins reaction with catalyst **4.6b** at 50 °C.

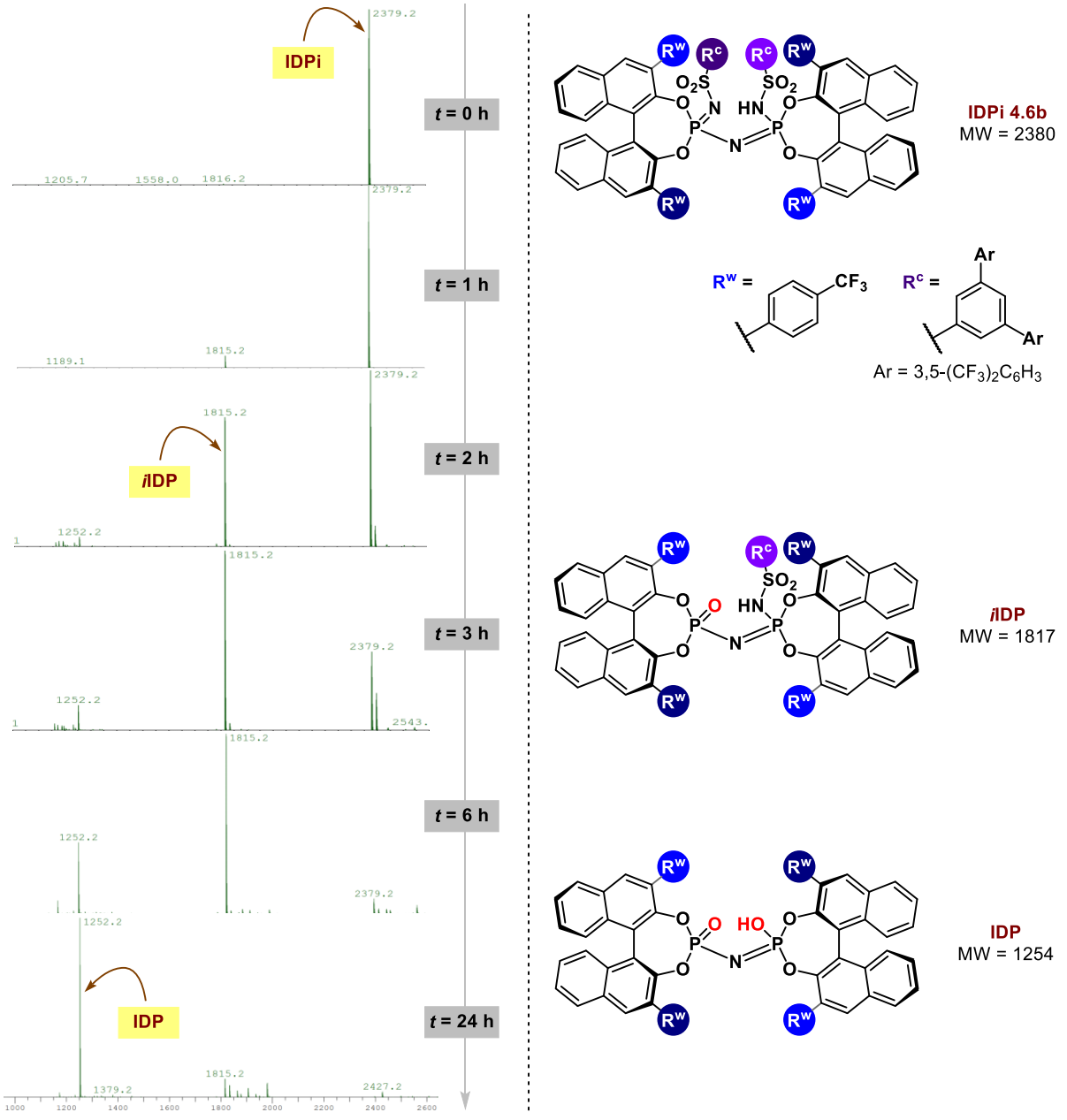

Figure 4.3. MS monitoring of the model Prins reaction with catalyst **4.6b** at 50 °C: proposed species formed in situ by inner core cleavage.

These results indicated that the IDPi catalyst was being transformed during the reaction, forming at least two new phosphorus-containing species. A combined analysis of the observed ^{31}P NMR signals and the *m/z* (and Δ*m/z*) values suggested that these species could arise from stepwise exchange of the arylsulfonylimino core groups by oxygen atoms, which corresponds to the respective *i*IDP and IDP structures (Figure 4.3). Based on their symmetry, these structures should give ^{31}P NMR a doublet of doublets and a singlet, respectively, which matched with the new signals observed in the ^{31}P NMR monitoring.

To elucidate the cause of the observed inner core cleavage on the IDPi structure, we performed several control experiments considering the following possibilities: solvent, temperature, presence of styrene, presence/amount of formaldehyde. (Figure 4.4).

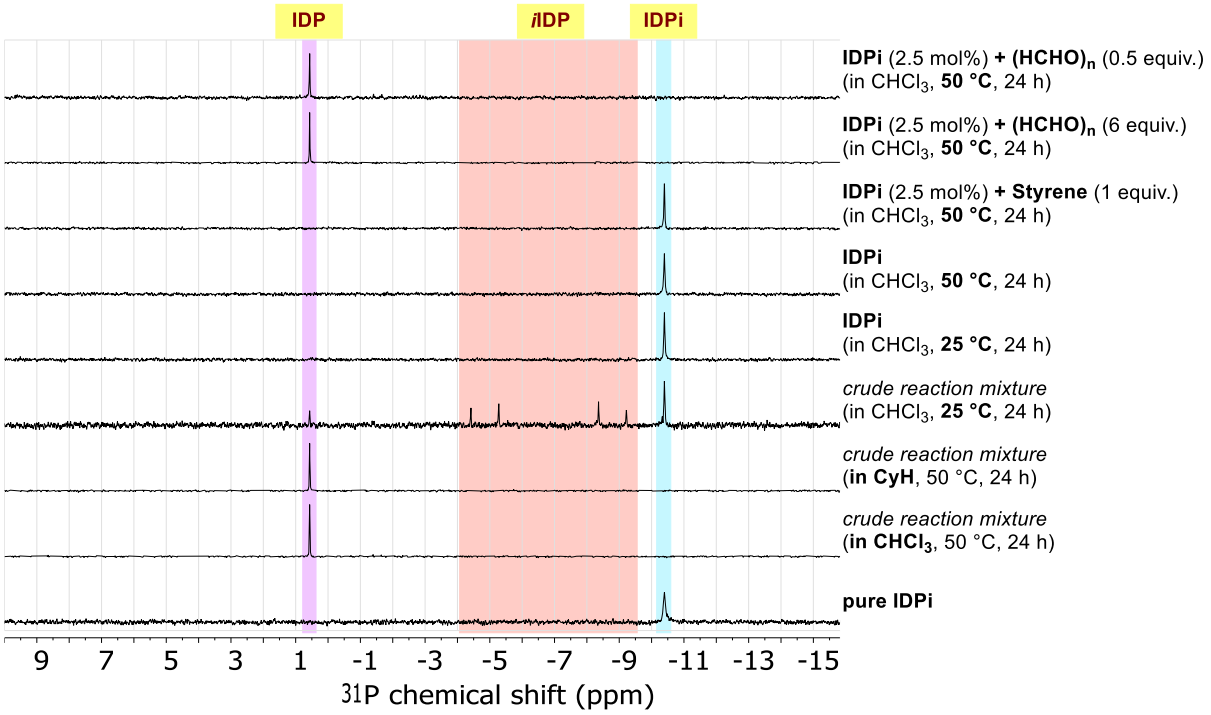

Figure 4.4. ^{31}P NMR spectra of the control experiments to determine the cause of the IDPi inner core cleavage.

The solvent was excluded as possible cleavage cause, since performing the reaction for 24 h at 50 °C resulted in the full inner core cleavage, regardless of whether chloroform or cyclohexane were used as solvents. At lower temperature (25 °C) the degree of inner core cleavage was less pronunciated, but it still took place, as can be seen from the ^{31}P NMR spectrum showing the signal of IDPi as major one, along with the signals of *i*IDP and IDP. The temperature proved not to be a decisive factor for the cleavage though, as the IDPi seemed to have remained unchanged after dissolving it in $CHCl_3$ for 24 h, either at 50 °C or at 25 °C. The presence of styrene also seems not to cause the cleavage, since a mixture of this olefin with a catalytic amount of IDPi at 50 °C did not result in any changes on the ^{31}P NMR spectrum.

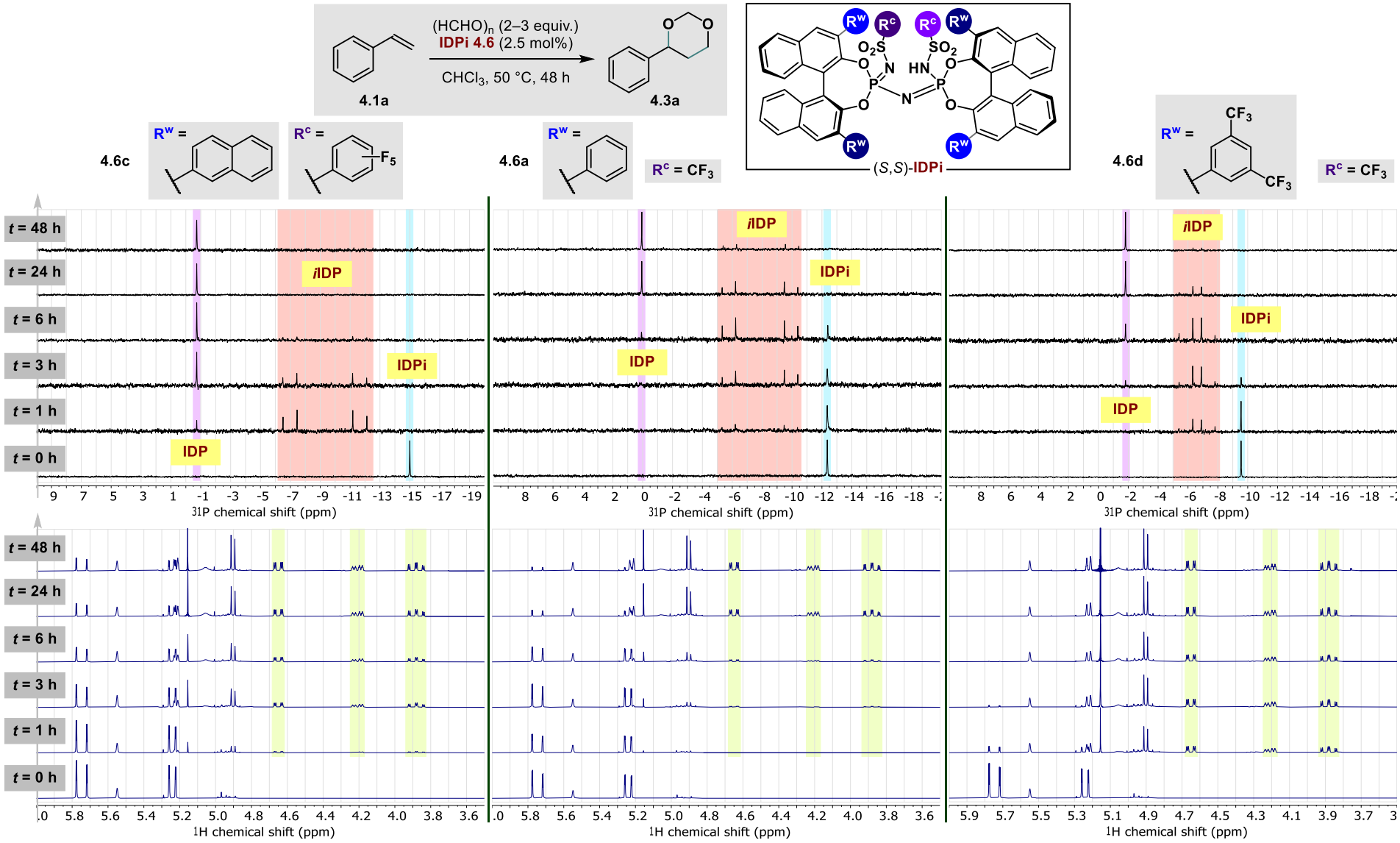

Figure 4.5. NMR monitorings (^{31}P and ^{1}H) for the model Prins reaction with catalysts **4.6c**, **4.6a** and **4.6d**.

Contrarily, mixtures of paraformaldehyde and IDPi (ratio 240:1) at 50 °C prompted full inner core cleavage, even with lower amounts of paraformaldehyde (ratio $(HCHO)_n$/IDPi 20:1). With these results, we can confidently assure that paraformaldehyde is causing the inner core cleavage for IDPi **4.6b**, and this process is accelerated at higher temperatures.

Next, we were curious about whether this formaldehyde-mediated inner core cleavage is an oddity displayed only with IDPi **4.6b** or if other members of this catalyst class undergo a similar process. Therefore, we performed similar NMR/MS monitorings over time for reaction mixtures of **4.1a** and **4.2a** in $CHCl_3$ at 50 °C, using IDPi catalysts **4.6c**, **4.6a**, and **4.6d** (Figure 4.5). The three studied catalysts indeed underwent the same inner core cleavage, although with some differences. For example, catalysts **4.6c** and **4.6b**, containing aromatic inner cores, started showing cleavage signals faster than their counterparts with a triflyl core (**4.6a** and **4.6d**). In addition, from the latter ones, the catalyst containing EWG-substituted wings (**4.6d**) seemed to be more labile toward this cleavage process than the IDPi with unsubstituted phenyl rings as wings **4.6a**.

A potential explanation for these differences can rely on electronic properties. For example, the aromatic sulfonylimino inner cores have weaker electron-withdrawing character and therefore more nucleophilic imino nitrogen atoms than a triflyl core; also, EWG-substituted wings can extend this effect to the phosphorus atoms, rendering it more electrophilic. More investigations are definitely required to gain information on the order of events taking place during this formaldehyde-mediated core cleavage, but we still present a simplified mechanistic proposal in Scheme 4.3, resembling a *metathesis* between the P=N and the C=O moieties.

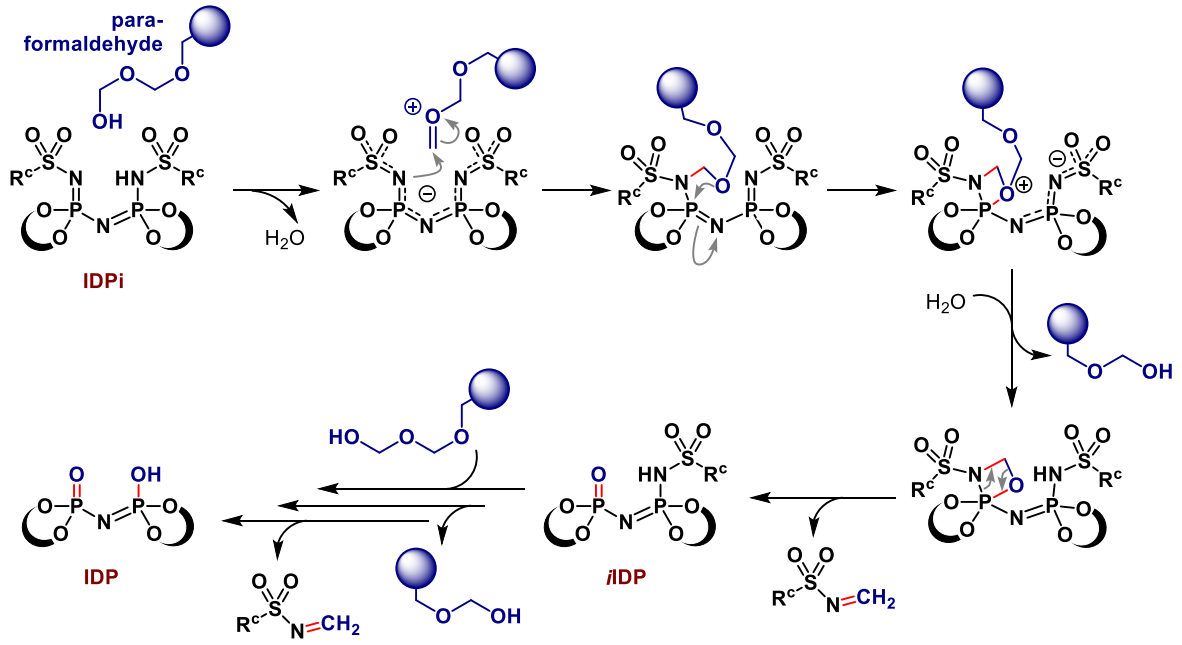

Scheme 4.3. Proposed *metathesis-like* mechanism for the formaldehyde-mediated IDPi inner core cleavage.

4.1.3 *i*IDPs: Fine-Tuning and Catalyst Design

The NMR studies on the formaldehyde-mediated inner core cleavage also revealed that the product from the model Prins reaction (**4.3a**) started forming upon the first core cleavage, namely when *i*IDP was present in the reaction mixture, but the conversion stopped once the second cleavage was completed and only IDP was present in the reaction mixture. This indicated that an intermediate species was the actual catalyst in the reaction, probably the *i*IDP, so we decided to prepare this acid containing 4-trifluoromethyl-phenyl as wing.

The first reported route to prepare *i*IDPs involved the preparation of two BINOL-derived fragments (a phosphoramidite and a phosphoryl azide) and their subsequent coupling via a Staudinger reaction.[59] Fortunately, during the work on the herein presented project, a more efficient and less time-consuming route toward *i*IDPs (and other diphosphate-based acids) was developed, where the hexachlorobisphosphazonium salt **4.7** reacts with a substituted, enantiopure BINOL (obtained by Pd-catalyzed cross-coupling chemistry from suitable coupling partners), a sulfonamide and water, in a one-flask process (Scheme 4.4).[63]

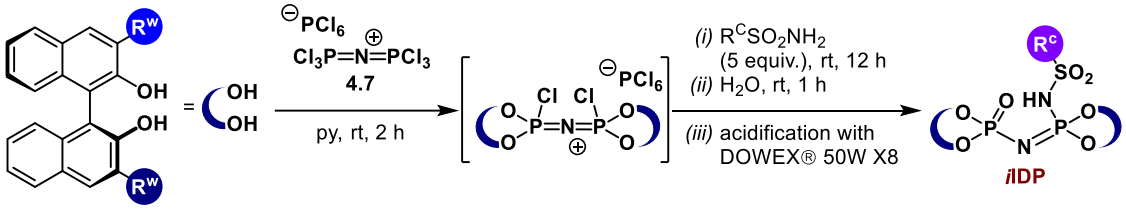

Scheme 4.4. Simplified one-flask synthesis of *i*IDPs.

Catalyst **4.5b** was prepared in this way and tested for the model Prins reaction at 50 °C, although with only 1 equiv. $(HCHO)_n$ to minimize possible core cleavage from *i*IDP to IDP. This experiment produced **4.3a** in 48% yield (relative to styrene; 95% relative to HCHO) and 89:11 er after only 12 h, illustrating the high catalytic activity of this *i*IDP; more importantly, without significant signs of core cleavage. Screening several reaction conditions with catalyst **4.5b** (Table 4.1), it was found that the enantioselectivity increases at lower temperature (25 °C); also, the catalyst tolerates the use of excess $(HCHO)_n$ at room temperature without undergoing significant core cleavage, and a solvent screening showed promising enantioselectivity in cyclohexane or methylcyclohexane.

Table 4.1. Reaction optimization for the model Prins reaction with catalyst **4.5b**.

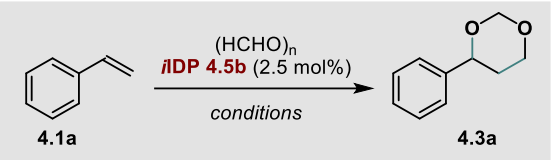

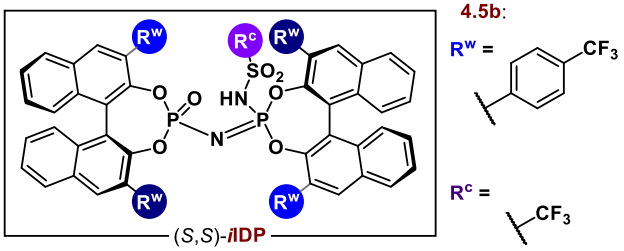

entry	temp. (°C)	equiv. $(HCHO)_n$	solvent	concent. (M)	time (h)	% yield 4.3a	er 4.3a
1	50	1	$CHCl_3$	0.2	12	48	89:11
2	**25**	1	$CHCl_3$	0.2	12	23	92.5:7.5
3	25	**3**	$CHCl_3$	0.2	48	74	91.5:8.5
4	25	3	**CH_2Cl_2**	0.2	48	70	88:12
5	25	3	**PhMe**	0.2	48	61	88:12
6	25	3	**PhH**	0.2	48	50	89.5:10.5
7	25	3	**CyH**	0.2	48	65	94:6
8	25	3	**MeCy**	0.2	48	48	94:6
9	25	3	**Et_2O**	0.2	48	3	85.5:14.5
10	25	3	**xylenes**	0.2	48	nr	n/d
11	25	3	***n*-hexane**	0.2	48	nr	n/d
12	25	3	CyH	**0.1**	48	32	94.5:5.5

Another parameter that could be used for the optimization of the reaction is the source of formaldehyde. Therefore, we compared paraformaldehyde with other HCHO sources, such as 1,3,5-trioxane (*sym*-trioxane, **4.2b**), formalin (aqueous 37% w/w solution of formaldehyde, **4.2c**) and methylal ($CH_2(OMe)_2$, **4.2d**), in the reaction using catalyst **4.5b** (CyH, 3 equiv. "HCHO", 25 °C, 24 h). Whereas paraformaldehyde led to **4.3a** in 38% yield (94:6 er), trioxane and formalin formed the product in lower yields (10% and 19%, respectively), but with relatively similar enantiomeric ratios (93:7 and 93.5:6.5, respectively). The reaction with methylal did not show any conversion under the tested conditions. Based on this, we continued the work on reaction development with paraformaldehyde as HCHO source (Scheme 4.5).

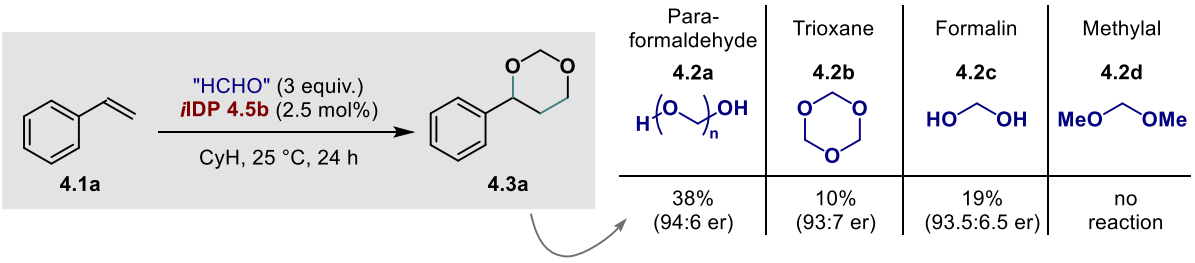

Scheme 4.5. Exploration of different formaldehyde sources.

To underscore the balance of acidity and confinement provided by the *i*IDP catalyst, a comparison study was performed with the corresponding IDP **4.4e** (similar confinement, less acidity) and *N*-triflylphosphoramide **4.4f** (*expected* relatively similar acidity, open active site).

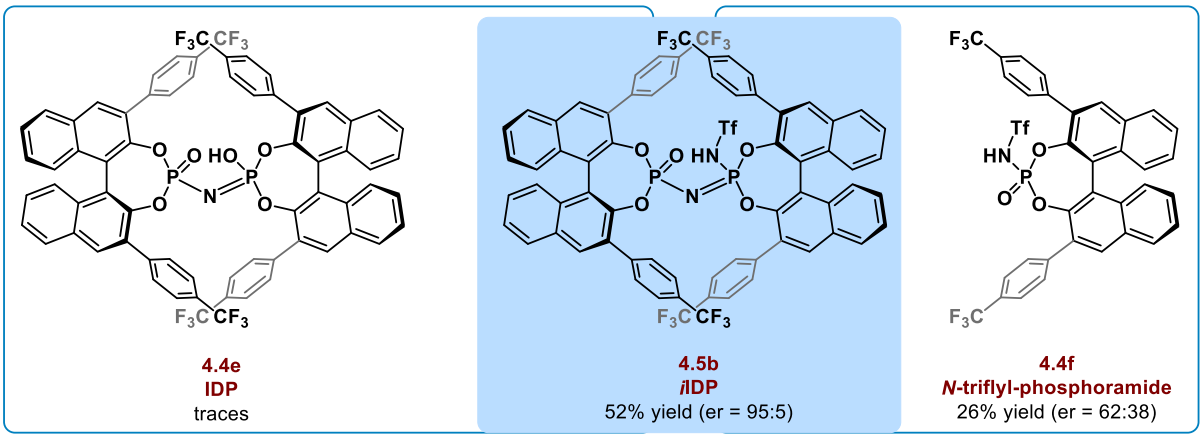

Scheme 4.6. Acidity and confinement: comparison of *i*IDP **4.5b** with the confined, less acidic IDP **4.4e**, and with the acidic, open *N*-triflylphosphoramide **4.4f**.

Indeed, whereas the *i*IDP **4.5b** gave 52% of **4.3a** (er = 94.5:5.5) after 36 h at rt in CyH, the acidic and open NTPA provided the Prins product in 26% yield after 36 h, but with significantly decreased enantioselectivity (er = 62:38); the confined but less acidic IDP led only to traces amounts of the 1,3-dioxane after 72 h (Scheme 4.6).

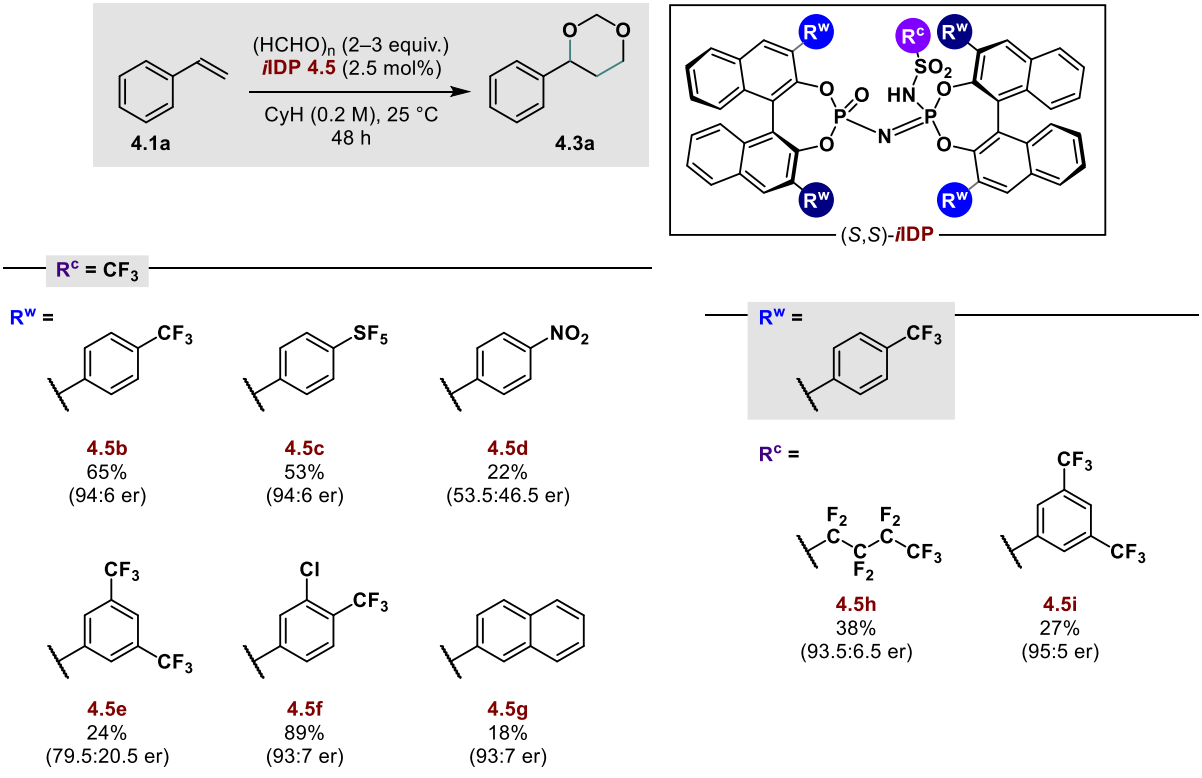

Scheme 4.7. Preliminary *i*IDP screening for the model Prins reaction.

Following the promising results using catalyst **4.5b**, we undertook the task of preparing and testing several other *i*IDPs for the model Prins reaction, anticipating to find a more reactive and selective Brønsted acid catalyst (Scheme 4.7). From these results, it is clear that other inner cores different than triflyl did not improve the reactivity, like the extended perfluoroalkyl chain of catalyst **4.5h**. While the aromatic core of **4.5i** proved beneficial for the selectivity, this was at the expense of decreasing the reactivity, which was probably also due to the significant core cleavage that was observed. Keeping the triflyl core, the presence of an EWG on the wing also seemed to be fundamental for the reactivity, as already presented in the preliminary general screening with the *i*IDP **4.5a** (Scheme 4.1), where no reactivity was observed in comparison to **4.5b**, and now with the lower reactivity displayed by *i*IDP **4.5g**, although without significant detriment in the enantioselectivity. Nevertheless, the sole presence of an EWG is not enough to achieve good reactivity/selectivity, but the type and position of these groups plays a role in the reactivity, as can be seen with the moderate activity displayed by catalysts **4.5d** or **4.5e**. Perfluorinated groups in the *para*-position of the wing appear to be beneficial for both reactivity and selectivity, and so does the presence of additional substituents in the *meta*-position as well. For example, catalyst **4.5f**, with a 3-Cl-4-CF_3-phenyl wing, produced **4.3a** in 89% yield with 93:7 er.

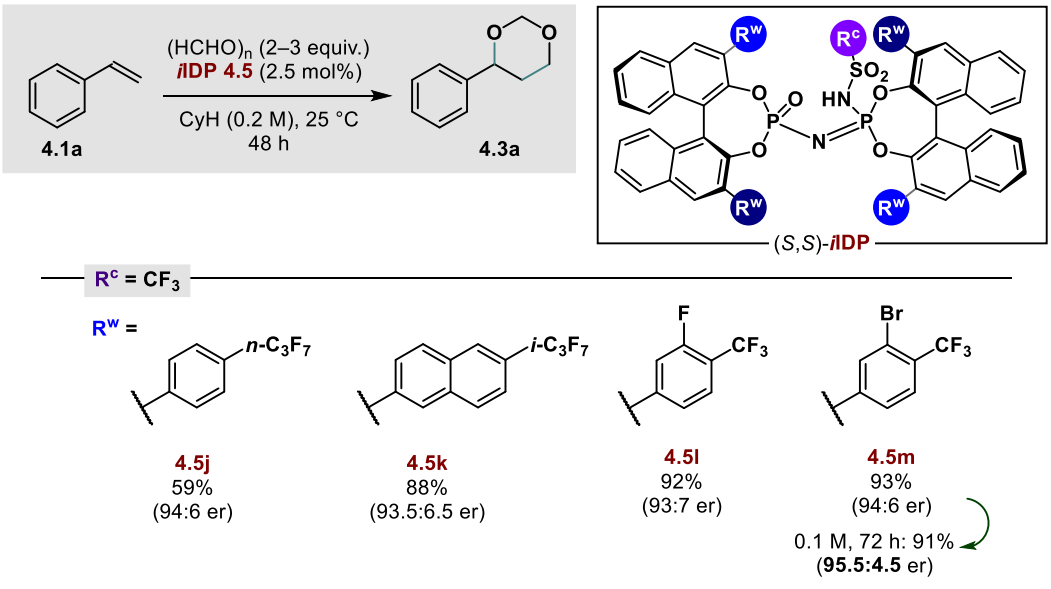

Scheme 4.8. Fine-tuning of the *i*IDP catalyst structure for the model Prins reaction.

These results prompted us to prepare other wings with perfluorinated chains in the *para*-position and/or with substituents in the *meta*-position. Wings combining *p*-CF_3 groups and halogens in the *meta*-position led us to the highly active and selective catalysts **4.5l** and **4.5m**. After fine-tuning the reaction conditions, the latter provided the Prins product in excellent yield and enantioselectivity (91%, 95.5:4.5 er) in CyH (0.1 M) at 25 °C for 72 h (Scheme 4.8).

It is noteworthy to highlight the positive effect of installing an EWG on the 2-naphthyl wing: whereas the catalyst with the unsubstituted wing had a poor performance, the *i*IDP **4.5k**, containing a 6-perfluoroisopropyl-substituted 2-naphthyl wing, led to a significant increase in reactivity without detectable detriment in the enantioselectivity. The preparation of this wing (as aryl triflate **4.8a**), depicted in Scheme 4.9, relied on a Cu-mediated Ullmann-type coupling of a naphthyl bromide and commercially available perfluoroisopropyl iodide. This approach proved efficient and step-economic, unlike reported procedures to attach perfluoroisopropyl groups on a naphthalene ring, requiring either volatile perfluoropropylene,[159] or previous transformation of the halide either to a diazonium salt[159b] or a boronic acid.[159a, 160]

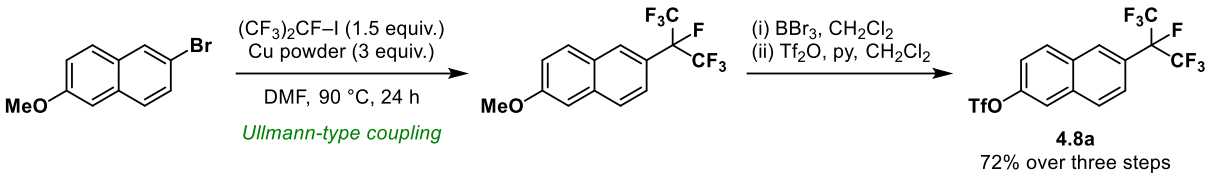

Scheme 4.9. Synthesis of the aryl triflate for the 6-perfluoroisopropyl-2-naphthyl wing of catalyst **4.5k**.

To determine the absolute configuration of the major enantiomer from the obtained 1,3-dioxane **4.3a**, enantioenriched samples of this compound were prepared by reacting the commercially available enantiomers of 1-phenylpropane-1,3-diol (**4.9a**) with paraformaldehyde and catalytic amounts of *p*-toluenesulfonic acid, following reported conditions.[161] By comparing the HPLC traces of these enantioenriched 1,3-dioxanes with the traces obtained from our *i*IDP-catalyzed Prins reaction, we could determine that the (*S*,*S*)-enantiomer of the *i*IDP catalyst selectively favors the formation of the (*R*)-enantiomer of the 1,3-dioxane **4.3a** (Scheme 4.10).

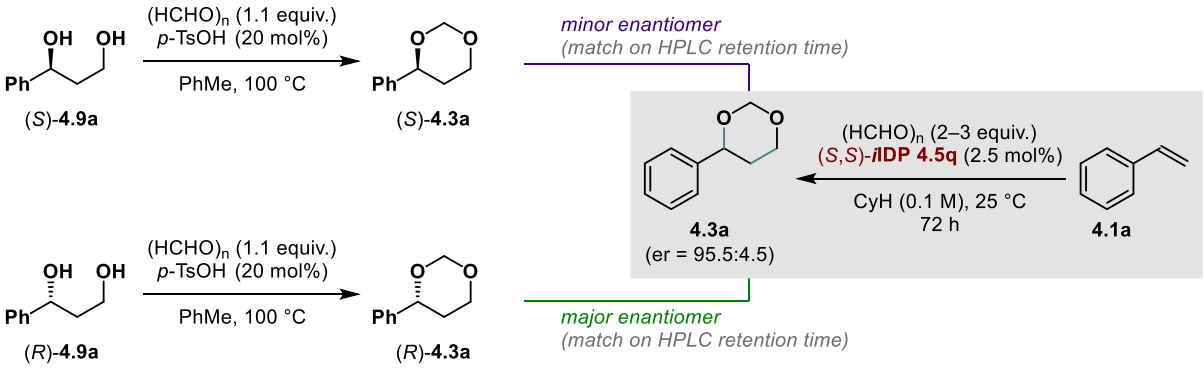

Scheme 4.10. Determination of absolute configuration of **4.3a** by comparison of HPLC-chromatograms with enantioenriched samples.

4.2 Substrate Scope and Further Modifications

4.2.1 Reaction Scope: Terminal Aryl Olefins

Encouraged by the positive results using *i*IDPs for the Prins reaction with the model substrate (styrene, **4.1a**), we explored several other (hetero)aryl olefins (terminal and internal), as well as some alkyl olefins as potential substrates for our enantioselective methodology.

PRELIMINARY SCOPE

Several commercially available terminal aryl olefins were tested in a preliminary substrate screening, using *i*IDP **4.5b** with the optimized conditions from the styrene reaction (in CyH at 25 °C).

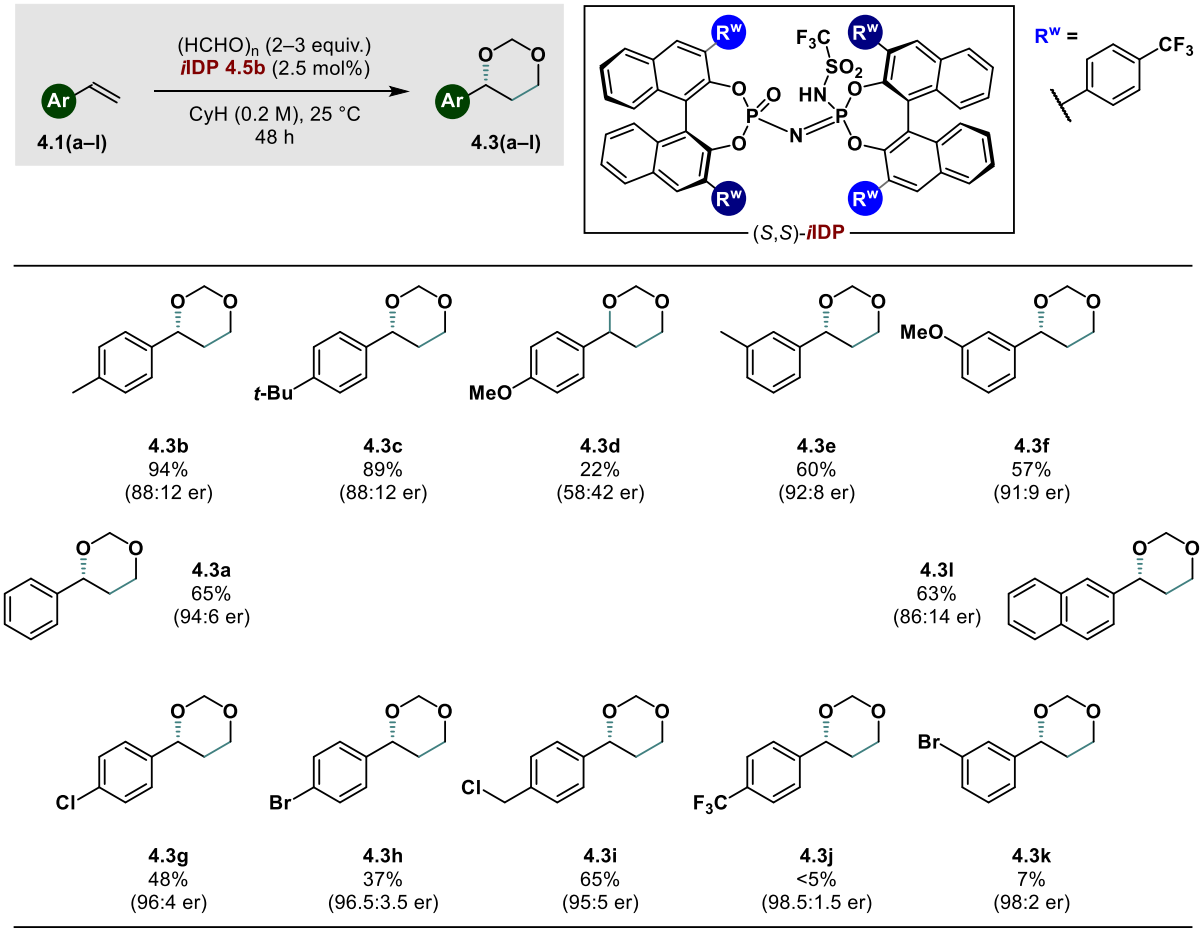

Scheme 4.11. Preliminary substrate scope of terminal aryl olefins using catalyst **4.5b**.

As can be seen in Scheme 4.11, in general the 1,3-dioxane products were obtained with moderate to good enantioselectivity, although with significant differences in yield. In general, aryl olefins containing an EDG on the aromatic ring displayed high reactivity, like the *p*-alkyl substituted ones (**4.1b** and **4.1c**), but also these reactions proceeded with lower enantioselectivity in comparison to the parent styrene. Although the methoxy group is also

electron-donating, product **4.3d** was formed in low yield and enantioselectivity, due to side reactions that led to complex reaction mixtures. Conversely, the presence of EWG on the aromatic ring rendered the olefins **4.1(g–k)** less nucleophilic, which was evidenced by the low to moderate yields of the corresponding 1,3-dioxanes. Remarkably, for these cases there seems to be an inverse relationship between reactivity (%yield) and enantioselectivity (er); thus, 1,3-dioxanes **4.3j** and **4.3k** were obtained with excellent enantioselectivity, but only in trace amounts under the tested conditions.

From this preliminary screening, two main challenges were recognized: *(i)* the presence of strong electron-donating groups in the *para*-position induces over-reactivity and hampers also the enantioinduction, and *(ii)* the presence of strong electron-withdrawing groups turns the reactions slow, but favoring at the same time the enantioinduction process.

ARYL OLEFINS WITH ELECTRON-DONATING GROUPS

*(unless otherwise stated, these results are obtained using catalyst **4.5b**)*

As already mentioned, in general the presence of EDG favored the reactivity of the olefin, but the 1,3-dioxanes were obtained with moderate or low enantioselectivity.

Olefins with moderately activated aromatic rings, such as the *p*-alkyl-substituted ones, were highly reactive. Gratifyingly, the presence of the less-activating chloromethyl group ($–CH_2Cl$) was also very well tolerated, and **4.3i** was obtained in 55% yield and with good enantioselectivity (95:5 er), and the primary benzyl chloride can act as a handle for posterior functionalization of the enantioenriched product. If the alkyl substitution is switched to the *meta*-position, the reactivity is not as high as in the previous cases, although the product is still formed with good enantioselectivity, as shown for **4.3e**.

The presence of the strongly activating methoxy group in the *para*-position turned out to be fairly challenging. With the available *i*IDP library, olefin **4.1d** in general reached full conversion rather quickly, but always producing complex mixtures, where the corresponding 1,3-dioxane **4.3d** was formed in low yield and with unsatisfactory enantioselectivity (22%, 58:42 er, after 36 h). Several screenings showed that less acidic catalysts were required to obtain a moderate degree of enantioinduction. For example, an *i*IDP without EWG on the wing, such as **4.5n**, increased the yield of **4.3d** to 45%, with 96% olefin conversion after 36 h, although without any improvement on the enantioinduction (57.5:42.5 er). If the expectedly less acidic IDP **4.4e** (containing 4-CF_3-phenyl wings) is used, **4.3d** is formed in 31% yield, with improved product selectivity (36% olefin conversion) and enantioselectivity (78:22 er); however, the reaction could not be sped up to a significant degree by tuning the reaction conditions (Scheme 4.12).

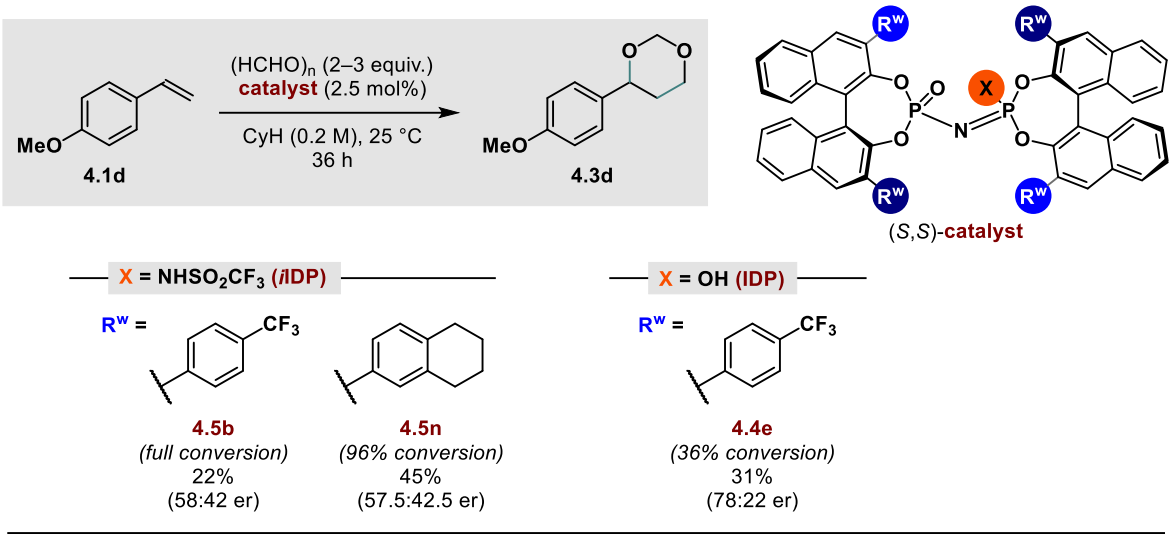

Scheme 4.12. Effect of the catalyst acidity on the Prins reaction of the highly activated 4-vinylanisole (**4.1d**).

Another strategy to produce enantioenriched 4-aryl-1,3-dioxanes containing an oxygenated substituent in the *para*-position, would consist in replacing the methoxy group for another oxygenated substituent (Scheme 4.13). Therefore, we tested the commercially available 4-vinylphenyl acetate (**4.1m**) for the Prins reaction, but still complex mixtures were obtained, where the 1,3-dioxane **4.3m** was formed along with a side product with further formaldehyde incorporation (as ring hydroxymethylation, **4.3m'**), and they could be partially isolated after a relatively difficult chromatographic separation.

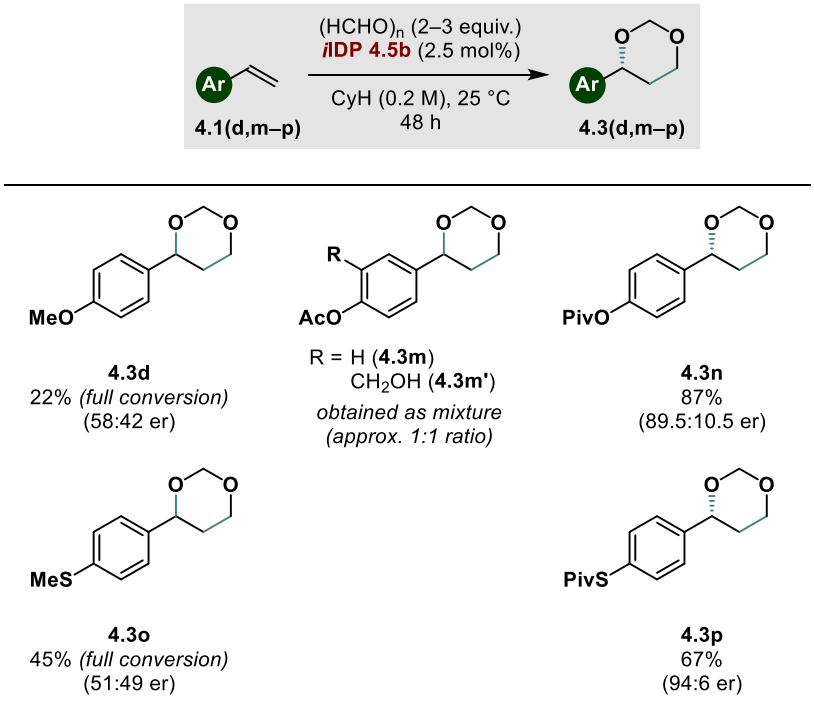

Scheme 4.13. From strong to moderate electron-withdrawing groups in the *para*-position of the aryl olefin.

To inhibit this additional reactivity, we prepared the bulkier pivalate derivative **4.1n** that, to our delight, produced a much simpler reaction mixture, consisting mostly of the desired 1,3-

dioxane **4.3n** (87%, 89.5:10.5 er), and without any signal of ring hydroxymethylation. Similarly, whereas 4-(methylthio)styrene **4.1o** was highly reactive (full conversion, but product **4.3o** in only 45% yield and 51:49 er), the less activated thiopivalate-derived olefin **4.1p** produced **4.3p** in 67% (94:6 er).

The strong electron-donating methoxy group proved less problematic when it was in the *meta*-position (**4.1f**), probably because in this case the mesomeric effect does not lead to stabilization of a benzylic cationic species, and the inductive effect (–I) is the dominant one. Building up on these last observations, and considering the relevance of *ortho*-dioxygenated aromatic rings (catechol derivatives) in natural products and medicinal chemistry,[162] we prepared and tested substrate **4.1q**, forming the corresponding 1,3-dioxane **4.3q** in 72% yield (full conversion) after 60 h, although only with moderate enantioselectivity (73.5:26.5 er). Olefin **4.1r**, presenting a less activating *ortho*-dioxygenation pattern, achieved 73% conversion, forming the 1,3-dioxane in 62% yield with very good enantioselectivity (94:6 er) (Scheme 4.14).

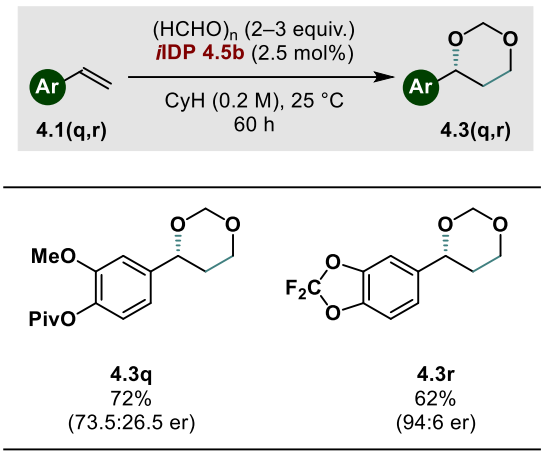

Scheme 4.14. *i*IDP-catalyzed Prins reaction of 3,4-dioxygenated aryl olefins.

ARYL OLEFINS WITH ELECTRON-WITHDRAWING GROUPS

*(unless otherwise stated, these results are obtained using catalyst **4.5b**)*

Not very surprisingly, the presence of electron-withdrawing groups on the aromatic ring translates into the olefin moiety being less nucleophilic, which is reflected in lower reaction rates. Other EWG-substituted aryl olefins were tested: the less deactivating 4-fluorine-substituted **4.1s** presented though excellent reactivity and moderate enantioselectivity (88%, 93:7 er, after 36 h), whereas the *meta*-isomer **4.1t** was less reactive but more selective (22%, 97:3 er, after 72 h). As previously shown, a similar situation was observed with the *para*- and *meta*-bromo-substituted olefins (**4.1h** and **4.1k**). Based on the results from the previous section, we considered to combine the effect of a *meta*-Br substituent with a *para*-EDG, to ideally increase the reactivity without sacrificing much of the enantioinduction provided by the *meta*-Br part. Hence, olefins **4.1u** and **4.1v** were prepared and tested, showing strikingly different behaviors, where the former was fully converted after 36 h and provided 1,3-dioxane (**4.3u**) in 56%, although with only 59:41 er, showing that the *p*-OMe group overrides the effect

from the *m*-Br substituent. In contrast, the latter olefin (**4.1v**) was less reactive (57% olefin conversion after 60 h) and cleanly transformed to **4.3v** in 44% yield, with an excellent enantiomeric ratio of 95.5:4.5. Similarly to poorly reactive olefins **4.1j** and **4.1k** (containing either 4-CF_3 or 3-Br substituents, respectively), the presence of an ethoxycarbonyl substituent (–CO_2Et) in the *para*-position significantly hampered the reactivity, and only 6% of product **4.3w** was obtained after 72 h (9% olefin conversion), although with exquisite enantioselectivity (97.5:2.5 er) (Scheme 4.15).

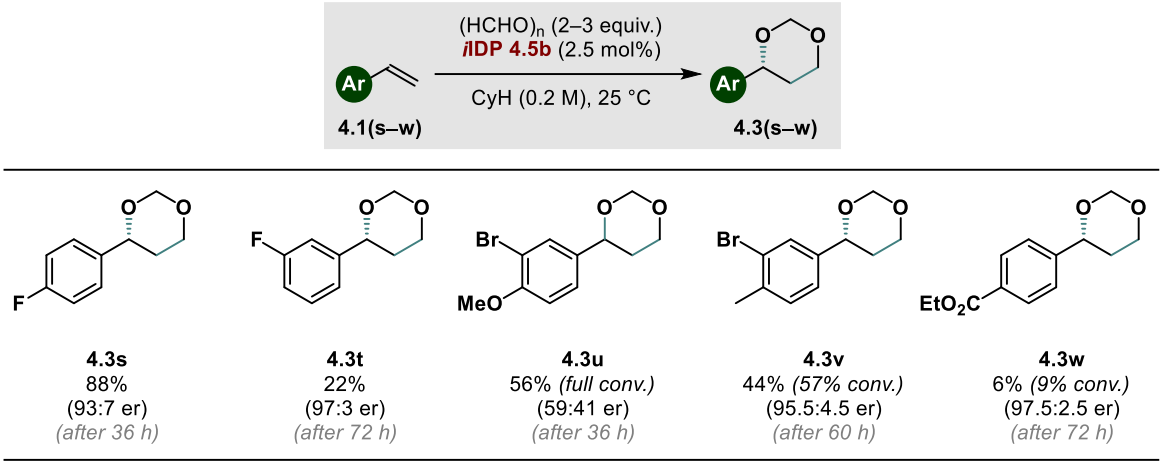

Scheme 4.15. Scope expansion for EWG-containing aryl olefins.

Increasing the conversion of these three olefins (**4.1j**, **4.1k** and **4.1w**) constituted a particular challenge, since increasing temperature was not helpful. At 50 °C, the *i*IDP readily underwent formaldehyde-mediated inner core cleavage (see Section 4.1.2) to produce the less acidic IDP, causing the desired Prins reaction to stop. Therefore, we considered to use the more acidic IDPis, but again the formaldehyde-mediated inner core cleavage was faster than the desired Prins reaction. In need of a more acidic *i*IDP, we decided to install additional EWG on the catalyst structure. So far, the fine-tuning of *i*IDPs (and IDPis) has involved modifying the wings (3,3'-positions of the BINOL backbone) and the inner "core" (sulfonylimino groups), but the backbone itself has remained almost unchanged, so we recognized in there some unexplored space for further catalyst structure development.

On the modifications of BINOL backbones

Modifications on the BINOL backbone have been performed since decades, mostly on the 6,6'-positions, due to their increased electron density, which allows an easy installment of synthetic handles. The majority of reports on 6,6'-disubstituted BINOL-derived compounds present the introduction of the following groups on the backbone:

- Halogen atoms: mostly bromine or iodine, acting as moderate EWG to modify the electronics of the BINOL, or to be used as synthetic handles for the installment of other types of groups.[163]

- Alkyl/silyl groups: either linear or bulky alkyl groups (*t*-Bu, adamantyl), or bulky silyl groups ((*i*-Pr)$_3$Si– or Ph$_3$Si–), to modify the lipophilicity of the structure and/or its geometry through a change of the dihedral angle.[164]
- Alkenyl groups: vinyl or styrenyl moieties, mostly used for later copolymerization with an olefin during the preparation of solid-supported catalysts.[165]
- Strong electron-withdrawing groups: similarly to the introduction of halogen atoms, these groups modify the electronic properties of the BINOL structure. Examples in literature include nitro groups (–NO_2),[166] alkoxycarbonyl groups (–CO_2R),[167] or linear perfluoroalkyl chains (–R^F: CF_3, C_2F_5, *n*-C_3F_7, *n*-C_4F_9, *n*-C_6F_{13}, *n*-C_8F_{17}).[168]

Based on the reports for the synthesis of 6,6'-bis(perfluoroalkyl)-substituted BINOL derivatives, we used 6,6'-dibromo protected BINOL **4.8b** as coupling partner for the installment of perfluoroalkyl groups (*n*-C_3F_7 and *i*-C_3F_7), via a Cu-mediated Ullmann-type reaction (similar to the synthesis of the wing toward catalyst **4.5k**). For each modified BINOL, once the 6,6'-substituents were installed, we followed a lithiation/functionalization sequence to generate coupling partners,[169] from which a standard methodology was followed toward the installment of wings (3,3') and posterior *i*IDP synthesis (Scheme 4.16).

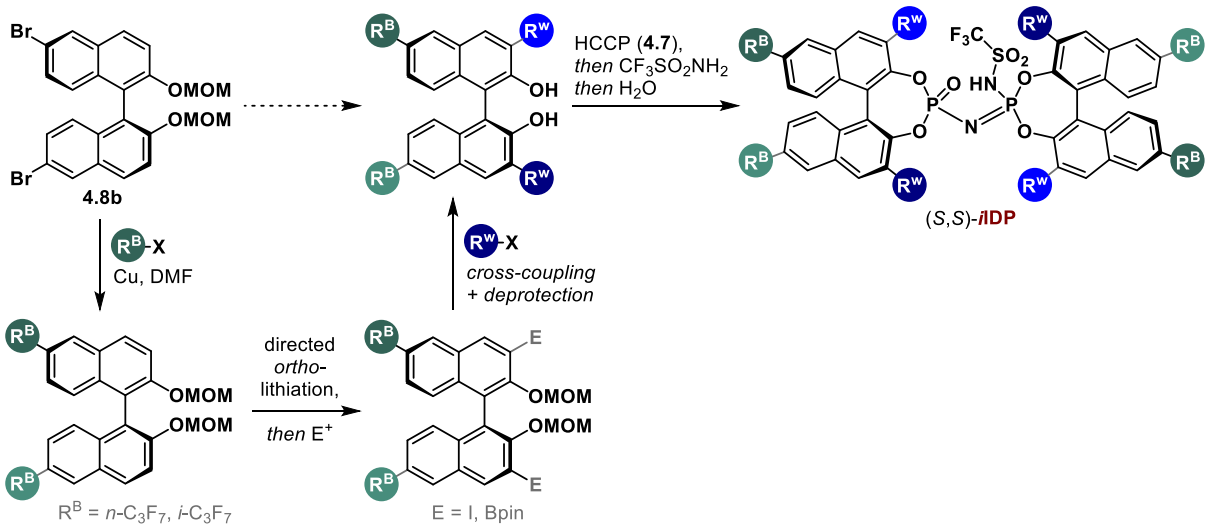

Scheme 4.16. Synthetic route toward 6,6'-disubstituted BINOLs and *i*IDPs.

To determine if the 6,6'-substituted *i*IDPs have any effect on the reactivity/selectivity of the Prins reaction, they were tested first for the model reaction (styrene + paraformaldehyde) for 24 h at room temperature (Scheme 4.17). In general, the presence of 6,6'-substituents led only to a slight decrease in enantioselectivity, but also to a striking improvement of the reactivity.

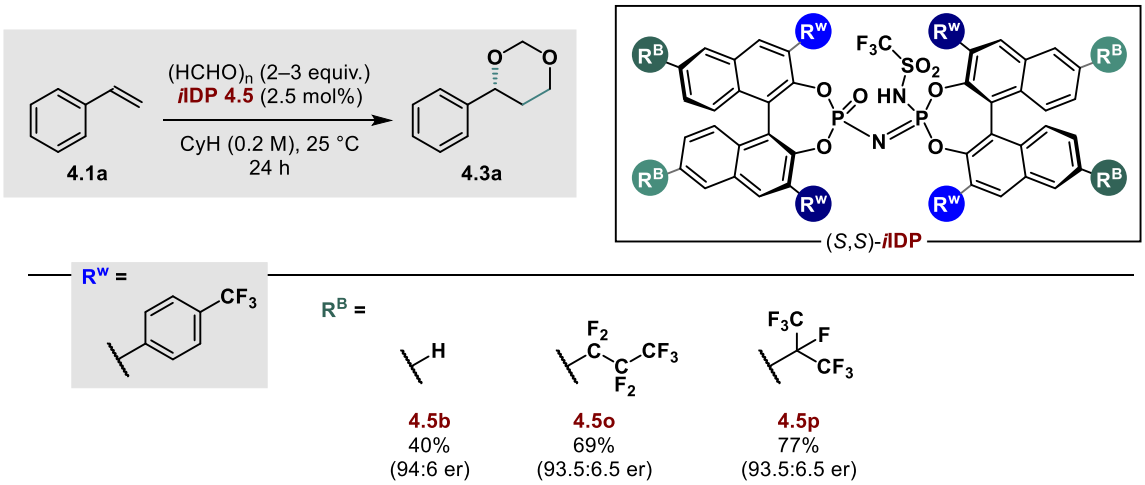

Scheme 4.17. Effect of 6,6'-substituted *i*IDPs in the model Prins reaction.

To underscore the effect of EWGs, both on the wings and on the BINOL backbone, the performance of catalysts **4.5a**, **4.5b** and **4.5p** for the model Prins reaction was assessed by NMR monitoring in $CDCl_3$. These experiments were set up in NMR tubes and monitored over time by ^1H NMR at room temperature, in the presence of Ph_3CH as internal standard to account for possible fluctuations in the amount of solvent. As expected, these reaction profiles proceeded slower than the reactions from the screenings, due to the lack of stirring, which played a key role considering the heterogeneity of the samples (low solubility of paraformaldehyde). Nevertheless, the obtained reaction profiles display striking differences in terms of olefin conversion and product formation, which can be attributed to the distinct structural features of the catalysts (Figure 4.6). For the case of **4.5a**, where neither the backbone nor the wings contain EWGs, barely any reactivity was observed. Trifluoromethyl-substituted wings from catalyst **4.5b** unequivocally translated into moderate reactivity (approx. 60% olefin conversion and 56% yield after 4 days), and the additional acidifying effect of the 6,6'-perfluoroisopropyl groups (catalyst **4.5p**) was evident by the excellent reactivity (over 98% olefin conversion and 86% yield after 4 days).

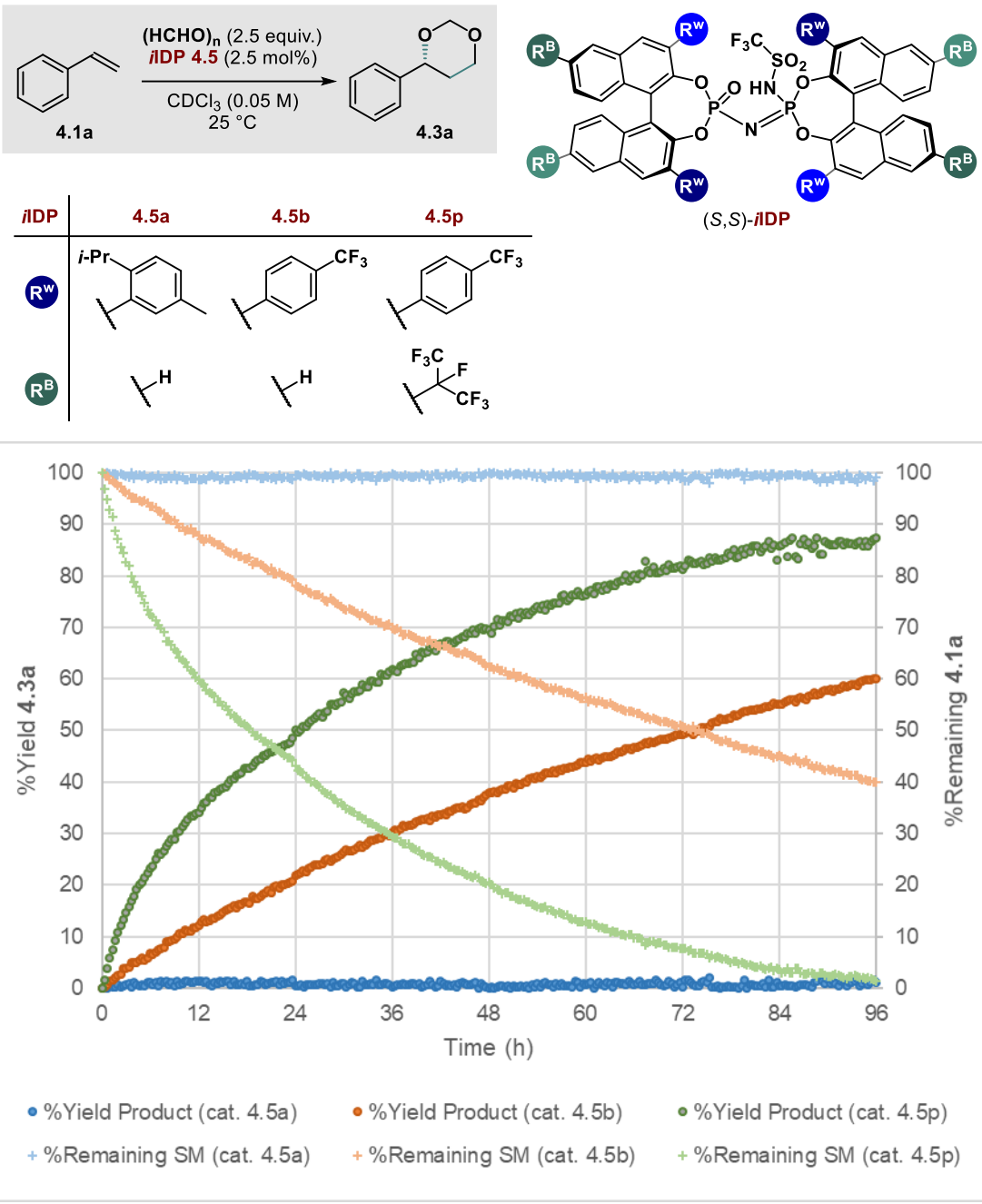

Figure 4.6. Reaction profiles (^{1}H NMR at 25 °C) for the model Prins reaction with catalysts **4.5a**, **4.5b**, and **4.5p**.

Motivated by these results, we tested this 6,6'-EWG-substituted *i*IDP (**4.5p**) for the Prins reaction of the challenging electron-deficient olefins **4.1j**, **4.1k** and **4.1w**. Gratifyingly, in all cases the reactivity was increased in comparison to the parent *i*IDP **4.5b**, at the expense of only a slight decrease in enantioselectivity (Scheme 4.18).

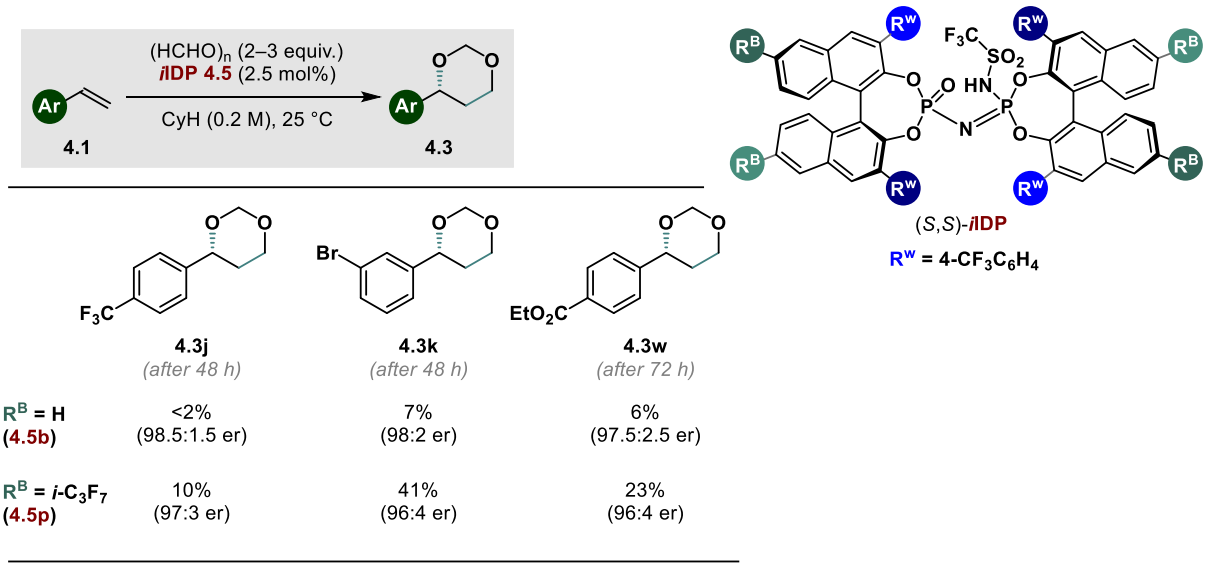

Scheme 4.18. Designed 6,6'-(i-C_3F_7)$_2$-substituted *i*IDPs in the Prins reaction of electron-deficient aryl olefins.

OTHER TERMINAL ARYL OLEFINS

*(unless otherwise stated, these results are obtained using catalyst **4.5b**)*

In addition to the previously shown examples, other terminal aryl olefins were tested with the purpose of expanding the substrate scope of the developed methodology. For example, olefins containing bigger rings, such as the naphthalene-derived ones (**4.1l** and **4.1z**) and the partially hydrogenated **4.1x**, as well as **4.1y**, containing a fluorene ring, reacted with **4.2a** to produce the corresponding 1,3-dioxanes, albeit with low to moderate enantioselectivity (Scheme 4.19). Olefin **4.1z** proved to be challenging, both from the reactivity and the enantioselectivity, probably due to the substitution in the *ortho*-position, which brings steric bulk close to the reactive olefin moiety. Gratifyingly, the presence of a smaller *ortho*-substituent proved beneficial, as olefin **4.1za** produced the corresponding 1,3-dioxane with good enantioselectivity (34% after 36 h, 83:17 er).

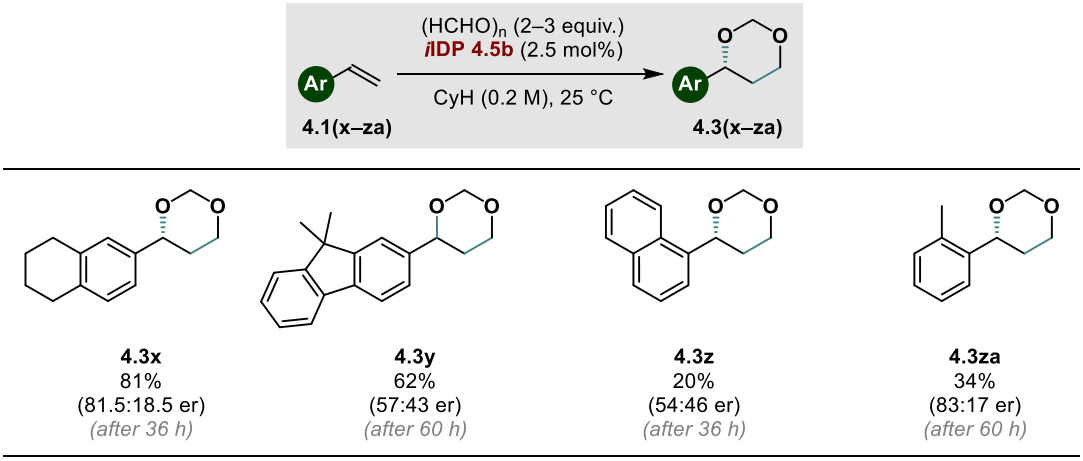

Scheme 4.19. Further substrate substitution patterns, including *ortho*-substituted aryl olefins.

We wondered about how a substrate containing two vinyl groups (**4.1zb**) would behave in an *i*IDP-catalyzed Prins reaction (Scheme 4.20). Using 2.5 equiv. of paraformaldehyde, the products from a single Prins reaction (**4.3zb**) and from the double reaction (**4.3zb'**) were obtained, in an approximate 2:1 ratio (the quantification via ^{1}H NMR was rather complicated due to overlapping signals in the olefin region). For the double Prins reaction, two diastereomers are formed in an approx. 6:1 ratio: a pair of enantiomers (*dl*: **4.3zb'**$_{dl}$) and a *meso* form (**4.3zb'** $_{meso}$). Whereas the product from a single Prins reaction (**4.3zb**) was formed with 89.5:10.5 er, the *dl* isomer of the double reaction product (**4.3zb'**$_{dl}$) was formed with excellent enantioselectivity (99:1 er), probably due to an amplification process from the partially enantioenriched "mono-Prins" product **4.3zb** following the Horeau's principle.[170]

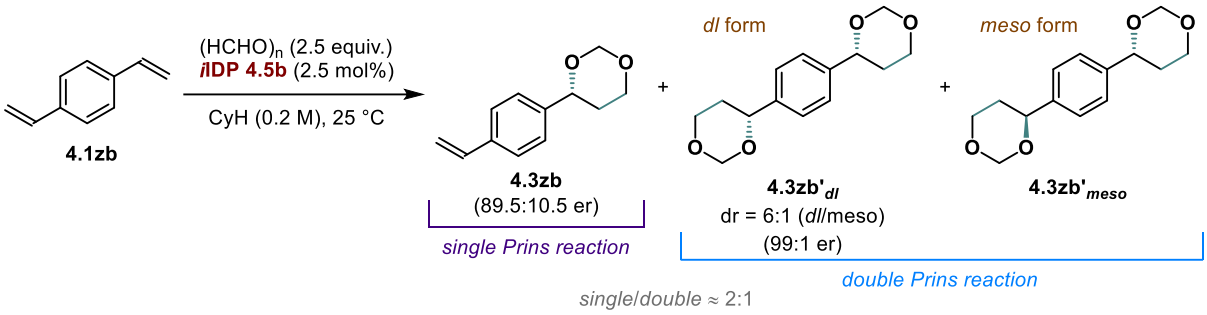

Scheme 4.20. Using 1,4-divinylbenzene as substrate: single and double Prins reaction.

Next, we studied the behavior of another bis-olefinic substrate, **4.1zc**, now containing both an aryl olefin and an alkyl olefin. The reaction proceeded in a chemoselective fashion forming the 1,3-dioxane **4.3zc** in 89% yield (er = 91.5:8.5), where only the aryl olefin moiety was transformed and the aliphatic olefin residue from the allyl group remained unchanged (Scheme 4.21).

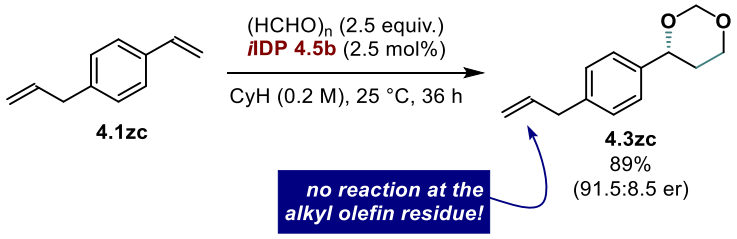

Scheme 4.21. 4-allylstyrene (**4.1zc**) as substrate: reaction selective for terminal *aryl* olefins.

Another group of substrates that we were interested in consisted in heteroaryl olefins. Thus, we prepared and tested the reactivity of olefins containing several heterocycles, such as thiophene, indole, carbazole and pyridine (Scheme 4.22). However, many of the substrates containing π-excessive heterocycles (thiophene and indole, **4.1(zd–zf)**) were overly reactive, presenting high conversion but producing very complex mixtures. From these examples, only the *N*-tosyl carbazole-derived olefin **4.1zg** presented moderate enantioselectivity in the transformation. Assuming that this extreme reactivity was partly due to the high electron density of these heterocycles, resembling the already discussed situation with the *p*-methoxy-

substituted styrene **4.1d**, we tried to test an olefinic substrate containing an electron-deficient heterocycle. However, 3-vinylpyridine **4.1zh** proved to be completely unreactive, even in the presence of the more acidic 6,6'-(*i*-C_3F_7)$_2$-substituted *i*IDP **4.5p**; this lack of reactivity quite likely arises from the acid-base reaction between substrate and catalyst, rendering the latter inactive for the activation of paraformaldehyde.

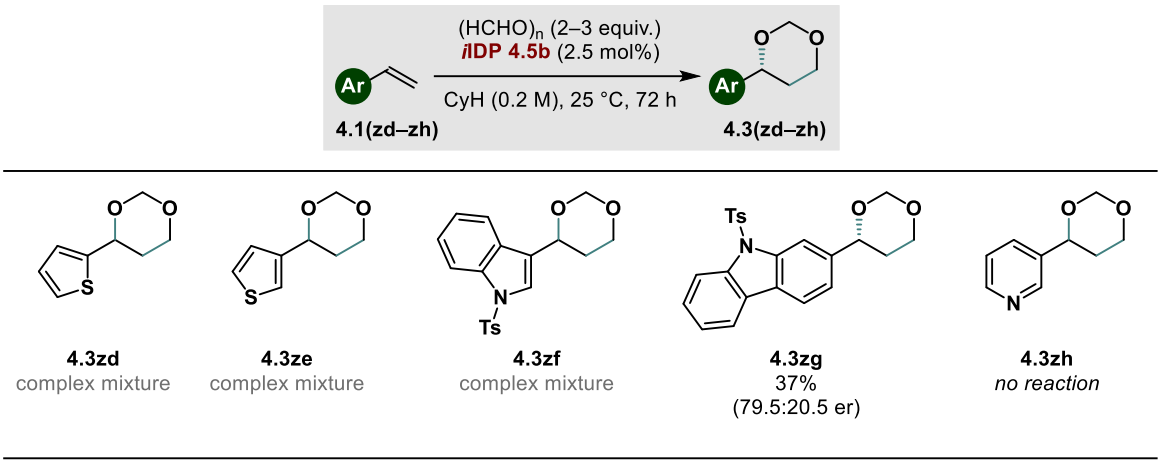

Scheme 4.22. Testing heteroaryl olefins in the *i*IDP-catalyzed Prins reaction.

Finally, the introduction of substituents on the α-position of the olefin moiety was explored. However, both α-methylstyrene (**4.1zi**) and α-ethylstyrene (**4.1zi'**) were extremely reactive in the presence of paraformaldehyde and catalyst **4.5b**, resulting in the formation of complex mixtures; unfortunately, in neither case were the expected 1,3-dioxanes observed.

FINE-TUNING OF THE SCOPE

After determining which types of substrates were tolerated in our developed methodology and could potentially be improved to meet satisfactory levels of reactivity and enantioselectivity, an extensive screening of chiral Brønsted acid catalysts and reaction conditions was performed. The improved results are summarized in Scheme 4.23.

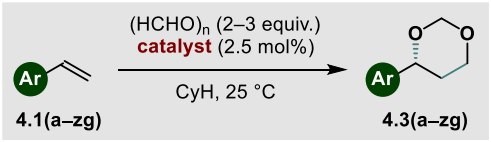

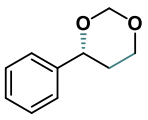

4.3a
89% (95.5:4.5 er)
*(with **4.5m**)*
72 h, 0.1 M

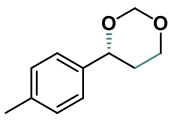

4.3b
89% (90:10 er)
*(with **4.5b**)*
72 h, 0.05 M

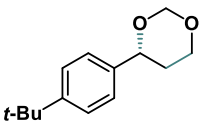

4.3c
89% (91.5:8.5 er)
*(with **4.5b**)*
72 h, 0.05 M

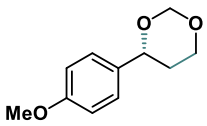

4.3d
31% (78:22 er)
*(with **4.4e**)*
36 h, 0.2 M

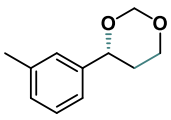

4.3e
88% (93:7 er)
*(with **4.5k**)*
72 h, 0.05 M

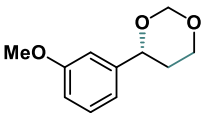

4.3f
87% (93:7 er)
*(with **4.5k**)*
72 h, 0.05 M

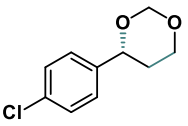

4.3g
88% (95.5:4.5 er)
*(with **4.5k**)*
96 h, 0.2 M

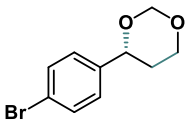

4.3h
74% (95.5:4.5 er)
*(with **4.5k**)*
5 d, 0.2 M

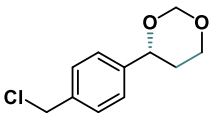

4.3i
57% (95.5:4.5 er)
*(with **4.5b**)*
5 d, 0.2 M

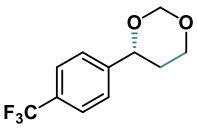

4.3j
10% (97:3 er)
*(with **4.5p**)*
5 d, 0.2 M

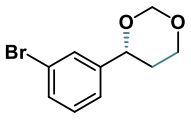

4.3k
41% (96:4 er)
*(with **4.5p**)*
5 d, 0.2 M

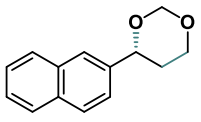

4.3l
79% (90.5:9.5 er)
*(with **4.5k**)*
72 h, 0.025 M

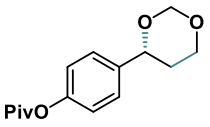

4.3n
83% (91:9 er)
*(with **4.5k**)*
72 h, 0.1 M

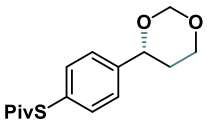

4.3p
88% (95:5 er)
*(with **4.5k**)*
72 h, 0.05 M

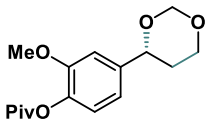

4.3q
72% (80:20 er)
*(with **4.5k**)*
48 h, 0.1 M

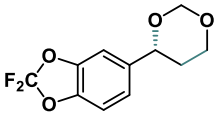

4.3r
57% (94.5:5.5 er)
*(with **4.5j**)*
72 h, 0.05 M

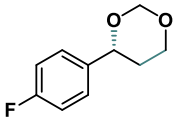

4.3s
82% (94.5:5.5 er)
*(with **4.5j**)*
96 h, 0.05 M

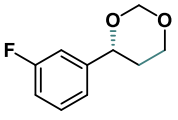

4.3t
52% (96.5:3.5 er)
*(with **4.5k**)*
5 d, 0.2 M

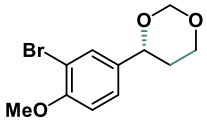

4.3u
34% (70.5:29.5 er)
*(with **4.5n**)*
5 d, 0.2 M

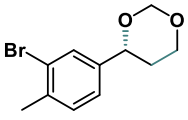

4.3v
67% (94:6 er)
*(with **4.5b**)*
5 d, 0.2 M

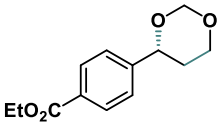

4.3w
23% (96:4 er)
*(with **4.5p**)*
5 d, 0.2 M

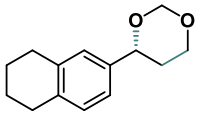

4.3x
81% (81.5:18.5 er)
*(with **4.5b**)*
72 h, 0.1 M

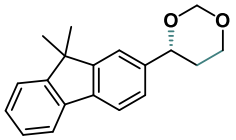

4.3y
62% (58:42 er)
*(with **4.5k**)*
96 h, 0.1 M

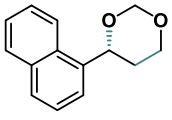

4.3z
33% (66.5:33.5 er)
*(with **4.5k**)*
5 d, 0.2 M

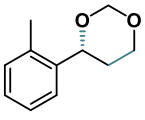

4.3za
78% (88.5:11.5 er)
*(with **4.5j**)*
7 d, 0.1 M

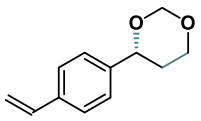

4.3zb
60% (89.5:10.5 er)
*(with **4.5b**)*
48 h, 0.1 M

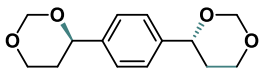

4.3zb'
30% (99:1 er)
*(with **4.5b**)*
48 h, 0.1 M

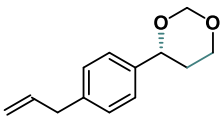

4.3zc
89% (91:9 er)
*(with **4.5b**)*
72 h, 0.05 M

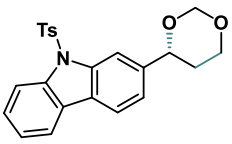

4.3zg
66% (83:17 er)
*(with **4.5k**)*
96 h, 0.025 M

Scheme 4.23. Improved conditions for the terminal aryl olefin scope of the *i*IDP-catalyzed Prins reaction.

4.2.2 Scope Limitations: Internal Aryl Olefins, and Alkyl Olefins

Motivated by the relative generality of the Prins reaction of terminal aryl olefins, both with electron-donating and electron-withdrawing groups, we decided to investigate the more challenging internal olefins.

When *trans*-*β*-methylstyrene (**4.10a**) was reacted with **4.2a** in the presence of catalyst **4.5b**, only trace amounts of product **4.11a** (*trans*-isomer) were observed by ^{1}H NMR after 4 days at room temperature, and HPLC analysis indicated an enantiomeric ratio of 58:42. By using the more acidic 6,6'-disubstituted *i*IDP **4.5p**, *trans*-4-phenyl-5-methyl-1,3-dioxane (**4.11a**) was formed after 4 days in 27% yield, with er = 57.5:42.5, and also a small amount (5%) of the *cis*-disubstituted 1,3-dioxane (**4.11a'**) was obtained (Scheme 4.24). To enhance reactivity, the *para*-methoxy-substituted internal olefin (*trans*-anethole, **4.10b**) was tested as substrate. In this case, catalyst **4.5b** was acidic enough to achieve full olefin conversion and provide the *trans*-isomer of the 1,3-dioxane **4.11b** in 48% yield, along with 7% of the *cis*-isomer **4.11b'**; contrarily to the terminal olefins, in this case the presence of the methoxy substituent rather led to better enantioselectivity (er_{trans} = 64.5:35.5).

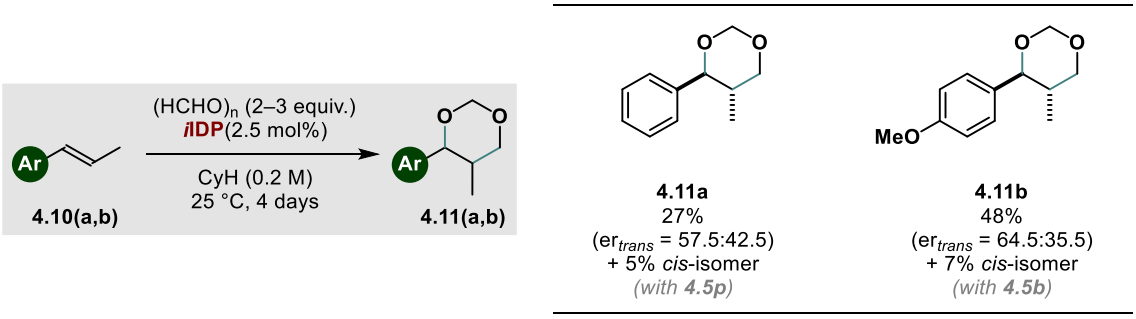

Scheme 4.24. Internal aryl olefins in the *i*IDP-catalyzed Prins reaction.

The particularly reactive 1*H*-indene (**4.10c**) was also examined. In this case, catalyst **4.5b** led to full olefin conversion, though provided the 1,3-dioxane **4.11c** in 26% yield after 4 days at 25 °C, exclusively as the *cis*-isomer (er_{cis} = 76.5:23.5). This compound is commercialized under the name *Indoflor*® as a fragrance, as its odor has been reported as "animalic, floral, civet, leather".[171] Unfortunately, after testing several other reaction conditions, neither the yield nor the selectivity could be improved (Scheme 4.25). Using the less acidic *i*IDP **4.5t** made the reaction slower (27% conversion, 8% yield after 4 days), but without significant change in the enantiomeric ratio (75.5:24.5 er).

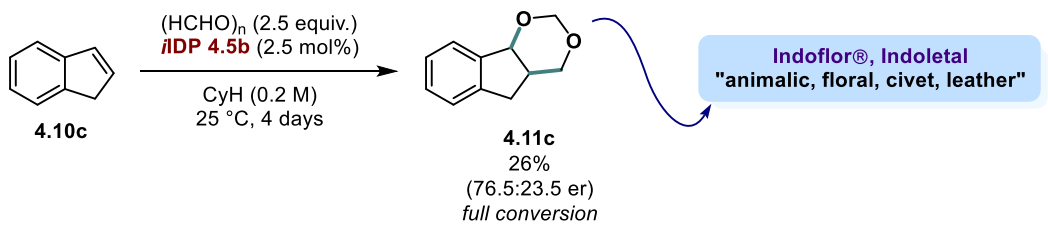

Scheme 4.25. Toward an asymmetric synthesis of Indoflor® by Prins reaction of 1*H*-indene (**4.10c**).

Finally, we were curious about the possibility of using alkyl olefins for our developed methodology. We chose 1-octene (**4.10d**) as substrate, but neither catalyst **4.5b** nor the more acidic **4.5p** led to the formation of any detectable product with paraformaldehyde. This lack of reactivity could not be solved even at higher temperatures (50 °C or 80 °C), eventually causing only the formaldehyde-mediated inner core cleavage of the *i*IDP catalysts. Switching to 4-phenyl-1-butene (**4.10e**), expecting that the aromatic ring could be used as a recognition element by the catalyst, proved unsuccessful and again no reactivity was observed under the tested conditions.

4.2.3 One Step Away from Enantioenriched 1,3-Diols

Acetals and ketals have been used for decades in organic synthesis as protecting groups, either of aldehydes/ketones or alcohols. However, whereas isopropylidene ketals (derived from acetone) or arylidene acetals (derived from aromatic aldehydes) have found use in several areas of synthesis, such as in carbohydrate synthetic chemistry, the simpler methylene acetals ("*formals*") have been considerably less used, mostly because of the difficulty to remove them without destroying the desired unprotected alcohol. The obtained Prins products (enantioenriched 1,3-dioxanes) can be regarded as formals of 1,3-diols, which are useful and valuable synthetic building blocks. Therefore, it would be ideal to find a strategy for the deprotection of the former into the latter without damaging the enantiopurity.

We considered though that the classical methods to effect this transformation (involving over-stoichiometric amounts of acid and/or high temperatures) could be too harsh and damage the obtained degree of enantiopurity for the 1,3-dioxanes, which contain a labile benzylic ether moiety. Indeed, 1,3-dioxane **4.3a** has been reported to undergo ring opening when treated with Ac_2O/H_2SO_4 to produce the diacetate **4.12a**,[172] which can further be transformed into the 1,3-diol **4.9a** upon saponification. However, when the enantiopure 1,3-dioxane (>99:1 er, obtained from preparative HPLC with a chiral column) was cleaved by this two-step process, the corresponding 1,3-diol is obtained in 67:33 er, evidencing that a strong racemization takes place during this ring-opening strategy (Scheme 4.26).[173]

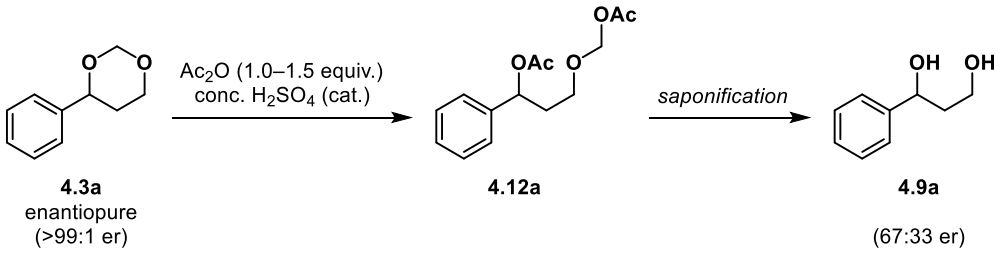

Scheme 4.26. Ring-opening of 1,3-dioxanes by acetolysis and saponification: loss of enantiopurity.

Fujioka reported a much milder process for the ring-opening deprotection of cyclic formals (1,3-dioxolanes or 1,3-dioxanes), using a combination of a trialkylsilyl triflate (TESOTf or TMSOTf)

and 2,2'-bipyridyl, followed by hydrolysis.[174] In his proposed mechanism, the less sterically-hindered oxygen atom of the cyclic formal interacts with the Lewis acid, followed by nucleophilic ring-opening by the bipyridyl at the acetalic moiety. The thus formed silylated pyridinium intermediate releases formaldehyde upon hydrolysis and provides the 1,3-diol, or a monosilylated derivative thereof, depending on the pH of the hydrolytic agent (Scheme 4.27).[175]

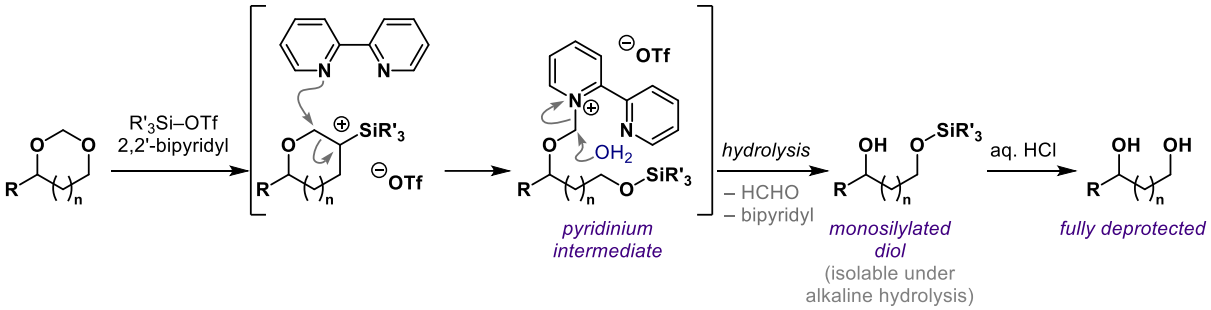

Scheme 4.27. Proposed mechanism for the ring-opening of cyclic formals with trialkylsilyl triflates and bipyridyl.

Since the proposed mechanism does not postulate a nucleophilic attack at the benzylic position, we considered that this strategy might be useful for us to not destroy the enantiopurity of the 1,3-dioxanes. In fact, when we applied these reaction conditions to our enantioenriched Prins product **4.3a** (er = 95.5:4.5), the 1,3-diol **4.9a** was obtained in 88% yield and, more importantly, without noticeable erosion of the enantiopurity (95:5 er) (Scheme 4.28).

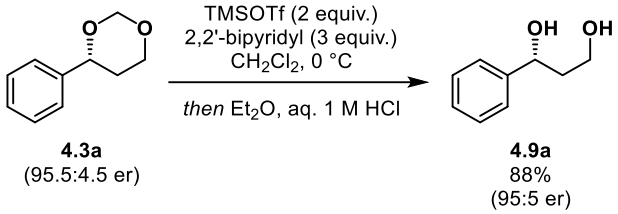

Scheme 4.28. Ring opening of 1,3-dioxane **4.3a** to the corresponding 1,3-diol using the conditions from Fujioka[175]: no loss of enantiopurity.

Diol **4.9a** represents a common intermediate in the synthetic routes toward several pharmaceutically active compounds, such as fluoxetine (Prozac®),[176] dapoxetine (Priligy®)[177] and tomoxetine (Strattera®).[176] The asymmetric syntheses of these compounds have a common starting material: the enantiopure 1,3-diol **4.9a**. This compound has been obtained with several asymmetric methods, such as enantioselective epoxidation of cinnamyl alcohol **4.12c**,[178] metal- or enzyme-catalyzed reduction of β-ketoester **4.12b**,[179] or lipase-catalyzed kinetic resolution of benzylic secondary alcohols[180] (Scheme 4.29). Even though these starting materials are relatively available, we recognized the potential applicability of our *i*IDP-catalyzed Prins reaction/1,3-dioxane opening sequence in the preparation of pharmaceutically active compounds from less functionalized, feedstock chemicals (styrene and paraformaldehyde).

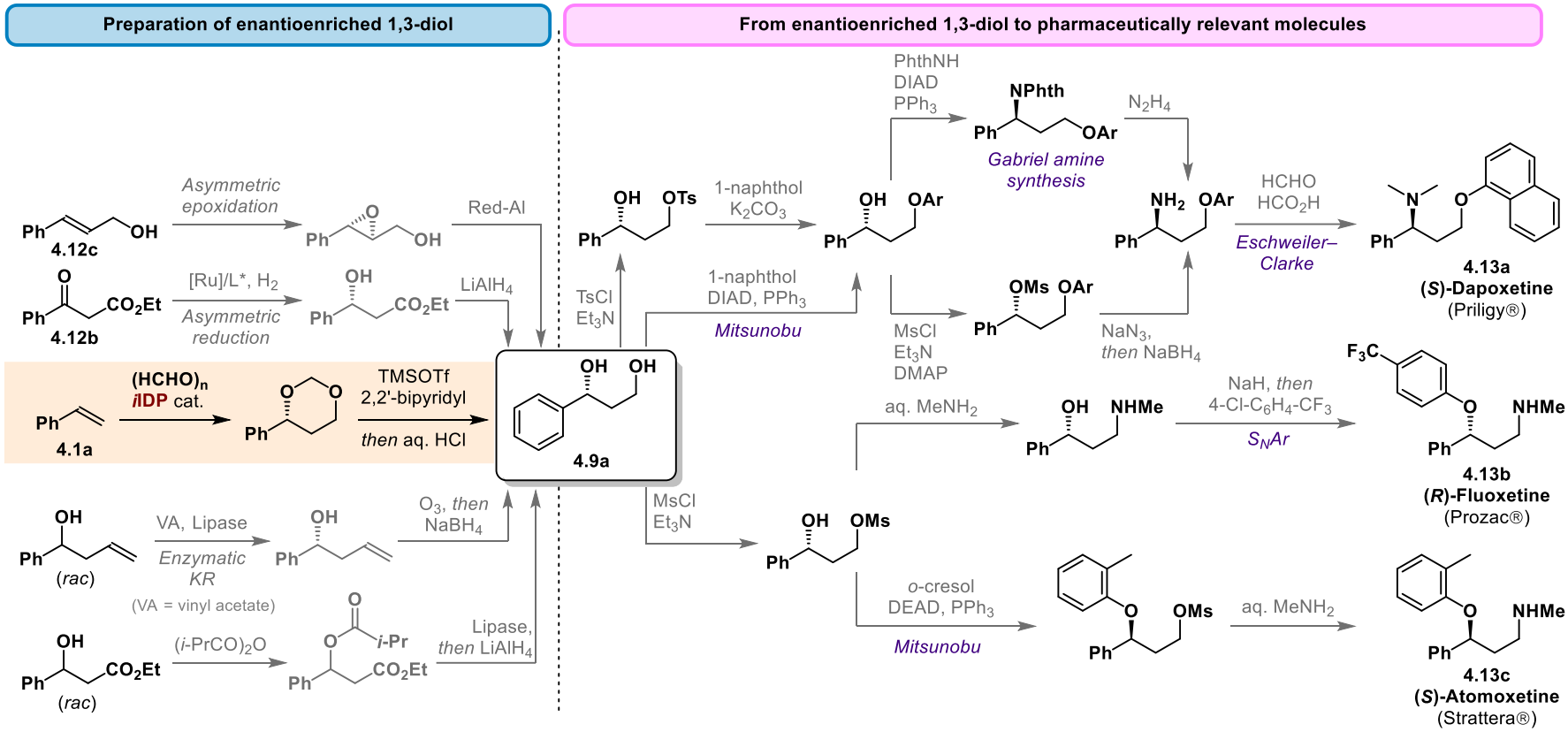

Scheme 4.29. Enantioenriched 1,3-diol **4.9a**: preparation routes and further transformation to pharmaceutically active compounds (dapoxetine, fluoxetine and atomoxetine).

4.2.4 Enantioenriched Deuterated 1,3-Dioxanes

The subtle differences that a C–D bond has in comparison to a C–H bond, such as a smaller vibrational frequency and a lower zero-point energy, have been exploited for decades toward the study of reaction mechanisms and biosynthetic pathways. Recently, medicinal chemistry has also focused the attention on deuterated molecules to modulate the metabolic stability of some drugs. This, in turn, has increased the demand for methods toward the selective introduction of deuterium atoms.[181]

Considering the previously presented application of the asymmetric Prins reaction as part of a synthetic route toward several pharmaceutically active compounds, as well as the commercial availability of paraformaldehyde-d_2 and the accessibility of deuterated styrene derivatives, we asked ourselves if these starting materials could be utilized to expand the scope of the developed enantioselective Prins reaction. In this way, enantiomerically-enriched deuterated 1,3-dioxanes could be prepared and further transformed toward deuterated 1,3-diols. Moreover, different combinations of protic or deuterated starting materials would allow us to control the position and degree of deuteration in the obtained products.

In analogy to the previously presented model Prins reaction, catalyst **4.5q** transformed a mixture of styrene (**4.1a**) and deuterated paraformaldehyde (**4.2e**) into the 1,3-dioxane-d_4 **4.3a(d_4)** in 62% yield with 95:5 er (Scheme 4.30).

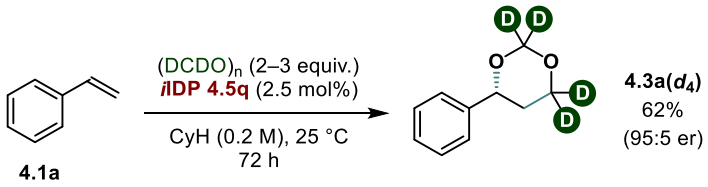

Scheme 4.30. The use of deuterated paraformaldehyde allows the synthesis of a 1,3-dioxane-d_4.

Motivated by this positive outcome, we prepared the doubly deuterated analog of styrene (styrene-β,β-d_2, **4.1zj**) adapting a reported route.[182] The synthesis started with the exchange of the acidic terminal alkyne proton in phenylacetylene for a deuterium atom. A subsequent regioselective hydrozirconation reaction using Schwartz's reagent afforded the terminal vinyl zirconium product, which underwent deuterodezirconation in the presence of D_2O to generate the targeted doubly deuterated olefin (Scheme 4.31).

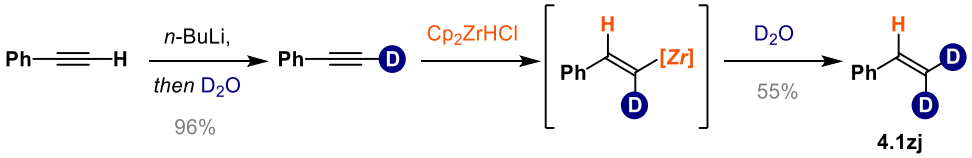

Scheme 4.31. Synthesis of styrene-β,β-d_2 (**4.1zj**).

Pleasantly, olefin **4.1zj** reacted with both protic (**4.2a**) and deuterated paraformaldehyde (**4.2e**) in the presence of catalyst **4.5q**, forming the corresponding 1,3-dioxanes, as d_2 or d_6 forms

(**4.3a(d_2)** and **4.3a(d_6)**), respectively, in good yields and excellent enantioselectivities (Scheme 4.32).

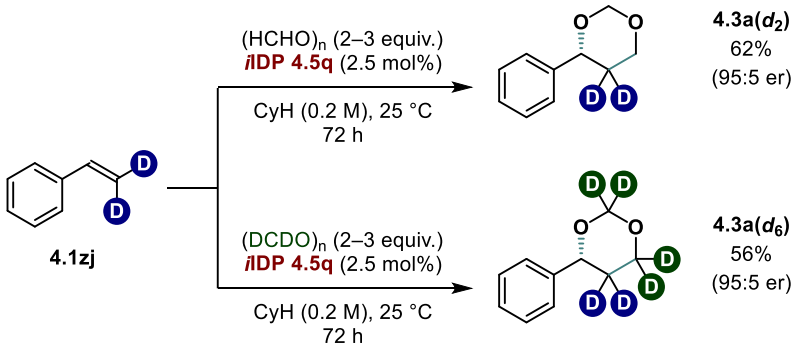

Scheme 4.32. Styrene-β,β-d_2 as substrate toward a 1,3-dioxane with tunable degrees of deuteration.

4.3 Mechanistic Investigations

According to several existing reports on mechanistic studies,[9, 134, 183] the acid-catalyzed Prins reaction is thought to proceed via a stepwise mechanism, as depicted in Scheme 4.33, where the olefin engages a nucleophilic addition to an acid-activated molecule of formaldehyde (aldehydium ion **4.M1**) to form an intermediate γ-hydroxybenzyl cation **4.M2**. The fate of this species explains the formation of multiple products, such as unsaturated alcohols, 1,3-glycols and esters thereof, and 1,3-dioxanes, among others. For example, the formation of the 1,3-dioxane **4.3a** can be explained if the intermediate **4.M2** further reacts with a second molecule of formaldehyde, forming a cationic hemiacetal **4.M3** that readily undergoes cyclization (**4.M4**).

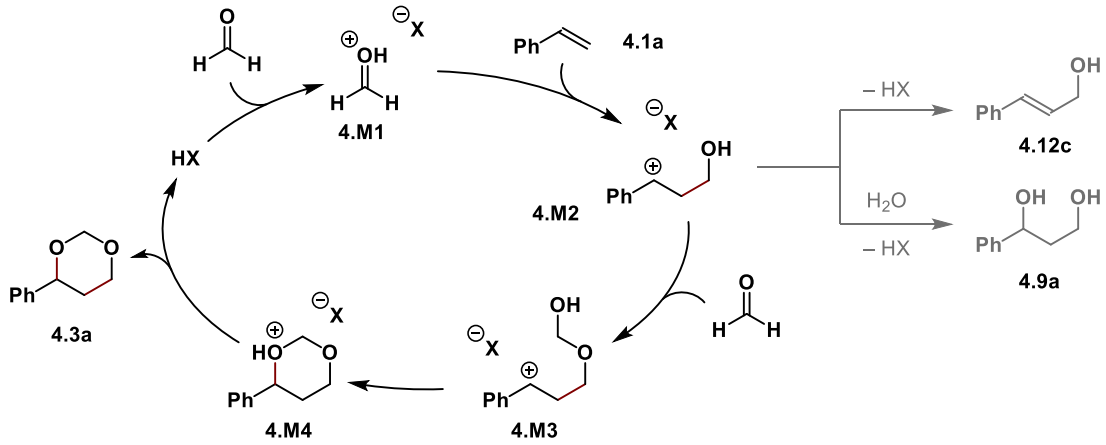

Scheme 4.33. Proposed stepwise mechanism for the Prins reaction of styrene and formaldehyde.

We were eager to gain some insight into the reaction pathway that operates in our developed methodology, and to determine how similar it is from the above-mentioned “accepted” mechanism. We hypothesized that some differences might exist, considering that our methodology uses an oligomeric form of formaldehyde (paraformaldehyde) rather than the monomer. Therefore, we first wanted to gain some insight about the role of the oligomeric

chain of paraformaldehyde, if any, and how the two units of formaldehyde required to form the 1,3-dioxane react with the olefin.

4.3.1 About The Reactive Formaldehyde Species

PRELIMINARY OBSERVATIONS AND HYPOTHESIS

On the early stages of Reaction Development, at the beginning of this project, we observed that using *substoichiometric* amounts (< 2 equiv.) of paraformaldehyde **4.2a** in the reaction with styrene (**4.1a**) in the presence of *i*IDP **4.5b** still resulted in the formation of the 1,3-dioxane **4.3a** as major product. This result was unexpected, since we had envisioned the reaction to begin with the slow release of formaldehyde monomer, which would be activated by the *i*IDP acid catalyst; also, we expected the γ-hydroxycarbocationic intermediate to undergo other pathways due to the low amount of formaldehyde available, thus forming unsaturated alcohols or 1,3-glycols. However, neither the 1,3-glycol **4.9a** nor the unsaturated alcohol (cinnamyl alcohol, **4.12c**) could be detected in the crude reaction mixture.

Also during the Reaction Development, as it was mentioned in Section 4.1.3, several formaldehyde sources (paraformaldehyde, *sym*-trioxane and formalin) were tested for the *i*IDP-catalyzed Prins reaction with styrene, observing differences in the reactivity, but almost no changes in the enantioselectivity of the transformation. To complement this results, we then decided to test the reaction using monomeric HCHO (**4.2f**), which we prepared following the procedure reported by Schlosser (cracking paraformaldehyde in the presence of Ts_2O, co-distilling the formed monomer with THF and collecting the solution at –78 °C).[121b] The obtained solution indeed contained formaldehyde monomer as major component, according to the ^{1}H NMR analysis of an aliquot thereof, and confirmed by volumetric analysis ([HCHO] ≈ 0.34 M, by treatment with excess Na_2SO_3 and subsequent acid-base titration). Interestingly, when the freshly obtained solution of monomeric HCHO was used in the Prins reaction of **4.1a** with *i*IDP **4.5b** at 25 °C, no signals of the 1,3-dioxane **4.3a** were detected in ^{1}H NMR after 24 h. It is worth to mention here that the use of methylal (**4.2d**, another monomeric formaldehyde derivative) as HCHO source did not result in any conversion.

Based on these results, we asked ourselves if an oligomeric structure of formaldehyde is required for the *i*IDP to catalyze the reaction (Scheme 4.34). Both paraformaldehyde (**4.2a**) and *sym*-trioxane (**4.2b**) are per se non-monomeric forms, namely a polymer and a cyclic trimer. Despite its oligomeric nature, **4.2b** is less reactive, probably because of the thermodynamic stability of the six-membered ring and the associated energetic penalty involved to generate reactive species from this stable ring. On the other side, formalin is known

to contain a mixture of poly(oxymethylene)glycols that interconvert with each other, and this equilibria can be affected by concentration and temperature.[184]

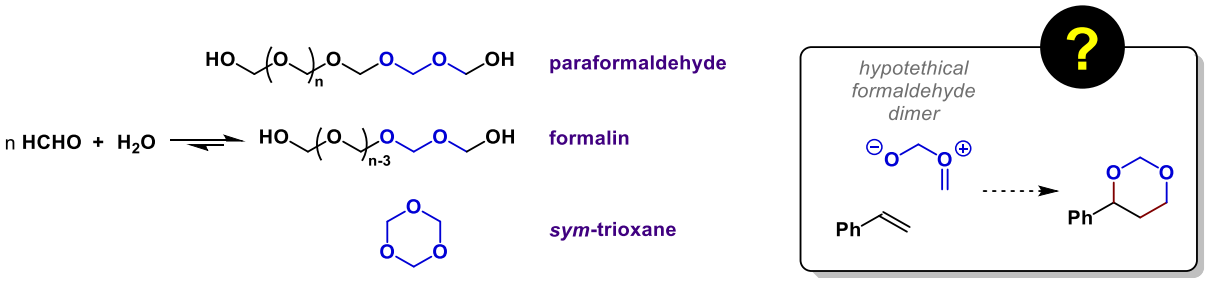

Scheme 4.34. Can a formaldehyde dimer be involved in the *i*IDP-catalyzed Prins reaction?

SOLUBLE FORMALDEHYDE OLIGOMERS

To delve into the role of oligomeric formaldehyde sources, we examined other types of oligomeric polyoxymethylenes. Methylal is essentially the smallest member of the family of poly(oxymethylene) dimethyl ethers (POMDMEs: MeO–$(CH_2O)_n$–Me). If the methoxy capping groups are replaced by acetates, the substances belong to the family of poly(oxymethylene) diacetates (POMDAs: AcO–$(CH_2O)_n$–Ac), which are commonly prepared by the reaction of formaldehyde oligomers (trioxane or paraformaldehyde) with acetic anhydride in the presence of a Lewis acid. We prepared the $POMDA_3$ (**4.2h**) by reaction of *sym*-trioxane and acetic anhydride in the presence of $ZnCl_2$, following the reported procedure from King and Stanonis (Scheme 4.35).

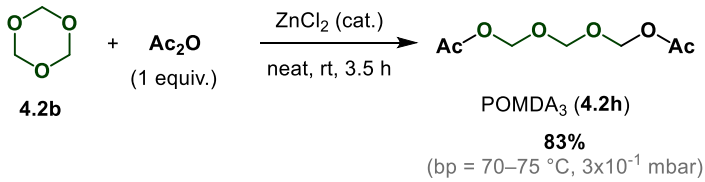

Scheme 4.35. Synthesis of $POMDA_3$ from *sym*-trioxane and acetic anhydride.

We next evaluated the performance of the obtained $POMDA_3$ and the commercially available $POMDME_2$ (**4.2i**) as formaldehyde sources, as well as the simplest series of those families (both commercially available): $POMDA_1$ (methylene diacetate, **4.2g**) and $POMDME_1$ (methylal, **4.2d**). When these formaldehyde surrogates were reacted with styrene and *i*IDP **4.5b** (2.5 mol%) in $CHCl_3$ at rt for 48 h, a difference in reactivity between the "oligomers" and the "monomers" was evident (Scheme 4.36): for the monomers, $POMDA_1$ barely presented one turnover (3% yield of the 1,3-dioxane **4.3a**) and, exactly as observed during earlier stages, $POMDME_1$ did not lead to any product. Contrarily, the oligomers performed better: $POMDA_3$ produced 24% of **4.3a** (er = 94:6), and using $POMDME_2$ resulted in 51% yield (er = 92:8).

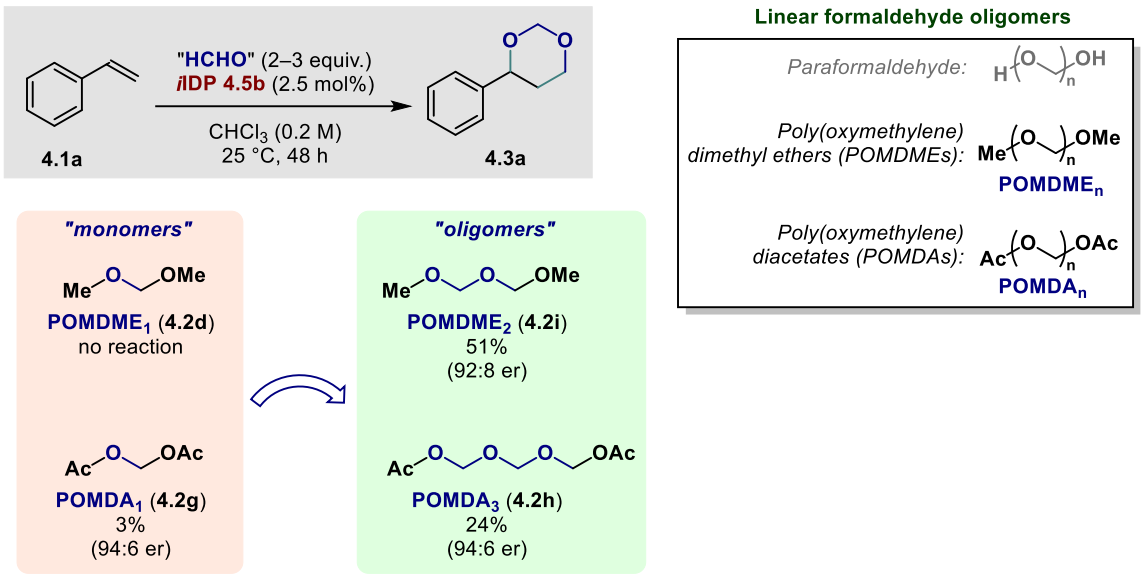

Scheme 4.36. Comparison of linear mono- and oligo-oxymethylenes as formaldehyde source.

4.3.2 Isotope-Labeling Studies

Deuterium-containing substances have played a key role in the elucidation of reaction mechanisms for decades, due to the kinetic isotope effects arising from the differences between the ^{1}H and the ^{2}H nuclei. Similarly, substances containing ^{13}C and, to a lesser extent, other isotopes (^{15}N, ^{18}O, among others) are broadly utilized in mechanistic experiments.[185] Therefore, we decided to design experiments with isotope-labeled substances to gain information about our developed organocatalytic, asymmetric, intermolecular Prins reaction.

COMPETITION EXPERIMENT: PARAFORMALDEHYDE VS. PARAFORMALDEHYDE-D_2

The previously presented results with POMDAs/POMDMEs reinforced our hypothesis that the reaction proceeds better with oligomeric formaldehyde sources. Therefore, we wondered if the two "*formaldehyde units*" that react with the olefin would come from different oligomer chains, or the olefin "captures" them from the same chain. To shed light on this mechanistic aspect, it would be necessary to have two different types of oligomeric species, such that they can be quantified when inserted into the reaction product. For this, we envisioned the use of paraformaldehyde ($(HCHO)_n$, **4.2a**) and the deuterated analogue thereof ($(DCDO)_n$, **4.2e**), both commercially available.

Our designed experiment consists in reacting an olefin with a mixture of **4.2a** and **4.2e**, to then determine the relative amount of ^{1}H (or ^{2}H) incorporation in the two "formaldehyde units" of the produced 1,3-dioxane (positions C-2 and C-6), and the degree of ^{1}H incorporation can be readily quantified by means of ^{1}H NMR spectroscopy. We anticipated two possible outcome scenarios (Scheme 4.37):

- *Each formaldehyde unit comes from a different chain:* a statistical mixture of 1,3-dioxane products should be obtained, taking into account the ratio of $(HCHO)_n$ to $(DCDO)_n$ (**4.2a** to **4.2e**) at the beginning of the experiment, as well as potential KIEs. These factors would result in the position C-2 and C-6 having different amounts of ^1H (and also of ^2H) from each other.
- *Both formaldehyde units come from the same paraformaldehyde chain:* every produced molecule of 1,3-dioxane should contain the same isotope (either H or D) on both positions C-2 and C-6. This would be reflected in a C-2/C-6 ^1H content ratio close to 1.

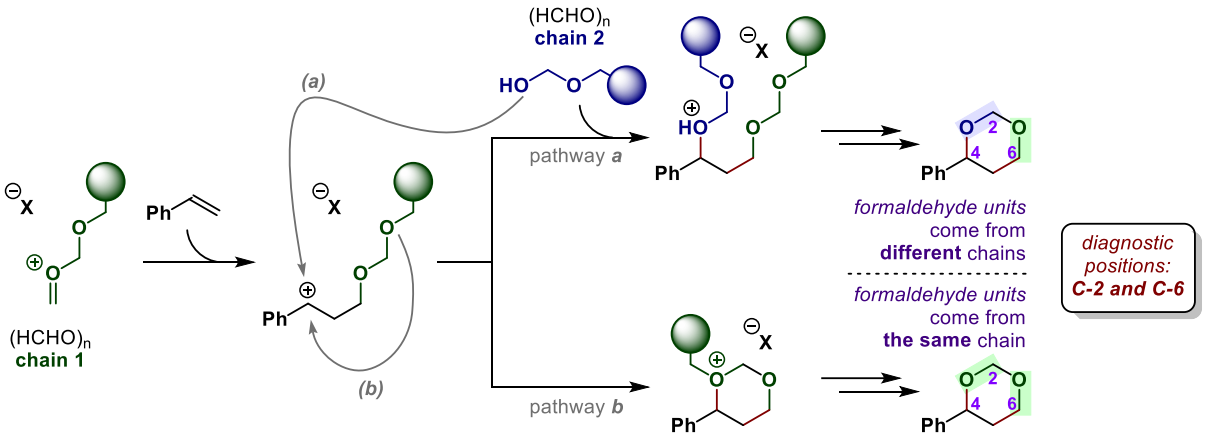

Scheme 4.37. How many paraformaldehyde chains? Possible scenarios for the Prins reaction.

We conducted experiments with different **4.2a**:**4.2e** ratios, in each case using either *p*-TsOH or *i*IDP **4.5b** as catalysts. After 24 h, all the reactions were stopped by adding Et_3N and immediately analyzed by ^1H NMR, obtaining the results shown in Table 4.2.

Table 4.2. ^{1}H NMR analysis of the Prins reaction of styrene (**4.1a**) with mixtures of paraformaldehyde (**4.2a**) and paraformaldehyde-d_2 (**4.2e**).

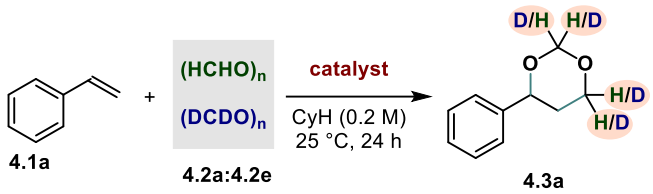

Catalyst	$(HCHO)_n$:$(DCDO)_n$ **4.2a:4.2e**	^{1}H NMR Integrals							Ratio H-2/H-6
		H-4	H-2_a	H-2_b	H-6_a	H-6_b	H-2: H-2_a + H-2_b	H-6: H-6_a + H-6_b	
*i*IDP **4.5b**	Only **4.2a**	1.00	0.96	1.11	1.02	1.03	2.07	2.05	1.01
	2:1	1.00	0.80	0.90	0.84	0.83	1.70	1.67	**1.02**
	1:1	1.00	0.70	0.80	0.73	0.73	1.49	1.47	**1.02**
	1:2	1.00	0.44	0.54	0.54	0.54	0.97	1.08	**0.90**
	Only **4.2e**	1.00	0.00	0.00	0.00	0.00	0.00	0.00	n/a
p-TsOH	Only **4.2a**	1.00	0.98	1.08	0.98	0.99	2.06	1.97	1.05
	2:1	1.00	0.61	0.65	0.98	1.00	1.26	1.98	**0.64**
	1:1	1.00	0.44	0.47	0.96	0.99	0.91	1.95	**0.47**
	1:2	1.00	0.31	0.34	0.70	0.71	0.65	1.41	**0.46**
	Only **4.2e**	1.00	0.00	0.00	0.00	0.00	0.00	0.00	n/a

The H-2/H-6 ratios indicate a striking difference between the two catalysts. The products from reactions with *i*IDP **4.5b** had ratios close to 1, regardless of the composition of the mixture of paraformaldehyde chains. Contrarily, the ratios from the reactions with *p*-TsOH as catalyst presented a clear deviation from 1 and there were also differences between the values depending on the composition of the **4.2a**/**4.2e** mixtures.

Before misinterpreting the obtained data, we wanted to determine a possible interference: *transacetalization*. Thus, we treated racemic **4.3a** with $(DCDO)_n$ in the presence of the two studied catalysts under the same conditions from the previous experiment, but in none of the cases differences in the ^{1}H integrals of C-2 and C-6 were obtained, allowing us to rule out transacetalization as potential side reaction (Scheme 4.38).

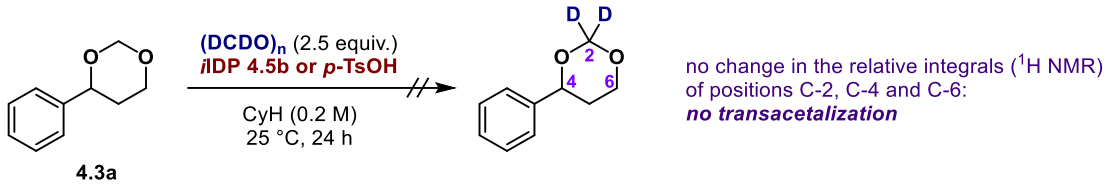

Scheme 4.38. Ruling out possible transacetalization of the 1,3-dioxane.

Connecting the obtained results with the anticipated possible scenarios of this experiment (Scheme 4.37), we could postulate that the *i*IDP-catalyzed Prins reaction proceeds by pathway ***(b)***, where both formaldehyde units come from the same paraformaldehyde chain. Conversely, the use of *p*-TsOH as catalyst results in formaldehyde capture from different chains. A plausible explanation for this difference can consist in the confined nature of the *i*IDP catalyst, in stark contrast to the open acidic site of *p*-TsOH, as depicted in Figure 4.7.

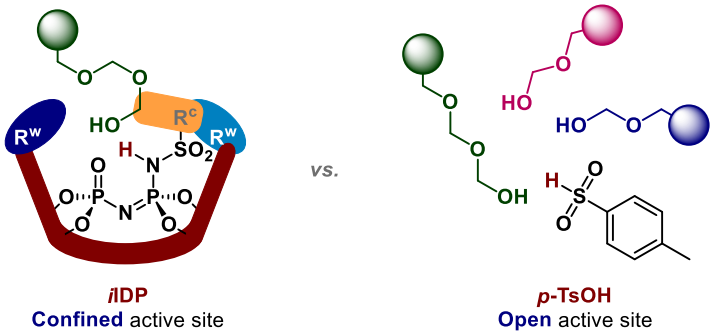

Figure 4.7. Key role of confinement in the observed "paraformaldehyde chain selectivity"

DEUTERIUM-LABELED SUBSTRATES: DIASTEREOSPECIFICITY

In light of the different pathways by which the reaction occurs when using either *i*IDPs or *p*-TsOH as catalyst for the Prins reaction, we wondered if the confinement might also have any influence on the order of events. In other words, whether the mechanism really proceeds in a stepwise fashion or not. For this, we conceived using substrates displaying *E*/*Z* isomerism, so that some information on diastereospecificity can be obtained. As shown in Section 4.2.2, *trans*-substituted olefins, such as *trans*-*β*-methyl-styrene (**4.10a**) or *trans*-anethole (**4.10b**), produced the corresponding *trans*-1,3-dioxanes as major products. However, their reduced reactivity in comparison to parent styrene in the presence of *p*-TsOH did not allow us to make any comparison between the two catalysts. Inspired by the synthetic ease to obtain deuterated styrene derivatives, such as the previously discussed styrene-*β*,*β*-d_2 **4.1zj**, we envisioned using *β*-monodeuterated styrenes, which could be available either as the *trans*- (*E*-, **4.1zk**) or as the *cis*- (*Z*-, **4.1zl**) isomer. Indeed, following a similar synthetic approach from phenylacetylene (or its deuterated analog), Schwartz's reagent and a source of H^+ (or D^+), both isomeric monodeuterated olefins could be prepared (Scheme 4.39).

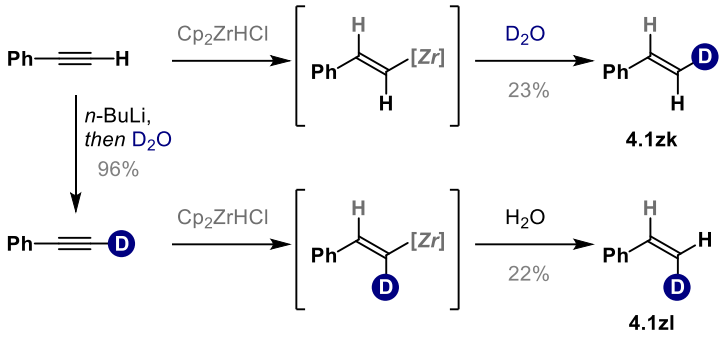

Scheme 4.39. Synthesis of both isomers of styrene-***β*-*d***.

With these olefins in hand, we tested their reaction with paraformaldehyde in the presence of an acid catalyst: either *p*-TsOH or *i*IDP **4.5b**. As can be seen on Scheme 4.40, when the two catalysts are compared, the crude reaction mixtures from the *trans*-olefin presented different signal patterns on ^{1}H NMR. The reaction with *i*IDP led to simpler coupling patterns than their counterpart with *p*-TsOH. When the *cis*-olefin reacted in the presence of *i*IDP, different signals were observed, attributable to the other diastereoisomer of the expected monodeuterated 1,3-dioxane. Additionally, the shapes of the signals for the *p*-TsOH case look like an additive overlap of the signals for both *i*IDP cases (*cis*- and *trans*- olefin): the *p*-TsOH-catalyzed reaction transforms the *trans*-olefin into a mixture of *cis*- and *trans*-1,3-dioxanes (*diastereomer scrambling*), in contrast to the observed diastereospecificity with *i*IDP as catalyst.

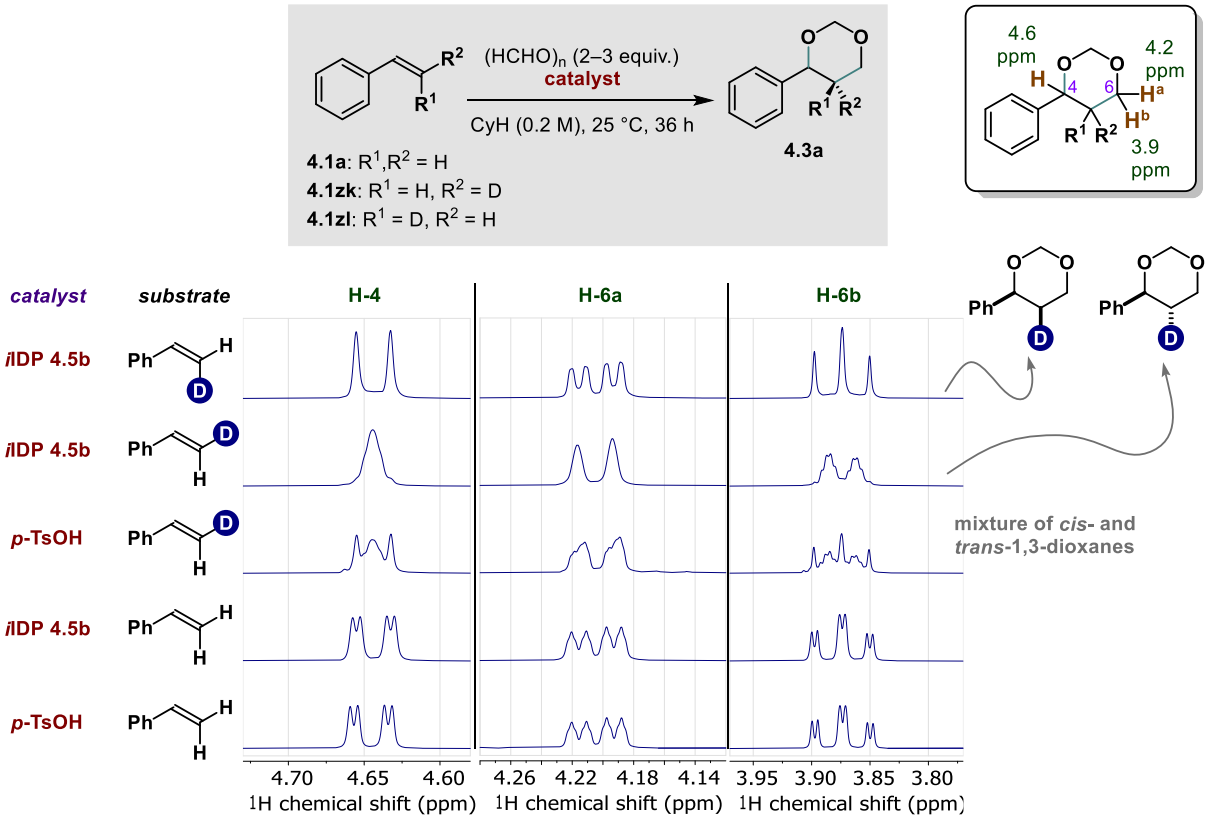

Scheme 4.40. ^{1}H NMR analysis of the Prins reaction of ***β*-deutero-styrenes (**4.1zk** and **4.1zl**) with **4.2a**.

At this point, we wondered if *p*-TsOH could be able to isomerize the olefins before the Prins reaction takes place. However, after stirring a mixture of *trans*-olefin **4.1zk** and *p*-TsOH (20 mol%) in $CHCl_3$ for 5 days at rt, neither the chemical shift nor the shape/coupling constant of the olefinic signals was detected on ^1H NMR, ruling out a possible "*pre-Prins*" isomerization.

Together, these results point out toward a parallel of stepwise/concerted pathways. The observed diastereomer scrambling with *p*-TsOH points out toward the intermediacy of a freely-rotating species *during* the Prins reaction, which we assume is the previously mentioned γ-hydroxycarbocation that originates after nucleophilic addition of the olefin to the activated aldehyde (Scheme 4.41). On the other hand, the results from the *i*IDP reactions go rather in direction of a more concerted pathway, where such a freely-rotating species is not formed or, if formed, then it is rather short-lived.

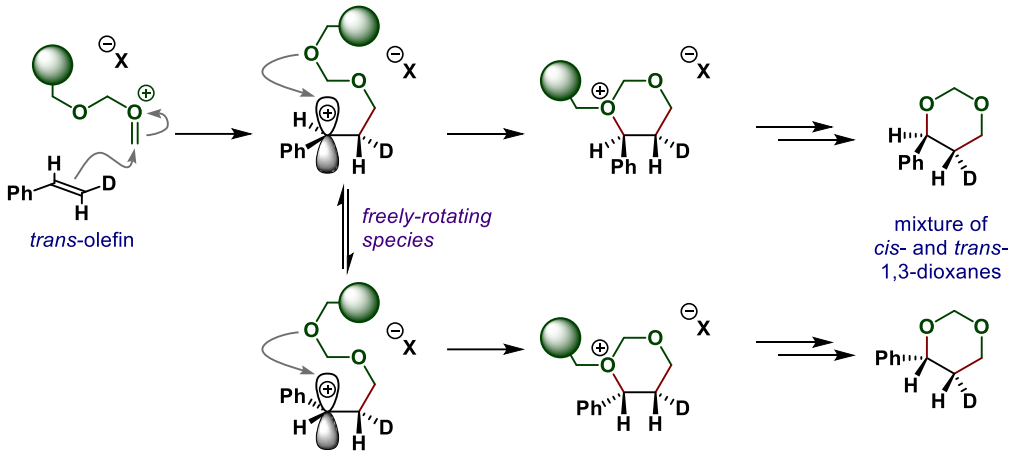

Scheme 4.41. Freely-rotating γ-hydroxycarbocation: diastereomer scrambling in the Prins reaction with *p*-TsOH.

4.3.3 Computations

(this part was conducted in collaboration with Dr. Rajat Maji)

EFFECT OF CONFINEMENT IN THE REACTION PATHWAY

In order to gain further insights into the reaction mechanism and to rationalize the mechanistic dissimilarities between the confined *i*IDP and the open *p*-TsOH, computational studies (level of theory: PBE-D3/def2-SVP) were performed. Due to the polymeric nature of paraformaldehyde, we considered a formaldehyde dimer-derived aldehydium ion as reactive species (a so-called "truncated electrophile"), with a methoxy group in the end (*capping group*) to resemble the polymeric chain of paraformaldehyde. The reaction of the ion-paired aldehydium ion (using the conjugate base of either *i*IDP or *p*-TsOH as counteranions) with styrene was studied by computing the corresponding transition states (TS) for the C–C bond-forming event (Scheme 4.42).

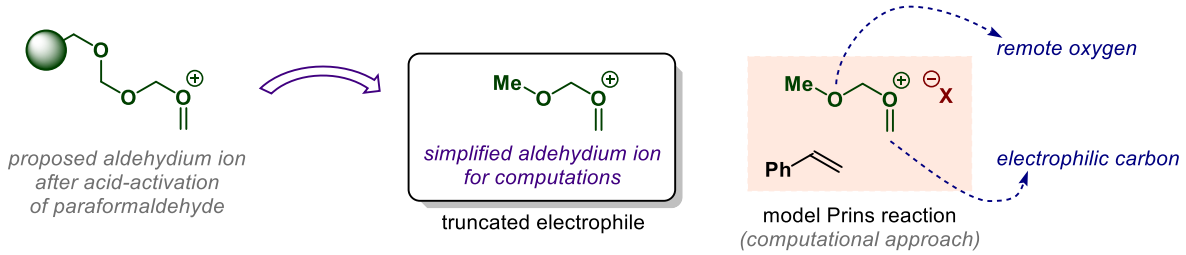

Scheme 4.42. Computational approach to study the Prins reaction.

The optimized TS in the presence of the *p*-toluenesulfonate anion (**TS1**) displays the electrophilic carbon atom of the aldehydium ion approaching both carbon atoms of the olefin moiety, resembling a non-classical "onium" ion, with some similarity to the halonium ions that participate in the accepted mechanism of alkene dihalogenation. In **TS1**, the distance between the benzylic carbon and the "*remote oxygen*" is 4.95 Å, which makes a concerted cyclization scenario rather unlikely (Figure 4.8). This arrangement suggests a stepwise operating pathway, where the benzylic carbocation intermediate can undergo free rotation, which can explain the observed *diastereomer scrambling* in the reaction with styrene-*β-d* (**4.1zk** and **4.1zl**).

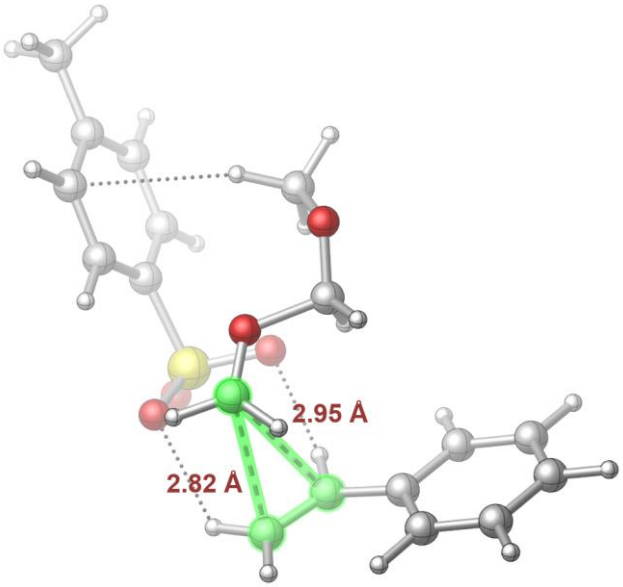

Figure 4.8. Computed transition state **TS1** (PBE-D3/def2-SVP); counteranion: conjugate base of *p*-TsOH.

A very different geometry was obtained from the optimized TS using the conjugate base of *i*IDP **4.5b** as counteranion (**TS2**). In this case, the aldehydium ion approaches the olefin moiety achieving a chair-like geometry, where the C–C bond-formation event takes place before the C–O bond formation. The distance between the terminal olefinic carbon and the electrophilic carbon is 1.96 Å, whereas the distance between the benzylic carbon and the "remote" oxygen is 3.08 Å. It is however interesting that the C···O distance in this case is significantly shorter than for the case of *p*-TsOH as catalyst (**TS1**), due to a change in the conformation of the formaldehyde dimer species, probably dictated by the confined nature of the *i*IDP anion.

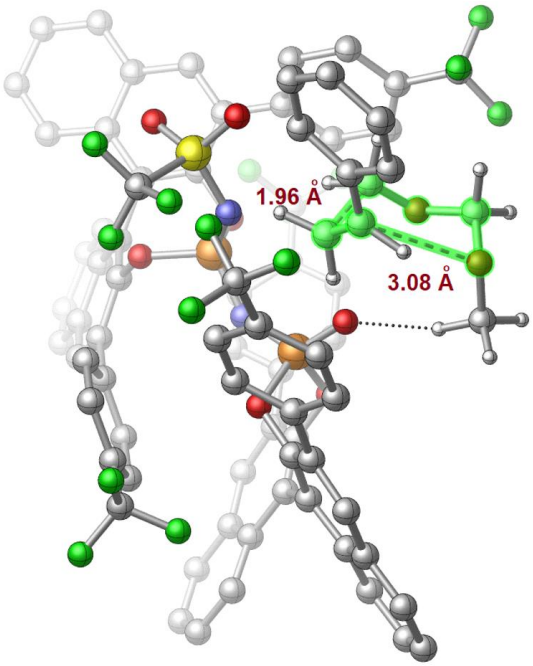

Figure 4.9. Computed transition state **TS2** (PBE-D3/def2-SVP); counteranion: conjugate base of *i*DP **4.5b**.

UNDERSTANDING THE ORIGIN OF ENANTIOSELECTIVITY

Next, we embarked on understanding the reason behind the observed enantioselectivity. To do so, we computed the TSs toward each enantiomer of the product (M06-2X/def2-TZVP+ CPCM(cyclohexane)//PBE-D3/def2-SVP). Due to the difference in computed energy between both transition states ($\Delta\Delta G^{\ddagger}$ = 2.68 kcal/mol), an enantiomeric ratio of 99:1 is predicted for the Prins reaction of styrene **4.1a** with catalyst **4.5b** at 298 K, being this in good agreement with the experimentally observed value (94:6 er). To identify the origin of the stereoinduction, a distortion-interaction analysis was conducted.[186] The main part of the calculated energy difference ($\Delta\Delta E^{\ddagger}_{gas}$ = 2.3 kcal/mol) can be ascribed to distortion effects ($\Delta\Delta E^{\ddagger}_{distortion}$ = 2.1 kcal/mol).

4.3.4 Proposed Catalytic Cycle

Bringing together all the pieces from the presented mechanistic information, we proposed a mechanism for the *i*DP-catalyzed Prins reaction (Scheme 4.43). At first, the Brønsted acid catalyst (***i*DP**) interacts with the oligomeric chain of paraformaldehyde (**4.2a**), probably on the terminal hemiacetal groups due to steric reasons (**4.CC1**), although we do not exclude the possibility of other oxygen atoms also acting as Lewis base if the oligomeric chain fits in the active site of the catalyst (**4.CC5**). Upon release of either water or a shorter oligomeric chain (depending where the protonation takes place), an aldehydium ion is formed (either **4.CC2** or **4.CC6**) and builds a contact ion pair with the chiral, enantiopure *i*DP anion, which, in turn, might force the oligomeric chain of this aldehydium ion to adopt a pseudo s-*cis* conformation.

At this point, the nucleophilic olefin moiety of styrene (**4.1a**) approaches the electrophilic carbon and the C–C bond-formation takes place via **TS2**. The incipient benzylic cation, which would arise at this step, is in close proximity to the so-called "remote oxygen" of the oligomeric chain, and readily undergoes the cyclization step. This means that the sequence of C–C and following C–O bond-forming events occurs in a rather *concerted* pathway (as suggested by the lack of diastereomer scrambling in the reactions with styrene-*β*-*d*), although also in a *highly asynchronous* fashion (as shown by the interatomic distances in **TS2**). It is noteworthy how this addition of a formaldehyde oligomer to the olefin has a certain resemblance to the transition states from [4+2] cycloaddition reactions. After the cyclization has occurred, the already formed 1,3-dioxane ring still hangs on the residual oligomeric chain (**4.CC3**), which gets cleaved on one of these proposed ways: either by itself to produce a new, shorter aldehydium ion paired with the *i*IDP anion (**4.CC4**), ready to react with another molecule of olefin; or with the aid of water, to produce a shorter paraformaldehyde chain and recover the catalyst in its Brønsted acidic form (***i*IDP**).

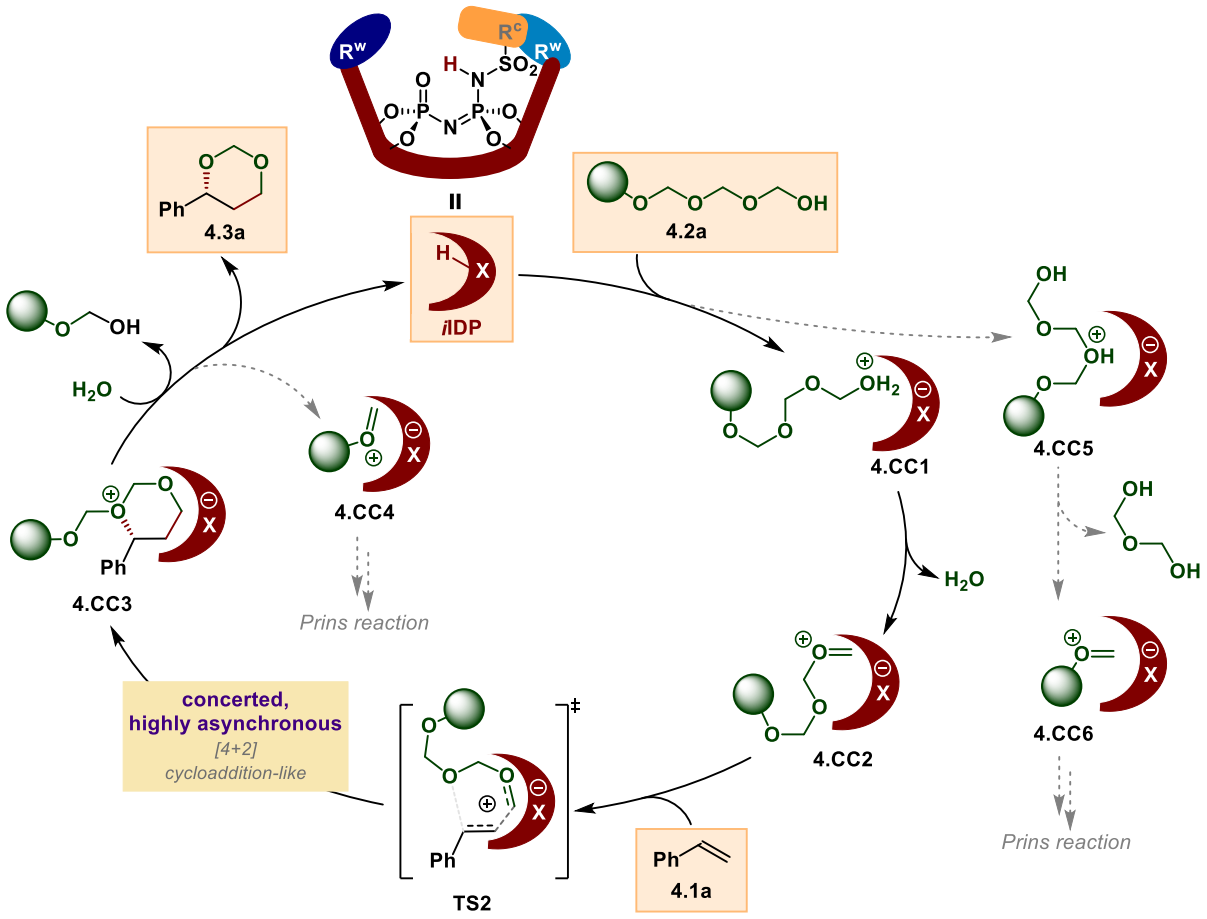

Scheme 4.43. Proposed catalytic cycle for the *i*IDP-catalyzed Prins reaction of styrene and paraformaldehyde.

Page left intentionally blank

5 Summary

Despite their significant potential, catalytic, asymmetric reactions of olefins with formaldehyde are rare and metal-free approaches have not previously been disclosed. We have developed a catalytic, asymmetric, intermolecular Prins reaction of aryl olefins and paraformaldehyde to form enantiomerically-enriched 1,3-dioxanes, using confined imino-imidodiphosphate (*i*IDP) Brønsted acid catalysts.

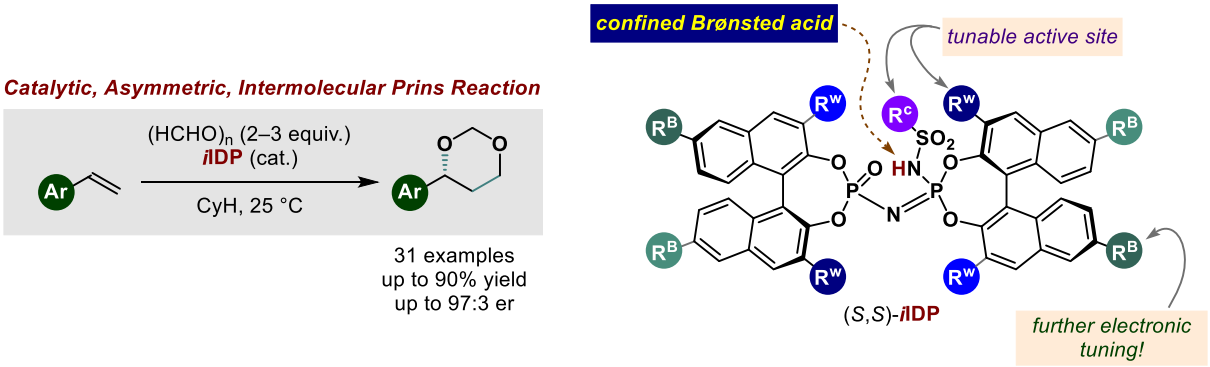

Scheme 5.1. The *i*IDP-catalyzed, asymmetric, intermolecular Prins reaction of terminal aryl olefins and paraformaldehyde.

Depending on the electronic properties of the olefin, influenced by the presence of substituents on the aromatic ring, different levels of acidity are required to obtain reactivity *and* selectivity, which allowed us to design a library of catalysts, from IDPs to highly acidic *i*IDPs. However, the more acidic IDPis activated paraformaldehyde in a way that resulted into cleavage of the inner core from the catalyst, by means of a metathesis-like process between the oxygen of the aldehyde and the sulfonylimino substituents on the inner core.

The enantioenriched 1,3-dioxanes could be transformed into the corresponding optically active 1,3-diols, which are valuable synthetic building blocks. Additionally, the scope of the *i*IDP-catalyzed asymmetric, intermolecular Prins reaction could be extended for the preparation of deuterated 1,3-dioxanes, with full control of the degree and the position of the deuteration by proper choice of the starting materials.

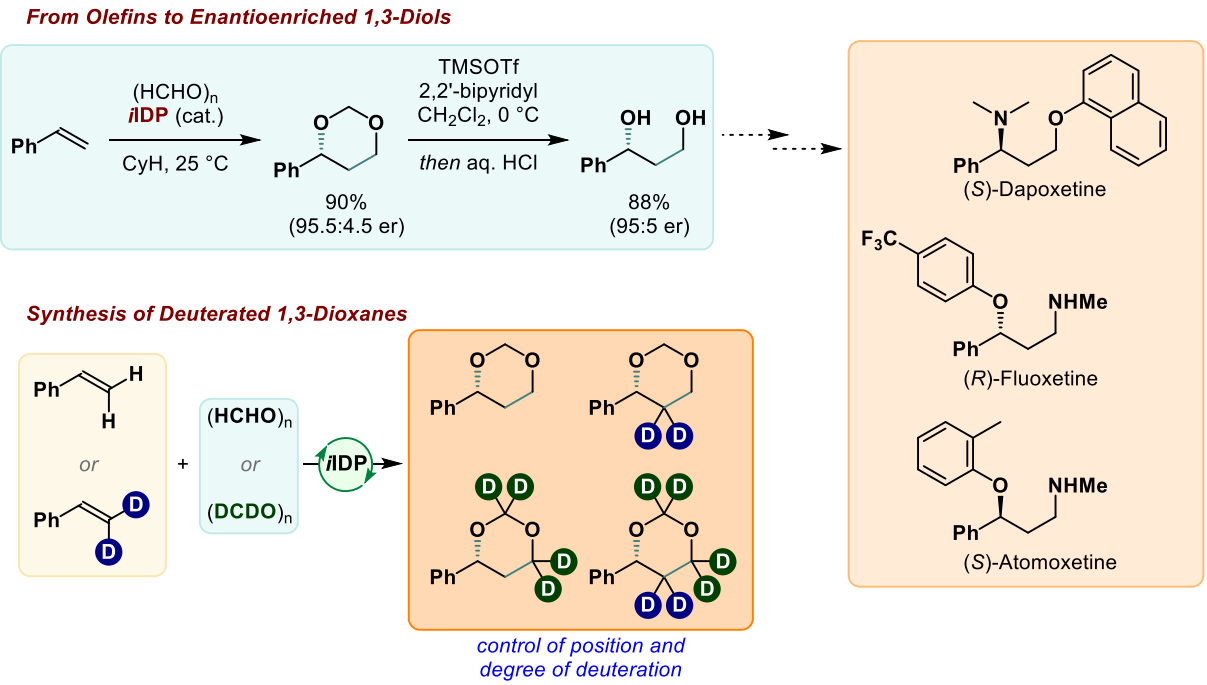

Scheme 5.2. Applications of the developed Prins reaction to the synthesis of 1,3-diols and deuterated derivatives thereof.

Based on isotope labeling experiments and computations, we propose a reaction mechanism where the confined nature of the *i*IDP catalyst leads to a concerted, highly asynchronous addition of an acid-activated formaldehyde oligomer to the olefin.

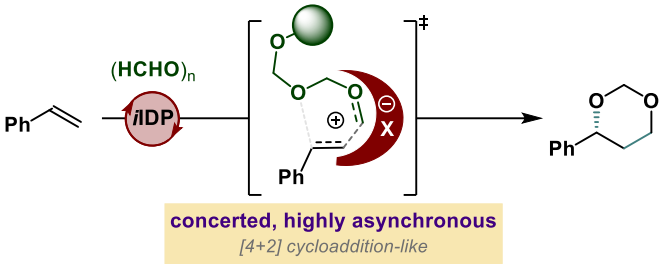

Scheme 5.3. Concerted, highly asynchronous reaction of styrene and an oligomeric formaldehyde chain in the confined cavity of the *i*IDP anion.

6 Outlook

6.1 Other Aldehydes and Olefins

Having disclosed the catalytic, asymmetric, intermolecular Prins reaction of aryl olefins and paraformaldehyde, we then envisioned expanding the scope of this transformation to other types of substrates. As already mentioned in Section 4.2.2, internal aryl olefins proved more challenging and further catalyst optimization will be required.

When considering other aldehydes different than formaldehyde, several additional challenges appear, such as: *(i)* lower electrophilicity, requiring stronger acids for their activation, *(ii)* the existence of enantiotopic faces (*re*/*si*) leads to 1,3-dioxanes containing two additional stereocenters, and *(iii)* if enolizable aldehydes are used, aldol reactions can further complicate the product selectivity of the transformation.

Gratifyingly, preliminary results indicate that the reaction of styrene (**4.1a**) and acetaldehyde (**6.1a**) can be catalyzed by IDPis (Scheme 6.1). Unlike for their reaction with formaldehyde, these acids are stable enough under the tested conditions and do not undergo inner core cleavage or any other kind of deactivation. Using IDPi **4.6d**, the 1,3-dioxane **6.2** was obtained as a mixture of diastereoisomers (**6.2a**, **6.2b** and **6.2c**), with the *all-cis* being the major one. Several presentations of acetaldehyde proved all reactive: monomer (**6.1a**), cyclic trimer (*paraldehyde*, **6.1b**) and cyclic tetramer (*metaldehyde*, **6.1c**). In all cases, *trans*-crotonaldehyde **6.3** was detected as side product by ^{1}H NMR, arising from the acid-catalyzed aldol condensation of acetaldehyde.

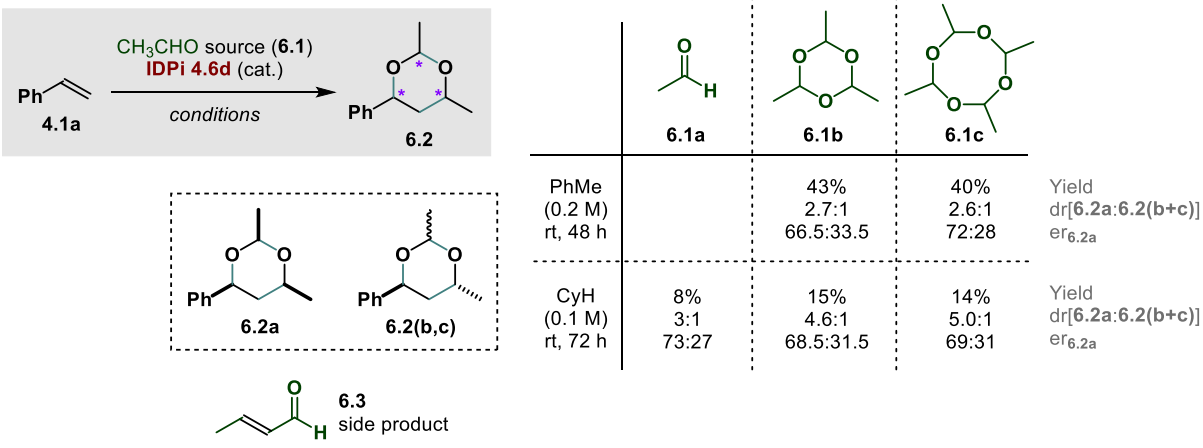

Scheme 6.1. IDPi-catalyzed Prins reaction of styrene and acetaldehyde.

6.2 Other Heteroatom-Stabilized Carbocations

We envisioned expanding the developed intermolecular Prins reaction by using other with heteroatom-stabilized carbocations. In collaboration with Dr. Sensheng Liu and Marian Guillén, we studied the three-component reaction of aryl olefins **4.1**, formaldehyde (as *sym*-trioxane **4.2b**) and sulfonamides/carbamates **6.3**/**6.4**, expecting to involve formaldehyde-derived iminium ions as electrophiles. Using the strong achiral Brønsted acid DNBSA (2,4-dinitrobenzenesulfonic acid hydrate) as catalyst, the corresponding 1,3-oxazinanes **6.5** were obtained (Scheme 6.2). However, the development of an asymmetric variant of this reaction has proven challenging and requires further work. For example, IDPi **4.6c** afforded product **6.5a** (using styrene **4.1a** and *p*-toluenesulfonamide **6.3a**), albeit only in 23% yield and with low enantioselectivity (56.5:43.5 er).

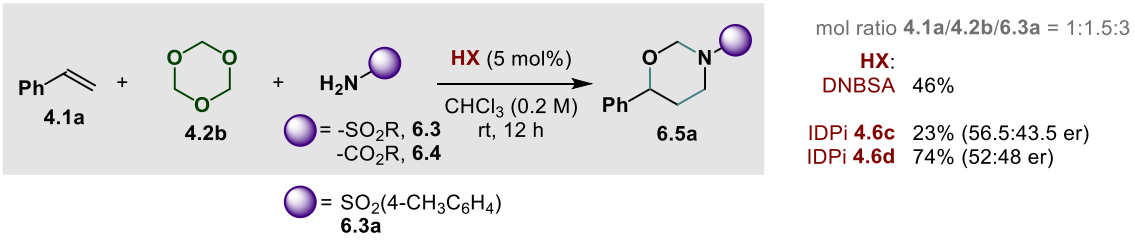

Scheme 6.2. Acid-catalyzed three-component reaction of olefins, *sym*-trioxane and sulfonamides/carbamates.

Considering the pseudo-[4+2] nature of the calculated TS for the Prins reaction with paraformaldehyde, we envisioned to elaborate on this toward a real [4+2] cycloaddition using olefins as dienophiles and a conjugated electrophile as diene. Preliminary experiments using acrolein in the reaction with styrene did not give any product. Gratifyingly, switching to salicyl alcohol **6.6**, as precursor of an *ortho*-quinone methide, reacted with styrene **4.1a**, using *i*IDP **4.5b** as catalyst, to form the corresponding 2-substituted chromane **6.7a** in low yield (22%), but with promising enantioselectivity (71.5:28.5 er). In addition to the further exploration of the transformation, efforts toward the elucidation of the reaction mechanism can be of interest to determine if a stepwise ("*classical Prins*"-like) or rather a concerted ("*Diels–Alder*"-like) pathway is operating in this case (Scheme 6.3).

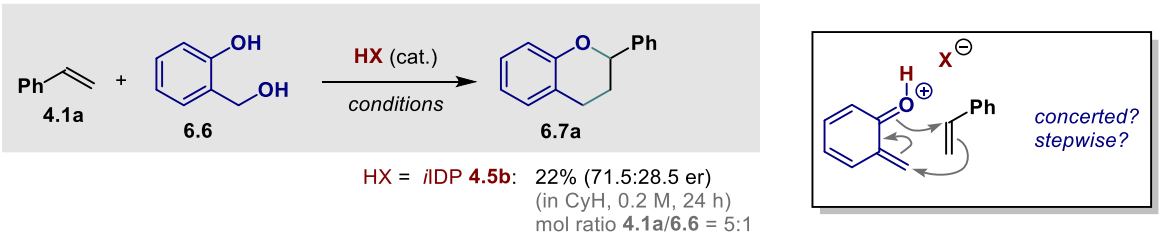

Scheme 6.3. Acid-catalyzed reaction of styrene and salicyl alcohol.

Another explored approach toward the use of olefins as dienophiles in [4+2] cycloadditions resembles the Povarov reaction, where aniline-derived iminium ions act as electrophilic diene and the cycloaddition product consists of a 1,2,3,4-tetrahydroquinoline ring. However, most of the asymmetric examples known to date involve the use of electron-rich olefins, such as enol ethers, enamines or conjugated dienes. As a first approach toward a three-component reaction of anilines, formaldehyde and olefins, we first studied *N*-protected-*N*-methoxymethyl anilines as precursors of formaldehyde-aniline-derived iminium ions and their reaction with styrene as model olefin. The reaction of the *N*-tosyl electrophile precursor 6.8 with styrene 4.1a, using IDPi 4.6d as catalyst, produced the expected nitrogenated heterocycle 6.9a in moderate yield (57%) after 4 days at rt, with moderate enantioselectivity (60:40 er). Similarly to the reaction of olefins and *ortho*-quinone methides, mechanistic studies could be beneficial to gain insight on the order of events for this Povarov reaction (Scheme 6.4).

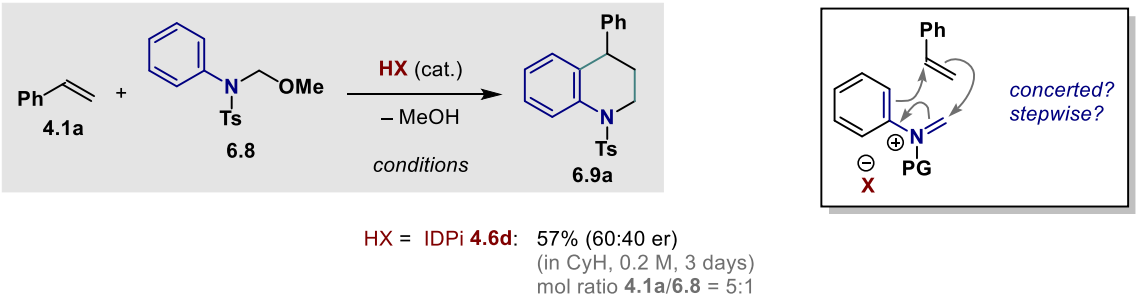

HX = IDPi **4.6d**: 57% (60:40 er)
(in CyH, 0.2 M, 3 days)
mol ratio **4.1a**/**6.8** = 5:1

Scheme 6.4. Acid-catalyzed Povarov reaction of formaldehyde-aniline iminium precursors and styrene.

Page left intentionally blank

7 Experimental Section

7.1 General Working Methods

Unless otherwise stated, all reactions were magnetically stirred and conducted in oven-dried (90 °C) or flame-dried glassware in anhydrous solvents under Ar, applying standard Schlenk techniques. Solvents and liquid reagents, as well as solutions of solid or liquid reagents were added via syringes, stainless steel or polyethylene cannulas through rubber septa or through a weak Ar counter-flow. Solid reagents were added through a weak Ar counter-flow. Cooling baths were prepared in Dewar vessels, filled with ice/water (0 °C), cooled acetone (> –78 °C) or dry ice/acetone (–78 °C). Heated oil baths were used for reactions requiring elevated temperatures. Solvents were removed under reduced pressure at 40 °C using a rotary evaporator, and unless otherwise stated, the remaining compound was dried in high vacuum (10^{-3} mbar) at ambient temperature. All given yields are isolated yields of chromatographically- and NMR spectroscopically-pure materials, unless otherwise stated.

Chemicals

Chemicals were purchased from commercial suppliers (including abcr, Acros, Alfa Aesar, Fluorochem, Merck, and TCI) and used without further purification unless otherwise stated. Et_3N was distilled from $LiAlH_4$ and stored under Ar prior to use. Pyridine was dried and stored over molecular sieves.

Catalysts **4.5d** and **4.5g** were prepared in our laboratory by Joyce Grimm, who kindly shared them for screening tests.

Solvents

Solvents (CyH, CH_2Cl_2, Et_2O, THF, PhMe) were dried by distillation from an appropriate drying agent in the technical department of the Max-Planck-Institut für Kohlenforschung and received in Schlenk flasks under Ar.[187] Other anhydrous solvents were purchased from commercial suppliers and used as received.

Inert Gas

Dry argon was purchased from Air Liquide with >99.5% purity.

Thin Layer Chromatography

Reactions were monitored by thin layer chromatography (TLC) on silica gel pre-coated plastic sheets (0.2 mm, Macherey-Nagel). Visualization was accomplished by irradiation with UV light

(254 nm and 366 nm) and/or phosphomolybdic acid (PMA) stain and/or Cerium Ammonium Molybdate (CAM) stain and/or permanganate ($KMnO_4$) stain. Preparative thin layer chromatography was performed on silica gel pre-coated glass plates SIL G-100, with fluorescent indicator UV_{254} (Macherey-Nagel).

Column Chromatography

Column chromatography was carried out using Merck silica gel (60 Å, 230−400 mesh, particle size 0.040−0.063 mm) or aluminum oxide (neutral, activated, Brockmann I, Sigma-Aldrich; activity adjustment individually specified) using technical grade solvents. Elution was accelerated using compressed air. Automated column chromatography was conducted on a Biotage® IsoleraTM ISO-4SW instrument, using SNAP Ultra HP-SphereTM 25 µm chromatography cartridges. All fractions containing a desired substance were combined and concentrated under reduced pressure, then redissolved in an appropriate solvent and filtered through cotton to remove silica residues.

Nomenclature

Nomenclature follows the suggestions proposed by the computer program ChemDraw Professional (version 20.1). Stereochemical configuration is graphically depicted in the structural formulas throughout this thesis following the recommendations from the IUPAC.[188]

Nuclear Magnetic Resonance Spectroscopy

^{1}H, ^{13}C, ^{11}B, ^{19}F, ^{31}P nuclear magnetic resonance (NMR) spectra were recorded on a Bruker AV-500, AV-400 or DPX-300 spectrometer in a suitable deuterated solvent. The solvent employed and respective measuring frequency are indicated for each experiment. Chemical shifts are reported with Me_4Si serving as a universal reference of all nuclides and with one or two decimal places. The resonance multiplicity is described as s (singlet), d (doublet), t (triplet), q (quadruplet), p (pentet), hept (heptet), m (multiplet), and b (broad). All spectra were recorded at 298 K unless otherwise noted, processed with the program MestReNova 11.0, and coupling constants are reported as observed. The residual deuterated solvent signal relative to Me_4Si was used as the internal reference in ^{1}H NMR spectra (e.g. $CDCl_3$ = 7.26 ppm) and are reported as follows: chemical shift in ppm (multiplicity, coupling constant *J* in Hz, number of protons). ^{11}B, ^{13}C, ^{19}F, ^{31}P NMR spectra were referenced according to Ξ-values (IUPAC recommendations 2008)[189] relative to the internal references set in ^{1}H NMR spectra (e.g. ^{13}C: Me_4Si, ^{19}F: CCl_3F, ^{31}P: H_3PO_4; each 0.00 ppm). All spectra are broadband decoupled unless otherwise noted.

Mass Spectrometry

Electron impact (EI) mass spectrometry (MS) was performed on a Finnigan MAT 8200 (70 eV) or MAT 8400 (70 eV) spectrometer. Electrospray ionization (ESI) mass spectrometry was conducted on a Bruker ESQ 3000 spectrometer. High resolution mass spectrometry (HRMS) was performed on a Finnigan MAT 95 (EI) or Bruker APEX III FTMS (7T magnet, ESI). The ionization method and mode of detection employed is indicated for the respective experiment and all masses are reported in atomic units per elementary charge (*m/z*) with an intensity normalized to the most intense peak.

Specific Rotations

Specific rotations $[\alpha_D^T]$ were measured with a Rudolph RA Autopol IV Automatic Polarimeter at the indicated temperature (*T*) with a sodium lamp (sodium D line, λ = 589 nm). Measurements were performed in an acid resistant 1 mL cell (50 mm length) with concentrations (g/(100 mL)) reported in the corresponding solvent.

High Performance Liquid Chromatography

High performance liquid chromatography (HPLC) was performed on Shimadzu LC-20AD liquid chromatograph (SIL-20AC auto sampler, CMB-20A communication bus module, DGU-20A5 degasser, CTO-20AC column oven, SPD-M20A diode array detector), Shimadzu LC-20AB liquid chromatograph (SIL-20ACHT auto sampler, DGU-20A5 degasser, CTO-20AC column oven, SPD-M20A diode array detector), or Shimadzu LC-20AB liquid chromatograph (reversed phase, SIL-20ACHT auto sampler, CTO-20AC column oven, SPD-M20A diode array detector) using columns with chiral stationary phases. All solvents used were HPLC-grade solvents, purchased from Merck. The column employed and respective solvent mixture are indicated for each experiment.

Gas Chromatography

Gas chromatography (GC) analyses on a chiral stationary phase were performed on HP 6890 and 5890 series instruments (split-mode capillary injection system, flame ionization detector (FID), hydrogen carrier gas). All of these analyses were conducted in the GC department of the Max-Planck-Institut für Kohlenforschung. The conditions employed are described in detail for the individual experiments.

Liquid Chromatography-Mass Spectrometry

Liquid chromatography-mass spectrometry (LC-MS) was performed on Shimadzu LC-MS 2020 liquid chromatograph. All solvents used were HPLC-grade solvents purchased from

Sigma-Aldrich. The column employed, the respective solvent mixture, and the MS parameters are indicated for each experiment.

Computations

All calculations presented in this paper were carried out with a development version of the ORCA suite of programs base on version 4.2.[190] Molecular geometries were optimized in the gas phase using the PBE functional[191] in conjunction with the D3 version of Grimme's dispersion correction with Becke–Johnson damping function,[192] using the resolution of identity approximation. The def2-SVP basis set was used for all atoms with matching auxiliary basis.[193] Analytic frequency calculations were performed to verify the nature of all stationary points (minima and transition states) and to calculate free energies and enthalpies at 298 K by using the rigid-rotor harmonic oscillator (RRHO) approximation. Solvation effect has been accounted by using CPCM (cyclohexane) solvation model,[194] as implemented in ORCA. An exhaustive manual conformational search was performed for possible catalyst-substrate orientations. Transition state (TS) structures were verified by the presence of a single imaginary vibrational frequency. Single-point energies are calculated at M06-2X/def2-TZVP[195] level of theory. Distortion-Interaction analysis[186] has been performed to determine the reason behind the stereoinduction. Molecular structures were generated using CYLview program[196] and VMD.[197]

7.2 Substrate Synthesis

GENERAL PROCEDURE A: *Wittig Olefination.*

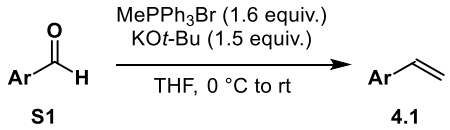

To a suspension of $MePPh_3Br$ (1.43 g, 4 mmol, 1.6 equiv.) in THF (9 mL), at 0 °C, KO*t*-Bu (421 mg, 3.75 mmol, 1.5 equiv.) was added and the mixture was further stirred vigorously for 30 min. At 0 °C, a solution of the aldehyde (**S1**, 2.5 mmol, 1 equiv., in 5 mL THF) was added dropwise to the formed phosphorus ylide. The mixture was further stirred at rt for 12 h. After checking full conversion, the mixture was diluted with MTBE (50 mL) and distilled water (50 mL), and the aqueous layer was extracted with MTBE (2 x 30 mL). The combined organic layers were washed with brine (1 x 30 mL), dried over anh. Na_2SO_4, filtered and concentrated under reduced pressure. Purification by flash column chromatography on silica gel (*n*-pentane/CH_2Cl_2) afforded the corresponding olefin **4.1**.

GENERAL PROCEDURE B: *Pd-catalyzed Aryl (Pseudo-)Halide Vinylation.*

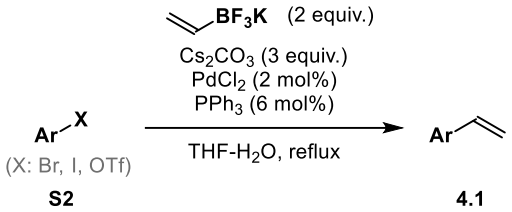

A mixture of aryl (pseudo-)halide (**S2**, 2.5 mmol, 1 equiv.), potassium vinyltrifluoroborate (5 mmol, 2 equiv.), $PdCl_2$ (0.05 mmol, 2 mol%), PPh_3 (0.15 mmol, 6 mol%), Cs_2CO_3 (7.5 mmol, 3 equiv.), distilled water (2.0 mL) and THF (9.5 mL) was stirred at rt and degassed by bubbling Ar for 10 min, then heated to reflux under Ar. After allowing to cool to rt and checking full conversion, the mixture was filtered through a short pad of Celite®, washing with MTBE (30 mL). The filtrate was washed with distilled water (1 x 30 mL) and brine (1 x 30 mL), then dried over anh. Na_2SO_4, filtered and concentrated under reduced pressure. Purification by flash column chromatography on silica gel (*n*-pentane/CH_2Cl_2) afforded the corresponding olefin **4.1**.

4-vinylphenyl pivalate (**4.1n**)

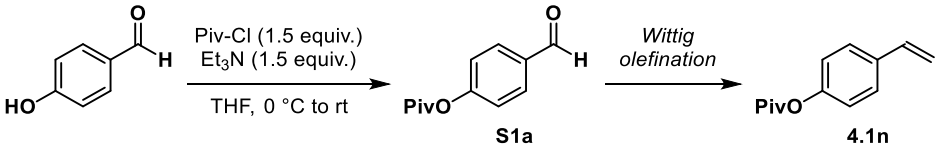

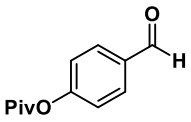

*4-formylphenyl pivalate (**S1a**): (Prepared following a reported procedure[198])*
In an oven-dried RB flask, 4-hydroxybenzaldehyde (1.22 g, 10 mmol, 1 equiv.) was dissolved in THF (10 mL) and cooled to 0 °C (ice/water bath). Under Ar, triethylamine (2.1 mL, 15 mmol, 1.5 equiv.) and pivaloyl chloride (1.8 mL, 15 mmol, 1.5 equiv., dropwise) were added and the mixture was further stirred at rt for 2 h. After checking full conversion (TLC monitoring), the mixture was treated with satd. aq. NH_4Cl (20 mL) and diluted with MTBE (30 mL), and the aqueous layer was extracted with MTBE (3 x 30 mL). The combined organic layers were washed with brine (1 x 30 mL), dried over anh. Na_2SO_4, filtered and concentrated under reduced pressure. Purification by flash column chromatography on silica gel (*i*-hexane/EtOAc 95:5 → 80:20) afforded the corresponding ester **S1a** as a white low-melting solid (1.63 g, 79%).

^{1}H NMR (501 MHz, $CDCl_3$): δ 9.99 (s, 1H), 7.91 (d, *J* = 8.6 Hz, 2H), 7.24 (d, *J* = 8.6 Hz, 2H), 1.37 (s, 9H). Spectroscopic data was consistent with the values reported in the literature.[199]

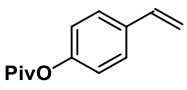

*4-vinylphenyl pivalate (**4.1n**):* Following *General Procedure A* with 4-formylphenyl pivalate (**S1b**, 516 mg, 2.5 mmol) as starting material. The crude

product was purified by flash column chromatography (eluent: *n*-pentane/CH_2Cl_2 90:10 → 70:30) to give **4.1n** as a colorless liquid (448 mg, 88%).

^{1}H NMR (501 MHz, $CDCl_3$): δ 7.41 (d, *J* = 8.5 Hz, 2H), 7.02 (d, *J* = 8.6 Hz, 2H), 6.70 (dd, *J* = 17.6, 10.9 Hz, 1H), 5.70 (dd, *J* = 17.6, 0.9 Hz, 1H), 5.24 (dd, *J* = 10.9, 0.9 Hz, 1H), 1.36 (s, 9H). ^{13}C NMR (126 MHz, $CDCl_3$): δ 177.2 (C), 150.8 (C), 136.1 (CH), 135.3 (C), 127.2 (CH), 121.7 (CH), 114.0 (CH_2), 39.2 (C), 27.3 (CH_3). ESI-HRMS: calculated for $C_{13}H_{16}O_2Na^+$ ([M+Na]$^+$): 227.1042, found: 227.1046.

methyl(4-vinylphenyl)sulfane (**4.1o**)

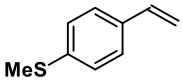

Following *General Procedure A* with 4-(methylthio)benzaldehyde (**S1b**, 381 mg, 2.5 mmol) as starting material. The crude product was purified by flash column chromatography (eluent: *n*-pentane/CH_2Cl_2 100:0 → 70:30) to give **4.1o** as a colorless liquid (365 mg, 97%).

^{1}H NMR (501 MHz, $CDCl_3$): δ 7.29 (d, *J* = 8.4 Hz, 2H), 7.17 (d, *J* = 8.4 Hz, 2H), 6.63 (dd, *J* = 17.5, 10.9 Hz, 1H), 5.66 (dd, *J* = 17.5, 0.9 Hz, 1H), 5.16 (dd, *J* = 10.9, 0.9 Hz, 1H), 2.45 (s, 3H). Spectroscopic data was consistent with the values reported in the literature.[200]

***S*-(4-vinylphenyl) 2,2-dimethylpropanethioate** (**4.1p**)

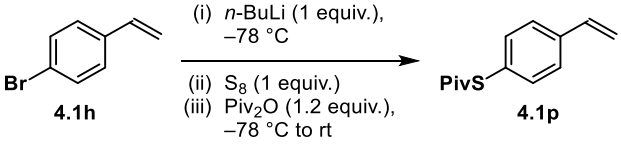

(Adapted from a reported procedure[201]): 4-bromostyrene (**4.1h**, 457 mg, 2.5 mmol, 1 equiv.), dissolved in a mixture of dry THF (6 mL) and dry *n*-hexane (6 mL), was treated with *n*-BuLi (2.5 M in hexanes, 1.0 mL, 2.5 mmol, 1.0 equiv.) dropwise at –78 °C. After stirring at –78 °C for 1.5 h, sulfur powder (80 mg, 2.5 mmol, 1.0 equiv.) was added in one portion and the mixture was stirred at 0 °C for 30 min. Pivalic anhydride (0.56 mL, 2.75 mmol, 1.1 equiv.) was added after cooling the reaction mixture again to –78 °C. After stirring for 1 h at –78 °C, the mixture was slowly warmed up to rt and further stirred for 24 h. The reaction was quenched with 10 mL distilled water and extracted with MTBE (3 x 25 mL). Then, the combined organic phase was washed with brine (1 x 30 mL), dried over anh. Na_2SO_4, filtered and concentrated under reduced pressure. Purification by flash column chromatography on silica gel (*n*-pentane/CH_2Cl_2 95:5 → 70:30) afforded the corresponding thioester **4.1p** as a light-yellow liquid (264 mg, 48%).

^{1}H NMR (501 MHz, $CDCl_3$): δ 7.43 (d, *J* = 8.4 Hz, 2H), 7.35 (d, *J* = 8.4 Hz, 2H), 6.72 (dd, *J* = 17.5, 10.9 Hz, 1H), 5.79 (dd, *J* = 17.6, 0.8 Hz, 1H), 5.31 (dd, *J* = 10.9, 0.8 Hz, 1H), 1.32 (s, 9H). ^{13}C NMR (126 MHz, $CDCl_3$): δ 204.7 (C), 138.6 (C), 136.3 (CH), 135.2 (CH), 127.5 (C),

127.0 (CH), 115.3 (CH_2), 47.1 (C), 27.6 (CH_3). ESI-HRMS: calculated for $C_{13}H_{16}OSNa^+$ ($[M+Na]^+$): 243.0814, found: 243.0818.

2-methoxy-4-vinylphenyl pivalate (**4.1q**)

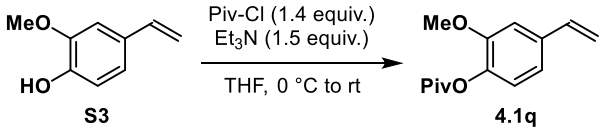

In an oven-dried RB flask, 2-methoxy-4-vinylphenol (**S3**, 750 mg, 5 mmol, 1 equiv.) was dissolved in THF (5 mL) and cooled to 0 °C (ice/water bath). Under Ar, triethylamine (1.0 mL, 7.5 mmol, 1.5 equiv.) and pivaloyl chloride (0.86 mL, 7 mmol, 1.4 equiv., dropwise) were added and the mixture was further stirred at rt for 2 h. After checking full conversion (TLC monitoring), the mixture was treated with satd. aq. NH_4Cl (20 mL) and diluted with MTBE (30 mL), and the aqueous layer was extracted with MTBE (3 x 30 mL). The combined organic layers were washed with brine (1 x 30 mL), dried over anh. Na_2SO_4, filtered and concentrated under reduced pressure. Purification by flash column chromatography on silica gel (*i*-hexane/EtOAc 95:5 → 70:30) afforded the corresponding ester **4.1q** as a white solid (1.01 g, 86%).

^{1}H NMR (501 MHz, $CDCl_3$): δ 7.01 – 6.93 (m, 3H), 6.68 (dd, *J* = 17.6, 10.9 Hz, 1H), 5.69 (dd, *J* = 17.6, 0.8 Hz, 1H), 5.24 (dd, *J* = 10.8, 0.8 Hz, 1H), 3.83 (s, 3H), 1.37 (s, 9H). ^{13}C NMR (126 MHz, $CDCl_3$): δ 176.8, 151.4, 140.2, 136.6, 136.5, 122.8, 119.1, 113.96, 110.1, 56.0, 39.2, 27.4. Spectroscopic data was consistent with the values reported in the literature.[202]

2,2-difluoro-5-vinylbenzo[*d*][1,3]dioxole (**4.1r**)

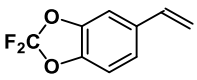

Following *General Procedure B* with 5-bromo-2,2-difluoro-1,3-benzodioxole (**S2a**, 593 mg, 2.5 mmol) as starting material. The crude product was purified by flash column chromatography (eluent: *n*-pentane/CH_2Cl_2 100:0 → 70:30) to give **4.1r** as a colorless liquid (337 mg, 73%).

^{1}H NMR (501 MHz, $CDCl_3$): δ 7.15 (d, *J* = 1.7 Hz, 1H), 7.07 (dd, *J* = 8.3, 1.7 Hz, 1H), 6.99 (d, *J* = 8.2 Hz, 1H), 6.66 (dd, *J* = 17.5, 10.9 Hz, 1H), 5.66 (d, *J* = 17.5 Hz, 1H), 5.25 (d, *J* = 10.9 Hz, 1H). ^{19}F NMR (471 MHz, $CDCl_3$): δ –50.24 (s, 2F). ^{13}C NMR (126 MHz, $CDCl_3$): δ 144.4 (C), 143.4 (C), 135.7 (CH), 134.3 (C), 131.8 (C, t, *J* = 255.1 Hz), 122.5 (CH), 114.3 (CH_2), 109.4 (CH), 106.6 (CH). Spectroscopic data was consistent with the values reported in the literature.[203] APPI-HRMS: calculated for $C_9H_7F_2O_2^+$ ($[M+H]^+$): 185.0409, found: 185.0410.

2-bromo-1-methoxy-4-vinylbenzene (**4.1u**)

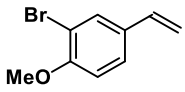

Following *General Procedure A* with 3-bromo-4-methoxybenzaldehyde (**S1c**, 538 mg, 2.5 mmol) as starting material. The crude product was purified by

flash column chromatography (eluent: *n*-pentane/CH_2Cl_2 100:0 → 80:20) to give **4.1u** as a very light yellow liquid (440 mg, 83%).

^{1}H NMR (501 MHz, CD_2Cl_2): δ 7.63 (d, *J* = 2.1 Hz, 1H), 7.33 (dd, *J* = 8.5, 2.2 Hz, 1H), 6.88 (d, *J* = 8.5 Hz, 1H), 6.61 (dd, *J* = 17.6, 10.9 Hz, 1H), 5.64 (dd, *J* = 17.5, 0.7 Hz, 1H), 5.18 (dd, *J* = 10.9, 0.8 Hz, 1H), 3.88 (s, 3H). ^{13}C NMR (126 MHz, CD_2Cl_2): δ 156.0, 135.4, 132.2, 131.1, 127.0, 113.2, 112.3, 112.1, 56.6. Spectroscopic data was consistent with the values reported in the literature.[204]

2-bromo-1-methyl-4-vinylbenzene (**4.1v**)

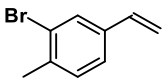

Following *General Procedure A* with 3-bromo-4-methylbenzaldehyde (**S1d**, 498 mg, 2.5 mmol) as starting material. The crude product was purified by flash column chromatography (eluent: *n*-pentane/CH_2Cl_2 100:0 → 70:30) to give **4.1v** as a colorless liquid (396 mg, 80%).

^{1}H NMR (501 MHz, $CDCl_3$): δ 7.58 (d, *J* = 1.8 Hz, 1H), 7.24 (dd, *J* = 7.8, 1.8 Hz, 1H), 7.18 (d, *J* = 7.8 Hz, 1H), 6.62 (dd, *J* = 17.6, 10.9 Hz, 1H), 5.71 (dd, *J* = 17.6, 0.7 Hz, 1H), 5.24 (d, *J* = 10.8 Hz, 1H), 2.39 (s, 3H). ^{13}C NMR (126 MHz, $CDCl_3$): δ 137.4 (C), 137.3 (C), 135.5 (CH), 130.9 (CH), 130.1 (CH), 125.25 (C), 125.19 (CH), 114.5 (CH_2), 22.8 (CH_3). Spectroscopic data was consistent with the values reported in the literature.[205] APPI-HRMS: calculated for $C_9H_{10}Br^+$ ([M+H]$^+$): 196.9961, found: 196.9962.

ethyl 4-vinylbenzoate (**4.1w**)

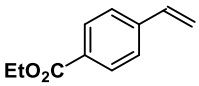

Following *General Procedure B* with ethyl 4-bromobenzoate (**S2b**, 573 mg, 2.5 mmol) as starting material. The crude product was purified by flash column chromatography (eluent: *n*-pentane/CH_2Cl_2 90:10 → 70:30) to give **4.1w** as a colorless liquid (399 mg, 91%).

^{1}H NMR (501 MHz, $CDCl_3$): δ 8.00 (d, *J* = 8.4 Hz, 2H), 7.46 (d, *J* = 8.4 Hz, 2H), 6.75 (dd, *J* = 17.6, 10.9 Hz, 1H), 5.86 (dd, *J* = 17.5, 0.8 Hz, 1H), 5.38 (dd, *J* = 10.9, 0.7 Hz, 1H), 4.37 (q, *J* = 7.1 Hz, 2H), 1.39 (t, *J* = 7.1 Hz, 3H). ^{13}C NMR (126 MHz, $CDCl_3$): δ 166.5, 142.0, 136.2, 130.0, 129.8, 126.2, 116.5, 61.0, 14.5. Spectroscopic data was consistent with the values reported in the literature.[206]

6-vinyl-1,2,3,4-tetrahydronaphthalene (**4.1x**)

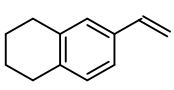

Following *General Procedure B* with 5,6,7,8-tetrahydronaphthalen-2-yl trifluoromethanesulfonate[207] (**S2c**, 1368 mg, 4.9 mmol) as starting material. The crude product was purified by flash column chromatography (eluent: *n*-pentane/CH_2Cl_2 100:0 → 80:20) to give **4.1x** as a colorless liquid (730 mg, 95%).

^{1}H NMR (501 MHz, $CDCl_3$): δ 7.18 (dd, *J* = 8.0, 1.9 Hz, 1H), 7.13 (s, 1H), 7.04 (d, *J* = 7.9 Hz, 1H), 6.68 (dd, *J* = 17.6, 10.9 Hz, 1H), 5.70 (dd, *J* = 17.6, 1.0 Hz, 1H), 5.18 (dd, *J* = 10.9, 1.1 Hz, 1H), 2.78 (d, *J* = 3.5 Hz, 4H), 1.82 (dq, *J* = 6.6, 3.6, 3.0 Hz, 4H). ^{13}C NMR (126 MHz, $CDCl_3$): δ 137.3 (C), 137.2 (C), 137.0 (CH), 135.0 (C), 129.4 (CH), 127.2 (CH), 123.4 (CH), 112.8 (CH_2), 29.6 (CH_2), 29.4 (CH_2), 23.4 (CH_2). Spectroscopic data was consistent with the values reported in the literature.[208]

9,9-dimethyl-2-vinyl-9*H*-fluorene (**4.1y**)

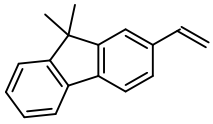

Following *General Procedure B* with 2-bromo-9,9-dimethyl-9*H*-fluorene (**S2d**, 683 mg, 2.5 mmol) as starting material. The crude product was purified by flash column chromatography (eluent: *n*-pentane/CH_2Cl_2 100:0 → 80:20) to give **4.1y** as a colorless liquid (422 mg, 77%).

^{1}H NMR (501 MHz, $CDCl_3$): δ 7.76 – 7.70 (m, 1H), 7.69 (d, *J* = 7.8 Hz, 1H), 7.51 (d, *J* = 1.5 Hz, 1H), 7.48 – 7.42 (m, 1H), 7.42 (dd, *J* = 7.8, 1.6 Hz, 1H), 7.34 (pd, *J* = 7.4, 1.5 Hz, 2H), 6.83 (dd, *J* = 17.6, 10.9 Hz, 1H), 5.83 (dd, *J* = 17.6, 0.9 Hz, 1H), 5.28 (dd, *J* = 10.9, 0.9 Hz, 1H), 1.52 (s, 6H). ^{13}C NMR (126 MHz, $CDCl_3$): δ 154.1 (C), 154.0 (C), 139.2 (C), 139.0 (C), 137.4 (CH), 136.9 (C), 127.4 (CH), 127.1 (CH), 125.7 (CH), 122.7 (CH), 120.4 (CH), 120.2 (CH), 120.1 (CH), 113.3 (CH_2), 46.9 (C), 27.3 (CH_3). Spectroscopic data was consistent with the values reported in the literature.[209]

1,4-divinylbenzene (**4.1zb**)

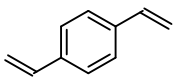

Following *General Procedure A*, but modifying some amounts to achieve double Wittig reaction, with terephthalaldehyde (**S1e**, 671 mg, 2.5 mmol) as starting material, and 2.05 equiv. $MePPh_3Br$ and 2.15 equiv. KO*t*-Bu. The crude product was purified by flash column chromatography (eluent: *n*-pentane/CH_2Cl_2 100:0 → 90:10), evaporating the solvents under reduced pressure at 25 °C, to give **4.1zb** as a colorless liquid (417 mg, 64%, to be stored at –20 °C).

^{1}H NMR (501 MHz, $CDCl_3$): δ 7.38 (s, 4H), 6.71 (dd, *J* = 17.6, 10.9 Hz, 2H), 5.75 (dd, *J* = 17.6, 0.9 Hz, 2H), 5.24 (dd, *J* = 10.9, 0.9 Hz, 2H). ^{13}C NMR (126 MHz, $CDCl_3$): δ 137.26 (C), 136.61 (CH), 126.53 (CH), 113.90 (CH_2). Spectroscopic data was consistent with the values reported in the literature.[210]

1-allyl-4-vinylbenzene (**4.1zc**)

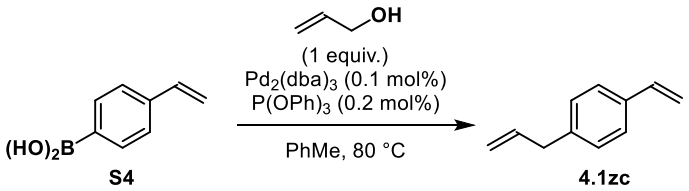

(Adapted from a reported procedure[211]): A mixture of $Pd_2(dba)_3$ (4.6 mg, 5 µmol, 0.1 mol%), 4-vinylphenyl boronic acid (**S3**, 888 mg, 6 mmol, 1.2 equiv.), $(PhO)_3P$ (2.5 µL, 10 µmol, 0.2 mol%) and allyl alcohol (290 mg, 5 mmol, 1 equiv.) in 1,4-dioxane (6.5 mL) was heated at 80 °C under Ar for 6 h. After cooling to rt, the reaction mixture was diluted with MTBE (50 mL) and washed with brine (1 x 30 mL), dried over anh. Na_2SO_4, filtered and concentrated under reduced pressure. Purification by flash column chromatography on silica gel (*n*-pentane) afforded the corresponding olefin **4.1zc** as a colorless liquid (480 mg, 67%).

^{1}H NMR (501 MHz, CD_2Cl_2): δ 7.35 (d, *J* = 8.1 Hz, 2H), 7.16 (d, *J* = 8.2 Hz, 2H), 6.71 (dd, *J* = 17.6, 10.9 Hz, 1H), 5.97 (ddt, *J* = 16.9, 10.1, 6.7 Hz, 1H), 5.72 (dd, *J* = 17.6, 1.0 Hz, 1H), 5.20 (dd, *J* = 10.9, 1.0 Hz, 1H), 5.13 – 5.03 (m, 2H), 3.38 (d, *J* = 6.8 Hz, 2H). ^{13}C NMR (126 MHz, CD_2Cl_2): δ 140.4 (C), 137.9 (CH), 137.0 (CH), 135.9 (C), 129.1 (CH), 126.6 (CH), 115.9 (CH_2), 113.3 (CH_2), 40.3 (CH_2). Spectroscopic data was consistent with the values reported in the literature.[212]

2-vinylthiophene (**4.1zd**)

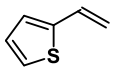

Following *General Procedure A* with thiophene-2-carbaldehyde (**S1f**, 561 mg, 5 mmol) as starting material. The crude product was purified by flash column chromatography (eluent: *n*-pentane/CH_2Cl_2 100:0 → 70:30) to give **4.1zd** as a colorless liquid (243 mg, 44%).

^{1}H NMR (501 MHz, CD_2Cl_2): δ 7.19 (d, *J* = 4.9 Hz, 1H), 7.02 – 6.95 (m, 2H), 6.84 (dd, *J* = 17.4, 10.9 Hz, 1H), 5.57 (d, *J* = 17.4 Hz, 1H), 5.14 (d, *J* = 10.8 Hz, 1H). ^{13}C NMR (126 MHz, CD_2Cl_2): δ 143.4, 130.3, 127.7, 126.3, 124.8, 113.4. Spectroscopic data was consistent with the values reported in the literature.[213]

3-vinylthiophene (**4.1ze**)

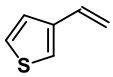

Following *General Procedure A* with thiophene-3-carbaldehyde (**S1g**, 561 mg, 5 mmol) as starting material. The crude product was purified by flash column chromatography (eluent: *n*-pentane/CH_2Cl_2 100:0 → 70:30) to give **4.1ze** as a colorless liquid (380 mg, 69%).

^{1}H NMR (501 MHz, CD_2Cl_2): δ 7.30 (ddd, *J* = 5.1, 2.9, 0.6 Hz, 1H), 7.26 (dd, *J* = 5.1, 1.4 Hz, 1H), 7.20 (dd, *J* = 2.8, 1.3 Hz, 1H), 6.73 (dd, *J* = 17.5, 10.9 Hz, 1H), 5.59 (dd, *J* = 17.6, 1.2 Hz,

1H), 5.20 (dd, *J* = 10.9, 1.2 Hz, 1H). ^{13}C NMR (126 MHz, CD_2Cl_2): δ 141.0, 131.4, 126.4, 125.1, 122.8, 113.8. Spectroscopic data was consistent with the values reported in the literature.[200]

1-tosyl-3-vinyl-1*H*-indole (**4.1zf**)

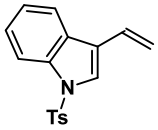

Following *General Procedure A* with 1-tosyl-1*H*-indole-3-carbaldehyde[214] (**S1h**, 599 mg, 2 mmol) as starting material. The crude product was purified by flash column chromatography (eluent: *n*-pentane/MTBE 98:2 → 70:30) to give **4.1zf** as a white solid (555 mg, 93%).

^{1}H NMR (501 MHz, $CDCl_3$): δ 7.99 (d, *J* = 8.2 Hz, 1H), 7.77 (d, *J* = 8.4 Hz, 2H), 7.74 (d, *J* = 7.9 Hz, 1H), 7.60 (s, 1H), 7.33 (t, *J* = 7.8 Hz, 1H), 7.27 (t, *J* = 7.0 Hz, 1H), 7.22 (d, *J* = 8.1 Hz, 2H), 6.77 (dd, *J* = 17.8, 11.3 Hz, 1H), 5.79 (dd, *J* = 17.8, 1.2 Hz, 1H), 5.35 (dd, *J* = 11.4, 1.2 Hz, 1H), 2.33 (s, 3H). ^{13}C NMR (126 MHz, $CDCl_3$): δ 145.2, 135.7, 135.3, 130.1, 129.2, 127.7, 127.0, 125.0, 124.2, 123.6, 121.1, 120.6, 115.5, 113.9, 21.7. Spectroscopic data was consistent with the values reported in the literature.[215]

9-tosyl-2-vinyl-9*H*-carbazole (**4.1zg**)

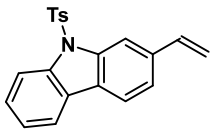

Following *General Procedure B*, employing 2-bromo-9-tosyl-9*H*-carbazole[216] (**S2e**, 500 mg, 1.25 mmol) as starting material. The crude product was purified by flash column chromatography (eluent: *n*-pentane/MTBE 90:10 → 70:30) to give **4.1zg** as a white low-melting solid (324 mg, 75%). ^{1}H NMR (501 MHz, $CDCl_3$) δ 8.36 (s, 1H), 8.30 (d, *J* = 8.4 Hz, 1H), 7.87 (d, *J* = 7.7 Hz, 1H), 7.83 (d, *J* = 8.0 Hz, 1H), 7.69 (d, *J* = 8.4 Hz, 2H), 7.51 – 7.43 (m, 2H), 7.35 (t, *J* = 7.5 Hz, 1H), 7.10 (d, *J* = 8.2 Hz, 2H), 6.91 (dd, *J* = 17.5, 10.9 Hz, 1H), 5.91 (d, *J* = 17.6 Hz, 1H), 5.36 (d, *J* = 10.9 Hz, 1H), 2.26 (s, 3H). ^{13}C NMR (126 MHz, $CDCl_3$) δ 145.0 (C), 139.1 (C), 139.0 (C), 137.4 (C), 137.2 (CH), 135.2 (C), 129.8 (CH), 127.5 (CH), 126.6 (CH), 126.4 (C), 126.2 (C), 124.1 (CH), 122.2 (CH), 120.1 (CH), 115.3 (CH), 114.6 (CH_2), 113.2 (CH), 21.6 (CH_3). ESI-HRMS: calculated for $C_{21}H_{17}NO_2SNa^+$ ([M+Na]$^+$): 370.0872, found: 370.0872.

3-vinylpyridine (**4.1zh**)

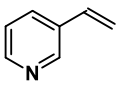

Following *General Procedure A* with nicotinaldehyde (**S1i**, 536 mg, 5 mmol) as starting material. The crude product was purified by flash column chromatography (eluent: *n*-pentane/MTBE 95:5 → 60:40) to give **4.1zh** as a colorless liquid (406 mg, 77%).

^{1}H NMR (501 MHz, $CDCl_3$) δ 8.60 (d, *J* = 2.2 Hz, 1H), 8.47 (dd, *J* = 4.8, 1.6 Hz, 1H), 7.72 (dt, *J* = 7.8, 2.0 Hz, 1H), 7.26 – 7.23 (m, 1H), 6.70 (dd, *J* = 17.7, 11.0 Hz, 1H), 5.82 (d, *J* = 17.6 Hz, 1H), 5.37 (d, *J* = 11.0 Hz, 1H). Spectroscopic data was consistent with the values reported in the literature.[217]

Styrene-β,β-*d*$_2$ (4.1zj)

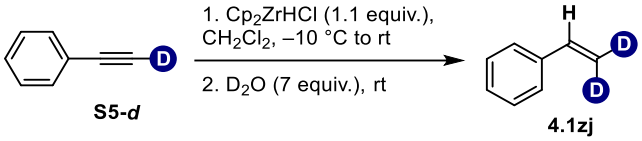

(Adapted from a reported procedure[182]): A two-necked RB flask under Ar atmosphere was charged with phenylacetylene-*d* (**S5-*d***)[182] (1.99 g, 19.5 mmol) and dry CH_2Cl_2 (50 mL). The flask was covered with aluminum foil and the mixture was cooled to –10 °C. Schwartz's Reagent (5.53 g, 21.5 mmol, 1.1 equiv.) was then added in three equal portions in rapid succession (over 2 min). The mixture was allowed to stir at –10 °C for 15 min, then the cold bath was removed and the stirring was continued at rt in the dark for 4 h. The flask was cooled to 0 °C, and the mixture was quenched with D_2O (2.5 mL, 99.9% D, 136.5 mmol, 7 equiv.) and stirred vigorously at rt for 12 h. The mixture was diluted with CH_2Cl_2 (50 mL), followed by the addition of anh. Na_2SO_4 and filtration, washing with CH_2Cl_2. The filtrate was concentrated under reduced pressure (400 mbar, water bath of rotavap at 25 °C; no heating, product is volatile) until 5–10 mL remained. *n*-Pentane (50 mL) was added and the mixture was filtered over a Celite® pad to remove the white precipitate; the filter cake was rinsed with *n*-pentane and the filtrate was again concentrated under reduced pressure (400 mbar, 25 °C). Purification by flash column chromatography on silica gel (*n*-pentane; removal of solvent on rotavap at 400 mbar, 25 °C) afforded the corresponding olefin **4.1zj** as a colorless liquid (1.13 g, 55%). Approx. 97% D-incorporation. ^{1}H NMR (501 MHz, $CDCl_3$) δ 7.45 – 7.40 (m, 2H), 7.37 – 7.31 (m, 2H), 7.26 (tt, *J* = 6.7, 1.3 Hz, 1H), 6.72 (d, *J* = 2.8 Hz, 1H). Spectroscopic data was consistent with the values reported in the literature.[218]

trans*-Styrene-(β)-*d (**4.1zk**) and ***cis*-Styrene-(β)-*d*** (**4.1zl**)

(Adapted from a reported procedure[182]): Prepared in a similar way to **4.1zj**, choosing between starting alkyne (**S5** or **S5-*d***) and electrophile quench (H_2O or D_2O).

trans*-Styrene-(β)-*d (**4.1zk**)

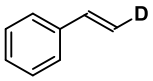

Prepared in a similar way to **4.1zj**: from **S5** (511 mg, 5 mmol) as starting material, and D_2O. The crude product was purified by flash column chromatography (eluent: *n*-pentane) to give **4.1zk** as a colorless liquid (153 mg, 29%), >95% D-incorporation. ^{1}H NMR (501 MHz, $CDCl_3$) δ 7.44 – 7.40 (m, 2H), 7.36 – 7.31 (m, 2H), 7.26 (ddt, *J* = 8.0, 6.4, 1.4 Hz, 1H), 6.73 (dt, *J* = 17.6, 1.7 Hz, 1H), 5.75 (d, *J* = 17.6 Hz, 1H), [5.25 (dd, *J* = 10.8, 0.9 Hz, 0.04H)]. ^{13}C NMR (126 MHz, $CDCl_3$) δ 137.7, 136.9, 128.7, 127.9, 126.4, 113.7 (t, *J* = 24.7 Hz). Spectroscopic data was consistent with the values reported in the literature.[219]

cis*-Styrene-(β)-*d (**4.1zl**)

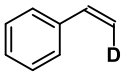

Prepared in a similar way to **4.1zj**: from **S5-*d*** (397 mg, 3.8 mmol) as starting material, and H_2O. The crude product was purified by flash column chromatography (eluent: *n*-pentane) to give **4.1zl** as a colorless liquid (88 mg, 22%), >95% D-incorporation.

^{1}H NMR (501 MHz, $CDCl_3$) δ 7.45 – 7.39 (m, 2H), 7.34 (t, *J* = 7.6 Hz, 2H), 7.26 (ddt, *J* = 8.0, 6.5, 1.4 Hz, 1H), 6.72 (dd, *J* = 10.9, 2.6 Hz, 1H), [5.76 (dd, *J* = 17.7, 0.9 Hz, 0.03H),] 5.24 (d, *J* = 10.9 Hz, 1H). ^{13}C NMR (126 MHz, $CDCl_3$) δ 137.7, 137.0, 128.7, 127.9, 126.4, 113.7 (t, *J* = 23.5 Hz). Spectroscopic data was consistent with the values reported in the literature.[182]

(methylenebis(oxy))bis(methylene) diacetate ($POMDA_3$, **4.2h**)

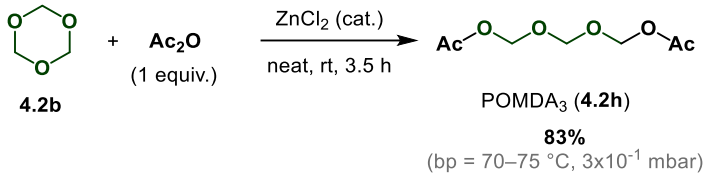

(Adapted from a reported procedure[220]): An oven-dried RB flask was charged with *sym*-trioxane (**4.2b**, 4.50 g, 50 mmol) and acetic anhydride (4.8 mL, 50 mmol, 1 equiv.), and cooled to approx. 5 °C (ice/water bath). $ZnCl_2$ (170 mg, 1.25 mmol, 2.5 mol%) was added in one portion, the flask was closed with a septum and the mixture was stirred at 5 °C for 15 min (during this time, it turns milky), and then further stirred at room temperature for 3.5 h. The reaction was stopped by adding distilled water (5 mL), diluted with Et_2O (50 mL) and neutralized by adding satd. aq. $NaHCO_3$ in small portions. The aqueous phase was extracted with Et_2O (2 x 50 mL), and the combined organic phase was dried over anh. Na_2SO_4, filtered and concentrated under reduced pressure. Purification of the obtained colorless liquid residue was performed by distillation at reduced pressure (0.3 mbar; oil bath: 130 °C), obtaining the desired tri(oxymethylene) diacetate **4.2h** (bp = 70–75 °C) as a colorless liquid (8.0 g, 83%).

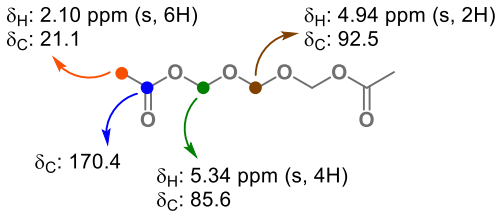

^{1}H NMR (501 MHz, $CDCl_3$) δ 5.34 (s, 4H), 4.94 (s, 2H), 2.10 (s, 6H). ^{13}C NMR (126 MHz, $CDCl_3$) δ 170.5 (C), 92.5 (CH_2), 85.7 (CH_2), 21.1 (CH_3). ESI-HRMS: calculated for $C_7H_{16}NO_6^+$ ($[M+NH_4]^+$): 210.0972, found: 210.0973.

7.3 *i*IDP-Catalyzed Intermolecular Prins Reaction

GENERAL PROCEDURE C: *Asymmetric Brønsted Acid-Catalyzed Intermolecular Prins Reaction.*

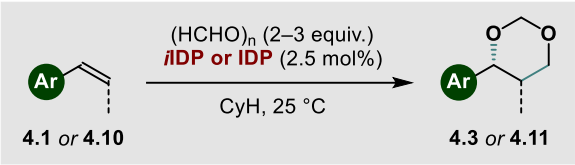

A mixture of paraformaldehyde **4.2a** (2.5 equiv.), chiral enantiopure Brønsted acid catalyst (*i*IDP or IDP, 2.5 mol%), dry cyclohexane (depending on the concentration, indicated in each case), and olefin **4.1** or **4.10** (1 equiv.) was vigorously stirred at room temperature (time indicated in each case). The reaction was stopped by adding distilled water, and extracted with MTBE (3x). The combined organic layers were washed with brine, then dried over anh. Na_2SO_4, filtered and concentrated under reduced pressure. Purification by column chromatography (silica gel; *n*-pentane/MTBE mixtures) afforded the corresponding enantioenriched 1,3-dioxane product (**4.3** or **4.11**).

(*R*)-4-phenyl-1,3-dioxane (**4.3a**)

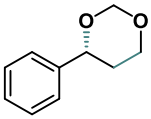

Following *General Procedure C* from styrene (**4.1a**, 29 µL, 0.25 mmol), with catalyst (*S*,*S*)-**4.5m** (2.5 mol%), in dry cyclohexane (2.5 mL, 0.1 M) for 72 h. Purification by flash column chromatography (eluent: *n*-pentane/MTBE 100:0 → 95:5) to give **4.3a** as a colorless liquid (36.4 mg, 89%, er = 95.5:4.5).

^{1}H NMR (501 MHz, $CDCl_3$) δ 7.40 – 7.35 (m, 4H), 7.32 – 7.28 (m, 1H), 5.23 (d, *J* = 6.3 Hz, 1H), 4.91 (d, *J* = 6.4 Hz, 1H), 4.66 (dd, *J* = 11.3, 2.5 Hz, 1H), 4.21 (dd, *J* = 11.5, 4.9 Hz, 1H), 3.89 (td, *J* = 11.9, 2.5 Hz, 1H), 2.11 (dddd, *J* = 13.5, 12.3, 11.3, 4.9 Hz, 1H), 1.76 – 1.70 (m, 1H). ^{13}C NMR (126 MHz, $CDCl_3$) δ 141.6 (C), 128.6 (CH), 128.0 (CH), 125.9 (CH), 94.3 (CH_2), 78.9 (CH), 67.1 (CH_2), 34.1 (CH_2). Spectroscopic data was consistent with the values reported in the literature.[137] ESI-HRMS: calculated for $C_{10}H_{12}O_2Na^+$ ([M+Na]$^+$): 187.0729, found: 187.0732. $[\alpha_D^{25}]$ = +32.1 (*c* = 0.746, $CHCl_3$). HPLC (Chiralpak IB-3 column, Heptane/*i*-PrOH 95:5, 1 mL/min, 25 °C, 220 nm): t_R = 3.6 min (major), 4.5 min (minor).

(*R*)-4-(*p*-tolyl)-1,3-dioxane (**4.3b**)

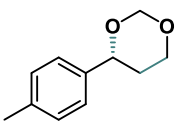

Following *General Procedure C* from 4-methylstyrene (**4.1b**, 33 µL, 0.25 mmol), with catalyst (*S*,*S*)-**4.5b** (2.5 mol%), in dry cyclohexane (5 mL, 0.05 M) for 72 h. Purification by flash column chromatography (eluent: *n*-pentane/MTBE 100:0 → 95:5) to give **4.3b** as a colorless liquid (39.5 mg, 89%, er = 90:10).

^{1}H NMR (501 MHz, $CDCl_3$) δ 7.27 (d, *J* = 8.1 Hz, 2H), 7.18 (d, *J* = 7.9 Hz, 2H), 5.21 (d, *J* = 6.3 Hz, 1H), 4.90 (d, *J* = 6.4 Hz, 1H), 4.62 (dd, *J* = 11.3, 2.5 Hz, 1H), 4.20 (dd, *J* = 11.4, 4.8 Hz,

1H), 3.87 (td, *J* = 11.9, 2.5 Hz, 1H), 2.35 (s, 3H), 2.10 (dddd, *J* = 13.5, 12.2, 11.2, 4.8 Hz, 1H), 1.74 – 1.66 (m, 1H). ^{13}C NMR (126 MHz, $CDCl_3$) δ 138.6 (C), 137.7 (C), 129.3 (CH), 125.9 (CH), 94.4 (CH_2), 78.8 (CH), 67.1 (CH_2), 34.1 (CH_2), 21.3 (CH_3). Spectroscopic data was consistent with the values reported in the literature.[137] ESI-HRMS: calculated for $C_{11}H_{14}O_2Na^+$ ([M+Na]$^+$): 201.0886, found: 201.0888. $[\alpha_D^{25}]$ = +32.9 (*c* = 0.517, $CHCl_3$). HPLC (Chiralpak IB-3 column, Heptane/*i*-PrOH 98:2, 0.5 mL/min, 25 °C, 220 nm): t_R = 7.3 min (major), 8.1 min (minor).

(*R*)-4-(4-(*tert*-butyl)phenyl)-1,3-dioxane (**4.3c**)

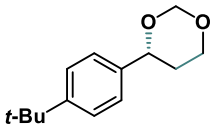

Following *General Procedure C* from 4-*tert*-butylstyrene (**4.1c**, 40 µL, 0.25 mmol), with catalyst (*S*,*S*)-**4.5b** (2.5 mol%), in dry cyclohexane (5 mL, 0.05 M) for 72 h. Purification by flash column chromatography (eluent: *n*-pentane/MTBE 100:0 → 95:5) to give **4.3c** as a white solid (49.1 mg, 89%, er = 91.5:8.5).
^{1}H NMR (501 MHz, $CDCl_3$) δ 7.39 (d, *J* = 8.4 Hz, 2H), 7.31 (d, *J* = 8.2 Hz, 2H), 5.21 (d, *J* = 6.3 Hz, 1H), 4.90 (d, *J* = 6.3 Hz, 1H), 4.63 (dd, *J* = 11.3, 2.5 Hz, 1H), 4.21 (dd, *J* = 11.4, 4.8 Hz, 1H), 3.88 (td, *J* = 11.9, 2.5 Hz, 1H), 2.14 (dddd, *J* = 13.4, 12.2, 11.3, 4.8 Hz, 1H), 1.76 – 1.68 (m, 1H), 1.32 (s, 9H). ^{13}C NMR (126 MHz, $CDCl_3$) δ 151.0 (C), 138.5 (C), 125.8 (CH), 125.5 (CH), 94.4 (CH_2), 78.8 (CH), 67.1 (CH_2), 34.7 (C), 33.8 (CH_2), 31.5 (CH_3). Spectroscopic data was consistent with the values reported in the literature.[137] ESI-HRMS: calculated for $C_{14}H_{20}O_2Na^+$ ([M+Na]$^+$): 243.1355, found: 243.1358. $[\alpha_D^{25}]$ = +29.8 (*c* = 0.450, $CHCl_3$). HPLC (Chiralpak AD-3 column, Heptane/*i*-PrOH 97:3, 0.5 mL/min, 25 °C, 220 nm): t_R = 6.2 min (major), 6.9 min (minor).

(*R*)-4-(4-methoxyphenyl)-1,3-dioxane (**4.3d**)

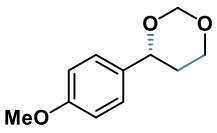

Following *General Procedure C* from 4-vinylanisole (**4.1d**, 33 µL, 0.25 mmol), with catalyst (*S*,*S*)-**4.4e** (2.5 mol%), in dry cyclohexane (1.25 mL, 0.2 M) for 36 h. Purification by flash column chromatography (eluent: *n*-pentane/MTBE 100:0 → 70:30) to give **4.3d** as a white solid (15.1 mg, 31%, er = 78:22).
^{1}H NMR (501 MHz, $CDCl_3$) δ 7.30 (d, *J* = 8.6 Hz, 2H), 6.90 (d, *J* = 8.8 Hz, 2H), 5.20 (d, *J* = 6.3 Hz, 1H), 4.89 (d, *J* = 6.3 Hz, 1H), 4.59 (dd, *J* = 11.2, 2.5 Hz, 1H), 4.20 (ddt, *J* = 11.5, 4.9, 1.4 Hz, 1H), 3.87 (td, *J* = 11.8, 2.5 Hz, 1H), 3.81 (s, 3H), 2.11 (dddd, *J* = 13.5, 12.3, 11.3, 4.9 Hz, 1H), 1.71 – 1.66 (m, 1H). ^{13}C NMR (126 MHz, $CDCl_3$) δ 159.4 (C), 133.8 (C), 127.3 (CH), 114.0 (CH), 94.4 (CH_2), 78.6 (CH), 67.1 (CH_2), 55.4 (CH_3), 34.0 (CH_2). Spectroscopic data was consistent with the values reported in the literature.[151c] ESI-HRMS: calculated for $C_{11}H_{14}O_3Na^+$ ([M+Na]$^+$): 217.0835, found: 217.0836. HPLC (Chiralpak AD-3 column, Heptane/*i*-PrOH 97:3, 0.5 mL/min, 25 °C, 220 nm): t_R = 11.2 min (major), 13.2 min (minor).

(*R*)-4-(*m*-tolyl)-1,3-dioxane (**4.3e**)

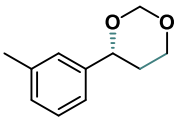

Following *General Procedure C* from 3-methylstyrene (**4.1e**, 33 µL, 0.25 mmol), with catalyst (*S*,*S*)-**4.5k** (2.5 mol%), in dry cyclohexane (5 mL, 0.05 M) for 72 h. Purification by flash column chromatography (eluent: *n*-pentane/MTBE 100:0 → 95:5) to give **4.3e** as a colorless liquid (39.4 mg, 88%, er = 93:7).
^{1}H NMR (501 MHz, $CDCl_3$) δ 7.25 (t, *J* = 7.6 Hz, 1H), 7.21 (s, 1H), 7.16 (d, *J* = 7.7 Hz, 1H), 7.11 (d, *J* = 7.6 Hz, 1H), 5.22 (d, *J* = 6.4 Hz, 1H), 4.90 (d, *J* = 6.3 Hz, 1H), 4.62 (dd, *J* = 11.3, 2.6 Hz, 1H), 4.21 (dd, *J* = 11.4, 4.9 Hz, 1H), 3.88 (td, *J* = 11.9, 2.5 Hz, 1H), 2.36 (s, 3H), 2.11 (dddd, *J* = 13.5, 12.3, 11.3, 4.8 Hz, 1H), 1.75 – 1.68 (m, 1H). ^{13}C NMR (126 MHz, $CDCl_3$) δ 141.5 (C), 138.3 (C), 128.7 (CH), 128.5 (CH), 126.6 (CH), 123.0 (CH), 94.4 (CH_2), 79.0 (CH), 67.1 (CH_2), 34.1 (CH_2), 21.6 (CH_3). ESI-HRMS: calculated for $C_{11}H_{14}O_2Na^+$ ([M+Na]$^+$): 201.0886, found: 201.0887. $[\alpha_D^{25}]$ = +40.5 (*c* = 0.430, $CHCl_3$). HPLC (Chiralpak IB-3 column, Heptane/*i*-PrOH 95:5, 1 mL/min, 25 °C, 220 nm): t_R = 3.4 min (major), 4.3 min (minor).

(*R*)-4-(3-methoxyphenyl)-1,3-dioxane (**4.3f**)

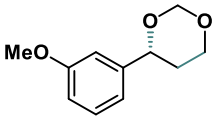

Following *General Procedure C* from 3-vinylanisole (**4.1f**, 34 µL, 0.25 mmol), with catalyst (*S*,*S*)-**4.5k** (2.5 mol%), in dry cyclohexane (5 mL, 0.05 M) for 72 h. Purification by flash column chromatography (eluent: *n*-pentane/MTBE 100:0 → 90:10) to give **4.3f** as a colorless oil (42.3 mg, 87%, er = 93:7).
^{1}H NMR (501 MHz, $CDCl_3$) δ 7.27 (t, *J* = 7.8 Hz, 1H), 6.97 – 6.91 (m, 2H), 6.84 (ddd, *J* = 8.3, 2.6, 1.0 Hz, 1H), 5.22 (d, *J* = 6.3 Hz, 1H), 4.90 (d, *J* = 6.3 Hz, 1H), 4.63 (dd, *J* = 11.3, 2.6 Hz, 1H), 4.20 (dd, *J* = 11.4, 4.8 Hz, 1H), 3.88 (td, *J* = 11.9, 2.5 Hz, 1H), 3.82 (s, 3H), 2.09 (dddd, *J* = 13.5, 12.2, 11.3, 4.9 Hz, 1H), 1.75 – 1.70 (m, 1H). ^{13}C NMR (126 MHz, $CDCl_3$) δ 159.9 (C), 143.2 (C), 129.6 (CH), 118.2 (CH), 113.6 (CH), 111.3 (CH), 94.3 (CH_2), 78.8 (CH), 67.1 (CH_2), 55.4 (CH_3), 34.1 (CH_2). ESI-HRMS: calculated for $C_{11}H_{14}O_3Na^+$ ([M+Na]$^+$): 217.0835, found: 217.0837. $[\alpha_D^{25}]$ = +42.2 (*c* = 0.465, $CHCl_3$). HPLC (Chiralpak IB-3 column, Heptane/*i*-PrOH 95:5, 1 mL/min, 25 °C, 220 nm): t_R = 4.9 min (major), 6.4 min (minor).

(*R*)-4-(4-chlorophenyl)-1,3-dioxane (**4.3g**)

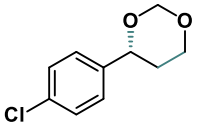

Following *General Procedure C* from 4-chlorostyrene (**4.1g**, 30 µL, 0.25 mmol), with catalyst (*S*,*S*)-**4.5k** (2.5 mol%), in dry cyclohexane (1.25 mL, 0.2 M) for 96 h. Purification by flash column chromatography (eluent: *n*-pentane/MTBE 100:0 → 95:5) to give **4.3g** as a colorless liquid (43.5 mg, 88%, er = 95.5:4.5).
^{1}H NMR (501 MHz, $CDCl_3$) δ 7.34 (d, *J* = 8.6 Hz, 2H), 7.30 (d, *J* = 8.6 Hz, 2H), 5.21 (d, *J* = 6.4 Hz, 1H), 4.88 (d, *J* = 6.4 Hz, 1H), 4.63 (dd, *J* = 11.3, 2.6 Hz, 1H), 4.20 (ddt, *J* = 11.5, 4.9, 1.4 Hz, 1H), 3.87 (td, *J* = 11.9, 2.5 Hz, 1H), 2.04 (dddd, *J* = 13.5, 12.3, 11.3, 4.9 Hz, 1H), 1.74 – 1.67 (m, 1H). ^{13}C NMR (126 MHz, $CDCl_3$) δ 140.2 (C), 133.6 (C), 128.8 (CH), 127.2 (CH), 94.3

(CH_2), 78.1 (CH), 66.9 (CH_2), 34.1 (CH_2). Spectroscopic data was consistent with the values reported in the literature.[137] ESI-HRMS: calculated for $C_{10}H_{11}ClO_2Na^+$ ([M+Na]$^+$): 221.0340, found: 221.0342. $[\alpha_D^{25}]$ = +45.1 (*c* = 0.532, $CHCl_3$). HPLC (Chiralpak IC-3 column, Heptane/*i*-PrOH 97:3, 0.5 mL/min, 25 °C, 220 nm): t_R = 8.0 min (minor), 8.7 min (major).

(*R*)-4-(4-bromophenyl)-1,3-dioxane (**4.3h**)

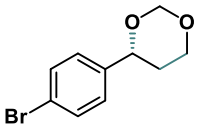

Following *General Procedure C* from 4-bromostyrene (**4.1h**, 33 µL, 0.25 mmol), with catalyst (*S*,*S*)-**4.5k** (2.5 mol%), in dry cyclohexane (1.25 mL, 0.2 M) for 5 days. Purification by flash column chromatography (eluent: *n*-pentane/MTBE 100:0 → 95:5) to give **4.3h** as a white solid (45.3 mg, 74%, er = 95.5:4.5). ^{1}H NMR (501 MHz, $CDCl_3$) δ 7.49 (d, *J* = 8.5 Hz, 2H), 7.25 (d, *J* = 8.4 Hz, 2H), 5.21 (d, *J* = 6.4 Hz, 1H), 4.88 (d, *J* = 6.4 Hz, 1H), 4.61 (dd, *J* = 11.3, 2.6 Hz, 1H), 4.20 (dd, *J* = 11.4, 4.8 Hz, 1H), 3.87 (td, *J* = 11.9, 2.4 Hz, 1H), 2.03 (dddd, *J* = 13.5, 12.3, 11.3, 4.9 Hz, 1H), 1.74 – 1.67 (m, 1H). ^{13}C NMR (126 MHz, $CDCl_3$) δ 140.7 (C), 131.7 (CH), 127.6 (CH), 121.7 (C), 94.3 (CH_2), 78.1 (CH), 66.9 (CH_2), 34.1 (CH_2). ESI-HRMS: calculated for $C_{10}H_{11}BrO_2Na^+$ ([M+Na]$^+$): 264.9835, found: 264.9836. $[\alpha_D^{25}]$ = +41.1 (*c* = 0.224, $CHCl_3$). HPLC (Chiralpak IC-3 column, Heptane/*i*-PrOH 97:3, 0.5 mL/min, 25 °C, 220 nm): t_R = 8.3 min (minor), 9.2 min (major).

(*R*)-4-(4-(chloromethyl)phenyl)-1,3-dioxane (**4.3i**)

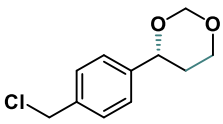

Following *General Procedure C* from 4-vinylbenzyl chloride (**4.1i**, 35 µL, 0.25 mmol), with catalyst (*S*,*S*)-**4.5b** (2.5 mol%), in dry cyclohexane (1.25 mL, 0.2 M) for 5 days. Purification by flash column chromatography (eluent: *n*-pentane/MTBE 100:0 → 90:10) to give **4.3i** as a white solid (30.1 mg, 57%, er = 95.5:4.5). ^{1}H NMR (501 MHz, $CDCl_3$) δ 7.39 (d, *J* = 8.4 Hz, 2H), 7.37 (d, *J* = 8.4 Hz, 2H), 5.22 (d, *J* = 6.4 Hz, 1H), 4.90 (d, *J* = 6.4 Hz, 1H), 4.66 (dd, *J* = 11.3, 2.6 Hz, 1H), 4.59 (s, 2H), 4.21 (dd, *J* = 11.5, 4.9 Hz, 1H), 3.88 (td, *J* = 11.8, 2.4 Hz, 1H), 2.07 (dddd, *J* = 13.4, 12.2, 11.3, 4.8 Hz, 1H), 1.76 – 1.69 (m, 1H). ^{13}C NMR (126 MHz, $CDCl_3$) δ 141.9 (C), 137.1 (C), 128.9 (CH), 126.3 (CH), 94.3 (CH_2), 78.4 (CH), 67.0 (CH_2), 46.1 (CH_2), 34.1 (CH_2). ^{13}C NMR (126 MHz, $CDCl_3$) δ 128.89, 126.26, 94.30, 78.46, 67.00, 46.09, 34.08. ESI-HRMS: calculated for $C_{11}H_{13}ClO_2Na^+$ ([M+Na]$^+$): 235.0496, found: 235.0498. $[\alpha_D^{25}]$ = +47.1 (*c* = 0.255, $CHCl_3$). HPLC (Chiralpak IC-3 column, Heptane/*i*-PrOH 98:2, 1 mL/min, 25 °C, 220 nm): t_R = 7.0 min (minor), 8.0 min (major).

(*R*)-4-(4-(trifluoromethyl)phenyl)-1,3-dioxane (**4.3j**)

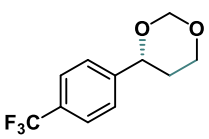

Following *General Procedure C* from 4-(trifluoromethyl)styrene (**4.1j**, 37 µL, 0.25 mmol), with catalyst (*S*,*S*)-**4.5p** (2.5 mol%), in dry cyclohexane (1.25

mL, 0.2 M) for 5 days. Purification by flash column chromatography (eluent: *n*-pentane/MTBE 100:0 → 95:5) to give **4.3j** as a white solid (5.8 mg, 10%, er = 97:3).

^{1}H NMR (501 MHz, $CDCl_3$) δ 7.62 (d, *J* = 8.1 Hz, 2H), 7.49 (d, *J* = 8.1 Hz, 2H), 5.24 (d, *J* = 6.4 Hz, 1H), 4.90 (d, *J* = 6.4 Hz, 1H), 4.72 (dd, *J* = 11.3, 2.6 Hz, 1H), 4.25 – 4.18 (m, 1H), 3.89 (td, *J* = 11.9, 2.5 Hz, 1H), 2.04 (dddd, *J* = 13.5, 12.2, 11.3, 4.9 Hz, 1H), 1.78 – 1.73 (m, 1H). ^{19}F NMR (471 MHz, $CDCl_3$) δ –62.54 (s, 3F). ^{13}C NMR (126 MHz, $CDCl_3$) δ 145.6 (C), 130.1 (q, *J* = 32.5 Hz, C), 126.1 (CH), 125.6 (q, *J* = 3.8 Hz, CH), 124.2 (q, *J* = 271.8 Hz, C), 94.2 (CH_2), 78.0 (CH), 66.9 (CH_2), 34.1 (CH_2). ESI-HRMS: calculated for $C_{11}H_{11}F_3O_2Na^+$ ([M+Na]$^+$): 255.0603, found: 255.0602. $[\alpha_D^{25}]$ = +40.2 (*c* = 0.249, $CHCl_3$). HPLC (Kromasil Amycoat RP column, CH_3CN/H_2O 50:50, 1 mL/min, 25 °C, 220 nm): t_R = 7.7 min (major), 8.5 min (minor).

(*R*)-4-(3-bromophenyl)-1,3-dioxane (**4.3k**)

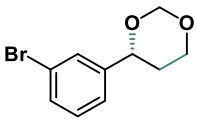

Following *General Procedure C* from 3-bromostyrene (**4.1k**, 33 µL, 0.25 mmol), with catalyst (*S*,*S*)-**4.5p** (2.5 mol%), in dry cyclohexane (1.25 mL, 0.2 M) for 5 days. Purification by flash column chromatography (eluent: *n*-pentane/MTBE 100:0 → 95:5) to give **4.3k** as a colorless liquid (25.0 mg, 41%, er = 96:4).

^{1}H NMR (501 MHz, $CDCl_3$) δ 7.54 (t, *J* = 1.9 Hz, 1H), 7.42 (ddd, *J* = 7.8, 2.0, 1.2 Hz, 1H), 7.29 (d, *J* = 7.9 Hz, 1H), 7.23 (t, *J* = 7.8 Hz, 1H), 5.21 (d, *J* = 6.4 Hz, 1H), 4.88 (d, *J* = 6.4 Hz, 1H), 4.62 (dd, *J* = 11.3, 2.6 Hz, 1H), 4.20 (dd, *J* = 11.5, 4.8 Hz, 1H), 3.87 (td, *J* = 11.9, 2.4 Hz, 1H), 2.04 (dddd, *J* = 13.4, 12.1, 11.3, 4.8 Hz, 1H), 1.75 – 1.70 (m, 1H). ^{13}C NMR (126 MHz, $CDCl_3$) δ 143.9 (C), 131.0 (CH), 130.2 (CH), 129.0 (CH), 124.4 (CH), 122.8 (C), 94.2 (CH_2), 78.0 (CH), 66.9 (CH_2), 34.1 (CH_2). ESI-HRMS: calculated for $C_{10}H_{11}BrO_2Na^+$ ([M+Na]$^+$): 264.9835, found: 264.9835. $[\alpha_D^{25}]$ = +35.5 (*c* = 0.609, $CHCl_3$). HPLC (Chiralpak IC-3 column, Heptane/*i*-PrOH 97:3, 0.5 mL/min, 25 °C, 220 nm): t_R = 8.0 min (minor), 8.6 min (major).

(*R*)-4-(naphthalen-2-yl)-1,3-dioxane (**4.3l**)

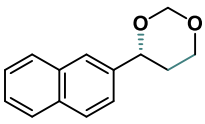

Following *General Procedure C* from 2-vinylnaphthalene (**4.1l**, 38.5 mg, 0.25 mmol), with catalyst (*S*,*S*)-**4.5k** (2.5 mol%), in dry cyclohexane (10 mL, 0.025 M) for 72 h. Purification by flash column chromatography (eluent: *n*-pentane/MTBE 100:0 → 90:10) to give **4.3l** as a white solid (42.1 mg, 79%, er = 90.5:9.5).

^{1}H NMR (501 MHz, $CDCl_3$) δ 7.88 – 7.81 (m, 4H), 7.53 – 7.44 (m, 3H), 5.29 (d, *J* = 6.4 Hz, 1H), 4.97 (d, *J* = 6.4 Hz, 1H), 4.83 (dd, *J* = 11.3, 2.6 Hz, 1H), 4.25 (dd, *J* = 11.4, 4.8 Hz, 1H), 3.94 (td, *J* = 11.8, 2.5 Hz, 1H), 2.25 – 2.13 (m, 1H), 1.85 – 1.79 (m, 1H). ^{13}C NMR (126 MHz, $CDCl_3$) δ 139.0 (C), 133.4 (C), 133.2 (C), 128.4 (CH), 128.2 (CH), 127.8 (CH), 126.3 (CH), 126.1 (CH), 124.6 (CH), 124.0 (CH), 94.4 (CH_2), 78.9 (CH), 67.1 (CH_2), 34.2 (CH_2). Spectroscopic data was consistent with the values reported in the literature.[137] ESI-HRMS: calculated for $C_{14}H_{14}O_2Na^+$ ([M+Na]$^+$): 237.0886, found: 237.0886. $[\alpha_D^{25}]$ = +21.0 (*c* = 0.591, $CHCl_3$). HPLC

(Chiralpak IB-3 column, Heptane/*i*-PrOH 80:20, 1 mL/min, 25 °C, 274 nm): t_R = 3.8 min (minor), 5.6 min (major).

(*R*)-4-(1,3-dioxan-4-yl)phenyl acetate (**4.3m**)

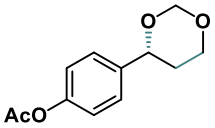

Following *General Procedure C* from 4-vinylphenyl acetate (**4.1m**, 3.8 µL, 0.025 mmol), with catalyst (*S*,*S*)-**4.5b** (2.5 mol%), in dry cyclohexane (0.125 mL, 0.2 M) for 48 h. Approx. 35% yield **4.3m**, by ^{1}H NMR using Ph_3CH as internal standard), complex mixture.

^{1}H NMR (501 MHz, $CDCl_3$): δ 7.38 (d, *J* = 8.3 Hz, 2H), 7.08 (d, *J* = 8.6 Hz, 2H), 5.21 (d, *J* = 6.3 Hz, 1H), 4.89 (d, *J* = 6.4 Hz, 1H), 4.65 (dd, *J* = 11.4, 2.6 Hz, 1H), 4.21 (dd, *J* = 11.4, 4.8 Hz, 1H), 3.87 (td, *J* = 11.9, 2.5 Hz, 1H), 2.30 (s, 3H), 2.02 (dddd, *J* = 13.4, 12.1, 11.3, 4.9 Hz, 1H), 1.76 – 1.68 (m, 1H). Spectroscopic data was consistent with the values reported in the literature.[142]

(*R*)-4-(1,3-dioxan-4-yl)phenyl pivalate (**4.3n**)

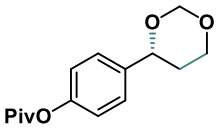

Following *General Procedure C* from 4-vinylphenyl pivalate (**4.1n**, 52 µL, 0.25 mmol), with catalyst (*S*,*S*)-**4.5k** (2.5 mol%), in dry cyclohexane (2.5 mL, 0.1 M) for 72 h. Purification by flash column chromatography (eluent: *n*-pentane/MTBE 100:0 → 80:20) to give **4.3n** as a white solid (54.9 mg, 83%, er = 91:9).

^{1}H NMR (501 MHz, $CDCl_3$) δ 7.38 (d, *J* = 8.5 Hz, 2H), 7.05 (d, *J* = 8.6 Hz, 2H), 5.21 (d, *J* = 6.4 Hz, 1H), 4.89 (d, *J* = 6.4 Hz, 1H), 4.65 (dd, *J* = 11.3, 2.5 Hz, 1H), 4.20 (ddt, *J* = 11.4, 5.0, 1.4 Hz, 1H), 3.87 (td, *J* = 11.9, 2.5 Hz, 1H), 2.07 (dddd, *J* = 13.5, 12.3, 11.3, 4.9 Hz, 1H), 1.75 – 1.68 (m, 1H), 1.35 (s, 9H). ^{13}C NMR (126 MHz, $CDCl_3$) δ 177.2 (C), 150.7 (C), 139.0 (C), 126.9 (CH), 121.6 (CH), 94.3 (CH_2), 78.3 (CH), 67.0 (CH_2), 39.2 (C), 34.2 (CH_2), 27.3 (CH_3). ESI-HRMS: calculated for $C_{15}H_{20}O_4Na^+$ ([M+Na]$^+$): 287.1254, found: 287.1252. $[\alpha_D^{25}]$ = +35.3 (*c* = 0.221, $CHCl_3$). HPLC (Chiralpak IB-3 column, Heptane/*i*-PrOH 98:2, 1 mL/min, 25 °C, 220 nm): t_R = 4.9 min (minor), 5.4 min (major).

(*R*)-4-(4-(methylthio)phenyl)-1,3-dioxane (**4.3o**)

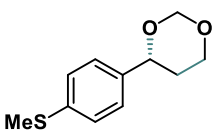

Following *General Procedure C* from methyl(4-vinylphenyl)sulfane (**4.1o**, 37.6 mg, 0.25 mmol; low-melting solid, added from a stock solution in CH_2Cl_2 followed by solvent removal in rotavap), with catalyst (*S*,*S*)-**4.5b** (2.5 mol%), in dry cyclohexane (1.25 mL, 0.2 M) for 48 h. Purification by flash column chromatography (eluent: *n*-pentane/MTBE 100:0 → 70:30) to give **4.3o** (23.7 mg, 45%, er = 51:49).

^{1}H NMR (501 MHz, $CDCl_3$): δ 7.30 (d, *J* = 8.5 Hz, 2H), 7.26 (d, *J* = 8.4 Hz, 2H), 5.21 (d, *J* = 6.3 Hz, 1H), 4.89 (d, *J* = 6.4 Hz, 1H), 4.61 (dd, *J* = 11.3, 2.5 Hz, 1H), 4.20 (dd, *J* = 11.3, 4.9 Hz,

1H), 3.87 (td, *J* = 11.8, 2.5 Hz, 1H), 2.48 (s, 3H), 2.08 (dddd, *J* = 13.4, 12.1, 11.3, 4.8 Hz, 1H), 1.74 – 1.67 (m, 1H). ^{13}C NMR (126 MHz, $CDCl_3$): δ 138.6 (C), 138.1 (C), 126.9 (CH), 126.5 (CH), 94.3 (CH_2), 78.5 (CH), 67.0 (CH_2), 34.0 (CH_2), 16.1 (CH_2). EI-HRMS: calculated for $C_{11}H_{14}O_2S^+$ ([M]$^+$): 210.0709, found: 210.0713.

HPLC (Chiralpak AD-3 column, Heptane/*i*-PrOH 97:3, 1 mL/min, 25 °C, 220 nm): t_R = 5.8 min, 6.4 min.

(*R*)-*S*-(4-(1,3-dioxan-4-yl)phenyl) 2,2-dimethylpropanethioate (**4.3p**)

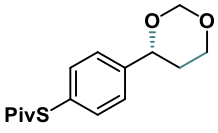

Following *General Procedure C* from *S*-(4-vinylphenyl) 2,2-dimethylpropanethioate (**4.1p**, 54 µL, 0.25 mmol), with catalyst (*S*,*S*)-**4.5k** (2.5 mol%), in dry cyclohexane (5 mL, 0.05 M) for 72 h. Purification by flash column chromatography (eluent: *n*-pentane/MTBE 100:0 → 85:15) to give **4.3p** as a white solid (61.7 mg, 88%, er = 95:5).

^{1}H NMR (501 MHz, $CDCl_3$) δ 7.41 (d, *J* = 8.4 Hz, 2H), 7.38 (d, *J* = 8.7 Hz, 2H), 5.22 (d, *J* = 6.3 Hz, 1H), 4.89 (d, *J* = 6.4 Hz, 1H), 4.67 (dd, *J* = 11.3, 2.6 Hz, 1H), 4.20 (dd, *J* = 11.5, 4.8 Hz, 1H), 3.88 (td, *J* = 11.9, 2.5 Hz, 1H), 2.06 (dddd, *J* = 13.4, 12.1, 11.2, 4.8 Hz, 1H), 1.77 – 1.70 (m, 1H), 1.32 (s, 9H). ^{13}C NMR (126 MHz, $CDCl_3$) δ 204.8 (C), 142.7 (C), 135.1 (CH), 127.5 (C), 126.5 (CH), 94.3 (CH_2), 78.3 (CH), 67.0 (CH_2), 47.1 (C), 34.1 (CH_2), 27.6 (CH_3). ESI-HRMS: calculated for $C_{15}H_{20}O_3SNa^+$ ([M+Na]$^+$): 303.1025, found: 303.1024. $[\alpha_D^{25}]$ = +42.1 (*c* = 0.826, $CHCl_3$). HPLC (Chiralcel OJ-3 column, Heptane/*i*-PrOH 95:5, 1 mL/min, 25 °C, 220 nm): t_R = 12.4 min (minor), 21.2 min (major).

(*R*)-4-(1,3-dioxan-4-yl)-2-methoxyphenyl pivalate (**4.3q**)

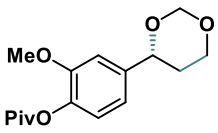

Following *General Procedure C* from 2-methoxy-4-vinylphenyl pivalate (**4.1q**, 68 µL, 0.25 mmol), with catalyst (*S*,*S*)-**4.5k** (2.5 mol%), in dry cyclohexane (2.5 mL, 0.1 M) for 48 h. Purification by flash column chromatography (eluent: *n*-pentane/MTBE 100:0 → 80:20) to give **4.3q** (53.0 mg, 72%, er = 80:20).

^{1}H NMR (501 MHz, $CDCl_3$): δ 7.02 (d, *J* = 1.9 Hz, 1H), 6.97 (d, *J* = 8.0 Hz, 1H), 6.88 (dd, *J* = 8.1, 1.9 Hz, 1H), 5.22 (d, *J* = 6.3 Hz, 1H), 4.89 (d, *J* = 6.4 Hz, 1H), 4.64 (dd, *J* = 11.2, 2.6 Hz, 1H), 4.20 (dd, *J* = 11.5, 4.9 Hz, 1H), 3.87 (td, *J* = 11.9, 2.5 Hz, 1H), 3.82 (s, 3H), 2.07 (dddd, *J* = 13.5, 12.2, 11.3, 4.8 Hz, 1H), 1.75 – 1.69 (m, 1H), 1.36 (s, 9H).

HPLC (Chiralcel OJ-3 column, Heptane/*i*-PrOH 95:5, 1 mL/min, 25 °C, 220 nm): t_R = 10.5 min (minor), 12.8 min (major).

(*R*)-5-(1,3-dioxan-4-yl)-2,2-difluorobenzo[*d*][1,3]dioxole (**4.3r**)

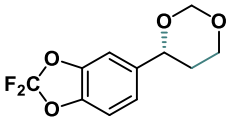

Following *General Procedure C* from 2,2-difluoro-5-vinylbenzo[*d*][1,3]dioxole (**4.1r**, 37 µL, 0.25 mmol), with catalyst (*S*,*S*)-**4.5j** (2.5 mol%), in dry cyclohexane (5 mL, 0.05 M) for 72 h. Purification by flash column chromatography (eluent: *n*-pentane/MTBE 100:0 → 90:10) to give **4.3r** as a colorless liquid (35.0 mg, 57%, er = 94.5:5.5).

^{1}H NMR (501 MHz, $CDCl_3$) δ 7.14 (d, *J* = 1.6 Hz, 1H), 7.06 (dd, *J* = 8.2, 1.6 Hz, 1H), 7.02 (d, *J* = 8.2 Hz, 1H), 5.20 (d, *J* = 6.4 Hz, 1H), 4.88 (d, *J* = 6.4 Hz, 1H), 4.63 (dd, *J* = 11.3, 2.6 Hz, 1H), 4.20 (dd, *J* = 11.5, 4.9 Hz, 1H), 3.86 (td, *J* = 11.9, 2.5 Hz, 1H), 2.03 (dddd, *J* = 13.4, 12.1, 11.2, 4.9 Hz, 1H), 1.74 – 1.68 (m, 1H). ^{19}F NMR (471 MHz, $CDCl_3$) δ –50.03 (d, *J* = 3.5 Hz, 2F). ^{13}C NMR (126 MHz, $CDCl_3$) δ 144.1 (C), 143.3 (C), 138.1 (C), 131.8 (t, *J* = 254.9 Hz, C), 121.0 (CH), 109.3 (CH), 107.6 (CH), 94.3 (CH_2), 78.1 (CH), 66.9 (CH_2), 34.3 (CH_2). EI-HRMS: calculated for $C_{11}H_{10}F_2O_4^+$ ([M]$^+$): 244.0540, found: 244.0542. $[\alpha_D^{25}]$ = +34.5 (*c* = 0.522, $CHCl_3$). HPLC (Chiralcel OJ-3 column, Heptane/*i*-PrOH 95:5, 1 mL/min, 25 °C, 220 nm): t_R = 5.2 min (major), 5.6 min (major).

(*R*)-4-(4-fluorophenyl)-1,3-dioxane (**4.3s**)

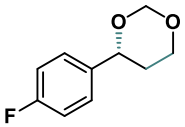

Following *General Procedure C* from 4-fluorostyrene (**4.1s**, 30 µL, 0.25 mmol), with catalyst (*S*,*S*)-**4.5j** (2.5 mol%), in dry cyclohexane (5 mL, 0.05 M) for 96 h. Purification by flash column chromatography (eluent: *n*-pentane/MTBE 100:0 → 95:5) to give **4.3s** as a yellow solid (37.4 mg, 82%, er = 94.5:5.5).

^{1}H NMR (501 MHz, $CDCl_3$) δ 7.35 (dd, *J* = 8.6, 5.5 Hz, 2H), 7.05 (t, *J* = 8.7 Hz, 2H), 5.21 (d, *J* = 6.3 Hz, 1H), 4.89 (d, *J* = 6.4 Hz, 1H), 4.63 (dd, *J* = 11.4, 2.5 Hz, 1H), 4.21 (dd, *J* = 11.6, 4.7 Hz, 1H), 3.87 (td, *J* = 11.9, 2.5 Hz, 1H), 1.74 – 1.67 (m, 1H). ^{19}F NMR (471 MHz, $CDCl_3$) δ –114.62 (s, 1F). ^{13}C NMR (126 MHz, $CDCl_3$) δ 162.5 (d, *J* = 245.8 Hz, C), 137.4 (d, *J* = 3.2 Hz, C), 127.6 (d, *J* = 8.1 Hz, CH), 115.5 (d, *J* = 21.3 Hz, CH), 94.3 (CH_2), 78.2 (CH), 67.0 (CH_2), 34.1 (CH_2). Spectroscopic data was consistent with the values reported in the literature.[146c] ESI-HRMS: calculated for $C_{10}H_{11}FO_2Na^+$ ([M+Na]$^+$): 205.0635, found: 205.0637. $[\alpha_D^{25}]$ = +34.1 (*c* = 0.369, $CHCl_3$). HPLC (Chiralpak IC-3 column, Heptane/*i*-PrOH 98:2, 1 mL/min, 25 °C, 220 nm): t_R = 4.5 min (minor), 4.9 min (major).

(*R*)-4-(3-fluorophenyl)-1,3-dioxane (**4.3t**)

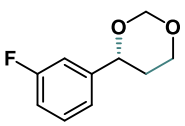

Following *General Procedure C* from 3-fluorostyrene (**4.1t**, 30 µL, 0.25 mmol), with catalyst (*S*,*S*)-**4.5k** (2.5 mol%), in dry cyclohexane (1.25 mL, 0.2 M) for 5 days. Purification by flash column chromatography (eluent: *n*-pentane/MTBE 100:0 → 95:5) to give **4.3t** as a colorless liquid (23.6 mg, 52%, er = 96.5:3.5).

^{1}H NMR (501 MHz, $CDCl_3$) δ 7.32 (td, *J* = 8.0, 5.9 Hz, 1H), 7.15 – 7.07 (m, 2H), 6.98 (tdd, *J* = 8.4, 2.6, 1.0 Hz, 1H), 5.22 (d, *J* = 6.4 Hz, 1H), 4.89 (d, *J* = 6.4 Hz, 1H), 4.65 (dd, *J* = 11.3, 2.6 Hz, 1H), 4.20 (ddt, *J* = 11.5, 4.9, 1.4 Hz, 1H), 3.87 (td, *J* = 11.9, 2.5 Hz, 1H), 2.05 (dddd, *J* = 13.5, 12.2, 11.3, 4.9 Hz, 1H), 1.77 – 1.71 (m, 1H). ^{19}F NMR (471 MHz, $CDCl_3$) δ –112.87 (s, 1F). ^{13}C NMR (126 MHz, $CDCl_3$) δ 163.1 (d, *J* = 245.9 Hz, C), 144.2 (d, *J* = 7.3 Hz, C), 130.1 (d, *J* = 8.0 Hz, CH), 121.3 (d, *J* = 2.8 Hz, CH), 114.7 (d, *J* = 20.8 Hz, CH), 112.9 (d, *J* = 22.4 Hz, CH), 94.2 (CH_2), 78.0 (d, *J* = 2.1 Hz, CH), 66.9 (CH_2), 34.0 (CH_2). ESI-HRMS: calculated for $C_{10}H_{11}FO_2Na^+$ ([M+Na]$^+$): 205.0635, found: 205.0637. $[\alpha_D^{25}]$ = +38.3 (*c* = 0.626, $CHCl_3$). HPLC (Chiralcel OJ-3 column, Heptane/*i*-PrOH 95:5, 1 mL/min, 25 °C, 220 nm): t_R = 5.8 min (minor), 6.4 min (major).

(*R*)-4-(3-bromo-4-methoxyphenyl)-1,3-dioxane (**4.3u**)

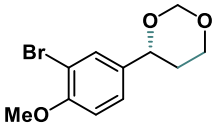

Following *General Procedure C* from 2-bromo-1-methoxy-4-vinylbenzene (**4.1u**, 53.3 mg, 0.25 mmol), with catalyst (*S*,*S*)-**4.5n** (2.5 mol%), in dry cyclohexane (1.25 mL, 0.2 M) for 5 days. Purification by flash column chromatography (eluent: *n*-pentane/MTBE 100:0 → 80:20) to give **4.3u** (23.2 mg, 34%, er = 70.5:29.5).

^{1}H NMR (501 MHz, CD_2Cl_2): δ 7.55 (dd, *J* = 2.1, 0.6 Hz, 1H), 7.28 (ddd, *J* = 8.5, 2.2, 0.7 Hz, 1H), 6.91 (d, *J* = 8.5 Hz, 1H), 5.13 (d, *J* = 6.3 Hz, 1H), 4.85 (d, *J* = 6.3 Hz, 1H), 4.57 (dd, *J* = 11.3, 2.6 Hz, 1H), 4.15 (ddt, *J* = 11.5, 4.9, 1.5 Hz, 1H), 3.87 (s, 3H), 3.83 (td, *J* = 11.8, 2.5 Hz, 1H), 1.99 (dddd, *J* = 13.4, 12.2, 11.3, 4.9 Hz, 1H), 1.71 – 1.65 (m, 1H). ^{13}C NMR (126 MHz, CD_2Cl_2): δ 155.8 (C), 135.9 (C), 131.3 (CH), 126.5 (CH), 112.2 (CH), 111.7 (C), 94.5 (CH_2), 77.9 (CH), 67.1 (CH_2), 56.7 (CH_3), 34.3 (CH_2). EI-HRMS: calculated for $C_{11}H_{13}BrO_3^+$ ([M]$^+$): 272.0043, found: 272.0044.

HPLC (Chiralpak AD-3 column, Heptane/*i*-PrOH 95:5, 1 mL/min, 25 °C, 220 nm): t_R = 6.0 min (major), 7.0 min (minor).

(*R*)-4-(3-bromo-4-methylphenyl)-1,3-dioxane (**4.3v**)

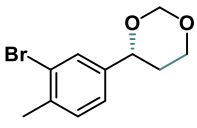

Following *General Procedure C* from 2-bromo-1-methyl-4-vinylbenzene (**4.1v**, 37 µL, 0.25 mmol), with catalyst (*S*,*S*)-**4.5b** (2.5 mol%), in dry cyclohexane (1.25 mL, 0.2 M) for 5 days. Purification by flash column chromatography (eluent: *n*-pentane/MTBE 100:0 → 95:5) to give **4.3v** as a colorless oil (43.2 mg, 67%, er = 94:6).

^{1}H NMR (501 MHz, $CDCl_3$) δ 7.56 (d, *J* = 1.6 Hz, 1H), 7.22 (d, *J* = 7.8 Hz, 1H), 7.19 (dd, *J* = 7.8, 1.6 Hz, 1H), 5.20 (d, *J* = 6.4 Hz, 1H), 4.87 (d, *J* = 6.4 Hz, 1H), 4.59 (dd, *J* = 11.3, 2.6 Hz, 1H), 4.19 (dd, *J* = 11.5, 4.9 Hz, 1H), 3.86 (td, *J* = 11.9, 2.4 Hz, 1H), 2.38 (s, 3H), 2.05 (dddd, *J* = 13.5, 12.2, 11.3, 4.9 Hz, 1H), 1.73 – 1.68 (m, 1H). ^{13}C NMR (126 MHz, $CDCl_3$) δ 141.1 (C),

137.4 (C), 130.9 (CH), 129.9 (CH), 125.1 (C), 124.7 (CH), 94.3 (CH_2), 77.8 (CH), 66.9 (CH_2), 34.0 (CH_2), 22.7 (CH_3). ESI-HRMS: calculated for $C_{11}H_{13}BrO_2Na^+$ ([M+Na]$^+$): 278.9991, found: 278.9993. $[\alpha_D^{25}]$ = +32.0 (*c* = 0.651, $CHCl_3$). HPLC (Chiralcel OJ-3 column, Heptane/*i*-PrOH 95:5, 1 mL/min, 25 °C, 220 nm): t_R = 6.2 min (minor), 7.6 min (major).

ethyl (*R*)-4-(1,3-dioxan-4-yl)benzoate (**4.3w**)

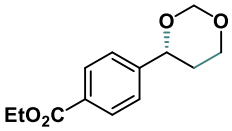

Following *General Procedure C* from ethyl 4-vinylbenzoate (**4.1w**, 43 µL, 0.25 mmol), with catalyst (*S*,*S*)-**4.5p** (2.5 mol%), in dry cyclohexane (1.25 mL, 0.2 M) for 5 days. Purification by flash column chromatography (eluent: *n*-pentane/MTBE 100:0 → 85:15) to give **4.3w** as a white solid (13.4 mg, 23%, er = 96:4).

^{1}H NMR (501 MHz, $CDCl_3$) δ 8.04 (d, *J* = 8.4 Hz, 2H), 7.44 (d, *J* = 8.2 Hz, 2H), 5.24 (d, *J* = 6.4 Hz, 1H), 4.90 (d, *J* = 6.4 Hz, 1H), 4.71 (dd, *J* = 11.3, 2.6 Hz, 1H), 4.38 (q, *J* = 7.1 Hz, 2H), 4.21 (dd, *J* = 11.5, 4.8 Hz, 1H), 3.89 (td, *J* = 11.9, 2.5 Hz, 1H), 2.04 (dddd, *J* = 13.4, 12.2, 11.3, 4.8 Hz, 1H), 1.78 – 1.72 (m, 1H), 1.39 (t, *J* = 7.1 Hz, 3H). ^{13}C NMR (126 MHz, $CDCl_3$) δ 166.5 (C), 146.5 (C), 130.0 (C), 129.9 (CH), 125.6 (CH), 94.2 (CH_2), 78.3 (CH), 66.9 (CH_2), 61.1 (CH_2), 34.1 (CH_2), 14.5 (CH_3). ESI-HRMS: calculated for $C_{13}H_{16}O_4Na^+$ ([M+Na]$^+$): 259.0941, found: 259.0944. $[\alpha_D^{25}]$ = +28.5 (*c* = 0.548, $CHCl_3$). HPLC (Chiralpak AD-3 column, Heptane/*i*-PrOH 95:5, 1 mL/min, 25 °C, 220 nm): t_R = 7.1 min (major), 8.4 min (minor).

(*R*)-4-(5,6,7,8-tetrahydronaphthalen-2-yl)-1,3-dioxane (**4.3x**)

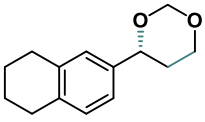

Following *General Procedure C* from 6-vinyl-1,2,3,4-tetrahydronaphthalene (**4.1x**, 42 µL, 0.25 mmol), with catalyst (*S*,*S*)-**4.5b** (2.5 mol%), in dry cyclohexane (2.5 mL, 0.1 M) for 72 h. Purification by flash column chromatography (eluent: *n*-pentane/MTBE 100:0 → 80:20) to give **4.3x** (44.2 mg, 81%, er = 81.5:18.5).

^{1}H NMR (501 MHz, $CDCl_3$): δ 7.11 – 7.04 (m, 3H), 5.21 (d, *J* = 6.4 Hz, 1H), 4.89 (d, *J* = 6.3 Hz, 1H), 4.58 (dd, *J* = 11.3, 2.5 Hz, 1H), 4.20 (dd, *J* = 11.4, 4.9 Hz, 1H), 3.87 (td, *J* = 11.8, 2.4 Hz, 1H), 2.82 – 2.72 (m, 4H), 2.12 (dtd, *J* = 13.6, 11.7, 4.8 Hz, 1H), 1.79 (p, *J* = 3.2 Hz, 4H), 1.70 (ddd, *J* = 13.7, 2.7, 1.5 Hz, 1H). ^{13}C NMR (126 MHz, $CDCl_3$): δ 138.7 (C), 137.4 (C), 137.0 (C), 129.4 (CH), 126.7 (CH), 123.1 (CH), 94.4 (CH_2), 79.0 (CH), 67.1 (CH_2), 34.0 (CH_2), 29.6 (CH_2), 29.3 (CH_2), 23.3 (CH_2). EI-HRMS: calculated for $C_{14}H_{18}O_2^+$ ([M]$^+$): 218.1301, found: 218.1301. HPLC (Chiralpak IC-3 column, Heptane/*i*-PrOH 98:2, 1 mL/min, 25 °C, 220 nm): t_R = 6.4 min (minor), 7.8 min (major).

4-(9,9-dimethyl-9*H*-fluoren-2-yl)-1,3-dioxane (**4.3y**)

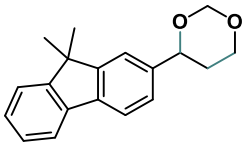

Following *General Procedure C* from 9,9-dimethyl-2-vinyl-9*H*-fluorene (**4.1y**, 55.1 mg, 0.25 mmol), with catalyst (*S*,*S*)-**4.5k** (2.5 mol%), in dry cyclohexane (2.5 mL, 0.1 M) for 96 h. Purification by flash column chromatography (eluent: *n*-pentane/MTBE 100:0 → 80:20) to give **4.3y** (43.5 mg, 62%, er = 58:42).

^{1}H NMR (501 MHz, $CDCl_3$): δ 7.74 – 7.68 (m, 2H), 7.48 (d, *J* = 1.5 Hz, 1H), 7.45 – 7.41 (m, 1H), 7.36 – 7.29 (m, 3H), 5.27 (d, *J* = 6.4 Hz, 1H), 4.94 (d, *J* = 6.3 Hz, 1H), 4.73 (dd, *J* = 11.3, 2.5 Hz, 1H), 4.24 (dd, *J* = 11.4, 4.9 Hz, 1H), 3.92 (td, *J* = 11.8, 2.5 Hz, 1H), 2.18 (dddd, *J* = 13.5, 12.2, 11.3, 4.8 Hz, 1H), 1.78 (dtt, *J* = 13.6, 2.5, 1.1 Hz, 1H), 1.49 (s, 6H). ^{13}C NMR (126 MHz, $CDCl_3$): δ 154.1 (C), 154.0 (C), 140.7 (C), 139.1 (C), 139.0 (C), 127.4 (CH), 127.1 (CH), 124.9 (CH), 122.7 (CH), 120.2 (CH), 120.15 (CH), 120.06 (CH), 94.4 (CH_2), 79.4 (CH), 67.2 (CH_2), 47.1 (C), 34.4 (CH_2), 27.33 (CH_3), 27.32 (CH_3). EI-HRMS: calculated for $C_{19}H_{20}O_2^+$ ($[M]^+$): 280.1458, found: 280.1463.

HPLC (Chiralpak AD-3 column, Heptane/*i*-PrOH 95:5, 1 mL/min, 25 °C, 220 nm): t_R = 3.8 min, 4.9 min.

4-(naphthalen-1-yl)-1,3-dioxane (**4.3z**)

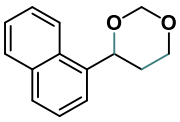

Following *General Procedure C* from 1-vinylnaphthalene (**4.1z**, 38.6 mg, 0.25 mmol), with catalyst (*S*,*S*)-**4.5k** (2.5 mol%), in dry cyclohexane (1.25 mL, 0.2 M) for 5 days. Purification by flash column chromatography (eluent: *n*-pentane/MTBE 100:0 → 80:20) to give **4.3z** (17.7 mg, 33%, er = 66.5:33.5).

^{1}H NMR (501 MHz, CD_2Cl_2): δ 8.09 (d, *J* = 8.3 Hz, 1H), 7.91 – 7.87 (m, 1H), 7.82 (d, *J* = 8.2 Hz, 1H), 7.66 (d, *J* = 7.2 Hz, 1H), 7.52 (dddd, *J* = 17.3, 8.4, 6.8, 1.6 Hz, 3H), 5.37 (dd, *J* = 11.3, 2.4 Hz, 1H), 5.27 (d, *J* = 6.3 Hz, 1H), 5.06 (d, *J* = 6.4 Hz, 1H), 4.23 (ddt, *J* = 11.4, 4.9, 1.4 Hz, 1H), 4.01 (td, *J* = 11.8, 2.4 Hz, 1H), 2.23 (dtd, *J* = 13.2, 11.9, 4.8 Hz, 1H), 1.95 – 1.89 (m, 1H). ^{13}C NMR (126 MHz, CD_2Cl_2): δ 137.6, 134.2, 130.6, 129.2, 128.5, 126.4, 125.9, 123.7, 123.5, 94.9, 76.5, 67.4, 33.7. EI-HRMS: calculated for $C_{14}H_{14}O_2^+$ ($[M]^+$): 214.0988, found: 214.0990.

HPLC (Kromasil Amycoat RP column, CH_3CN/H_2O 50:50, 1 mL/min, 25 °C, 220 nm): t_R = 8.1 min, 10.5 min.

(*R*)-4-(*o*-tolyl)-1,3-dioxane (**4.3za**)

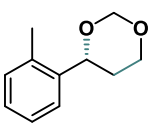

Following *General Procedure C* from 2-methylstyrene (**4.1za**, 32 µL, 0.25 mmol), with catalyst (*S*,*S*)-**4.5j** (2.5 mol%), in dry cyclohexane (2.5 mL, 0.1 M) for 7 days. Purification by flash column chromatography (eluent: *n*-pentane/MTBE 100:0 → 95:5) to give **4.3za** as a colorless liquid (34.7 mg, 78%, er = 88.5:11.5).

^{1}H NMR (501 MHz, $CDCl_3$) δ 7.50 (dd, *J* = 7.6, 1.7 Hz, 1H), 7.25 (t, *J* = 8.4 Hz, 1H), 7.20 (td, *J* = 7.4, 1.5 Hz, 1H), 7.15 (d, *J* = 7.4 Hz, 1H), 5.24 (d, *J* = 6.3 Hz, 1H), 4.93 (d, *J* = 6.3 Hz, 1H), 4.83 (dd, *J* = 11.2, 2.4 Hz, 1H), 4.22 (dd, *J* = 11.4, 4.8 Hz, 1H), 3.89 (td, *J* = 11.9, 2.4 Hz, 1H), 2.35 (s, 3H), 2.09 (dddd, *J* = 13.6, 12.3, 11.2, 4.8 Hz, 1H), 1.73 – 1.66 (m, 1H). ^{13}C NMR (126 MHz, $CDCl_3$) δ 139.5 (C), 134.4 (C), 130.5 (CH), 127.7 (CH), 126.5 (CH), 125.9 (CH), 94.5 (CH_2), 76.2 (CH), 67.2 (CH_2), 32.8 (CH_2), 19.1 (CH_3). ESI-HRMS: calculated for $C_{11}H_{14}O_2Na^+$ ([M+Na]$^+$): 201.0886, found: 201.0888. $[\alpha_D^{25}]$ = +37.6 (*c* = 0.622, $CHCl_3$). HPLC (Chiralpak IC-3 column, Heptane/*i*-PrOH 97:3, 0.5 mL/min, 25 °C, 220 nm): t_R = 9.1 min (minor), 10.1 min (major).

(*R*)-4-(4-vinylphenyl)-1,3-dioxane (**4.3zb**)

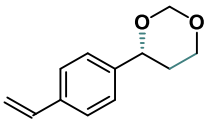

Following *General Procedure C* from 1,4-divinylbenzene (**4.1zb**, 36 µL, 0.25 mmol), paraformaldehyde **2a** (18.8 mg, 0.625 mmol, 2.5 equiv.), with catalyst (*S*,*S*)-**4.5b** (2.5 mol%), in dry cyclohexane (2.5 mL, 0.1 M) for 48 h. Purification by preparative TLC (eluent: *i*-hexane/MTBE 93:7) to give **4.3zb** (28.0 mg, 60%, er = 89.5:10.5). Also **4.3zb'** could be isolated (18.0 mg, 30% based on diolefin, er = 99:1).

4.3zb: ^{1}H NMR (501 MHz, $CDCl_3$): δ 7.41 (d, *J* = 8.3 Hz, 2H), 7.33 (d, *J* = 8.2 Hz, 2H), 6.71 (dd, *J* = 17.6, 10.9 Hz, 1H), 5.74 (dd, *J* = 17.6, 1.0 Hz, 1H), 5.24 (dd, *J* = 11.0, 1.0 Hz, 1H), 5.22 (d, *J* = 6.6 Hz, 1H), 4.90 (d, *J* = 6.4 Hz, 1H), 4.64 (dd, *J* = 11.3, 2.6 Hz, 1H), 4.20 (dd, *J* = 11.4, 4.9 Hz, 1H), 3.88 (td, *J* = 11.9, 2.4 Hz, 1H), 2.09 (dddd, *J* = 13.6, 12.2, 11.3, 4.8 Hz, 1H), 1.75 – 1.68 (m, 1H). Spectroscopic data was consistent with the values reported in the literature.[221]

HPLC (Chiralpak AD-3 column, Heptane/*i*-PrOH 97:3, 1 mL/min, 25 °C, 220 nm): t_R = 4.2 min (major), 4.6 min (minor).

1,4-di((*R*)-1,3-dioxan-4-yl)benzene (**4.3zb'**)

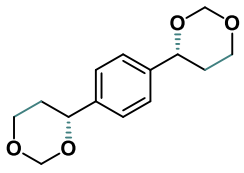

^{1}H NMR (501 MHz, $CDCl_3$): δ 7.37 (s, 4H), 5.21 (d, *J* = 6.3 Hz, 2H), 4.90 (d, *J* = 6.4 Hz, 2H), 4.65 (dd, *J* = 11.2, 2.5 Hz, 2H), 4.20 (dd, *J* = 11.4, 4.9 Hz, 2H), 3.88 (td, *J* = 11.9, 2.5 Hz, 2H), 2.08 (ddddd, *J* = 13.4, 12.3, 11.3, 4.9, 1.1 Hz, 2H), 1.75 – 1.68 (m, 2H). Spectroscopic data was consistent with the values reported in the literature.[221]

HPLC (Chiralpak AD-3 column, Heptane/*i*-PrOH 95:5, 1 mL/min, 25 °C, 220 nm): t_R = 11.4 min (major), 12.6 min (minor).

(*R*)-4-(4-allylphenyl)-1,3-dioxane (**4.3zc**)

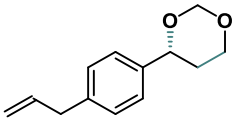

Following *General Procedure C* from 1-allyl-4-vinylbenzene (**4.1zc**, 40 µL, 0.25 mmol), with catalyst (*S*,*S*)-**4.5b** (2.5 mol%), in dry cyclohexane (5 mL, 0.05 M) for 72 h. Purification by flash column chromatography (eluent: *n*-pentane/MTBE 100:0 → 95:5) to give **4.3zc** as a colorless liquid (45.3 mg, 89%, er = 91:9). ^{1}H NMR (501 MHz, $CDCl_3$) δ 7.31 (d, *J* = 8.1 Hz, 2H), 7.19 (d, *J* = 8.2 Hz, 2H), 5.96 (ddt, *J* = 16.9, 10.1, 6.7 Hz, 1H), 5.21 (d, *J* = 6.3 Hz, 1H), 5.09 (dq, *J* = 9.5, 1.7 Hz, 1H), 5.06 (p, *J* = 1.6 Hz, 1H), 4.90 (d, *J* = 6.3 Hz, 1H), 4.63 (dd, *J* = 11.3, 2.5 Hz, 1H), 4.21 (dd, *J* = 11.4, 4.9 Hz, 1H), 3.88 (td, *J* = 11.8, 2.4 Hz, 1H), 3.39 (d, *J* = 6.7 Hz, 2H), 2.11 (dddd, *J* = 13.4, 12.2, 11.3, 4.8 Hz, 1H), 1.73 – 1.68 (m, 1H). ^{13}C NMR (126 MHz, $CDCl_3$) δ 139.8 (C), 139.4 (C), 137.5 (CH), 128.8 (CH), 126.1 (CH), 116.0 (CH_2), 94.4 (CH_2), 78.8 (CH), 67.1 (CH_2), 40.0 (CH_2), 34.0 (CH_2). ESI-HRMS: calculated for $C_{13}H_{16}O_2Na^+$ ([M+Na]$^+$): 227.1042, found: 227.1041. $[\alpha_D^{25}]$ = +29.4 (*c* = 0.639, $CHCl_3$). HPLC (Chiralpak IC-3 column, Heptane/*i*-PrOH 97:3, 0.5 mL/min, 25 °C, 220 nm): t_R = 9.4 min (minor), 10.4 min (major).

(*R*)-2-(1,3-dioxan-4-yl)-9-tosyl-9*H*-carbazole (**4.3zg**)

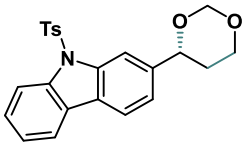

Following *General Procedure C* from 9-tosyl-2-vinyl-9*H*-carbazole (**4.1zg**, 86.9 mg, 0.25 mmol), with catalyst (*S*,*S*)-**4.5m** (2.5 mol%), in dry cyclohexane (10 mL, 0.025 M) for 96 h. Purification by flash column chromatography (eluent: *n*-pentane/MTBE 100:0 → 80:20) to give **4.3zg** as a light-yellow solid (67.0 mg, 66%, er = 83:17).

^{1}H NMR (501 MHz, $CDCl_3$) δ 8.34 (s, 1H), 8.31 (dt, *J* = 8.5, 0.9 Hz, 1H), 7.89 (d, *J* = 8.0 Hz, 1H), 7.88 (d, *J* = 7.7 Hz, 0H), 7.48 (ddd, *J* = 8.5, 7.3, 1.3 Hz, 1H), 7.43 (dd, *J* = 8.1, 1.5 Hz, 1H), 7.35 (td, *J* = 7.5, 1.0 Hz, 1H), 7.10 (d, *J* = 8.4 Hz, 1H), 5.30 (d, *J* = 6.3 Hz, 1H), 4.98 (d, *J* = 6.3 Hz, 1H), 4.85 (dd, *J* = 11.3, 2.7 Hz, 1H), 4.27 (ddt, *J* = 11.4, 4.9, 1.4 Hz, 1H), 3.95 (td, *J* = 11.8, 2.4 Hz, 1H), 2.18 (dddd, *J* = 13.5, 12.3, 11.3, 4.8 Hz, 1H), 1.87 – 1.81 (m, 1H). ^{13}C NMR (126 MHz, $CDCl_3$) δ 145.0 (C), 141.4 (C), 138.8 (C), 138.6 (C), 135.1 (C), 129.8 (CH), 127.5 (CH), 126.6 (CH), 126.3 (C), 126.1 (C), 124.1 (CH), 121.8 (CH), 120.2 (CH), 120.1 (CH), 115.3 (CH), 112.9 (CH), 94.4 (CH_2), 79.2 (CH), 67.1 (CH_2), 34.5 (CH_2), 21.6 (CH_3). ESI-HRMS: calculated for $C_{23}H_{21}NO_4SNa^+$ ([M+Na]$^+$): 430.1084, found: 430.1085. $[\alpha_D^{25}]$ = +26.1 (*c* = 0.964, $CHCl_3$). HPLC (Chiralpak IB-3 column, Heptane/*i*-PrOH 95:5, 1 mL/min, 25 °C, 261 nm): t_R = 10.0 min (major), 11.4 min (minor).

(4*S,5*S**)-5-methyl-4-phenyl-1,3-dioxane** (**4.11a**)

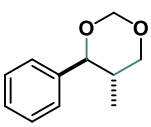

Following *General Procedure C* from *trans*-*β*-methylstyrene (**4.10a**, 3.2 µL, 0.025 mmol), with catalyst (*S*,*S*)-**4.5p** (2.5 mol%), in dry cyclohexane (0.125 mL,

0.2 M) for 4 days. ^{1}H NMR analysis of the crude (using Ph_3CH as internal standard) revealed 27% yield of **4.11a** (er = 57.5:42.5), along with 5% of the *cis*-isomer.

Trans-isomer: ^{1}H NMR (501 MHz, $CDCl_3$) δ 7.40 – 7.28 (m, 5H), 5.21 (d, *J* = 6.2 Hz, 1H), 4.84 (d, *J* = 6.3 Hz, 1H), 4.12 (d, *J* = 10.1 Hz, 1H), 4.11 (d, *J* = 11.7 Hz, 1H), 3.42 (t, *J* = 11.2 Hz, 1H), 2.17 – 2.07 (m, 1H), 0.60 (d, *J* = 6.8 Hz, 3H). ^{13}C NMR (126 MHz, $CDCl_3$) δ 139.6 (C), 128.5 (CH), 128.4 (CH), 127.5 (CH), 94.3 (CH_2), 86.4 (CH), 73.2 (CH_2), 36.5 (CH), 12.7 (CH_3). Spectroscopic data was consistent with the values reported in the literature.[151c]

HPLC (Chiralcel OJ-3R column, CH_3CN/H_2O 50:50, 1 mL/min, 25 °C, 220 nm): t_R = 9.2 min, 9.9 min.

(4*S,5*S**)-4-(4-methoxyphenyl)-5-methyl-1,3-dioxane** (**4.11b**)

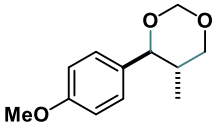

Following *General Procedure C* from *trans*-anethole (**4.10b**, 3.7 µL, 0.025 mmol), with catalyst (*S*,*S*)-**4.5b** (2.5 mol%), in dry cyclohexane (0.125 mL, 0.2 M) for 4 days. ^{1}H NMR analysis of the crude (using Ph_3CH as internal standard) revealed 48% yield of **4.11b** (er = 64.5:35.5), along with 7% of the *cis*-isomer.

Trans-isomer: ^{1}H NMR (501 MHz, CD_2Cl_2): δ 7.30 – 7.24 (m, 2H), 6.91 – 6.85 (m, 2H), 5.11 (d, *J* = 6.2 Hz, 1H), 4.80 (d, *J* = 6.3 Hz, 1H), 4.06 (dd, *J* = 11.3, 4.6 Hz, 1H), 4.05 (d, *J* = 10.0 Hz, 1H), 3.80 (s, 3H), 3.38 (t, *J* = 11.2 Hz, 1H), 2.11 – 1.98 (m, 1H), 0.56 (d, *J* = 6.7 Hz, 3H). ^{13}C NMR (126 MHz, CD_2Cl_2): δ 159.9 (C), 132.4 (C), 129.0 (CH), 114.0 (CH), 94.5 (CH_2), 86.0 (CH), 73.3 (CH_2), 55.6 (CH_3), 36.8 (CH), 12.7 (CH_3). Spectroscopic data was consistent with the values reported in the literature.[151c]

HPLC (Chiralcel OJ-3R column, CH_3CN/H_2O 50:50, 1 mL/min, 25 °C, 220 nm): t_R = 8.6 min, 10.0 min.

(4a*R,9b*S**)-4,4a,5,9b-tetrahydroindeno[1,2-*d*][1,3]dioxine** (**4.11c**)

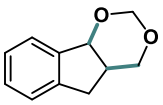

Following *General Procedure C* from 1*H*-indene (**4.10c**, 2.9 µL, 0.025 mmol), with catalyst (*S*,*S*)-**4.5b** (2.5 mol%), in dry cyclohexane (2.5 mL, 0.1 M) for 4 days. ^{1}H NMR analysis of the crude (using Ph_3CH as internal standard) revealed 26% yield of **4.11c** (er = 76.5:23.5).

^{1}H NMR (501 MHz, $CDCl_3$) δ 7.42 (d, *J* = 7.0 Hz, 1H), 7.34 – 7.28 (m, 2H), 7.27 – 7.23 (m, 1H), 5.08 (d, *J* = 4.8 Hz, 1H), 4.92 (d, *J* = 6.2 Hz, 1H), 4.80 (d, *J* = 6.2 Hz, 1H), 4.07 (dd, *J* = 11.9, 4.5 Hz, 1H), 3.94 (dd, *J* = 11.9, 3.8 Hz, 1H), 3.10 (dd, *J* = 15.5, 7.9 Hz, 1H), 2.91 (dd, *J* = 15.5, 7.3 Hz, 1H), 2.41 (tt, *J* = 7.6, 3.9 Hz, 1H). ^{13}C NMR (126 MHz, $CDCl_3$): δ 144.5 (C), 141.5 (C), 129.1 (CH), 127.0 (CH), 125.6 (CH), 124.9 (CH), 91.1 (CH_2), 79.4 (CH), 67.6 (CH_2), 38.5 (CH), 33.1 (CH_2). Spectroscopic data was consistent with the values reported in the literature.[136]

HPLC (Chiralcel OJ-3R column, CH_3CN/H_2O 50:50, 1 mL/min, 25 °C, 220 nm): t_R = 5.2 min, 7.1 min.

(*R*)-4-phenyl-1,3-dioxane-5,5-*d*$_2$ (4.3a(*d*$_2$))

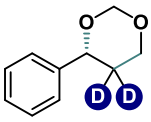

Following *General Procedure C* from styrene-β,β-*d*$_2$ (**4.1zj**, 32 µL, 0.25 mmol), paraformaldehyde **4.2a** (18.8 mg, 0.625 mmol, 2.5 equiv.), with catalyst (*S*,*S*)-**4.5m** (2.5 mol%), in dry cyclohexane (2.5 mL, 0.1 M) for 72 h. Purification by flash column chromatography (eluent: *n*-pentane/MTBE 100:0 → 95:5) to give **4.3a(*d*$_2$)** as a colorless liquid (30.4 mg, 73%, er = 95:5).

^{1}H NMR (501 MHz, $CDCl_3$) δ 7.41 – 7.33 (m, 4H), 7.33 – 7.26 (m, 1H), 5.23 (d, *J* = 6.3 Hz, 1H), 4.90 (d, *J* = 6.4 Hz, 1H), 4.65 (s, 1H), 4.21 (d, *J* = 11.4 Hz, 1H), 3.88 (dt, *J* = 11.5, 1.9 Hz, 1H). ^{13}C NMR (126 MHz, $CDCl_3$) δ 141.6 (C), 128.6 (CH), 128.0 (CH), 125.9 (CH), 94.3 (CH_2), 78.8 (CH), 67.0 (CH_2). *The carbon atom from the CD_2 group was not visible.* EI-HRMS: calculated for $C_{10}H_{10}D_2O_2^+$ ([M]$^+$): 166.0957, found: 166.0958. $[\alpha_D^{25}]$ = +27.5 (*c* = 0.793, $CHCl_3$). HPLC (Chiralpak IB-3 column, Heptane/*i*-PrOH 95:5, 1 mL/min, 25 °C, 220 nm): t_R = 3.6 min (major), 4.5 min (minor).

(*R*)-4-phenyl-1,3-dioxane-2,2,6,6-*d*$_4$ (4.3a(*d*$_4$))

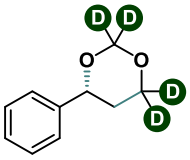

Following *General Procedure C* from styrene (**4.1a**, 29 µL, 0.25 mmol), paraformaldehyde-*d*$_2$ **4.2e** (20.0 mg, 0.625 mmol, 2.5 equiv.), with catalyst (*S*,*S*)-**4.5m** (2.5 mol%), in dry cyclohexane (2.5 mL, 0.1 M) for 72 h. Purification by flash column chromatography (eluent: *n*-pentane/MTBE 100:0 → 95:5) to give **4.3a(*d*$_4$)** as a colorless liquid (26.1 mg, 62%, er = 95:5).

^{1}H NMR (501 MHz, $CDCl_3$) δ 7.40 – 7.34 (m, 4H), 7.33 – 7.28 (m, 1H), 4.66 (dd, *J* = 11.3, 2.6 Hz, 1H), 2.09 (ddt, *J* = 13.2, 11.2, 1.8 Hz, 1H), 1.72 (dd, *J* = 13.5, 2.6 Hz, 1H). ^{13}C NMR (126 MHz, $CDCl_3$) δ 141.6 (C), 128.6 (CH), 128.0 (CH), 125.9 (CH), 78.8 (CH), 33.9 (CH_2). *The carbon atoms from CD_2 groups were not visible.* EI-HRMS: calculated for $C_{10}H_8D_4O_2^+$ ([M]$^+$): 168.1083, found: 168.1084. $[\alpha_D^{25}]$ = +43.5 (*c* = 0.409, $CHCl_3$). HPLC (Chiralpak IB-3 column, Heptane/*i*-PrOH 95:5, 1 mL/min, 25 °C, 220 nm): t_R = 3.6 min (major), 4.5 min (minor).

(*R*)-4-phenyl-1,3-dioxane-2,2,5,5,6,6-*d*$_6$ (4.3a(*d*$_6$))

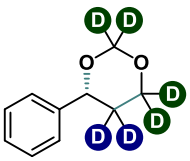

Following *General Procedure C* from styrene-β,β-*d*$_2$ (**4.1zj**, 32 µL, 0.25 mmol), paraformaldehyde-*d*$_2$ **4.2e** (20.0 mg, 0.625 mmol, 2.5 equiv.), with catalyst (*S*,*S*)-**4.5m** (2.5 mol%), in dry cyclohexane (2.5 mL, 0.1 M) for 72 h. Purification by flash column chromatography (eluent: *n*-pentane/MTBE 100:0 → 95:5) to give **4.3a(*d*$_6$)** as a colorless liquid (23.8 mg, 56%, er = 95:5).

^{1}H NMR (501 MHz, $CDCl_3$) δ 7.40 – 7.34 (m, 4H), 7.32 – 7.28 (m, 1H), 4.65 (s, 1H). ^{13}C NMR (126 MHz, $CDCl_3$) δ 141.6 (C), 128.6 (CH), 128.0 (CH), 125.9 (CH), 78.7 (CH). *The carbon atoms from CD_2 groups were not visible.* ESI-HRMS: calculated for $C_{10}H_6D_6O_2Na^+$ ([M+Na]$^+$):

193.1106, found: 193.1110. $[\alpha_D^{25}]$ = +44.2 (*c* = 0.371, $CHCl_3$). HPLC (Chiralpak IB-3 column, Heptane/*i*-PrOH 95:5, 1 mL/min, 25 °C, 220 nm): t_R = 3.6 min (major), 4.5 min (minor).

(*R*)-1-phenylpropane-1,3-diol (**4.9a**)

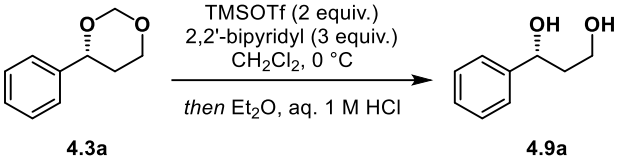

4.3a **4.9a**

(Adapted from a reported procedure[175]): An oven-dried RB flask was charged with **4.3a** (164 mg, 1 mmol, er = 95.5:4.5), dry CH_2Cl_2 (2 mL) and 2,2'-bipyridyl (469 mg, 3 mmol, 3 equiv.). After cooling the mixture at 0 °C, TMSOTf (0.36 mL, 2 mmol, 2 equiv.) was added dropwise followed by further stirring at 0 °C for 2 h. After checking full conversion of **4.3a** by TLC, Et_2O (10 mL) and aq. 1 M HCl (10 mL, 10 mmol, 10 equiv.) were added in one portion at 0 °C and the reaction mixture was stirred for 1.5 h. The mixture was then extracted with EtOAc (3 x 30 mL) and the combined organic phase was washed with satd. aq. $NaHCO_3$ (1 x 30 mL), dried over anh. Na_2SO_4, filtered and concentrated under reduced pressure. Purification by flash column chromatography on silica gel (*i*-hexane/EtOAc 90:10 → 60:40) afforded the corresponding 1,3-diol **4.9a** as a colorless oil (134 mg, 88%, er = 95:5).

^{1}H NMR (501 MHz, $CDCl_3$) δ 7.39 – 7.33 (m, 4H), 7.32 – 7.25 (m, 1H), 4.96 (dd, *J* = 8.8, 3.7 Hz, 1H), 3.89 – 3.83 (m, 2H), 2.08 – 1.89 (m, 2H). Spectroscopic data was consistent with the values reported in the literature.[222] HPLC (Chiralpak IC-3 column, Heptane/*i*-PrOH 95:5, 1 mL/min, 25 °C, 220 nm): t_R = 16.3 min (minor), 22.8 min (major).

7.4 Catalyst Synthesis

7.4.1 Precursors

GENERAL PROCEDURE D: *Ullmann-type coupling of aryl bromides and perfluoroalkyl iodides.*

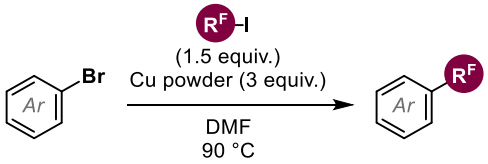

Activation of copper: Copper powder (5 g) was stirred for 30 min in aq. HCl 1 M (100 mL), and then filtered with a Büchner funnel, washing with distilled water (2 x 100 mL), ethanol (1 x 50 mL), acetone (1 x 50 mL) and Et_2O (1 x 50 mL). The obtained solid was transferred to a flask and dried under vacuum (10^{-3} mbar) overnight.

Ullmann-type coupling: An oven-dried Schlenk flask under Ar atmosphere was charged with freshly activated Cu powder (3 equiv.), aryl bromide (1 equiv.), and dry DMF (0.6 M for aryl

bromide). After degassing the mixture by bubbling Ar for 5 min, the perfluoroalkyl iodide (1.5 equiv.) was added in one portion and the flask was closed under Ar. The mixture was stirred vigorously at 90 °C (oil bath) for 24–72 h. After cooling to rt, the mixture was diluted with MTBE, treated with water (dropwise at first, then in one portion) and vigorously stirred for 10 min at rt. Afterwards, the mixture was passed through a Celite® pad, washing with MTBE. The aqueous layer was further extracted with MTBE (3x) and the combined organic layers were washed with aq. HCl 2 M, water and brine. The extract was dried over anh. Na_2SO_4, filtered and concentrated under reduced pressure. If necessary, further purification was conducted by column chromatography, or the crude mixture was used for the next reaction steps.

GENERAL PROCEDURE E: *Preparation of aryl triflates from phenols.*

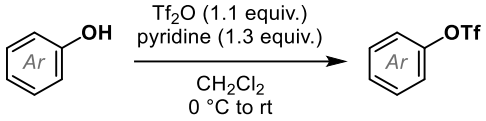

(Adapted from a reported procedure[207]) An oven-dried RB flask was charged with phenol substrate (1 equiv.) and dry CH_2Cl_2 (0.5 M for substrate). This solution was cooled to 0 °C (ice/water) and treated with pyridine (1.3 equiv.). Trifluoromethanesulfonic anhydride (1.1 equiv.) was added dropwise at 0 °C and the mixture was stirred vigorously at rt overnight. The reaction was stopped by dropwise addition of aq. HCl 1 M and further diluted with MTBE. The aqueous layer was extracted with MTBE, and the combined organic phases were washed subsequently with satd. aq. $NaHCO_3$, water, and brine. After drying over anh. Na_2SO_4, the organic phase was filtered and concentrated under reduced pressure. Purification by flash column chromatography on silica gel (*n*-pentane) afforded the corresponding aryl triflate**.**

2-bromo-4-iodo-1-(trifluoromethyl)benzene (**S6a**)

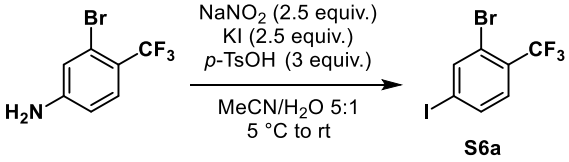

S6a

(Adapted from a reported procedure[223]) To a mixture of 3-bromo-4-(trifluoromethyl)aniline (3.0 g, 15 mmol, 1 equiv.), acetonitrile (65 mL) and *p*-toluenesulfonic acid monohydrate (7.13 g, 45 mmol, 3 equiv.), at 0–5 °C, was added a solution of $NaNO_2$ (1.72 g, 30 mmol, 2 equiv.) and KI (5.19 g, 37.5 mmol, 2.5 equiv.) in distilled water (12 mL), dropwise over 5 min. The mixture was allowed to reach room temperature and further stirred for 30 min, then poured onto distilled water (30 mL), neutralized with satd. aq. $NaHCO_3$ (20 mL) and extracted with MTBE (3 x 30 mL). The combined organic phases were washed with satd. aq. $NaHCO_3$ (1 x 20 mL), aq. $Na_2S_2O_3$ 10% (1 x 20 mL), water (1 x 20 mL) and brine (1 x 20 mL), successively; then dried over anh. Na_2SO_4, filtered and concentrated under reduced pressure. Purification by flash

column chromatography on silica gel (*n*-pentane) afforded the corresponding aryl iodide **S6a** as a colorless liquid (4.32 g, 82%).

^{1}H NMR (501 MHz, $CDCl_3$) δ 8.09 (d, *J* = 0.9 Hz, 1H), 7.76 (dd, *J* = 8.3, 0.9 Hz, 1H), 7.38 (d, *J* = 8.3 Hz, 2H). ^{19}F NMR (471 MHz, $CDCl_3$) δ –62.90 (s, 3F). ^{13}C NMR (126 MHz, $CDCl_3$) δ 143.2 (CH), 136.7 (CH), 130.0 (d, *J* = 31.9 Hz, C), 129.0 (q, *J* = 5.2 Hz, CH), 123.0 (q, *J* = 273.4 Hz, C), 121.0 (C), 98.9 (C). Spectroscopic data was consistent with the values reported in the literature.[224] EI-HRMS: calculated for $C_7H_3BrF_3I^+$ ([M]$^+$): 349.8410, found: 349.8409.

6-(perfluoropropan-2-yl)naphthalen-2-yl trifluoromethanesulfonate (**4.8a**)

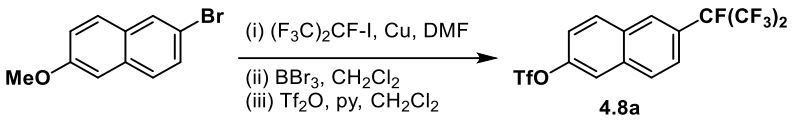

4.8a

2-methoxy-6-(perfluoropropan-2-yl)naphthalene:

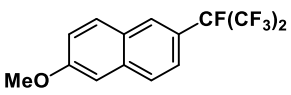

Following *General Procedure D* from 6-bromo-2-methoxynaphthalene (3.56 g, 15 mmol, 1 equiv.) and perfluoroisopropyl iodide (3.2 mL, 22.5 mmol, 1.5 equiv.). The obtained organic extract was used directly for the next reaction.

^{1}H NMR (501 MHz, $CDCl_3$): δ 8.04 (s, 1H), 7.83 (t, *J* = 9.4 Hz, 2H), 7.59 (d, *J* = 8.1 Hz, 1H), 7.24 (dd, *J* = 8.9, 2.6 Hz, 1H), 7.17 (d, *J* = 2.5 Hz, 1H), 3.95 (s, 3H). ^{19}F NMR (471 MHz, $CDCl_3$) δ –75.51 (d, *J* = 7.3 Hz, 6F), –181.74 (hept, *J* = 7.4 Hz, 1F).

6-(perfluoropropan-2-yl)naphthalen-2-ol:

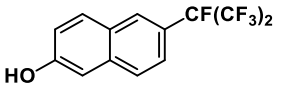

An oven-dried RB flask was charged with the product from the previous Ullmann coupling and dry CH_2Cl_2 (300 mL). This solution was cooled to –10 °C (salt/ice) and, using an addition funnel, BBr_3 (45 mL, 1 M in CH_2Cl_2, 45 mmol, 3 equiv.) was added dropwise over 10 min. The mixture was vigorously stirred at –10 °C for 30 min, and then at rt for 6 h. After cooling to 0 °C, the reaction was stopped by dropwise addition of MeOH (50 mL, with the addition funnel) and further diluted with distilled water (200 mL). The aqueous layer was extracted with CH_2Cl_2 (2 x 50 mL), and the combined organic phases were washed with brine (1 x 100 mL). After drying over anh. Na_2SO_4, the organic phase was filtered and concentrated under reduced pressure, affording an off-white solid, which was used directly for the next reaction.

^{1}H NMR (501 MHz, CD_2Cl_2) δ 8.18 (s, 1H), 8.01 (d, *J* = 8.9 Hz, 1H), 7.98 (d, *J* = 8.9 Hz, 1H), 7.69 (d, *J* = 8.8 Hz, 1H), 7.58 (d, *J* = 2.5 Hz, 1H), 7.34 (dd, *J* = 8.9, 2.4 Hz, 1H). ^{19}F NMR (471 MHz, CD_2Cl_2) δ –75.76 (d, *J* = 6.8 Hz, 6F), –182.06 (hept, *J* = 7.1 Hz, 1F).

*6-(perfluoropropan-2-yl)naphthalen-2-yl trifluoromethanesulfonate (**4.8a**):*

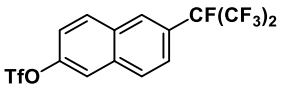

Following *General Procedure E* from the product from the previous deprotection (assuming 45 mmol). Purification by flash column chromatography (eluent: *n*-pentane) to give **4.8a** as a light yellow oil that solidified upon standing as white solid (4.78 g, 72% over three steps).

^{1}H NMR (501 MHz, CD_2Cl_2) δ 8.25 (s, 1H), 8.09 (d, *J* = 9.1 Hz, 1H), 8.07 (d, *J* = 8.9 Hz, 1H), 7.88 (d, *J* = 2.5 Hz, 1H), 7.77 (d, *J* = 8.8 Hz, 1H), 7.53 (dd, *J* = 9.0, 2.5 Hz, 1H). ^{19}F NMR (471 MHz, CD_2Cl_2) δ –73.10 (s, 3F), –75.73 (d, *J* = 7.4 Hz, 6F), –182.12 (hept, *J* = 7.2 Hz, 1F). ^{13}C NMR (126 MHz, CD_2Cl_2) δ 149.0, 134.7, 132.2, 132.0 (d, *J* = 2.3 Hz), 130.0 (d, *J* = 2.4 Hz), 127.0 (d, *J* = 12.2 Hz), 125.8 (d, *J* = 20.5 Hz), 123.7 (d, *J* = 9.7 Hz), 122.2 (d, *J* = 28.1 Hz), 121.6, 119.92 (d, *J* = 27.5 Hz), 119.63, 119.2 (d, *J* = 320.9 Hz). EI-HRMS: calculated for $C_{14}H_6F_{10}O_3S^+$ ([M]$^+$): 443.9873, found: 443.9880.

4-(perfluoropropyl)phenyl trifluoromethanesulfonate (**S6b**)

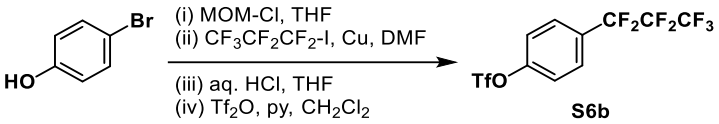

1-bromo-4-(methoxymethoxy)benzene:

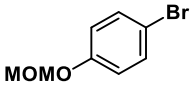

(Adapted from a reported procedure[225]*)* To a solution of 4-bromophenol (3.46 g, 20 mmol, 1 equiv.) in dry THF (65 mL) at 0 °C, NaH (960 mg of 60% suspension in oil, 24 mmol, 1.2 equiv.) was added portionwise and, after stirring 15 min, MOM-Cl (1.8 mL, 22 mmol, 1.1 equiv.) was added in one portion. The mixture was slowly warmed up to rt and further stirred for 24 h. The reaction was quenched by carefully adding satd. aq. NH_4Cl, diluted with 50 mL distilled water and extracted with MTBE (3 x 25 mL). Then, the combined organic phase was washed with brine (1 x 30 mL), dried over anh. Na_2SO_4, filtered and concentrated under reduced pressure. The obtained crude was directly used for the next step, without further purification.

^{1}H NMR (501 MHz, CD_2Cl_2) δ 7.39 (d, *J* = 9.0 Hz, 2H), 6.93 (d, *J* = 9.0 Hz, 2H), 5.14 (s, 2H), 3.44 (s, 3H). ^{13}C NMR (126 MHz, CD_2Cl_2) δ 156.9, 132.6, 118.6, 114.3, 95.0, 56.3. Spectroscopic data was consistent with the values reported in the literature.[225]

1-(methoxymethoxy)-4-(perfluoropropyl)benzene:

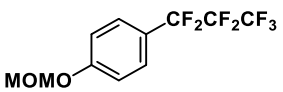

Following *General Procedure D* from the previously obtained 1-bromo-4-(methoxymethoxy)benzene (1.08 g, 5 mmol, 1 equiv.) and perfluoropropyl iodide (2.2 mL, 15 mmol, 3 equiv.). The obtained organic extract was used directly for the next reaction.

^{1}H NMR (501 MHz, CD_2Cl_2) δ 7.51 (d, *J* = 8.8 Hz, 2H), 7.15 (d, *J* = 8.9 Hz, 2H), 5.23 (s, 2H), 3.47 (s, 3H). ^{19}F NMR (471 MHz, CD_2Cl_2) δ –80.42 (t, *J* = 10.0 Hz, 3F), –110.96 (q, *J* = 10.2 Hz, 2F), –126.75 (s, 2F). ^{13}C NMR (126 MHz, CD_2Cl_2) δ 160.6 (C), 128.7 (t, *J* = 6.6 Hz, CH), 116.6 (CH), 94.7 (CH_2), 56.5 (CH_3).

4-(perfluoropropyl)phenol:

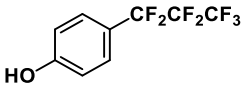

A RB flask was charged with the crude product from the previous Ullmann coupling (1.18 g, ~3.8 mmol), 1,4-dioxane (8 mL), MeOH (1 mL), and aq. HCl 6 M (3 mL, 18 mmol, ~5 equiv.). The mixture was heated to 90 °C overnight and, after cooling to rt, it was diluted with CH_2Cl_2 (50 mL) and distilled water (50 mL). The aqueous layer was further extracted with CH_2Cl_2 (3 x 20 mL) and the combined organic layers were washed with brine (1 x 30 mL). After drying over anh. Na_2SO_4, the organic phase was filtered and concentrated under reduced pressure, affording an orange oil, which was used directly for the next reaction.

^{1}H NMR (501 MHz, CD_2Cl_2) δ 7.47 (d, *J* = 8.6 Hz, 2H), 6.96 (d, *J* = 8.8 Hz, 2H), 5.57 (s, 1H). ^{19}F NMR (471 MHz, CD_2Cl_2) δ –80.44 (t, *J* = 9.9 Hz, 3F), –110.85 (q, *J* = 9.9 Hz, 2F), –126.83 (s, 2F). ^{13}C NMR (126 MHz, CD_2Cl_2) δ 159.3 (C), 129.0 (t, *J* = 6.5 Hz, CH), 116.0 (CH).

*4-(perfluoropropyl)phenyl trifluoromethanesulfonate (**S6b**):*

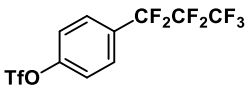

Following *General Procedure E* from the product from the previous deprotection (856 mg, ~3.25 mmol, 1 equiv.). Purification by flash column chromatography (eluent: *n*-pentane) to give aryl triflate **S6b** as a colorless liquid (442 mg, 17% over four steps).

^{1}H NMR (501 MHz, CD_2Cl_2) δ 7.74 (d, *J* = 8.8 Hz, 2H), 7.48 (d, *J* = 8.8 Hz, 2H). ^{19}F NMR (471 MHz, CD_2Cl_2) δ –73.06 (s, 3F), –80.35 (t, *J* = 10.0 Hz, 3F), –111.86 (q, *J* = 10.0 Hz, 2F), –126.53 (s, 2F). ^{13}C NMR (126 MHz, CD_2Cl_2) δ 152.4 (C), 129.7 (t, *J* = 6.5 Hz, CH), 122.5 (CH), 119.1 (q, *J* = 320.7 Hz, C). APCI-HRMS: calculated for $C_{10}H_4F_{10}O_3S^+$ ([M]$^+$): 393.9716, found: 393.9716.

5,6,7,8-tetrahydronaphthalen-2-yl trifluoromethanesulfonate (**S6c**)

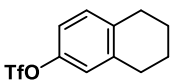

Following *General Procedure E* from 5,6,7,8-tetrahydronaphth-2-ol (1.49 g, 10 mmol). Purification by flash column chromatography (eluent: *n*-pentane) to give aryl triflate **S6c** as a colorless liquid (2.67 g, 94%).

^{1}H NMR (501 MHz, $CDCl_3$) δ 7.11 (d, *J* = 8.6 Hz, 1H), 6.97 (d, *J* = 8.2 Hz, 2H), 2.82 – 2.74 (m, 4H), 1.80 (p, *J* = 3.4 Hz, 4H). ^{19}F NMR (471 MHz, $CDCl_3$) δ –72.98 (s, 3F). ^{13}C NMR (126 MHz, $CDCl_3$) δ 147.4 (C), 139.8 (C), 137.8 (C), 130.8 (CH), 121.5 (CH), 118.9 (q, *J* = 321 Hz, C),

118.3 (CH), 29.6 (CH_2), 29.0 (CH_2), 22.9 (CH_2), 22.7 (CH_2). Spectroscopic data was consistent with the values reported in the literature.[207]

3,3'',5,5''-tetrakis(trifluoromethyl)-[1,1':3',1''-terphenyl]-5'-sulfonamide (**S7a**) *and* **((3,3'',5,5''-tetrakis(trifluoromethyl)-[1,1':3',1''-terphenyl]-5'-yl)sulfonyl)phosphorimidoyl trichloride** (**S7b**)

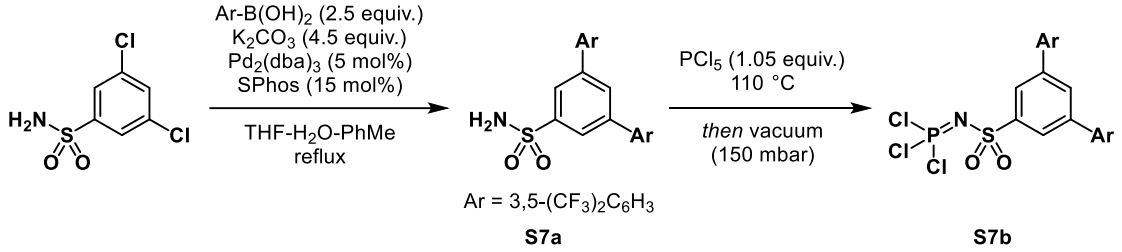

<u>*Suzuki Coupling:*</u> In a flask, THF (14 mL), distilled water (4.5 mL) and PhMe (14 mL) were mixed and degassed by bubbling Ar for 10 min. Then, $Pd_2(dba)_3$ (229 mg, 0.25 mmol, 5 mol%) and SPhos (308 mg, 0.75 mmol, 15 mol%) were added and the mixture was stirred under Ar at 60 °C for 45 min. After cooling down to room temperature, 3,5-dichlorobenzenesulfonamide (1.13 g, 5 mmol, 1 equiv.), 3,5-bis(trifluoromethyl)phenylboronic acid (3.22 g, 12.5 mmol, 2.5 equiv.), and K_2CO_3 (3.1 g, 22.5 mmol, 4.5 equiv.) were added, and the mixture was heated under Ar at 95 °C overnight. After cooling down, the mixture was diluted with MTBE (100 mL) and H_2O (50 mL), and the aqueous phase was extracted with MTBE (2 x 30 mL). The combined organic extracts were washed with distilled water (1 x 50 mL), and brine (1 x 50 mL). Purification by column chromatography (silica gel, *i*-hexane/EtOAc mixture) afforded sulfonamide **S7a** (2.91 g, 98% yield) as an off-white solid.

^{1}H NMR (501 MHz, CD_3CN) δ 8.38 (s, 4H), 8.31 (t, *J* = 1.7 Hz, 1H), 8.27 (d, *J* = 1.7 Hz, 2H), 8.10 (s, 2H), 5.85 (s, 2H). ^{19}F NMR (471 MHz, CD_3CN) δ –63.21 (s, 12F).

ESI-HRMS: calculated for $C_{22}H_{10}F_{12}NO_2S^-$ ($[M–H]^-$): 580.0246, found: 580.0251.

<u>*Phosphazene Formation:*</u> *(Adapted from a reported procedure[61a])* A flame-dried Schlenk flask was charged under Ar with sulfonamide **S7a** (587 mg, 1 mmol, 1 equiv.), PCl_5 (221 mg, 1.05 mmol, 1.05 equiv.) and 1.0 mL dry PhMe. The system was attached to a flask with KOH pellets (to trap the generated HCl), and the mixture was heated under Ar flow at 110 °C for 3 h. Subsequently, the system was connected to a vacuum pump set to 500 mbar (to remove PhMe) and then to 150 mbar (to sublime off excess PCl_5), keeping the heating at 110 °C for 2 h. The obtained solid was dried under high-vacuum at room temperature overnight, affording phosphazene **S7b** (649 mg, 90% yield) as a light brown solid.

^{1}H NMR (501 MHz, $CDCl_3$) δ 8.24 (d, *J* = 1.6 Hz, 2H), 8.08 (s, 4H), 7.98 (s, 2H), 7.96 (t, *J* = 1.7 Hz, 1H). ^{19}F NMR (471 MHz, $CDCl_3$) δ –62.76 (s, 12F). ^{31}P NMR (203 MHz, $CDCl_3$) δ 5.42.

7.4.2 Substituted BINOL derivatives and Catalysts

*(Catalysts **4.5a**,[59] **4.5c**,[63] and **4.5e**[63] have already been reported in literature)*

GENERAL PROCEDURE F: *Ortho-lithiation of protected BINOL and electrophilic quenching.*

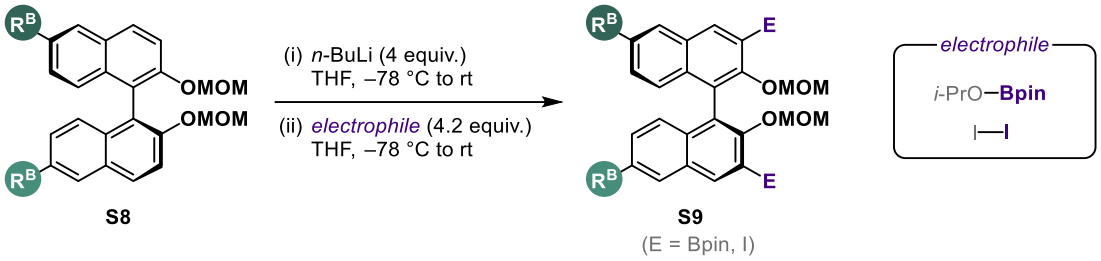

An oven-dried RB flask, equipped with a magnetic stir bar, was charged under Ar with **S8** (1 equiv.) and THF (0.1 M for substrate). After cooling the mixture at –78 °C, *n*-BuLi (2.5 M in hexanes, 4 equiv.) was added dropwise over 10 min. After the addition was completed, the mixture was stirred for 30 min at –78 °C and then for further 3 h at room temperature. The mixture was cooled again to –78 °C and the "*electrophile*" (4.2 equiv.) was added dropwise over 5 min, followed by stirring at rt for 16 h (overnight). The reaction was quenched at 0 °C by adding 1 mL MeOH, followed by dilution with distilled water. The mixture was extracted with MTBE (3x), and the combined organic phase was washed with brine, dried over anh. Na_2SO_4, filtered and concentrated under reduced pressure. Purification by column chromatography or recrystallization afforded the corresponding 3,3'-disubstituted-BINOL derivative **S9**.

(*S*)-2,2'-bis(methoxymethoxy)-6,6'-bis(perfluoropropyl)-1,1'-binaphthalene (**S8b**) *and* **(*S*)-3,3'-diiodo-2,2'-bis(methoxymethoxy)-6,6'-bis(perfluoropropyl)-1,1'-binaphthalene** (**S9b**)

(*S*)-2,2'-bis(methoxymethoxy)-6,6'-bis(perfluoropropyl)-1,1'-binaphthalene (**S8b**)

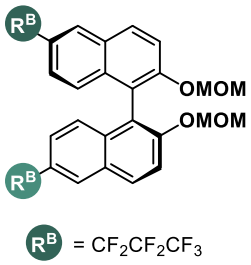

Following *General Procedure D* (Ullmann-type coupling) from (*S*)-6,6'-dibromo-2,2'-bis(methoxymethoxy)-1,1'-binaphthalene[226] (**4.8b**, 1.18 g, 2.23 mmol), perfluoropropyl iodide (1.0 mL, 6.7 mmol, 3 equiv.) and copper (0.85 g, 13.4 mmol, 6 equiv.). Purification by flash column chromatography (eluent: *n*-pentane/MTBE mixtures) to give **S8b** as a yellow solid (626 mg, 40%).

^{1}H NMR (501 MHz, CD_2Cl_2) δ 8.20 (s, 2H), 8.13 (d, *J* = 9.1 Hz, 2H), 7.74 (d, *J* = 9.1 Hz, 2H), 7.37 (d, *J* = 9.0 Hz, 2H), 7.25 (d, *J* = 9.0 Hz, 2H), 5.15 (d, *J* = 7.0 Hz, 2H), 5.08 (d, *J* = 7.0 Hz, 2H), 3.17 (s, 6H). ^{19}F NMR (471 MHz, CD_2Cl_2) δ –80.39 (t, *J* = 9.7 Hz, 6F), –111.19 (q, *J* = 10.6, 10.0 Hz, 4F), –126.43 (s, 4F). ^{13}C NMR (126 MHz, CD_2Cl_2) δ 155.1 (C), 135.7 (C), 131.2 (CH), 128.9 (C), 128.3 (t, *J* = 7.3 Hz, CH), 126.4 (CH), 124.3 (t, *J* = 24.3 Hz, C), 123.3 (t, *J* = 5.7 Hz, CH), 120.3 (C), 118.2 (CH), 95.2 (CH_2), 56.3 (CH_3).

ESI-HRMS: calculated for $C_{30}H_{20}F_{14}O_4Na^+$ ([M+Na]$^+$): 733.1030, found: 733.1030.

(*S*)-3,3'-diiodo-2,2'-bis(methoxymethoxy)-6,6'-bis(perfluoropropyl)-1,1'-binaphthalene (**S9b**)

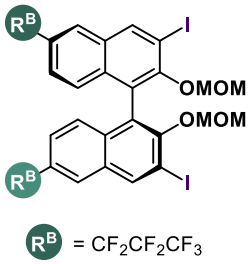

Following *General Procedure F* from **S8b** (600 mg, 0.84 mmol) and iodine (879 mg, 3.46 mmol, 4.1 equiv.). Purification by flash column chromatography (eluent: *n*-pentane/MTBE mixtures) to give **S9b** as a yellow solid (487 mg, 60%).

^{1}H NMR (501 MHz, CD_2Cl_2) δ 8.72 (s, 2H), 8.11 (s, 2H), 7.46 (d, *J* = 9.0 Hz, 2H), 7.31 (d, *J* = 8.9 Hz, 2H), 4.82 (d, *J* = 5.9 Hz, 2H), 4.78 (d, *J* = 5.8 Hz, 2H), 2.51 (s, 6H). ^{19}F NMR (471 MHz, CD_2Cl_2) δ –80.36 (t, *J* = 9.9 Hz, 6F), –111.56 (q, *J* = 9.7 Hz, 4F), –126.48 (s, 4F). ^{13}C NMR (126 MHz, CD_2Cl_2) δ 155.1 (C), 141.8 (CH), 135.5 (C), 131.4 (C), 127.8 (CH), 127.0 (t, *J* = 7.2 Hz, CH), 126.3 (t, *J* = 24.4 Hz, C), 126.1 (C), 124.0 (t, *J* = 5.8 Hz, CH), 100.2 (CH_2), 94.7 (C), 56.6 (CH_3).

ESI-HRMS: calculated for $C_{30}H_{18}F_{14}I_2O_4Na^+$ ([M+Na]$^+$): 984.8963, found: 984.8964.

(*S*)- 2,2'-bis(methoxymethoxy)-6,6'-bis(perfluoropropan-2-yl)-1,1'-binaphthalene (**S8c**) *and* **(*S*)-2,2'-(2,2'-bis(methoxymethoxy)-6,6'-bis(perfluoropropan-2-yl)-[1,1'-binaphthalene]-3,3'-diyl)bis(4,4,5,5-tetramethyl-1,3,2-dioxaborolane)** (**S9c**)

(*S*)-2,2'-bis(methoxymethoxy)-6,6'-bis(perfluoropropan-2-yl)-1,1'-binaphthalene (**S8c**)

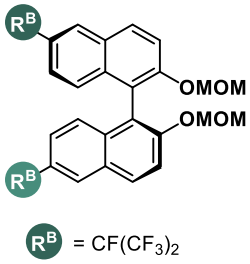

Following *General Procedure D* (Ullmann-type coupling) from (*S*)-6,6'-dibromo-2,2'-bis(methoxymethoxy)-1,1'-binaphthalene[226] (**4.8b**, 1.19 g, 2.23 mmol), heptafluoro-2-iodopropane (0.95 mL, 6.68 mmol, 3 equiv.) and copper (0.85 g, 13.4 mmol, 6 equiv.). Purification by flash column chromatography (eluent: *n*-pentane/MTBE mixtures) to give **S8c** as a yellow solid (1.10 g, 70%).

^{1}H NMR (501 MHz, CD_2Cl_2) δ 8.21 (s, 2H), 8.10 (d, *J* = 9.1 Hz, 2H), 7.73 (d, *J* = 9.1 Hz, 2H), 7.40 (d, *J* = 9.1 Hz, 2H), 7.25 (d, *J* = 9.1 Hz, 2H), 5.14 (d, *J* = 6.9 Hz, 2H), 5.09 (d, *J* = 7.0 Hz, 2H), 3.17 (s, 6H). ^{19}F NMR (471 MHz, CD_2Cl_2) δ –75.84 (d, *J* = 7.0 Hz, 12F), –182.07 (hept, *J* = 7.8, 7.2 Hz, 2F). ^{13}C NMR (126 MHz, CD_2Cl_2) δ 154.8 (C), 135.1 (C), 131.0 (CH), 129.12 (C), 129.11 (C), 127.0 (d, *J* = 11.8 Hz, CH), 126.6 (d, *J* = 2.3 Hz, CH), 122.5 (d, *J* = 9.8 Hz, CH), 122.3 (d, *J* = 20.6 Hz, C), 120.2 (C), 119.9 (C), 118.2 (CH), 95.3 (CH_2), 56.2 (CH_3). ESI-HRMS: calculated for $C_{30}H_{20}F_{14}O_4Na^+$ ([M+Na]$^+$): 733.1030, found: 733.1034. $[\alpha_D^{25}]$ = –41.2 (*c* = 0.61, CH_2Cl_2).

(*S*)-2,2'-(2,2'-bis(methoxymethoxy)-6,6'-bis(perfluoropropan-2-yl)-[1,1'-binaphthalene]-3,3'-diyl)bis(4,4,5,5-tetramethyl-1,3,2-dioxaborolane) (**S9c**)

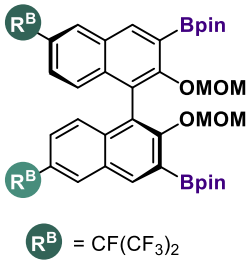

Following *General Procedure F* from **S8c** (1.00 g, 1.41 mmol) and 2-isopropoxy-4,4,5,5-tetramethyl-1,3,2-dioxaborolane (1.2 mL, 5.91 mmol, 4.2 equiv.). Purification by recrystallization (with hexanes) afforded the corresponding bis-boronate **S9c** as a yellow solid (989 mg, 73%).

^{1}H NMR (501 MHz, CD_2Cl_2) δ 8.59 (s, 2H), 8.26 (d, *J* = 2.2 Hz, 2H), 7.48 (dd, *J* = 9.1, 2.0 Hz, 2H), 7.36 (d, *J* = 9.1 Hz, 2H), 4.92 (d, *J* = 6.4 Hz, 2H), 4.82 (d, *J* = 6.4 Hz, 2H), 2.21 (s, 6H), 1.40 (s, 24H). ^{11}B NMR (161 MHz, CD_2Cl_2) δ 30.20. ^{19}F NMR (471 MHz, CD_2Cl_2) δ –75.86 (d, *J* = 7.2 Hz, 12F), –182.12 (hept, *J* = 7.4 Hz, 2F). ^{13}C NMR (126 MHz, CD_2Cl_2) δ 159.7 (C), 140.7 (CH), 136.9 (C), 131.2 (C), 129.7 (d, *J* = 2.1 Hz, C), 127.9 (d, *J* = 2.3 Hz, CH), 127.4 (d, *J* = 11.3 Hz, CH), 127.1 (C), 125.4 (C), 124.7 (C), 123.2 (d, *J* = 10.4 Hz, CH), 123.1 (C), 123.0 (C), 122.3 (d, *J* = 28.1 Hz, C), 120.0 (d, *J* = 28.0 Hz, C), 117.9 (C), 100.8 (CH_2), 95.4 (C), 93.3 (C), 93.0 (C), 92.7 (C), 91.6 (C), 91.4 (C), 91.1 (C), 84.6 (C), 55.7 (CH_3), 25.08 (CH_3), 25.06 (CH_3). ESI-HRMS: calculated for $C_{42}H_{42}B_2F_{14}O_8Na^+$ ([M+Na]$^+$): 985.2734, found: 985.2738. $[\alpha_D^{25}]$ = –31.6 (*c* = 0.72, CH_2Cl_2).

GENERAL PROCEDURE G: *Suzuki coupling and MOM deprotection.*

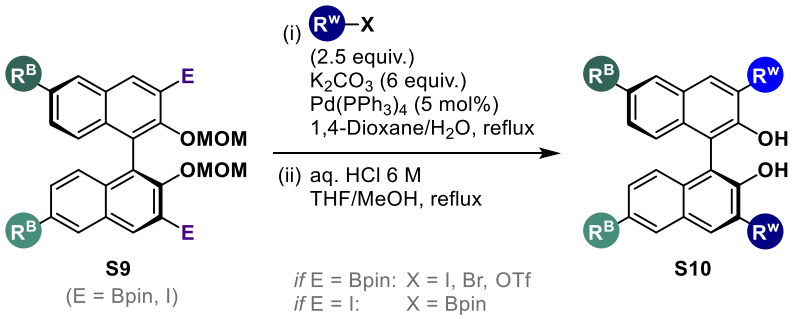

Suzuki coupling: In a flask under Ar, coupling partners **S9** (1 equiv.) and R^W–X (2.5 equiv.), and solid K_2CO_3 (6 equiv.) were dissolved in a 4:1 *v/v* mixture of 1,4-dioxane/water (0.1 M for **S9**). After degassing the mixture by bubbling Ar for 10 min, $Pd(PPh_3)_4$ (5 mol%) was added and the resulting mixture was heated to reflux for 18 h. The reaction mixture was cooled to room temperature and filtered through a short pad of Celite®, washing with CH_2Cl_2. The filtrate was washed with water, and with brine, then dried over anh. Na_2SO_4, filtered and concentrated under reduced pressure.

MOM deprotection: The obtained crude (from the cross-coupling step) was redissolved in a mixture of THF/MeOH 3:1 *v/v* (approx. 0.05 M), treated with aq. HCl 6 M (24 equiv.) and heated in a closed flask to 50 °C overnight (the flask should have a considerable headspace to avoid overpressure and explosions). After cooling to room temperature, the mixture was diluted with CH_2Cl_2 and water, and the aqueous phase was further extracted with CH_2Cl_2 (3x). The

combined organic phases were washed with brine and, after drying over anh. Na_2SO_4, the extract was filtered and concentrated under reduced pressure. Purification by flash column chromatography on silica gel (*n*-pentane/CH_2Cl_2 or *n*-pentane/MTBE mixtures) afforded the corresponding 3,3'-disubstituted BINOL-derivatives (*S*)-**S10**.

GENERAL PROCEDURE H: *Single-flask synthesis of iIDPs (and IDPs).*

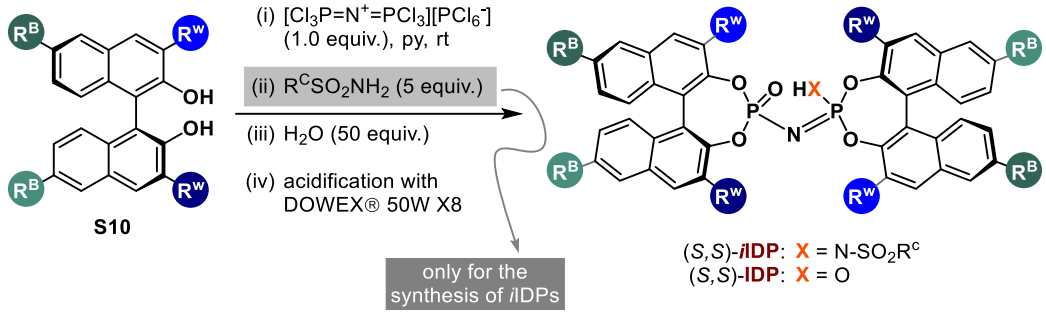

This is a slight adaptation from a reported procedure by our group.[63]

A- *Synthesis and purification*

An oven-dried Schlenk flask was charged with hexachlorobisphosphazonium hexachlorophosphate[63] (1 equiv.) and the corresponding (*S*)-BINOL (**S10**, 2.1 equiv.) under Ar. After drying the mixture under vacuum (10^{-3} mbar) for 30 min at rt and switching back to Ar atmosphere, pyridine (0.2 M for **S10**) was added in one portion and the mixture was vigorously stirred for 2 h.

Intermediate step **only** for the synthesis of *i*IDPs: Trifluoromethanesulfonamide (5 equiv.) was added in one portion and the mixture was further stirred at rt overnight.

(Both procedures continue here): Distilled water (50 equiv.) was added and the mixture was further stirred for 2 h. The reaction was stopped by diluting the mixture with CH_2Cl_2 and slowly adding aq. HCl 3 M (excess to neutralize pyridine: exothermic neutralization!); after stirring for 30 min, the aqueous phase was extracted with CH_2Cl_2 (3x). The combined organic phases were washed with distilled water, and brine, then dried over anh. Na_2SO_4, filtered and concentrated under reduced pressure. Purification by flash column chromatography on silica gel (*n*-hexane/EtOAc mixtures) afforded the corresponding catalysts as salts.

B- *Acidification*

DOWEX® 50W X8 (approx. 5 g/100 mg catalyst to acidify) was suspended in aq. H_2SO_4 0.5 M, transferred to a glass column with stopcock, and washed thoroughly with more acid (approximately 20 times the volume of the DOWEX pad) until the eluate was colorless. Then, the resin pad was washed with distilled water (until the eluate is neutral to pH indicator paper), ethanol and Et_2O, in that order. For each of these washing operations, ~10–20 times of pad volume was used as volume of the washing agent.

The purified catalyst salt (after column, dissolved in Et_2O) was added to the DOWEX pad (packed in Et_2O) and the eluate was collected in test tubes (adding more Et_2O to not let the

DOWEX pad run dry). The eluted fractions were re-added to the DOWEX pad to ensure full acidification: the collection and re-acidification was done 3x in total. After washing the DOWEX pad with Et_2O, the eluate was concentrated under reduced pressure and the obtained residue was re-dissolved in a small amount of Et_2O and treated with *n*-pentane (20 mL). After removing the solvents under reduced pressure, the obtained solid was further freeze-dried with liquid N_2 (3x) and dried overnight under high-vacuum, thus affording the acidified catalyst (either *i*IDP **4.5**, or IDP).

(*S*)-3,3'-bis(4-(trifluoromethyl)phenyl)-[1,1'-binaphthalene]-2,2'-diol (**S10a**)

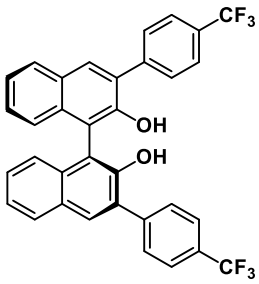

Following *General Procedure G* from (*S*)-2,2'-(2,2'-bis(methoxymethoxy)-[1,1'-binaphthalene]-3,3'-diyl)bis(4,4,5,5-tetramethyl-1,3,2-dioxaborolane) **S9a**[227] (940 mg, 1.5 mmol) and 4-bromobenzotrifluoride (1012 mg, 4.5 mmol, 3 equiv.) as coupling partners. The crude product was purified by flash column chromatography (eluent: *n*-pentane/MTBE 100:0 → 90:10) to give **S10a** as an off-white solid (793 mg, 92%).

^{1}H NMR (501 MHz, $CDCl_3$) δ 8.06 (s, 2H), 7.96 (d, *J* = 8.3 Hz, 2H), 7.87 (d, *J* = 8.0 Hz, 4H), 7.74 (d, *J* = 7.9 Hz, 4H), 7.44 (ddd, *J* = 8.2, 6.8, 1.3 Hz, 2H), 7.37 (ddd, *J* = 8.2, 6.8, 1.3 Hz, 2H), 7.23 (d, *J* = 8.4 Hz, 2H), 5.31 (s, 2H). ^{19}F NMR (471 MHz, $CDCl_3$) δ –62.49 (s, 6F). ^{13}C NMR (126 MHz, $CDCl_3$) δ 150.2 (C), 141.3 (C), 133.2 (C), 132.2 (CH), 130.1 (CH), 125.4 (q, *J* = 32.2 Hz, C), 129.6 (C), 129.5 (C), 128.9 (CH), 128.2 (CH), 125.4 (q, *J* = 3.8 Hz, CH), 125.0 (CH), 124.2 (CH), 112.1 (C). Spectroscopic data was consistent with the values reported in the literature.[228] $[\alpha_D^{25}]$ = –65.3 (*c* = 0.44, $CHCl_3$); literature (for (*R*)-enantiomer): $[\alpha_D^{23}]$ = +48.1 (*c* = 0.21, $CHCl_3$).[228]

Imino-imidodiphosphate (*i*IDP) **4.5b**

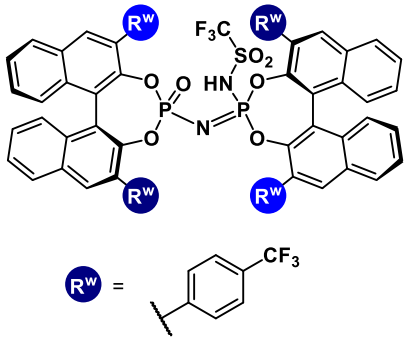

Following *General Procedure H* from **S10a** (603 mg, 1.0 mmol) as starting material. The crude product was purified by flash column chromatography (eluent: *n*-pentane/CH_2Cl_2 100:0 → 70:30) and acidified with DOWEX® 50W X8, to give **4.5b** as an off-white solid (530 mg, 77%).

^{1}H NMR (501 MHz, CD_2Cl_2) δ 8.22 (d, *J* = 8.2 Hz, 2H), 8.12 (d, *J* = 17.0 Hz, 2H), 8.07 (dd, *J* = 8.3, 5.3 Hz, 2H), 7.84 (dddd, *J* = 12.5, 8.1, 5.8, 2.2 Hz, 2H), 7.72 – 7.57 (m, 12H), 7.52 – 7.39 (m, 8H), 7.03 (d, *J* = 8.1 Hz, 2H), 6.98 (d, *J* = 8.1 Hz, 2H), 6.78 (d, *J* = 8.0 Hz, 2H), 6.72 (d, *J* = 8.0 Hz, 2H). ^{19}F NMR (471 MHz, CD_2Cl_2) δ –62.58 (s, 3F), –62.73 (s, 3F), –62.77 (s, 3F), –63.16 (s, 3F), –80.03 (s, 3F). ^{31}P NMR (203 MHz, CD_2Cl_2) δ –2.35 (d, *J* = 111.5 Hz), –7.81 (d, *J* = 111.4 Hz).

^{13}C NMR (126 MHz, CD_2Cl_2) δ 144.3, 144.2, 143.9, 143.8, 143.7, 140.4, 140.1, 140.0, 132.94, 132.87, 132.8, 132.7 (CH), 132.5, 132.33, 132.27, 132.1 (CH), 131.6 (CH), 131.1 (CH), 130.8 (CH), 130.3, 130.2 (CH), 130.1 (CH), 130.0 (CH), 129.8, 129.6, 129.4 (CH), 129.3 (CH), 129.2 (CH), 128.5 (CH), 128.2 (CH), 127.9 (CH), 127.8 (CH), 127.7 (CH), 127.5 (CH), 127.42 (CH), 127.36 (CH), 127.22 (CH), 127.19 (CH), 127.1 (CH), 127.0 (CH), 125.84 (CH), 125.81 (CH), 125.11 (CH), 125.07 (CH), 125.00 (CH), 124.97 (CH), 124.73 (CH), 124.69 (CH), 124.0, 123.94, 123.91, 122.7, 122.5. ESI-HRMS: calculated for $C_{69}H_{36}F_{15}N_2O_7P_2S^-$ ([M–H]$^-$): 1383.1485, found: 1383.1483. $[\alpha_D^{25}]$ = +314.0 (*c* = 0.23, $CHCl_3$).

Imino-imidodiphosphate (*i*IDP) **4.5h**

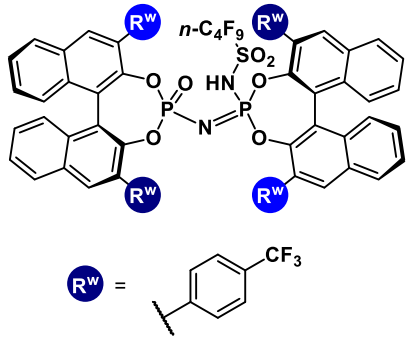

Following *General Procedure H* from **S10a** (59 mg, 0.1 mmol, 2.1 equiv.) as starting material, and using *n*-$C_4F_9SO_2NH_2$ (75 mg, 0.25 mmol, 5 equiv.) instead of $TfNH_2$. The crude product was purified by flash column chromatography (eluent: *n*-pentane/CH_2Cl_2 100:0 → 70:30) and acidified with DOWEX® 50W X8, to give **4.5h** as an off-white solid (51 mg, 67%).

^{1}H NMR (501 MHz, $CDCl_3$) δ 8.17 (t, *J* = 7.2 Hz, 2H), 8.04 (dt, *J* = 18.9, 5.8 Hz, 4H), 7.80 (ddd, *J* = 11.9, 8.8, 6.4 Hz, 1H), 7.72 – 7.52 (m, 12H), 7.52 – 7.35 (m, 8H), 7.01 (d, *J* = 8.1 Hz, 2H), 6.93 (d, *J* = 7.9 Hz, 2H), 6.74 (d, *J* = 8.1 Hz, 2H), 6.70 (d, *J* = 8.0 Hz, 2H). ^{19}F NMR (471 MHz, $CDCl_3$) δ –62.45 (s, 3F), –62.46 (s, 3F), –62.48 (s, 3F), –63.04 (s, 3F), –80.95 (t, *J* = 9.7 Hz, 3F), –113.42 (dt, *J* = 64.9, 11.9 Hz, 2F), –121.48 (s, 2F), –126.18 (q, *J* = 16.7 Hz, 2F). ^{31}P NMR (203 MHz, $CDCl_3$) δ –2.61 (d, *J* = 106.9 Hz), –6.80 (d, *J* = 107.2 Hz). ^{13}C NMR (126 MHz, $CDCl_3$) δ 140.1, 139.6, 139.5, 133.0, 132.7, 132.6, 132.5, 132.4, 132.2, 132.1, 131.9, 131.8, 131.0, 130.4, 130.0, 129.7, 129.7, 129.1, 129.0, 128.8, 128.1, 127.8, 127.5, 127.4, 127.3, 127.3, 127.1, 126.8, 126.8, 126.6, 125.7, 125.7, 125.7, 125.6, 124.8, 124.8, 124.8, 124.7, 124.7, 124.7, 124.6, 124.6, 124.4 *(spectrum with low signal-to-noise ratio despite high concentration)*. ESI-HRMS: calculated for $C_{72}H_{36}F_{21}N_2O_7P_2S^-$ ([M–H]$^-$): 1533.1389, found: 1533.1387.

(*S*)-3,3'-bis(3-chloro-4-(trifluoromethyl)phenyl)-[1,1'-binaphthalene]-2,2'-diol (**S10b**)

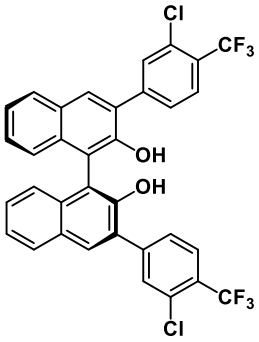

Following *General Procedure G* from **S9a**[227] (313 mg, 0.5 mmol) and 4-bromo-2-chloro-1-(trifluoromethyl)benzene (389 mg, 1.5 mmol, 3 equiv.) as coupling partners. The crude product was purified by flash column chromatography (eluent: *n*-pentane/MTBE 100:0 → 80:20) to give **S10b** as a light yellow solid (261 mg, 81%).

^{1}H NMR (501 MHz, CD_2Cl_2) δ 8.11 (s, 2H), 8.00 (d, *J* = 8.2 Hz, 2H), 7.98 – 7.94 (m, 2H), 7.82 (d, *J* = 8.2 Hz, 2H), 7.79 (d, *J* = 8.2 Hz, 2H), 7.46 (ddd, *J* = 8.2, 6.8, 1.2 Hz, 2H), 7.39 (ddd, *J* = 8.3, 6.8, 1.3 Hz, 2H), 7.19 (dd, *J* = 8.4, 1.1 Hz, 2H), 5.45 (s, 2H). ^{19}F NMR (471 MHz, CD_2Cl_2) δ –62.59 (s, 6F). ^{13}C NMR (126 MHz, CD_2Cl_2) δ 150.5, 143.4, 133.8, 132.8, 132.7, 132.3, 129.9, 129.2, 128.7, 128.4, 128.3, 127.9 (q, *J* = 5.2 Hz), 127.4 (d, *J* = 31.5 Hz), 125.3, 124.4, 123.6 (d, *J* = 272.8 Hz), 112.4. ESI-HRMS: calculated for $C_{34}H_{17}Cl_2F_6O_2^-$ ([M–H]$^-$): 641.0515, found: 641.0517.

Imino-imidodiphosphate (*i*IDP) **4.5f**

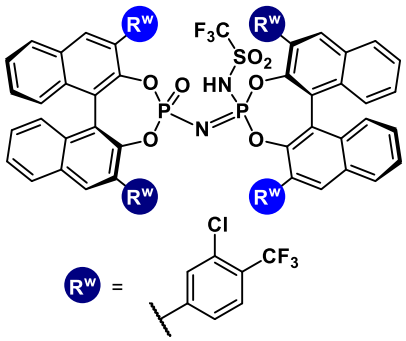

Following *General Procedure H* from **S10b** (129 mg, 0.2 mmol) as starting material. The crude product was purified by flash column chromatography (eluent: *i*-pentane/EtOAc 95:5 → 70:30) and acidified with DOWEX® 50W X8, to give **4.5f** as a light yellow solid (119 mg, 80%).

^{1}H NMR (501 MHz, CD_2Cl_2) δ 8.22 – 8.04 (m, 6H), 7.83 (ddd, *J* = 8.0, 6.3, 1.3 Hz, 2H), 7.74 – 7.55 (m, 11H), 7.54 – 7.32 (m, 9H), 7.19 (d, *J* = 16.6 Hz, 2H), 6.59 – 6.40 (m, 2H). ^{19}F NMR (471 MHz, CD_2Cl_2) δ –62.25 (s, 3F), –62.41 (s, 3F), –62.46 (s, 3F), –62.91 (s, 3F), –80.22 (s, 3F). ^{31}P NMR (203 MHz, CD_2Cl_2) δ –1.70 (d, *J* = 102.2 Hz), –5.89 (d, *J* = 102.2 Hz). ^{13}C NMR (126 MHz, CD_2Cl_2) δ 144.1, 144.0, 141.7, 133.0, 132.8, 132.7, 132.6, 132.4, 132.3, 132.2, 132.0, 131.8, 131.7, 131.4, 131.2, 131.0, 129.6, 129.5, 129.4, 129.3, 128.9, 128.5, 128.4, 128.2, 128.0, 128.0, 128.0, 127.8, 127.8, 127.5, 127.4, 127.2, 127.1, 127.0, 124.0. ESI-HRMS: calculated for $C_{69}H_{32}Cl_4F_{15}N_2O_7P_2S^-$ ([M–H]$^-$): 1518.9926, found: 1518.9926.

(*S*)-3,3'-bis(4-(perfluoropropyl)phenyl)-[1,1'-binaphthalene]-2,2'-diol (**S10c**)

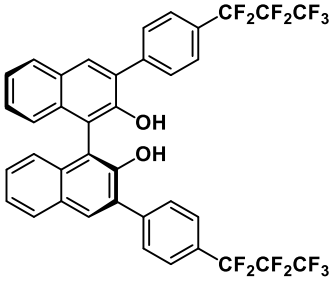

Following *General Procedure G* from **S9a**[227] (626 mg, 1 mmol) and 4-(perfluoropropyl)phenyl trifluoromethanesulfonate (**S6b**, 633 mg, 2.3 mmol, 2.3 equiv.) as coupling partners. The crude product was purified by flash column chromatography (eluent: *n*-pentane/CH_2Cl_2 100:0 → 70:30) to give **S10c** as a white foamy solid (467 mg, 64%).

^{1}H NMR (501 MHz, CD_2Cl_2) δ 8.11 (s, 2H), 7.99 (d, *J* = 8.2 Hz, 2H), 7.93 (d, *J* = 8.5 Hz, 4H), 7.72 (d, *J* = 8.3 Hz, 4H), 7.45 (ddd, *J* = 8.0, 6.8, 1.2 Hz, 2H), 7.37 (ddd, *J* = 8.2, 6.8, 1.3 Hz, 2H), 7.21 (d, *J* = 8.5 Hz, 2H), 5.45 (s, 2H). ^{19}F NMR (471 MHz, CD_2Cl_2) δ –80.32 (t, *J* = 10.0 Hz, 6F), –111.71 (q, *J* = 9.8 Hz, 4F), –126.50 (s, 4F). ^{13}C NMR (126 MHz, CD_2Cl_2) δ 150.6, 142.1, 133.7, 132.6, 130.4, 130.0, 129.7, 129.1, 128.3, 128.0, 127.1 (t, *J* = 6.4 Hz), 125.1, 124.4, 112.5. ESI-HRMS: calculated for $C_{38}H_{19}F_{14}O_2^-$ ([M–H]$^-$): 773.1167, found: 773.1172. $[\alpha_D^{25}]$ = –37.1 (*c* = 0.18, $CHCl_3$).

Imino-imidodiphosphate (*i*IDP) **4.5j**

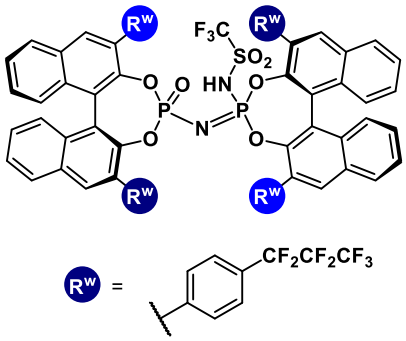

Following *General Procedure H* from **S10c** (119 mg, 0.15 mmol) as starting material. The crude product was purified by flash column chromatography (eluent: *n*-pentane/CH_2Cl_2 100:0 → 70:30) and acidified with DOWEX® 50W X8, to give **4.5j** as an off-white solid (132 mg, 98%).

^{1}H NMR (501 MHz, CD_2Cl_2) δ 8.22 (dd, *J* = 8.3, 5.6 Hz, 2H), 8.16 (s, 1H), 8.12 (s, 1H), 8.07 (t, *J* = 8.6 Hz, 2H), 7.88 – 7.79 (m, 2H), 7.73 (s, 1H), 7.67 – 7.57 (m, 9H), 7.53 (dt, *J* = 16.7, 8.4 Hz, 5H), 7.46 – 7.35 (m, 5H), 7.00 (d, *J* = 8.1 Hz, 2H), 6.93 (d, *J* = 8.1 Hz, 2H), 6.78 (d, *J* = 8.2 Hz, 2H), 6.74 (d, *J* = 8.2 Hz, 2H). ^{19}F NMR (471 MHz, CD_2Cl_2) δ –79.96 (s, 3F), –80.35 – –80.54 (m, 12F), –110.29 – –112.62 (m, 8F), –126.48 – –126.70 (m, 8F). ^{31}P NMR (203 MHz, CD_2Cl_2) δ -1.53 (d, *J* = 107.7 Hz), -7.14 (d, *J* = 108.4 Hz). ^{13}C NMR (151 MHz, CD_2Cl_2) δ 144.3, 144.2, 143.9, 143.8, 143.02, 142.96, 140.6, 140.3, 140.2, 133.03, 133.01, 132.9, 132.84, 132.83, 132.78, 132.77, 132.7, 132.60, 132.58, 132.49, 132.48, 132.4, 132.3, 132.24, 132.21, 132.20, 132.1, 132.02, 132.00, 131.7, 131.2, 130.7, 130.5, 130.1, 129.99, 129.91, 129.4, 129.3, 129.2, 128.6, 128.4, 128.3, 128.1, 127.91, 127.86, 127.8, 127.7, 127.5, 127.40, 127.36, 127.32, 127.28, 127.19, 127.16, 127.04, 126.97, 126.7, 126.63, 126.58, 126.53, 126.49, 126.25, 126.21, 126.16, 124.00, 123.98, 123.97, 123.95, 122.74, 122.72, 122.5, 121.6, 121.3, 121.1, 120.70, 120.68, 119.7, 119.4, 119.24, 119.19, 119.02, 118.96, 118.6, 117.7, 117.5, 117.3, 117.2, 117.1, 117.0, 116.4, 115.8, 115.7, 115.6, 114.2, 114.0, 111.05, 110.99, 110.8, 110.7, 110.54, 110.49, 109.5, 109.3, 109.2, 109.05, 108.99, 108.8, 108.7, 108.5, 107.6, 107.5, 107.3, 107.2, 107.0. ESI-HRMS: calculated for $C_{77}H_{36}F_{31}N_2O_7P_2S^-$ ([M–H]$^-$): 1783.1229, found: 1783.1237. $[\alpha_D^{25}]$ = +336.0 (*c* = 0.17, $CHCl_3$).

(*S*)-6,6'''-bis(perfluoropropan-2-yl)-[2,2':4',1'':3'',2'''-quaternaphthalene]-2'',3'-diol (**S10d**)

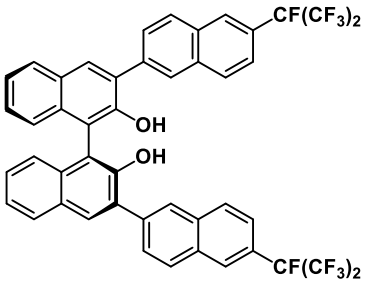

Following *General Procedure G* from **S9a**[227] (313 mg, 0.5 mmol) and 6-(perfluoropropan-2-yl)naphthalen-2-yl trifluoromethanesulfonate (**S6**, 489 mg, 1.1 mmol, 2.2 equiv.) as coupling partners. The crude product was purified by flash column chromatography (eluent: *n*-pentane/MTBE 100:0 → 90:10) to give **S10d** as a light yellow solid (410 mg, 94%).

^{1}H NMR (501 MHz, CD_2Cl_2) δ 8.31 (s, 2H), 8.24 (s, 2H), 8.19 (s, 2H), 7.71 (d, *J* = 8.8 Hz, 2H), 7.46 (ddd, *J* = 8.1, 6.8, 1.2 Hz, 2H), 7.39 (ddd, *J* = 8.3, 6.8, 1.4 Hz, 2H), 7.28 (dd, *J* = 8.4, 1.1 Hz, 2H), 5.53 (s, 2H). ^{19}F NMR (471 MHz, CD_2Cl_2) δ –75.72 (d, *J* = 7.3 Hz), –181.95 (hept, *J* = 7.5 Hz). ^{13}C NMR (126 MHz, CD_2Cl_2) δ 150.9, 138.0, 134.6, 133.7, 132.5 (CH), 132.2 (d, *J* = 2.1 Hz), 130.5, 130.1, 129.68 (CH), 129.66 (CH), 129.1 (CH), 129.0 (CH), 128.6 (CH), 128.1 (CH), 126.7 (d, *J* = 11.8 Hz, CH), 125.0 (CH), 124.5 (CH), 124.4, 122.5, 122.3 (q, *J* = 9.4 Hz, CH), 120.1 (d, *J* = 28.6 Hz), 112.8. ESI-HRMS: calculated for $C_{46}H_{23}O_2F_{14}^-$ ([M–H]$^-$): 873.1480, found: 873.1480. $[\alpha_D^{25}]$ = +36.3 (*c* = 0.25, $CHCl_3$).

Imino-imidodiphosphate (*i*IDP) **4.5k**

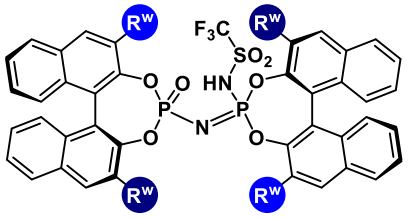

Following *General Procedure H* from **S10d** (350 mg, 0.40 mmol) as starting material. The crude product was purified by flash column chromatography (eluent: *i*-hexane/EtOAc 97:3 → 80:20) and acidified with DOWEX® 50W X8, to give **4.5k** as an off-light yellow solid (261 mg, 69%).

^{1}H NMR (501 MHz, CD_2Cl_2) δ 8.22 (t, *J* = 7.0 Hz, 2H), 8.14 – 8.04 (m, 5H), 7.98 – 7.87 (m, 7H), 7.80 (dt, *J* = 19.9, 6.9 Hz, 2H), 7.71 (dd, *J* = 8.9, 5.3 Hz, 2H), 7.66 – 7.41 (m, 18H), 7.39 (d, *J* = 8.7 Hz, 2H), 7.36 (s, 1H), 7.32 (s, 1H), 6.85 (dd, *J* = 8.7, 1.9 Hz, 1H), 6.77 (dd, *J* = 8.7, 1.9 Hz, 1H), 6.42 – 6.33 (m, 2H). ^{19}F NMR (471 MHz, CD_2Cl_2) δ –75.69 – –76.12 (m, 24F), –80.84 (s, 3F), –181.95 (dhept, *J* = 21.5, 7.1 Hz, 2F), –182.19 (dhept, *J* = 21.9, 7.1 Hz, 2F). ^{31}P NMR (203 MHz, CD_2Cl_2) δ –4.69 (d, *J* = 120.7 Hz), –9.79 (d, *J* = 120.3 Hz). ^{13}C NMR (126 MHz, CD_2Cl_2) δ 144.4, 144.1, 136.3, 136.1, 135.8, 134.3, 134.2, 134.1, 134.0, 133.6, 133.5, 133.18, 133.15, 133.1, 133.0, 132.6, 132.5, 132.43, 132.38, 132.3, 132.12, 132.06, 132.0, 131.9, 131.7, 131.6, 129.8, 129.72, 129.67, 129.6, 129.5, 129.4, 129.3, 129.2, 129.1, 128.8, 128.7, 128.6, 128.5, 128.4, 128.2, 128.1, 128.0, 127.84, 127.77, 127.64, 127.56, 127.5, 127.3, 127.1, 126.9, 126.4, 126.2, 126.1, 124.8, 124.7, 124.6, 124.5, 124.4, 124.24, 124.17, 124.15, 124.1, 123.92, 123.88, 123.86, 122.72, 122.70, 122.4, 122.2, 121.9, 121.7, 121.6. ESI-HRMS: calculated for $C_{93}H_{44}F_{31}N_2O_7P_2S^-$ ([M–H]$^-$): 1983.1855, found: 1983.1863. $[\alpha_D^{25}]$ = +232.7 (*c* = 0.21, $CHCl_3$).

(*S*)-3,3'-bis(3-fluoro-4-(trifluoromethyl)phenyl)-[1,1'-binaphthalene]-2,2'-diol (**S10e**)

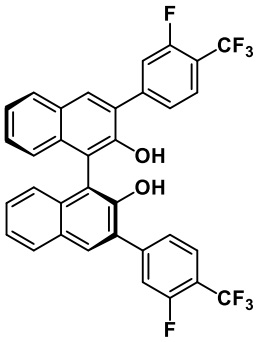

Following *General Procedure G* from **S9a**[227] (313 mg, 0.5 mmol) and 4-bromo-2-fluoro-1-(trifluoromethyl)benzene (210 µL, 1.5 mmol, 3 equiv.) as coupling partners. The crude product was purified by flash column chromatography (eluent: *n*-pentane/MTBE 100:0 → 90:10) to give **S10e** as a yellow solid (285 mg, 93%).

^{1}H NMR (501 MHz, CD_2Cl_2) δ 8.11 (s, 2H), 8.00 (d, *J* = 8.1 Hz, 2H), 7.74 (t, *J* = 7.6 Hz, 2H), 7.69 (s, 2H), 7.67 (d, *J* = 2.6 Hz, 2H), 7.46 (ddd, *J* = 8.2, 6.8, 1.2 Hz, 2H), 7.39 (ddd, *J* = 8.3, 6.8, 1.3 Hz, 2H), 7.20 (dd, *J* = 8.4, 1.0 Hz, 2H), 5.47 (s, 2H). ^{19}F NMR (471 MHz, CD_2Cl_2) δ –61.45 (d, *J* = 12.7 Hz, 6F), –115.71 (q, *J* = 12.4 Hz, 2F). ^{13}C NMR (126 MHz, CD_2Cl_2) δ 159.9 (dd, *J* = 254.8, 2.1 Hz), 150.5, 144.6 (d, *J* = 8.6 Hz), 133.8, 132.7, 129.9, 129.3, 128.7, 128.53 (d, *J* = 1.4 Hz), 127.4 (dq, *J* = 7.4, 3.0, 2.2 Hz), 125.8 (d, *J* = 3.5 Hz), 125.3, 124.3, 123.3 (q, *J* = 271.9 Hz), 118.5 (d, *J* = 21.4 Hz), 117.3 (dd, *J* = 33.0, 12.5 Hz), 112.4. ESI-HRMS: calculated for $C_{34}H_{17}F_8O_2^-$ ([M–H]$^-$): 609.1106, found: 609.1109.

Imino-imidodiphosphate (*i*IDP) **4.5l**

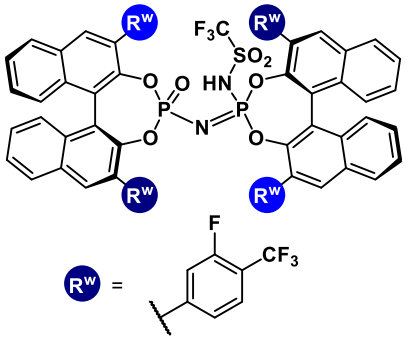

Following *General Procedure H* from **S10e** (122 mg, 0.20 mmol) as starting material. The crude product was purified by flash column chromatography (eluent: *i*-hexane/EtOAc 95:5 → 70:30) and acidified with DOWEX® 50W X8, to give **4.5l** as a light brown solid (72 mg, 51%).

^{1}H NMR (501 MHz, CD_2Cl_2) δ 8.18 (dd, *J* = 11.4, 8.2 Hz, 2H), 8.14 (s, 1H), 8.08 – 8.02 (m, 3H), 7.80 – 7.73 (m, 3H), 7.68 – 7.64 (m, 3H), 7.62 – 7.53 (m, 6H), 7.47 – 7.37 (m, 8H), 7.00 (d, *J* = 5.5 Hz, 1H), 6.98 (d, *J* = 5.4 Hz, 1H), 6.42 (t, *J* = 7.8 Hz, 0H), 6.37 (t, *J* = 7.6 Hz, 2H), 6.34 (d, *J* = 8.1 Hz, 1H), 6.25 (d, *J* = 8.1 Hz, 1H). ^{19}F NMR (471 MHz, CD_2Cl_2) δ –60.86 (d, *J* = 12.6 Hz, 3F), –61.14 (d, *J* = 8.5 Hz, 3F), –61.17 (d, *J* = 7.4 Hz, 3F), –61.53 (d, *J* = 12.4 Hz, 3F), –80.30 (s, 3F), –115.57 (q, *J* = 13.5 Hz, 1F), –115.67 (q, *J* = 12.7 Hz, 1F), –115.96 (q, *J* = 12.2 Hz, 1F), –116.03 (q, *J* = 12.7 Hz, 1F). ^{31}P NMR (203 MHz, CD_2Cl_2) δ 0.73 (d, *J* = 84.2 Hz), –2.40 (d, *J* = 84.2 Hz). ^{13}C NMR (126 MHz, CD_2Cl_2) δ 160.3, 158.3, 149.1, 144.3, 144.0, 143.8, 142.8, 133.0, 132.9, 132.8, 132.0, 131.9, 131.7, 131.7, 131.7, 131.6, 131.5, 130.9, 130.8, 129.4, 129.3, 129.2, 129.1, 128.1, 128.0, 127.9, 127.7, 127.6, 127.6, 127.3, 127.2, 127.1, 127.0, 127.0, 126.8, 126.8, 126.8, 126.7, 126.5, 126.5, 126.5, 126.5, 126.2, 126.2, 126.2, 126.0, 126.0, 125.4, 125.3, 125.2, 125.1, 124.1, 124.1, 123.9, 123.9, 123.4, 123.2, 123.2, 121.9, 119.2, 119.0, 118.5, 118.3, 118.3, 118.2, 118.1, 118.1. ESI-HRMS: calculated for $C_{69}H_{32}F_{19}N_2O_7P_2S^-$ ([M–H]$^-$): 1455.1108, found: 1455.1111.

(*S*)-3,3'-bis(3-bromo-4-(trifluoromethyl)phenyl)-[1,1'-binaphthalene]-2,2'-diol (**S10f**)

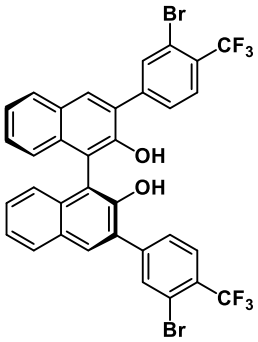

Following *General Procedure G* from **S9a**[227] (626 mg, 1 mmol) and 2-bromo-4-iodo-1-(trifluoromethyl)benzene (**S6a**, 633 mg, 2.3 mmol, 2.3 equiv.) as coupling partners. The crude product was purified by flash column chromatography (eluent: *n*-pentane/CH_2Cl_2 100:0 → 70:30) to give **S10f** as a white foamy solid (467 mg, 64%).

^{1}H NMR (501 MHz, CD_2Cl_2) δ 8.16 (s, 2H), 8.10 (s, 2H), 8.00 (d, *J* = 7.3 Hz, 2H), 7.84 (d, *J* = 8.2 Hz, 2H), 7.81 (d, *J* = 8.4 Hz, 2H), 7.46 (ddd, *J* = 8.1, 6.8, 1.2 Hz, 2H), 7.39 (ddd, *J* = 8.2, 6.8, 1.3 Hz, 2H), 7.19 (d, *J* = 8.4 Hz, 2H), 5.44 (s, 2H). ^{19}F NMR (471 MHz, CD_2Cl_2) δ –62.59 (s, 6F). ^{13}C NMR (126 MHz, CD_2Cl_2) δ 150.5 (C), 143.4 (C), 136.3 (CH), 133.8 (C), 132.7 (CH), 129.9 (C), 129.2 (CH), 129.00 (C), 128.97 (CH), 128.7 (CH), 128.2 (C), 128.1 (q, *J* = 5.4 Hz, CH), 125.3 (CH), 124.4 (CH), 123.6 (d, *J* = 272.9 Hz, C), 120.0 (C), 112.4 (C). ESI-HRMS: calculated for $C_{34}H_{17}Br_2F_6O_2^-$ ([M–H]$^-$): 728.9505, found: 728.9514. $[\alpha_D^{25}]$ = –37.6 (*c* = 0.20, $CHCl_3$).

Imino-imidodiphosphate (*i*IDP) **4.5m**

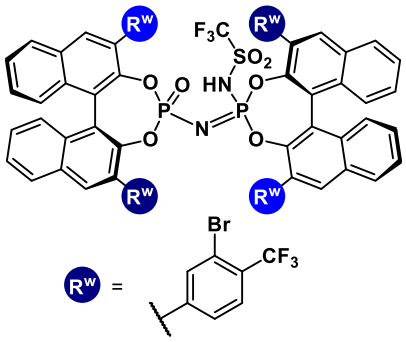

Following *General Procedure H* from **S10f** (384 mg, 0.52 mmol) as starting material. The crude product was purified by flash column chromatography (eluent: *n*-pentane/CH_2Cl_2 100:0 → 70:30) and acidified with DOWEX® 50W X8, to give **4.5m** as an off-white solid (286 mg, 67%).

^{1}H NMR (501 MHz, CD_2Cl_2) δ 8.22 (s, 1H), 8.15 (s, 1H), 8.09 (t, *J* = 6.7 Hz, 4H), 7.86 (dd, *J* = 13.5, 6.0 Hz, 3H), 7.80 (d, *J* = 8.6 Hz, 1H), 7.76 (d, *J* = 8.5 Hz, 1H), 7.73 – 7.64 (m, 5H), 7.61 (d, *J* = 7.3 Hz, 2H), 7.48 – 7.28 (m, 9H), 7.25 (s, 1H), 6.99 (t, *J* = 9.0 Hz, 2H), 6.69 (d, *J* = 8.2 Hz, 1H), 6.59 (d, *J* = 8.2 Hz, 1H). ^{19}F NMR (471 MHz, CD_2Cl_2) δ –62.24 (s, 3F), –62.51 (s, 3F), –62.64 (s, 3F), –63.04 (s, 3F), –80.13 (s, 3F). ^{31}P NMR (203 MHz, CD_2Cl_2) δ –3.53 (d, *J* = 111.3 Hz), –7.76 (d, *J* = 111.3 Hz). ^{13}C NMR (126 MHz, CD_2Cl_2) δ 144.1, 144.0, 143.9, 143.7, 143.6, 142.7, 141.7, 141.6, 141.5, 141.4, 136.2, 135.6, 135.5, 135.4, 132.8, 132.7, 132.61, 132.55, 132.4, 132.3, 132.2, 131.94, 131.90, 131.7, 131.4, 131.3, 131.00, 130.97, 130.78, 130.76, 129.7, 129.6, 129.5, 129.4, 129.2, 128.9, 128.8, 128.64, 128.55, 128.2, 128.0, 127.92, 127.88, 127.84, 127.81, 127.75, 127.5, 127.4, 127.3, 127.2, 127.0, 124.7, 124.52, 124.46, 124.3, 124.02, 124.00, 123.84, 123.82, 122.8, 122.7, 122.5, 122.4, 122.1, 120.2, 120.0, 119.8, 119.7. ESI-HRMS: calculated for $C_{69}H_{32}Br_4F_{15}N_2O_7P_2S^-$ ([M–H]$^-$): 1694.7906, found: 1694.7904. $[\alpha_D^{25}]$ = +279.3 (*c* = 0.23, $CHCl_3$).

(*S*)-5,5''',6,6''',7,7''',8,8'''-octahydro-[2,2':4',1'':3'',2'''-quaternaphthalene]-2'',3'-diol (**S10g**)

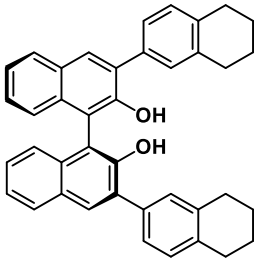

Following *General Procedure G* from **S9a**[227] (943 mg, 1.5 mmol) and 5,6,7,8-tetrahydronaphthalen-2-yl trifluoromethanesulfonate (**S6c**, 1.68 g, 6 mmol, 4 equiv.) as coupling partners. The crude product was purified by flash column chromatography (eluent: *n*-pentane/CH_2Cl_2 90:10 → 50:50) to give **S10g** as a white solid (698 mg, 85%).

^{1}H NMR (501 MHz, $CDCl_3$) δ 7.98 (s, 2H), 7.90 (d, *J* = 8.0 Hz, 2H), 7.46 – 7.41 (m, 4H), 7.37 (ddd, *J* = 8.1, 6.7, 1.3 Hz, 2H), 7.29 (ddd, *J* = 8.2, 6.8, 1.3 Hz, 2H), 7.22 (d, *J* = 8.3 Hz, 2H), 7.19 (d, *J* = 7.8 Hz, 2H), 5.38 (s, 2H), 2.84 (q, *J* = 6.1 Hz, 8H), 1.85 (dq, *J* = 6.6, 3.5, 3.1 Hz, 8H). ^{13}C NMR (126 MHz, $CDCl_3$) δ 150.3 (C), 137.6 (C), 137.1 (C), 134.7 (C), 133.0 (C), 131.1 (CH), 130.9 (C), 130.3 (CH), 129.6 (C), 129.5 (CH), 128.5 (CH), 127.2 (CH), 126.8 (CH), 124.5 (CH), 124.3 (CH), 112.7 (C), 29.7 (CH_2), 29.4 (CH_2), 23.4 (CH_2).

Imino-imidodiphosphate (*i*IDP) **4.5n**

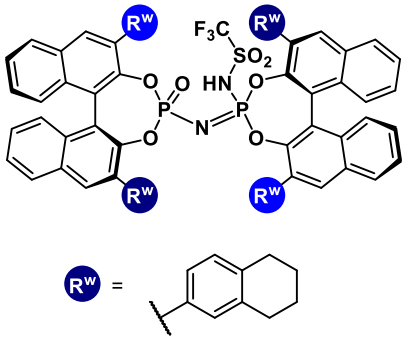

Following *General Procedure H* from **S10g** (83.5 mg, 0.15 mmol) as starting material. The crude product was purified by flash column chromatography (eluent: *n*-pentane/MTBE 100:0 → 70:30) and acidified with DOWEX® 50W X8, to give **4.5n** as an off-white solid (84 mg, 85%).

^{1}H NMR (501 MHz, CD_2Cl_2) δ 8.22 – 7.91 (m, 6H), 7.83 – 7.62 (m, 3H), 7.60 – 7.45 (m, 5H), 7.40 (d, *J* = 8.7 Hz, 2H), 7.37 – 7.15 (m, 6H), 7.13 – 6.89 (m, 6H), 6.87 – 6.66 (m, 2H), 6.62 – 6.49 (m, 1H), 6.45 – 6.22 (m, 1H), 2.89 – 1.36 (m, 32H). ^{19}F NMR (471 MHz, CD_2Cl_2) δ –79.49 (s, 3F). ^{31}P NMR (203 MHz, CD_2Cl_2) δ –6.68 (d, *J* = 120.3 Hz), –10.99 (d, *J* = 133.5 Hz). ^{13}C NMR (126 MHz, CD_2Cl_2) δ 137.7, 137.5, 132.5, 132.3, 132.3, 132.1, 130.9, 130.8, 130.3, 130.1, 129.7, 129.5, 129.4, 129.2, 129.1, 128.9, 127.9, 127.7, 127.3, 127.2, 127.2, 126.9, 126.7, 126.3, 29.8, 29.6, 29.5, 29.3, 23.7, 23.5, 23.4, 23.3. ESI-HRMS: calculated for $C_{81}H_{64}F_3N_2O_7P_2S^-$ ([M–H]$^-$): 1327.3867, found: 1327.3868.

(*S*)-6,6'-bis(perfluoropropyl)-3,3'-bis(4-(trifluoromethyl)phenyl)-[1,1'-binaphthalene]-2,2'-diol (**S10h**)

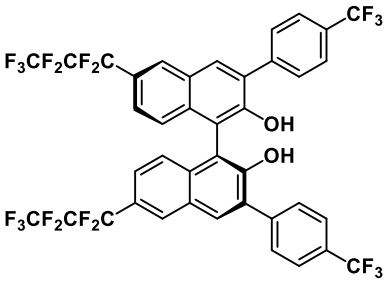

Following *General Procedure G* from **S9b** (165 mg, 0.17 mmol) and (4-(trifluoromethyl)phenyl)boronic acid (81 mg, 0.43 mmol, 2.5 equiv.) as coupling partners. The crude product was purified by flash column chromatography (eluent: *n*-pentane/MTBE 100:0 → 90:10) to give **S10h** as a light yellow solid (112 mg, 72%).

^{1}H NMR (501 MHz, CD_2Cl_2) δ 8.27 (s, 2H), 8.21 (s, 2H), 7.89 (d, *J* = 7.9 Hz, 4H), 7.79 (d, *J* = 8.2 Hz, 4H), 7.51 (d, *J* = 8.0 Hz, 2H), 7.33 (d, *J* = 9.0 Hz, 2H), 5.63 (s, 2H). ^{19}F NMR (471 MHz, CD_2Cl_2) δ –62.90, –80.30 (t, *J* = 9.9 Hz), –111.30 (qd, *J* = 9.5, 3.1 Hz), –126.30. ^{13}C NMR (126 MHz, CD_2Cl_2) δ 152.7 (C), 140.9 (C), 135.2 (C), 133.5 (CH), 131.5 (C), 130.6 (C), 130.5 (CH), 130.3 (C), 128.9 (t, *J* = 6.9 Hz, CH), 128.8 (C), 125.9 (q, *J* = 3.7 Hz, CH), 125.5 (d, *J* = 76.8 Hz, C), 125.3 (CH), 124.9 (t, *J* = 6.1 Hz, CH), 123.6 (C), 112.4 (C). ESI-HRMS: calculated for $C_{40}H_{17}F_{20}O_2^-$ ([M–H]$^-$): 909.0915, found: 909.0922.

Imino-imidodiphosphate (*i*IDP) **4.5o**

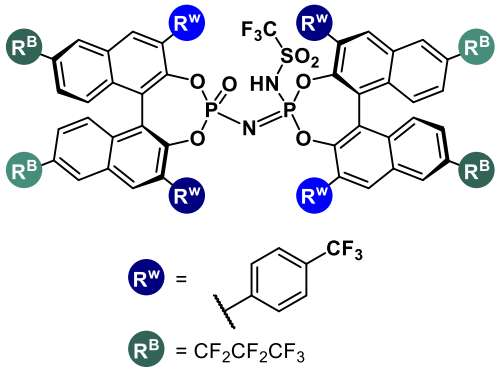

Following *General Procedure H* from **S10h** (87.7 mg, 0.096 mmol) as starting material. The crude product was purified by flash column chromatography (eluent: *n*-pentane/MTBE 100:0 → 70:30) and acidified with DOWEX® 50W X8, to give **4.5o** as a yellow solid (39 mg, 41%).

^{1}H NMR (501 MHz, CD_2Cl_2) δ 8.50 (s, 2H), 8.38 (s, 2H), 8.28 (d, *J* = 8.8 Hz, 2H), 7.89 (s, 1H), 7.85 – 7.78 (m, 2H), 7.73 (dd, *J* = 9.0, 4.7 Hz, 2H), 7.67 (d, *J* = 8.4 Hz, 2H), 7.63 (d, *J* = 8.5 Hz, 2H), 7.60 – 7.55 (m, 4H), 7.50 (t, *J* = 9.0 Hz, 3H), 7.46 (d, *J* = 8.2 Hz, 2H), 6.97 – 6.87 (m, 6H), 6.81 (d, *J* = 8.4 Hz, 2H). ^{19}F NMR (471 MHz, CD_2Cl_2) δ –62.81 (s, 3F), –62.87 (s, 6F), –63.28 (s, 3F), –79.97 (s, 3F), –80.12 – –80.36 (m, 12 F), –110.69 – –112.86 (m, 8F), –126.06 – –126.40 (m, 8F). ^{31}P NMR (203 MHz, CD_2Cl_2) δ –1.73 (d, *J* = 102.7 Hz), –6.27 (d, *J* = 104.2 Hz).

^{13}C NMR (126 MHz, CD_2Cl_2) δ 146.3, 146.1, 145.9, 139.7, 139.3, 139.1, 134.7, 134.7, 134.5, 134.5, 134.4, 134.3, 134.1, 134.0, 134.0, 133.9, 133.7, 133.6, 133.4, 133.4, 132.5, 132.1, 131.3, 131.1, 130.8, 130.4, 130.2, 130.1, 129.9, 128.9, 128.1, 128.1, 127.9, 127.8, 126.1, 126.1, 126.1, 126.1, 125.7, 125.3, 125.3, 125.3, 125.0, 125.0, 125.0, 124.8, 124.8, 123.8, 123.8, 123.7, 123.4, 122.4, 122.4. ESI-HRMS: calculated for $C_{81}H_{32}F_{43}N_2O_7P_2S^-$ ([M–H]$^-$): 2055.0725, found: 2055.0744.

(*S*)-6,6'-bis(perfluoropropan-2-yl)-3,3'-bis(4-(trifluoromethyl)phenyl)-[1,1'-binaphthalene]-2,2'-diol (**S10i**)

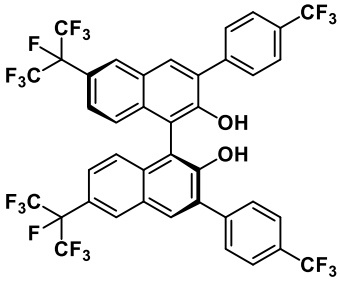

Following *General Procedure G* from **S9c** (500 mg, 0.52 mmol) and 4-bromobenzotrifluoride (182 µL, 1.30 mmol, 2.5 equiv.) as coupling partners. The crude product was purified by flash column chromatography (eluent: *n*-pentane/MTBE 100:0 → 80:20) to give **S10i** as a white solid (427 mg, 90%).

^{1}H NMR (501 MHz, CD_2Cl_2) δ 8.30 (s, 2H), 8.21 (s, 2H), 7.90 (d, *J* = 8.1 Hz, 4H), 7.80 (d, *J* = 8.1 Hz, 4H), 7.56 (d, *J* = 9.0 Hz, 2H), 7.37 (d, *J* = 9.0 Hz, 2H), 5.60 (s, 2H). ^{19}F NMR (471 MHz, CD_2Cl_2) δ –62.90 (s, 6F), –75.79 (h, *J* = 6.4 Hz, 12F), –182.09 (hept, *J* = 6.9 Hz, 2F). ^{13}C NMR (126 MHz, CD_2Cl_2) δ 152.5 (C), 141.0 (C), 134.6 (C), 133.4 (CH), 131.5 (C), 130.5 (CH), 130.4 (q, *J* = 32.5 Hz, C), 129.1 (d, *J* = 2.1 Hz, C), 128.0 (C), 127.7 (d, *J* = 11.8 Hz, CH), 125.9 (q, *J* = 3.7 Hz, CH), 125.6 (d, *J* = 2.2 Hz, CH), 124.1 (d, *J* = 9.5 Hz, CH), 123.7 (C), 123.2 (d, *J* = 20.4 Hz, C), 122.3 (d, *J* = 27.6 Hz, C), 121.5 (C), 120.0 (d, *J* = 28.1 Hz, C), 112.2 (C), 93.0 (hept, *J* = 33.1 Hz, C), 91.4 (hept, *J* = 33.2 Hz, C). ESI-HRMS: calculated for $C_{40}H_{17}F_{20}O_2^-$ ([M–H]$^-$): 909.0915, found: 909.0927. $[\alpha_D^{25}]$ = –61.4 (*c* = 0.17, $CHCl_3$).

Imino-imidodiphosphate (*i*IDP) **4.5p**

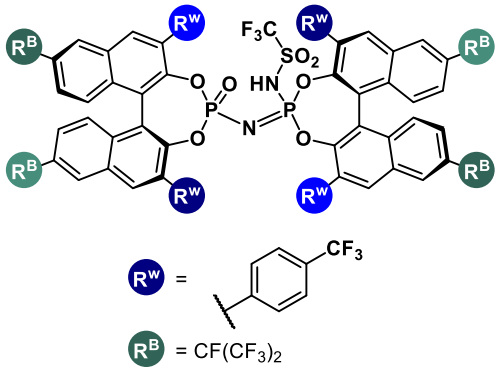

Following *General Procedure H* from **S10i** (326 mg, 0.35 mmol) as starting material. The crude product was purified by flash column chromatography (eluent: *i*-hexane/EtOAc 95:5 → 85:15) and acidified with DOWEX® 50W X8, to give **4.5p** as a light yellow solid (326 mg, 91%).

^{1}H NMR (501 MHz, CD_2Cl_2) δ 8.55 (s, 2H), 8.39 (s, 2H), 8.25 (d, *J* = 7.0 Hz, 2H), 7.91 – 7.81 (m, 4H), 7.76 (t, *J* = 9.0 Hz, 2H), 7.69 – 7.59 (m, 7H), 7.56 (d, *J* = 9.2 Hz, 1H), 7.47 (t, *J* = 8.8 Hz, 4H), 6.92 – 6.83 (m, 6H), 6.80 (d, *J* = 8.1 Hz, 2H). ^{19}F NMR (471 MHz, CD_2Cl_2) δ –62.86 (s, 6F), –62.88 (s, 3F), –63.27 (s, 3F), –75.52 – –75.59 (m, 16F), –75.66 (dp, *J* = 20.8, 8.2 Hz, 8F), –79.94 (s, 3F), –182.13 (q, *J* = 6.9 Hz, 3F), –182.24 (p, *J* = 7.3 Hz, 1F). ^{31}P NMR (203 MHz, CD_2Cl_2) δ –1.75 (d, *J* = 101.0 Hz), –5.93 (d, *J* = 100.8 Hz). ^{13}C NMR (126 MHz, CD_2Cl_2) δ 139.8, 139.3, 139.1, 134.7, 134.5, 134.4, 133.7, 133.6, 133.5, 133.2, 133.0, 132.3, 131.9, 131.5, 130.8, 130.2, 130.1, 129.9, 128.3, 128.0, 127.9, 126.1, 125.5, 125.32, 125.29, 124.9, 124.7, 123.8, 123.7, 123.2, 122.2, 120.1. ESI-HRMS: calculated for $C_{81}H_{32}F_{43}N_2O_7P_2S^-$ ([M–H]$^-$): 2055.0725, found: 2055.0740. $[\alpha_D^{25}]$ = +227.7 (*c* = 0.19, $CHCl_3$).

Imidodiphosphate (IDP) **4.4e**

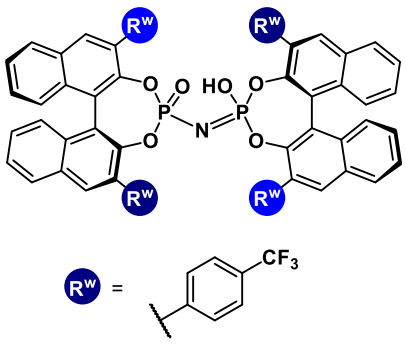

Following *General Procedure H* from **S10a** (33 mg, 0.05 mmol) as starting material, without adding any sulfonamide. The crude product was purified by flash column chromatography (eluent: *n*-pentane/MTBE 100:0 → 60:40) and acidified with DOWEX® 50W X8, to give **4.4e** as an off-white solid (31 mg, 88%).

^{1}H NMR (501 MHz, CD_2Cl_2) δ 8.20 (d, *J* = 5.8 Hz, 2H), 8.13 – 7.97 (m, 3H), 7.94 – 7.31 (m, 20H), 7.29 – 7.10 (m, 2H), 7.07 – 6.54 (m, 5H). ^{19}F NMR (471 MHz, CD_2Cl_2) δ –62.67 (s, 6F), –62.78 (s, 6F). ^{31}P NMR (203 MHz, CD_2Cl_2) δ 0.63. ^{13}C NMR (126 MHz, CD_2Cl_2) δ 132.9, 132.6, 132.5, 132.1, 132.0, 131.4, 131.3, 130.5, 130.5, 130.1, 129.4, 129.2, 129.2, 129.1, 128.6, 127.7, 127.5, 127.1, 126.9, 125.3, 125.2, 124.1. ESI-HRMS: calculated for $C_{68}H_{36}F_{12}NO_6P_2^-$ ([M–H]$^-$): 1252.1832, found: 1252.1835.

N-triflyl-phosphoramide 4.4f

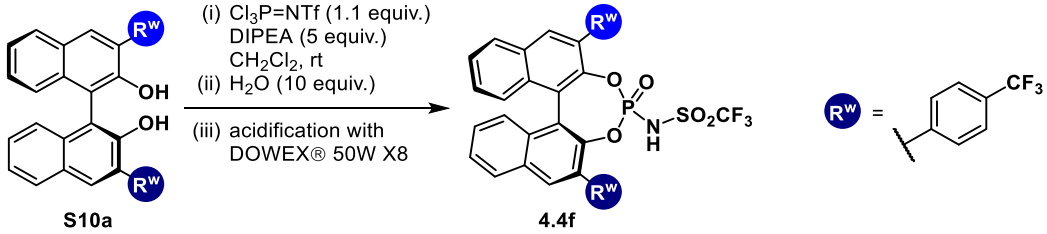

(Adapted from a reported procedure[229]):

In an oven-dried Schlenk flask under Ar, 3,3'-disubstituted (*S*)-BINOL (**S10a**, 58 mg, 0.1 mmol, 1 equiv.) was dissolved in CH_2Cl_2 (0.5 mL). At room temperature, DIPEA (90 µL, 0.5 mmol, 5 equiv.) was added, followed by *N*-triflylphosphorimidoyl trichloride (Cl_3P=NTf, 18 µL, 0.11 mmol, 1.1 equiv.). After stirring at room temperature for 30 min, distilled water (18 µL, 10 equiv.) were added and the mixture was further stirred for 30 min. The reaction was stopped by diluting the mixture with CH_2Cl_2 (10 mL) and slowly adding aq. HCl 3 M (2 mL); after stirring for 30 min, the aqueous phase was extracted with CH_2Cl_2 (3 x 20 mL). The combined organic phases were washed with distilled water, and brine, then dried over anh. Na_2SO_4, filtered and concentrated under reduced pressure. Purification by flash column chromatography on silica gel (*n*-hexane/EtOAc mixtures) afforded the corresponding catalyst as salts. Acidification with DOWEX® 50W X8 (see *General Procedure H*) afforded the corresponding *N*-triflylphosphoramide **4.4f** as a white solid (71 mg, 92% yield).

^{1}H NMR (501 MHz, CD_2Cl_2) δ 8.19 (s, 1H), 8.12 (s, 1H), 8.09 (d, *J* = 8.2 Hz, 1H), 8.07 (d, *J* = 8.3 Hz, 1H), 7.81 (d, *J* = 8.1 Hz, 2H), 7.72 – 7.67 (m, 4H), 7.67 – 7.63 (m, 3H), 7.59 (ddd, *J* = 8.1, 5.3, 2.7 Hz, 1H), 7.50 – 7.43 (m, 2H), 7.41 – 7.36 (m, 2H). ^{19}F NMR (471 MHz, CD_2Cl_2) δ –63.11 (s, 3F), –63.43 (s, 3F), –78.49 (s, 3F). ^{31}P NMR (203 MHz, CD_2Cl_2) δ –5.04 (s). ^{13}C NMR (126 MHz, CD_2Cl_2) δ 143.3 (d, *J* = 11.7 Hz), 142.8 (d, *J* = 9.4 Hz), 140.0 (d, *J* = 42.6 Hz), 132.7 (d, *J* = 2.6 Hz), 132.6, 132.5, 132.4, 132.4, 131.0, 130.6, 130.3 (dd, *J* = 32.5, 10.5 Hz), 129.2 (d, *J* = 15.5 Hz), 127.9 (d, *J* = 3.4 Hz), 127.4 (d, *J* = 6.6 Hz), 127.3, 125.8 (q, *J* = 3.8 Hz), 125.4 (q, *J* = 3.8 Hz), 123.5 (d, *J* = 31.7 Hz), 123.1 (d, *J* = 2.7 Hz), 122.5 (d, *J* = 2.1 Hz). ESI-HRMS: calculated for $C_{35}H_{18}F_9NO_5PS^-$ ([M–H]$^-$): 766.0505, found: 766.0514.

Imidodiphosphorimidate 4.6l

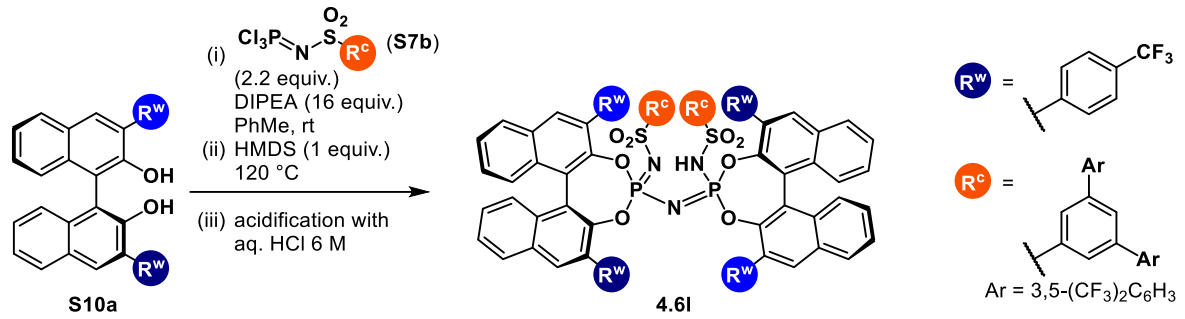

(Adapted from a reported procedure[61a]):

In an oven-dried Schlenk flask under Ar, trichlorophosphazene **S7b** (236 mg, 0.33 mmol, 2.2 equiv.) and 3,3'-disubstituted (*S*)-BINOL (**S10a**, 181 mg, 0.32 mmol, 2.1 equiv.) were dissolved in PhMe (2.0 mL). At room temperature, DIPEA (0.42 mL, 2.4 mmol, 16 equiv.) was added and the mixture was stirred for 30 min. After this time, HMDS (31 µL, 0.15 mmol, 1 equiv.) was added and the mixture was heated at 120 °C for 48 h. At room temperature, the mixture is diluted with CH_2Cl_2 (15 mL) and treated with aq. HCl 6 M (10 mL). After stirring vigorously for 30 min, the aqueous phase was extracted with CH_2Cl_2 (3 x 20 mL). The combined organic phases were washed with distilled water, and brine, then dried over anh. Na_2SO_4, filtered and concentrated under reduced pressure. Purification by flash column chromatography on silica gel (*n*-hexane/MTBE 95:5 → 80:20) afforded the corresponding IDPi as salt. This salt was redissolved in CH_2Cl_2 (20 mL), treated with aq. HCl 6 M (15 mL) and stirred vigorously for 30 min. The organic phase was diluted with dry PhMe (20 mL) and the solvent was concentrated under reduced pressure; the residue was redissolved in PhMe (20 mL) and concentrated. After freeze-drying with liquid N_2 under vacuum, the corresponding IDPi **4.6l** was obtained as a light yellow solid (201 mg, 56% yield).

^{1}H NMR (501 MHz, $CDCl_3$) δ 8.22 (d, *J* = 7.1 Hz, 2H), 8.18 – 8.12 (m, 3H), 7.96 (s, 4H), 7.92 – 7.89 (m, 4H), 7.84 – 7.76 (m, 7H), 7.74 (d, *J* = 1.7 Hz, 3H), 7.70 – 7.65 (m, 2H), 7.59 (ddd, *J* = 8.4, 6.9, 1.4 Hz, 2H), 7.54 – 7.48 (m, 4H), 7.45 (d, *J* = 8.5 Hz, 3H), 7.37 (d, *J* = 8.7 Hz, 4H), 7.22 – 7.13 (m, 8H), 6.89 (d, *J* = 8.2 Hz, 4H), 6.82 (d, *J* = 8.4 Hz, 4H). ^{19}F NMR (471 MHz, $CDCl_3$) δ –62.44 (s, 6F), –62.82 (s, 3F), –62.91 (s, 3F). ^{31}P NMR (203 MHz, $CDCl_3$) δ –3.05 (s). ^{13}C NMR (126 MHz, $CDCl_3$) δ 140.8, 139.6, 138.8, 138.3, 132.9, 132.7, 132.4, 132.2, 131.5, 131.4, 131.1, 131.1, 130.0, 129.7, 129.5, 129.4, 129.0, 129.0, 128.6, 128.1, 127.5, 127.4, 127.2, 126.7, 125.7, 125.6, 125.4, 125.3, 124.3, 123.9, 122.5, 122.1. ESI-HRMS: calculated for $C_{112}H_{54}F_{36}N_3O_8P_2S_2^-$ ([M–H]$^-$): 2378.2258, found: 2378.2216.

7.5 Computations

(in collaboration with Dr. Rajat Maji)

7.5.1 "Open" vs. "confined" acid: Understanding the "cavity effect"

The results from the experiments with deuterium-containing reagents showed a significant difference in the reaction pathways, when either *p*-TsOH or an *i*IDP are utilized as catalysts. Inspired by the work of Kupova and coworkers,[230] we conducted several computational calculations to study the addition of styrene (**4.1a**) to a formaldehyde-derived aldehydium ion ("*truncated electrophile*"), in the presence of the anion from the deprotonated catalyst (either *p*-TsOH or *i*IDP, Scheme 7.1). It is worth to mention that, in contrast to the study from Kupova, our proposed truncated electrophile does not contain a terminal –OH group, in order to describe more accurately the oligomeric structure of paraformaldehyde, as well as to avoid the participation of hydrogen-bond interactions in the calculations.

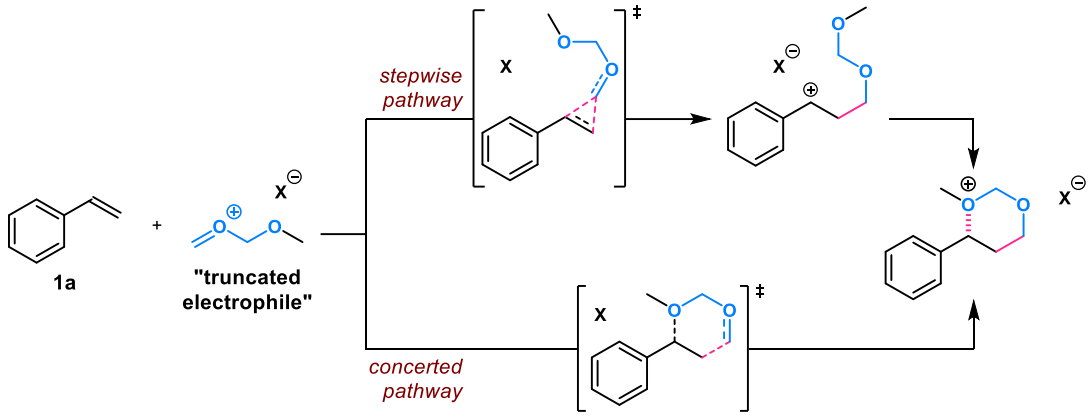

Scheme 7.1. Effect of confinement on the operative reaction pathway.

The results from the computations were the following (see Table 7.1):

(a) With the *p*-toluenesulfonate anion:

A transition state-assembly **TS1** was found, resembling the structure of an "-onium cation", where both carbon atoms from the olefin approach the electrophile (distances C···C: 2.82 Å and 2.95 Å, respectively). Notably, the distance between the benzylic carbon and the remote oxygen found to be 4.95 Å. Changing the displacement variable along the imaginary vibration mode indicates that the observed TS leads to a more stable non-cyclized intermediate (Figure 7.1). The intermediacy of such a carbocation matches the observed differences for the Prins reaction of β-deuterostyrenes (*cis*-/*trans*-scrambling, Scheme 4.40).

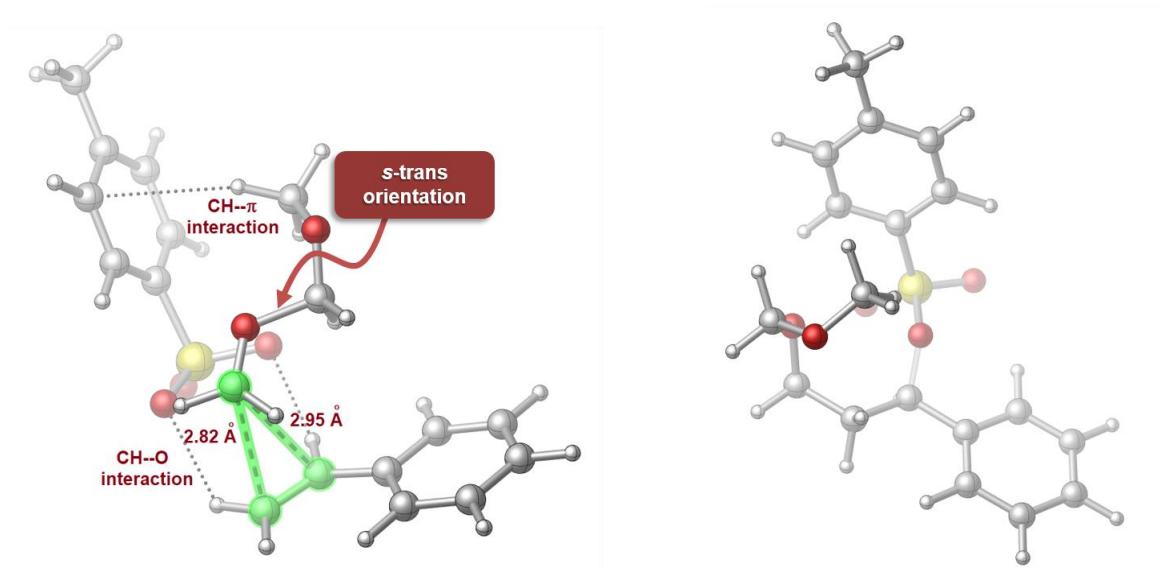

Figure 7.1. TS1 (left) and subsequent intermediate (right), computed at the PBE-D3/def2-SVP level of theory.

(b) With the *i*IDP anion:

In the presence of a confined, enantiopure (*S*,*S*)-*i*IDP anion (catalyst **4.5b**), **TS2** was obtained, where the distance between the atoms forming the C–C bond is around 2 Å (Figure 7.2). A *highly asynchronous, concerted* chair-like TS structure was obtained where C–C bond formation happens prior to the O–C bond formation.

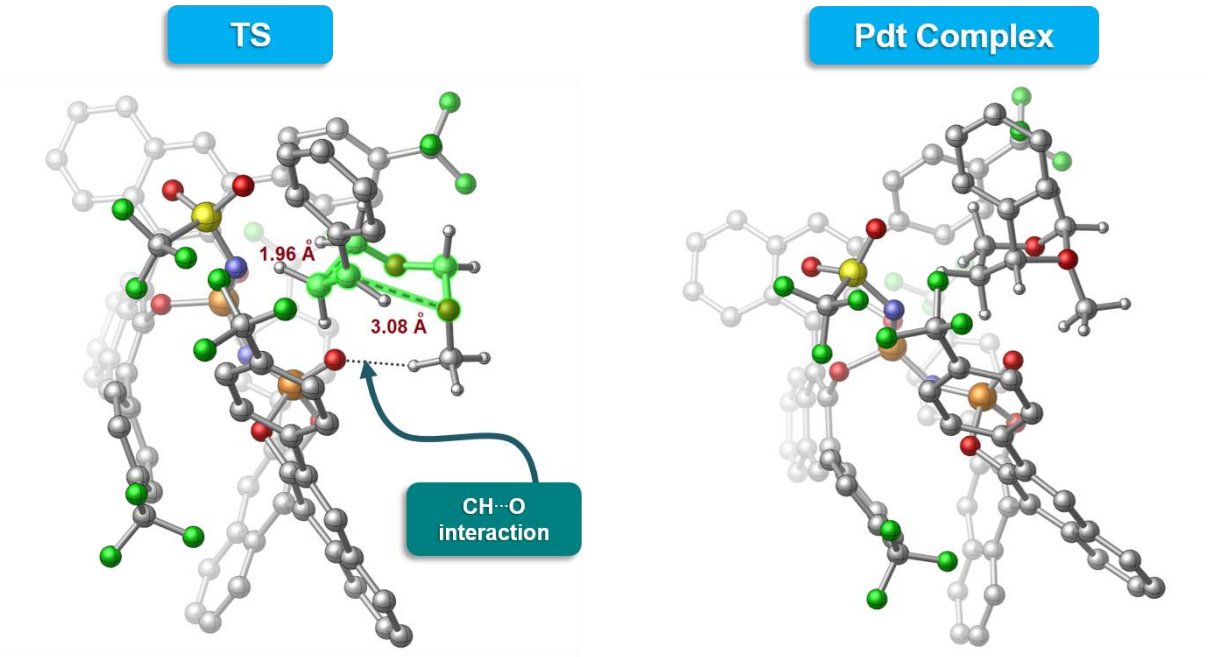

Figure 7.2. TS2 (left) and subsequent intermediate (right), computed at the PBE-D3/def2-SVP level of theory

Furthermore, the confined cavity induces the dimeric electrophile to adopt a conformation where the nucleophilic oxygen atom stays closer to the benzylic center (C···O distance = 3.02 Å, Figure 7.3). By slight displacement from the TS structure toward product and subsequent optimization, a quick collapse of the TS to the formation of the C–O bond is observed,

leading to direct cyclization. This implies that the carbocationic intermediate is virtually non-existent within the catalyst cavity and the transformation follows rather a dynamically concerted pathway. Again, this result is in agreement with the observed high stereospecificity for the *i*IDP-catalyzed Prins reaction with β-deutero-styrenes (Scheme 4.40).

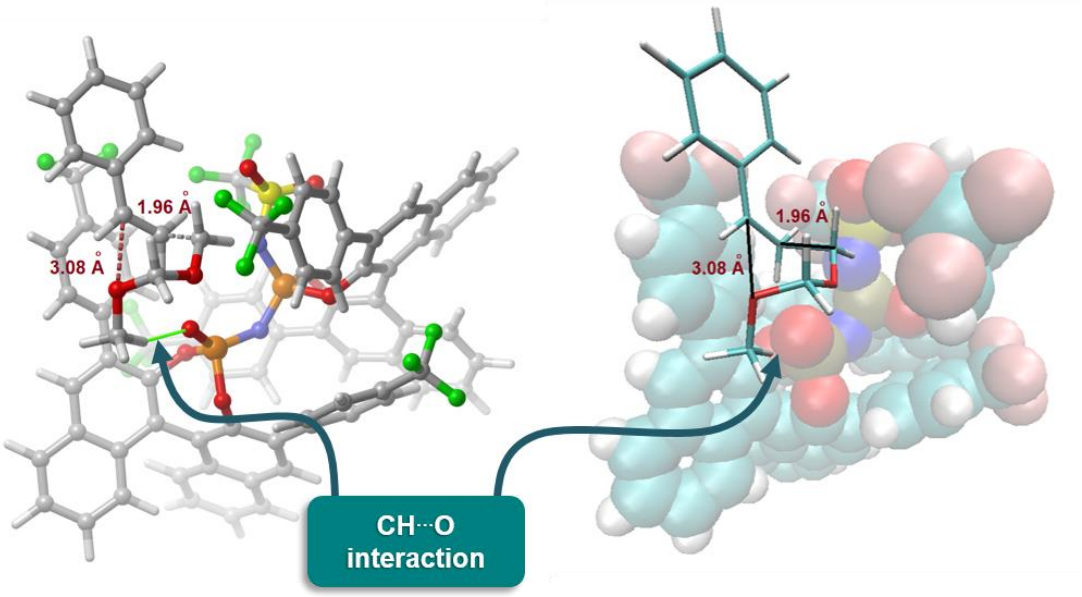

Figure 7.3. Different perspective of **TS2** (180° rotation).

Table 7.1. Comparison of *p*-TsOH and *i*IDP: TS energetics at the M06-2X/def2-TZVP+ CPCM(cyclohexane)//PBE-D3/def2-SVP level of theory

Catalyst	**TS No.**	**PBE RRHO corrections**	**M06-2X/def2-TZVP single point** *(solvent: CyH)*	**Imaginary Freq.**	**$\Delta G^{\ddagger}$ Final**
p-TsOH	**TS1**	0.08029937	–1473.3172402	–118.36	–1473.2369
*i*IDP **4.5b**	**TS2**	0.20723631	–6444.626477	–303.94	–6444.4191

7.5.2 Understanding the Stereoselectivity

Next, we turned our attention to understand the reason for the enantioselectivity in presence of *i*IDP catalysts. For this, we chose the reaction of styrene **4.1a** and our "*truncated electrophile*", in the presence of *i*IDP **4.5b**, modeling the transition states toward the formation of each enantiomer of product **4.3a**. Both TS structures adopt a chair-like conformation, where the initial C–C bond formation precedes the subsequent C–O collapse (Figure 7.4).

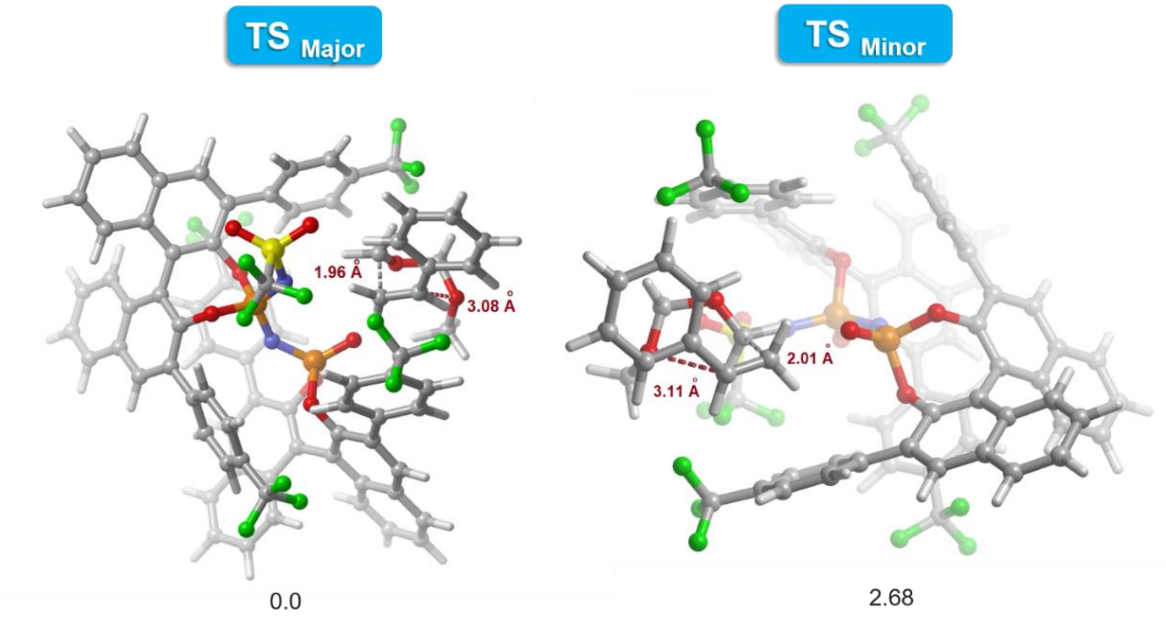

Figure 7.4. Enantio-determining TS structures ($\Delta\Delta G^{\ddagger}$ in kcal/mol, computed at the M06-2X/def2-TZVP+ CPCM(cyclohexane)//PBE-D3/def2-TZVP+ CPCM(cyclohexane)//PBE-D3/def2-SVP level of theory)

Based on the free energy difference of the optimized TS structures at 298 K (Table 7.2), the predicted enantioselectivity (er = 99:1, at the M06-2X/def2-TZVP+ CPCM(cyclohexane)//PBE-D3/def2-SVP level of theory) is in good agreement with the experimental value (er = 94.5:5.5).

Table 7.2. TS energetics for the formation of each enantiomer of the Prins product, at the M06-2X/def2-TZVP+ CPCM(cyclohexane)//PBE-D3/def2-SVP level of theory.

Product Enantiomer	**PBE RRHO corrections**	**M06-2X/def2-TZVP single point *(solvent: CyH)***	**Imaginary Freq.**	**$\Delta G^{\ddagger}$ Final**	**$\Delta\Delta G^{\ddagger}$** (kcal/mol)
(R) (major) (**TS2**)	0.20723631	–6444.626477	–303.94	–6444.4191	0.00
(S) (minor) (**TS3**)	0.20778449	–6444.62259	–218.51	–6444.4148	2.68

Employing the Distortion-Interaction (DI) analysis, we observed that the energy difference between two enantiodifferentiating TS structures (**TS2** and **TS3**) originates from unfavorable distortion effects (see Table 7.3). Notably, in the TS leading to the minor enantiomer ((*S*)-**4.3a**), the catalyst counteranion is more distorted to accommodate the substrate. This also highlights the importance of suitable cavity size in achieving the required stereoinduction.

Table 7.3. Distortion-Interaction Analysis to understand the selectivity for the intermolecular Prins reaction.

TS No.	**M06-2X/def2-TZVP single point** *(gas phase)*	**Relative Energy** ($\Delta\Delta E_{gas}^{\ddagger}$, kcal/mol)
TS2	–6444.604631	2.30
TS3	–6444.600944	
Substrates Only ($\Delta\Delta E_{sub}^{\ddagger}$)		
Subst_**TS2**	–578.2826397	1.80
Subst_**TS3**	–578.2797785	
Catalyst Only ($\Delta\Delta E_{sub}^{\ddagger}$)		
Cat_**TS2**	–5866.1760818	0.31
Cat_**TS3**	–5866.1755331	
Total Net Distortion in **TS3** ($\Delta\Delta E_{dist\_total}^{\ddagger}$)		2.11
Total Interaction		0.19

7.5.3 Optimized Cartesian Coordinates (PBE-D3/def2-SVP)

TS1

Imaginary frequency = –118.36

6	0.309765654	2.168394803	-4.772646504
6	-3.210091370	2.445729570	-3.813448554
6	-3.878021551	1.263455240	-3.887938443
6	-1.363069515	0.363249689	-4.812650625
1	-2.600244514	2.621436679	-2.908428959
1	-1.716191108	-0.606101640	-4.424772065
1	-1.898678693	0.934241161	-5.594539834
1	-3.794768531	0.549184652	-3.054697460
1	-4.505487574	0.987669131	-4.753220614
6	-3.131247154	3.489231942	-4.843029242
6	-2.395916903	4.665985368	-4.557559103
6	-3.715564084	3.363627105	-6.127972461
6	-2.250269814	5.677933697	-5.515206722
1	-1.938630721	4.772728775	-3.561098725
6	-3.567799065	4.373823326	-7.085928996
1	-4.299705516	2.464190313	-6.377186331
6	-2.834350208	5.535086418	-6.784553947
1	-1.678042390	6.585705581	-5.270521004
1	-4.031078087	4.258379705	-8.077737089
1	-2.720488873	6.327834172	-7.539276926
1	-0.191970100	2.768726722	-3.987697593
8	1.642528572	2.133900196	-4.726747662
8	-0.234364225	0.751602790	-4.400134999
1	-0.045678090	2.358552746	-5.806026537
6	2.231642092	2.129213312	-3.405952143
1	1.519341999	2.530010610	-2.656681391
1	2.486754755	1.088820139	-3.120519308
1	3.152599698	2.739063418	-3.460383396
6	2.326861454	-1.596067410	-1.736840092
6	3.249564435	-0.988350780	-0.862354280
6	2.810385934	0.114355028	-0.094109592
6	1.502364593	0.598911362	-0.202145865
6	0.606896061	-0.013388563	-1.096015320
6	1.011705431	-1.117797506	-1.854646775
1	2.644863080	-2.464907348	-2.335614475
1	3.511871720	0.597507366	0.605350303
1	1.159639655	1.452028553	0.402244434
1	0.286164081	-1.592061289	-2.530451357
6	4.656585436	-1.511910775	-0.719529056
1	4.792268666	-2.032136517	0.252810354
1	4.908373766	-2.233998579	-1.520369513
1	5.402153722	-0.691090569	-0.748735630
16	-1.034628695	0.717816856	-1.306169216
8	-1.601204191	0.895102297	0.052595099
8	-0.730012780	2.031415180	-2.014959988
8	-1.798983758	-0.242888708	-2.196740597

Pdt Complex of TS-1

6	1.904935274	1.195780359	-5.945826078
6	-2.183595069	1.154219433	-5.129353783
6	-1.253111596	1.703414690	-6.207701061
6	-0.274302118	0.685445063	-6.807152178
1	-2.740560205	0.290061751	-5.556596905
1	-0.805885348	-0.259588630	-7.039992011
1	0.128521349	1.099687811	-7.762331168
1	-1.894370561	2.069380016	-7.037648722
1	-0.685675830	2.575477599	-5.825107441
6	-3.187900814	2.142490524	-4.552826482
6	-3.988352427	1.732608812	-3.465148112
6	-3.355546101	3.442529915	-5.064972567
6	-4.938475020	2.600308470	-2.912683112
1	-3.847799487	0.725010946	-3.043617506
6	-4.309829269	4.311953195	-4.510559824
1	-2.740180448	3.793340895	-5.905195887
6	-5.104693671	3.894512102	-3.434417855
1	-5.554759600	2.263240303	-2.065141320
1	-4.426712400	5.325343587	-4.924149778
1	-5.851341005	4.576454887	-2.999678989
1	2.163807085	1.518466170	-6.982047268
8	1.715357775	2.381852630	-5.225252903
8	0.810359440	0.314866041	-5.963317723
1	2.741249382	0.599838696	-5.505807392
6	1.610408945	2.187864580	-3.819687721
1	1.636032172	3.189625457	-3.349583114
1	0.664933970	1.676000750	-3.543589184
1	2.464791579	1.584220105	-3.430614221
6	1.526954847	-0.915004104	-0.977531512
6	2.647355114	-1.361074767	-1.709227781
6	2.467858367	-1.715072631	-3.065256748
6	1.217140900	-1.617461421	-3.684401405
6	0.128620291	-1.165222708	-2.924668974
6	0.262368720	-0.819090299	-1.573187949
1	1.647235112	-0.642322389	0.082417858
1	3.331120276	-2.071330689	-3.649431145
1	1.075571504	-1.858501363	-4.745764663
1	-0.616911332	-0.485508090	-1.004037618
6	4.006387335	-1.468069231	-1.067633498
1	3.993147792	-1.123151777	-0.016282516
1	4.371011624	-2.516424849	-1.078232410
1	4.757126907	-0.863524877	-1.617624029
16	-1.467235256	-0.994315406	-3.698227065
8	-2.517393727	-1.210431526	-2.683126637
8	-1.383384438	0.644006025	-4.014930723
8	-1.514684905	-1.731984988	-4.977291949

Major Enantiomer

TS2

Imaginary frequency = –303.94

15	-0.350462660	-0.707857142	-0.915583153
8	1.304920371	-0.442088428	-0.875304737
8	-0.401092100	-2.158833370	-0.094144834
6	2.106661865	-1.471763661	-1.324712369
6	2.683255150	-1.377551937	-2.634508182
6	3.492737395	-2.432592931	-3.052841452
6	3.703150434	-3.592599035	-2.260868885
6	4.492995495	-4.681615483	-2.736651511
6	4.647773043	-5.832884973	-1.981073810
6	4.005526864	-5.940784647	-0.718856508
6	3.246274670	-4.892060319	-0.219904400
6	3.089977215	-3.682149334	-0.959096556
6	2.323483310	-2.564666583	-0.476138952
6	1.737057841	-2.541124537	0.892434573
6	2.553742004	-2.670314868	2.070551533
6	3.976887007	-2.773352330	2.020174177
6	4.727537645	-2.880975063	3.182560684
6	4.094613691	-2.893525644	4.453983059
6	2.717266728	-2.765889413	4.539005165
6	1.917061276	-2.632419317	3.364651662
6	0.515134020	-2.411367190	3.449674139
6	-0.277308375	-2.216997190	2.320120299
6	0.364696808	-2.310863199	1.042226951
6	2.461080860	-0.211489797	-3.526637446
1	3.997439749	-2.371286599	-4.028826066
1	4.968653634	-4.592350653	-3.725870999
1	5.255136887	-6.667998591	-2.361177780
1	4.107351672	-6.866217840	-0.132055071
1	2.748013989	-4.989427657	0.754255394
1	4.479643601	-2.737912185	1.044422425
1	5.823900682	-2.948319489	3.116980909
1	4.700108194	-2.987199328	5.367913649
1	2.215965761	-2.748616390	5.519432872
1	0.047714876	-2.381164301	4.445784560
6	-1.712729870	-1.862142053	2.448619521
6	2.365701138	1.113045322	-3.033535867
6	2.257352348	2.199721432	-3.905925300
6	2.239877083	1.996696787	-5.297521404
6	2.298570430	0.687305555	-5.804498068
6	2.397426061	-0.399004175	-4.926986327
6	-2.112106174	-0.968008863	3.467919673
6	-3.448018934	-0.590684128	3.615944492
6	-4.419472363	-1.089245049	2.731579761
6	-4.043958059	-1.990934483	1.722683368
6	-2.705088318	-2.373973265	1.582843829
1	2.384741186	1.291451104	-1.952508604
1	2.420192450	-1.419694635	-5.336329071
1	-1.354627071	-0.525281164	4.130331718

1	-2.422853415	-3.073632498	0.786366311
7	-0.924325763	0.407850240	0.080496172
15	-1.763561981	1.730126608	-0.077984057
8	-1.172715720	2.928965534	0.900848551
8	-3.211788544	1.428272560	0.676338291
6	-1.200882747	2.710447001	2.271776657
6	0.012545470	2.308853780	2.916342821
6	-0.036614436	2.094097713	4.291511365
6	-1.243302290	2.217194416	5.033788122
6	-1.282812001	1.933683782	6.432131552
6	-2.475927448	1.977972327	7.135864605
6	-3.683301451	2.299801165	6.460377762
6	-3.676915996	2.599050231	5.105263292
6	-2.461677956	2.588839683	4.356596592
6	-2.414755513	2.871199387	2.945409133
6	-3.629808846	3.256505261	2.177413767
6	-4.413566319	4.414472702	2.519438850
6	-4.034118255	5.329096723	3.545990088
6	-4.821360715	6.430656858	3.849212493
6	-6.027657635	6.674506518	3.141118613
6	-6.409588161	5.821745237	2.117867615
6	-5.614086571	4.690238365	1.769704692
6	-5.962938678	3.854249097	0.675615898
6	-5.171350075	2.779339754	0.288741133
6	-4.006811551	2.498366764	1.066135978
6	1.262045536	2.080179010	2.148995572
1	0.884617383	1.811340432	4.823606711
1	-0.343265948	1.663254527	6.938956796
1	-2.493084182	1.749822795	8.212147093
1	-4.634801257	2.303165051	7.013015177
1	-4.619793299	2.817490176	4.586872802
1	-3.097361598	5.159001367	4.093739965
1	-4.503310026	7.124890908	4.641701088
1	-6.646822699	7.547910964	3.395294334
1	-7.329347246	6.012320543	1.543303078
1	-6.876635613	4.081732729	0.105717839
6	-5.486901177	2.006926538	-0.937302043
6	1.689239079	2.961639788	1.131753548
6	2.860118344	2.706623630	0.408464735
6	3.629219166	1.566088344	0.692496017
6	3.229669991	0.694068140	1.719293788
6	2.055792327	0.946388200	2.432352813
6	-5.811451605	2.700143695	-2.125301513
6	-6.141846271	2.005652859	-3.292674225
6	-6.147730590	0.598930790	-3.294160104
6	-5.806757127	-0.103586947	-2.125406965
6	-5.476094862	0.594755579	-0.959431701
1	1.095071811	3.853450746	0.899497003
1	1.723923607	0.225716314	3.193679844
1	-5.753165088	3.797436607	-2.137564398
1	-5.214350921	0.040090347	-0.050564018

7	-1.918198301	2.334350986	-1.569375602
16	-2.385677135	3.810531546	-2.016244120
8	-2.934120134	3.733303535	-3.398092214
8	-3.099875997	4.620755386	-1.006640865
6	-0.728341443	4.710209123	-2.263681236
9	-0.155982786	4.315017831	-3.421571863
9	-0.945115443	6.027182989	-2.321438645
1	2.266718503	0.521722777	-6.890682519
1	2.185928478	3.217830041	-3.498463526
1	3.823023473	-0.202680751	1.945143603
1	3.176023455	3.396553982	-0.386852078
1	-6.373401022	2.560225237	-4.213832373
1	-5.794364117	-1.202018138	-2.132394581
1	-4.805658880	-2.393609697	1.040124749
1	-3.731880121	0.116215403	4.407643893
6	-3.180301401	-1.474585316	-5.381383840
6	-0.941325495	1.047382112	-5.874785185
6	-1.088437394	1.124442680	-4.485766939
6	-2.961851932	0.607993836	-4.230427050
1	-0.689418770	0.060181057	-6.299283540
1	-2.993785173	1.096203588	-3.239193642
1	-0.669683501	0.327304039	-3.844303487
1	-1.156522553	2.116184995	-4.018675188
6	-1.195809302	2.100416836	-6.822601396
6	-0.956055614	1.846091934	-8.201175438
6	-1.670064317	3.383384026	-6.426253405
6	-1.155522331	2.845806914	-9.153957970
1	-0.592143873	0.851862394	-8.503225942
6	-1.880218536	4.371560925	-7.388627942
1	-1.888824992	3.594660901	-5.368312530
6	-1.617803601	4.110416127	-8.746984095
1	-0.953322610	2.646945501	-10.216659061
1	-2.249863766	5.360395042	-7.079653466
1	-1.776554870	4.900973721	-9.496425638
8	-0.876735121	-0.949958273	-2.300807036
1	-3.851358098	-2.329474001	-5.144598075
8	-1.917799466	-1.874041361	-5.763340684
8	-3.149086014	-0.708125553	-4.152806823
1	-3.606500519	-0.852018146	-6.195724613
6	-1.314170861	-2.838849167	-4.886601581
1	-1.965907543	-3.737572537	-4.796254580
1	-0.356820021	-3.132957770	-5.355627032
1	-1.124496677	-2.405473772	-3.882128196
9	0.129568549	4.447705949	-1.264338275
6	-6.531419440	-0.129542244	-4.553123926
6	-5.846066200	-0.631150102	2.886937636
6	2.212298570	3.185928453	-6.223559345
6	4.876108269	1.244374190	-0.090080188
9	-5.836393230	0.341233100	-5.638877749
9	-7.841407022	0.019637122	-4.855074847
9	-6.284277761	-1.462361938	-4.483810018

9	-6.646436605	-1.089204477	1.891991107
9	-6.386853230	-1.041294605	4.061055423
9	-5.935956026	0.728653375	2.875044934
9	5.041844667	2.061932598	-1.157633103
9	5.993756415	1.343279013	0.672441512
9	4.846765496	-0.033219726	-0.565469212
9	1.922980613	2.834045801	-7.503732680
9	1.290292174	4.105943740	-5.839617708
9	3.408720423	3.823686356	-6.249632691
1	-3.468708274	1.138792599	-5.059631103

Pdt Complex of TS-2

15	-0.225277632	-0.680068078	-0.972679886
8	1.424072934	-0.421800409	-0.813249345
8	-0.322946432	-2.146897613	-0.182876001
6	2.269932429	-1.432871618	-1.213977968
6	2.953455641	-1.302545907	-2.469223410
6	3.824488687	-2.328276617	-2.831523459
6	3.988272189	-3.500061593	-2.045662681
6	4.841246129	-4.562779105	-2.469302561
6	4.946965509	-5.729804176	-1.729638571
6	4.189999008	-5.881116397	-0.537353238
6	3.367472927	-4.858163472	-0.087678376
6	3.258960529	-3.632184791	-0.808629614
6	2.433591980	-2.538470610	-0.369455765
6	1.743065288	-2.542798130	0.950191087
6	2.470936236	-2.688785815	2.184773797
6	3.893363222	-2.801079455	2.240878365
6	4.555134185	-2.926388178	3.454479786
6	3.830130506	-2.947017761	4.675363324
6	2.451315172	-2.809463705	4.658625667
6	1.741725104	-2.658938924	3.429391795
6	0.339157605	-2.427952689	3.414482133
6	-0.368167560	-2.223113074	2.232074687
6	0.362873934	-2.310624377	1.002447038
6	2.738983662	-0.137513499	-3.363726364
1	4.412075351	-2.238109041	-3.757730276
1	5.406077294	-4.440620459	-3.406784867
1	5.604156215	-6.544156514	-2.069781134
1	4.253503517	-6.819487958	0.034072674
1	2.781924773	-4.987880932	0.832746254
1	4.469169718	-2.762605119	1.306550995
1	5.652802373	-3.002468580	3.469049360
1	4.365456567	-3.054508847	5.630622749
1	1.877917144	-2.798302155	5.598784033
1	-0.199042455	-2.399403558	4.374211789
6	-1.809451905	-1.869848451	2.263874409
6	2.495774356	1.164719381	-2.866473656
6	2.300131565	2.243965892	-3.732047023
6	2.347746900	2.056824816	-5.123964541
6	2.608621408	0.774593244	-5.640396343

6	2.795912994	-0.304667699	-4.768531655
6	-2.273219179	-0.970299179	3.250303942
6	-3.619374126	-0.608419313	3.321434461
6	-4.536260319	-1.129994495	2.393528119
6	-4.094719936	-2.029549904	1.409489135
6	-2.744764724	-2.394924373	1.344513152
1	2.454983732	1.335861407	-1.785781023
1	2.980183408	-1.306228719	-5.185520729
1	-1.557529526	-0.513035638	3.948313500
1	-2.409368700	-3.093558245	0.567681092
7	-0.854783023	0.419505446	0.001976848
15	-1.644365151	1.776167289	-0.128092666
8	-1.042237636	2.919414868	0.909749969
8	-3.115351669	1.477462032	0.585546313
6	-1.096932490	2.649366211	2.268795247
6	0.101734820	2.210036131	2.916302273
6	0.027769256	1.940244969	4.280759255
6	-1.189510204	2.047566481	5.007942238
6	-1.254883242	1.709358600	6.393089814
6	-2.458109941	1.742343816	7.079934019
6	-3.650093391	2.108435638	6.399868896
6	-3.618132273	2.460909024	5.057952443
6	-2.392006957	2.462122369	4.327031698
6	-2.319094472	2.801230822	2.929239938
6	-3.516349039	3.242178324	2.162512449
6	-4.279565327	4.400284185	2.548007004
6	-3.890270924	5.263397834	3.614663804
6	-4.658573001	6.366330957	3.958831513
6	-5.854977005	6.662766613	3.254045527
6	-6.245728579	5.860946668	2.193606502
6	-5.469072602	4.730074224	1.803240330
6	-5.828092537	3.944435973	0.676025727
6	-5.054478388	2.872256335	0.245308140
6	-3.896420151	2.541039398	1.014767442
6	1.364219610	2.006051976	2.163364040
1	0.936599741	1.626140210	4.816430851
1	-0.326937840	1.406382910	6.902885741
1	-2.495219653	1.472385123	8.145985039
1	-4.609698996	2.105372100	6.938333900
1	-4.548719315	2.720400901	4.535506369
1	-2.960687811	5.052828063	4.160576588
1	-4.332763626	7.020859485	4.781385113
1	-6.459135193	7.536669731	3.540553500
1	-7.157813852	6.092802835	1.621962785
1	-6.739416767	4.207707904	0.118032622
6	-5.398377352	2.150469562	-1.004067341
6	1.809117734	2.914861691	1.176762673
6	3.001677315	2.687320090	0.480310845
6	3.772183435	1.544703357	0.754755803
6	3.350087721	0.642511374	1.744993107
6	2.157307595	0.869219823	2.434717111

6	-5.779730440	2.891945650	-2.145813649
6	-6.148342768	2.248362093	-3.329966096
6	-6.131839127	0.843520661	-3.400684290
6	-5.737916635	0.092904433	-2.280258004
6	-5.372374326	0.740813808	-1.094980724
1	1.212155466	3.805503560	0.945070408
1	1.810861561	0.126152468	3.167285396
1	-5.733566889	3.989368720	-2.111539891
1	-5.060407919	0.146776102	-0.228490820
7	-1.743381766	2.437930144	-1.591894117
16	-2.227826098	3.920413526	-2.002615507
8	-2.867922916	3.879744508	-3.343719374
8	-2.854285587	4.728711464	-0.934247168
6	-0.564640749	4.772114911	-2.346787848
9	-0.089377548	4.389225548	-3.551532183
9	-0.734038048	6.096748392	-2.354398595
1	2.669163603	0.626305439	-6.728832378
1	2.107278709	3.243346267	-3.320740526
1	3.938779933	-0.260097084	1.958612801
1	3.331804121	3.399070613	-0.289735899
1	-6.418376782	2.842076908	-4.215603029
1	-5.703515175	-1.003337493	-2.341907644
1	-4.813200218	-2.445000142	0.688697111
1	-3.952511558	0.103782108	4.089010538
6	-3.074280988	-0.773892804	-5.670178958
6	-1.162794733	0.868690271	-5.925601682
6	-1.459499534	1.228000349	-4.482971029
6	-2.887867879	0.897482706	-4.071478010
1	-3.003476336	1.009827985	-2.983301748
1	-0.767004016	0.696249282	-3.803569311
1	-1.279293696	2.307114442	-4.336107847
6	-1.846600958	1.657021202	-7.014167121
6	-1.803629563	1.192740231	-8.346344879
6	-2.474740806	2.887960655	-6.733277895
6	-2.397666580	1.931558912	-9.377012771
1	-1.306350355	0.237381616	-8.573549360
6	-3.058765264	3.629037899	-7.771679150
1	-2.504930555	3.284599396	-5.707152082
6	-3.028206405	3.153778485	-9.090831881
1	-2.361607511	1.556051910	-10.410748875
1	-3.543387522	4.589149938	-7.540118889
1	-3.491775057	3.737958526	-9.900026729
8	-0.656892667	-0.900433313	-2.394659575
1	-3.298933528	-1.834425926	-5.885241449
8	-1.577310368	-0.617773769	-6.130950894
8	-3.178924112	-0.503701848	-4.368119587
1	-3.574221500	-0.065617761	-6.362535660
6	-0.686745429	-1.569701480	-5.446087957
1	-0.986928689	-2.570458928	-5.804335376
1	0.337040164	-1.325357706	-5.778243676
1	-0.777500469	-1.469960273	-4.343798840

9	0.352873057	4.451582942	-1.414616174
1	-3.645161299	1.523984196	-4.581854542
6	-5.977051139	-0.697930122	2.479488752
6	2.053264926	3.207068326	-6.051731330
6	-6.512866958	0.173687253	-4.692672201
6	5.048613794	1.261291501	0.005774605
9	-6.087429073	0.659911423	2.480239202
9	-6.569185831	-1.132119969	3.620110247
9	-6.717548186	-1.157425393	1.440723503
9	5.174829829	2.026530934	-1.105753725
9	5.111002828	-0.040204551	-0.392849189
9	6.147201026	1.481624068	0.771218263
9	-5.838826429	0.723078913	-5.756417605
9	-7.829081094	0.309792451	-4.976289757
9	-6.232857796	-1.152380092	-4.703080983
9	2.458118351	4.390738299	-5.547199532
9	2.639054176	3.047766239	-7.262820388
9	0.708117959	3.317610120	-6.284662801
1	-0.071652148	0.818995950	-6.109600953

Minor Enantiomer

TS3

Imaginary frequency = –218.51

15	0.253838804	-0.454155665	-0.961983513
8	1.896310758	-0.267044521	-0.685069088
8	0.068537367	-2.002785687	-0.371781025
6	2.767344764	-1.256077453	-1.084121068
6	3.606149452	-1.014353934	-2.223563299
6	4.501633952	-2.020067913	-2.583419239
6	4.553186828	-3.270014912	-1.911892945
6	5.435412045	-4.306525181	-2.340449890
6	5.439076607	-5.542658614	-1.714342600
6	4.547930052	-5.791008911	-0.636499365
6	3.691982210	-4.797434008	-0.183497660
6	3.682320211	-3.505342853	-0.787525345
6	2.825563682	-2.440464094	-0.338384582
6	2.011970474	-2.553519085	0.903139187
6	2.622453815	-2.825652239	2.179561161
6	4.033389354	-2.958515047	2.354197242
6	4.579979119	-3.204632007	3.606029316
6	3.745467437	-3.332388086	4.748000168
6	2.374421048	-3.178156848	4.618360531
6	1.781888264	-2.903946164	3.349150487
6	0.387738123	-2.655160262	3.227322600
6	-0.205440681	-2.325606089	2.010916081
6	0.636060689	-2.303063477	0.851075921
6	3.530566758	0.242696054	-3.009209242
1	5.199564755	-1.850251361	-3.416994114
1	6.106090956	-4.107045097	-3.190818055
1	6.119575492	-6.336115277	-2.057978365
1	4.532613633	-6.782149644	-0.158470438

1	3.002351307	-5.002168664	0.646819844
1	4.693124155	-2.833391945	1.485660386
1	5.671571468	-3.292035924	3.713998068
1	4.190175957	-3.535609633	5.733702546
1	1.716932140	-3.248276948	5.499055344
1	-0.237956685	-2.714170887	4.131007489
6	-1.642765413	-1.961494770	1.947388296
6	3.233208493	1.494479564	-2.420132431
6	3.158715755	2.657224358	-3.194518925
6	3.390474092	2.603952086	-4.578848701
6	3.716029250	1.373812106	-5.180150589
6	3.772758586	0.212530891	-4.405113105
6	-2.194073854	-1.152903791	2.967165045
6	-3.541708956	-0.788703615	2.949982733
6	-4.371011238	-1.216953778	1.899984586
6	-3.842829803	-2.030204938	0.883531456
6	-2.491570938	-2.395670478	0.904954055
1	3.048923292	1.560198015	-1.342557284
1	3.982828364	-0.748453765	-4.896369148
1	-1.543955459	-0.765549026	3.765024273
1	-2.086606997	-3.023924332	0.101286700
7	-0.385154424	0.541678701	0.119557104
15	-1.236279475	1.861645793	0.018794157
8	-0.800302892	2.933625221	1.202968111
8	-2.753275401	1.449023179	0.549791281
6	-1.035589665	2.571484590	2.520278792
6	0.072460705	2.091738764	3.288967473
6	-0.176018758	1.729119261	4.610342342
6	-1.480512533	1.779573625	5.174743119
6	-1.723079619	1.347411165	6.513252078
6	-3.007522283	1.319201307	7.032778319
6	-4.105668075	1.714559656	6.223486164
6	-3.902582167	2.158798796	4.924486349
6	-2.589829977	2.227724319	4.367798910
6	-2.338921633	2.662693335	3.018057513
6	-3.436340182	3.118483342	2.120366199
6	-4.288092195	4.229225726	2.449904246
6	-4.089031465	5.041388148	3.604841417
6	-4.941642826	6.098040923	3.890389881
6	-6.035930802	6.395375263	3.035546630
6	-6.239956854	5.642853114	1.890101673
6	-5.371293891	4.561159485	1.557800876
6	-5.535871720	3.830011600	0.351629322
6	-4.668852847	2.806733811	-0.020964375
6	-3.627935536	2.467495462	0.899190538
6	1.416101899	1.920940681	2.681782583
1	0.658206869	1.380209355	5.238091448
1	-0.865436226	1.020811182	7.121960940
1	-3.180766232	0.976518368	8.063930216
1	-5.128468308	1.661368184	6.625789559
1	-4.761169119	2.438034884	4.299306153

1	-3.239553670	4.827371195	4.267647971
1	-4.763784949	6.714794884	4.784324603
1	-6.709214950	7.231714884	3.276478349
1	-7.070270417	5.877571136	1.206030630
1	-6.371843195	4.096191013	-0.312675995
6	-4.791582081	2.146431442	-1.343793559
6	1.985012175	2.887174208	1.822409000
6	3.239174140	2.674992838	1.238263796
6	3.950196379	1.492759153	1.503771747
6	3.406314216	0.533409678	2.374310328
6	2.151352834	0.744816963	2.949440029
6	-5.141455915	2.918003754	-2.474945571
6	-5.282944625	2.329705509	-3.735086642
6	-5.047597154	0.954408890	-3.899108756
6	-4.684712607	0.174699263	-2.787288622
6	-4.565058963	0.762215084	-1.525023505
1	1.435430895	3.809696853	1.598099496
1	1.710908313	-0.039765951	3.581479687
1	-5.258941803	4.005529994	-2.368797546
1	-4.283290405	0.140653563	-0.668139414
7	-1.247739962	2.649130525	-1.391144480
16	-1.631178624	4.193167440	-1.637011259
8	-2.214324507	4.345995238	-2.996303269
8	-2.252121399	4.920752660	-0.511368247
6	0.092033677	4.968326808	-1.821085542
9	0.922460689	4.553152639	-0.847968786
9	0.637578041	4.617991227	-3.011323827
1	3.910891269	1.323312105	-6.261845819
1	2.913396570	3.614395417	-2.717185401
1	3.950772962	-0.398157973	2.581045288
1	-5.549948150	2.947453209	-4.604433596
1	-4.487739713	-0.900080613	-2.910636782
1	-4.494297476	-2.374672055	0.067768297
1	-3.942732207	-0.143395936	3.743804201
6	-2.387211068	3.054157502	-5.739330826
6	0.313784752	0.939949736	-6.426654098
6	0.202670891	0.352573382	-5.177913561
6	-0.917788719	1.780108952	-4.296148711
1	-0.892126373	1.127729435	-3.398136586
1	-0.233633617	2.643212489	-4.346657202
1	-0.502836694	-0.469150505	-4.984311509
1	1.049705367	0.387377019	-4.477809176
8	-0.125709585	-0.454859001	-2.415401245
1	-2.985544460	3.733656814	-5.098726943
8	-1.247501811	3.632158687	-6.233883394
8	-2.095118331	1.894372792	-4.856399060
1	-2.994323888	2.595578744	-6.543026582
6	-0.982986998	4.994408587	-5.863614176
1	-1.290523707	5.192613720	-4.818070621
1	0.106911520	5.143579431	-5.967646544
1	-1.513752002	5.686254325	-6.553196154

9	-0.003386088	6.300492011	-1.777592517
6	-5.225372892	0.307575789	-5.244550559
6	-5.814207842	-0.783004790	1.888450875
6	3.247445996	3.829243847	-5.439620531
9	-6.467046626	-0.211357347	-5.406224720
9	-4.350562043	-0.718202087	-5.444121130
9	-5.040033965	1.189889903	-6.269232000
9	2.105191025	3.757229846	-6.211390164
9	3.152360705	4.968131912	-4.725877371
9	4.272703066	3.965310412	-6.311783671
9	-6.531049669	-1.379747900	2.874226234
9	-6.428967949	-1.068327994	0.714991341
9	-5.929710353	0.559693485	2.086177223
6	-0.668772161	0.867871831	-7.482611554
6	-0.504265785	1.690015271	-8.629044596
6	-1.836749278	0.066905712	-7.374300709
6	-1.473787101	1.710093804	-9.633417020
1	0.388126402	2.330216490	-8.698810491
6	-2.809935993	0.099271700	-8.375706826
1	-1.996792318	-0.560929277	-6.487892980
6	-2.629855796	0.917622005	-9.505631328
1	-1.341281083	2.353467978	-10.515862459
1	-3.720805807	-0.506067556	-8.267266551
1	-3.399094421	0.940397595	-10.292650412
1	1.155026804	1.631976978	-6.595754831
1	3.665623723	3.430813180	0.563522529
6	5.292573236	1.226921050	0.872961492
9	5.574495778	2.097311203	-0.127282654
9	5.353300387	-0.026796273	0.342036445
9	6.302912498	1.310551115	1.774764466

Page left intentionally blank

8 References

[1] M. Bender. *ChemBioEng. Rev.* **2014**, *1*, 136–147.

[2] H. A. Dieck, R. F. Heck. *J. Am. Chem. Soc.* **1974**, *96*, 1133–1136.

[3] O. Diels, K. Alder. *Liebigs Ann. Chem.* **1928**, *460*, 98–122.

[4] O. Roelen. Verfahren zur Herstellung von sauerstoffhaltigen Verbindungen. Patent DE849548C, 1938.

[5] (a) P. J.-L. Hérisson, Y. Chauvin. *Makromolekulare Chemie* **1971**, *141*, 161–176; (b) R. H. Grubbs, P. L. Burk, D. D. Carr. *J. Am. Chem. Soc.* **1975**, *97*, 3265–3267.

[6] K. B. Sharpless. *Angew. Chem. Int. Ed.* **2002**, *41*, 2024–2032.

[7] J. Smidt, W. Hafner, R. Jira, J. Sedlmeier, R. Sieber, R. Rüttinger, H. Kojer. *Angew. Chem.* **1959**, *71*, 176–182.

[8] (a) W. S. Knowles. *Angew. Chem. Int. Ed.* **2002**, *41*, 1998–2007; (b) R. Noyori. *Angew. Chem. Int. Ed.* **2002**, *41*, 2008–2022.

[9] I. M. Pastor, M. Yus. *Curr. Org. Chem.* **2007**, *11*, 925–957.

[10] F. Doro, N. Akeroyd, F. Schiet, A. Narula. *Angew. Chem. Int. Ed.* **2019**, *58*, 7174–7179.

[11] J. K. Smith, History of Catalysis. In *Encyclopedia of Catalysis*, John Wiley & Sons, Inc.: 2010; pp 1–34.

[12] R. van Santen, Catalysis in Perspective: Historic Review. In *Catalysis: From Principles to Applications*, 1st ed.; M. Beller, A. Renken, R. van Santen, Eds. Wiley-VCH Verlag GmbH & Co. KGaA: 2012; pp 3–19.

[13] S. Zahn, T. M. Swager. *Angew. Chem. Int. Ed.* **2002**, *41*, 4225–4230.

[14] B. M. Trost. *P. Natl. Acad. Sci. USA* **2004**, *101*, 5348–5355.

[15] *Press release: The Nobel Prize in Chemistry 2021*. https://www.nobelprize.org/prizes/chemistry/2021/press-release/ (accessed 2021-10-12).

[16] V. Oliveira, M. Cardoso, L. Forezi. *Catalysts* **2018**, *8*, 605.

[17] Z. G. Hajos, D. R. Parrish. *J. Org. Chem.* **1974**, *39*, 1615–1621.

[18] U. Eder, G. Sauer, R. Wiechert. *Angew. Chem. Int. Ed.* **1971**, *10*, 496–497.

[19] B. List. *Tetrahedron* **2002**, *58*, 5573–5590.

[20] (a) S. Bahmanyar, K. N. Houk. *J. Am. Chem. Soc.* **2001**, *123*, 11273–11283; (b) S. Bahmanyar, K. N. Houk. *J. Am. Chem. Soc.* **2001**, *123*, 12911–12912.

[21] B. List, L. Hoang, H. J. Martin. *P. Natl. Acad. Sci. USA* **2004**, *101*, 5839–5842.

[22] B. List, R. A. Lerner, C. F. Barbas. *J. Am. Chem. Soc.* **2000**, *122*, 2395–2396.

[23] (a) C. F. Barbas, III. *Angew. Chem. Int. Ed.* **2008**, *47*, 42–47; (b) A. Dondoni, A. Massi. *Angew. Chem. Int. Ed.* **2008**, *47*, 4638–4660.

[24] K. A. Ahrendt, C. J. Borths, D. W. C. MacMillan. *J. Am. Chem. Soc.* **2000**, *122*, 4243–4244.

[25] J. Seayad, B. List. *Org. Biomol. Chem.* **2005**, *3*, 719–724.

[26] S. Mayer, B. List. *Angew. Chem. Int. Ed.* **2006**, *45*, 4193–4195.

[27] M. Mahlau, B. List. *Angew. Chem. Int. Ed.* **2013**, *52*, 518–533.

[28] IUPAC, Compendium of Chemical Terminology (the "Gold Book"). 2nd ed.; A. D. McNaught, A. Wilkinson, Eds. Blackwell Scientific Publications: Oxford, 1997. ISBN: 0-9678550-9-8. DOI: 10.1351/goldbook.

[29] P. Vachal, E. N. Jacobsen. *J. Am. Chem. Soc.* **2002**, *124*, 10012–10014.

[30] J. P. Malerich, K. Hagihara, V. H. Rawal. *J. Am. Chem. Soc.* **2008**, *130*, 14416–14417.

[31] A. G. Doyle, E. N. Jacobsen. *Chem. Rev.* **2007**, *107*, 5713–5743.

[32] B. List. *Chem. Rev.* **2007**, *107*, 5413–5415.

[33] (a) T. Akiyama, J. Itoh, K. Yokota, K. Fuchibe. *Angew. Chem. Int. Ed.* **2004**, *43*, 1566–1568; (b) D. Uraguchi, M. Terada. *J. Am. Chem. Soc.* **2004**, *126*, 5356–5357.

[34] M. Hatano, K. Moriyama, T. Maki, K. Ishihara. *Angew. Chem. Int. Ed.* **2010**, *49*, 3823–3826.

[35] (a) D. Parmar, E. Sugiono, S. Raja, M. Rueping. *Chem. Rev.* **2014**, *114*, 9047–9153; (b) D. Parmar, E. Sugiono, S. Raja, M. Rueping. *Chem. Rev.* **2017**, *117*, 10608–10620.

[36] K. Kaupmees, N. Tolstoluzhsky, S. Raja, M. Rueping, I. Leito. *Angew. Chem. Int. Ed.* **2013**, *52*, 11569–11572.

[37] L. M. Yagupolskii, V. N. Petrik, N. V. Kondratenko, L. Sooväli, I. Kaljurand, I. Leito, I. A. Koppel. *J. Chem. Soc. Perk. T. 2* **2002**, 1950–1955.

[38] D. Nakashima, H. Yamamoto. *J. Am. Chem. Soc.* **2006**, *128*, 9626–9627.

[39] S. Vellalath, I. Čorić, B. List. *Angew. Chem. Int. Ed.* **2010**, *49*, 9749–9752.

[40] (a) G. Pousse, A. Devineau, V. Dalla, L. Humphreys, M.-C. Lasne, J. Rouden, J. Blanchet. *Tetrahedron* **2009**, *65*, 10617–10622; (b) N. D. Shapiro, V. Rauniyar, G. L. Hamilton, J. Wu, F. D. Toste. *Nature* **2011**, *470*, 245–249.

[41] C. H. Cheon, H. Yamamoto. *J. Am. Chem. Soc.* **2008**, *130*, 9246–9247.

[42] B. List, P. S. J. Kaib. *Synlett* **2015**, *27*, 156–158.

[43] (a) S. C. Pan, B. List. *Chem.-Asian J.* **2008**, *3*, 430–437; (b) M. Hatano, T. Maki, K. Moriyama, M. Arinobe, K. Ishihara. *J. Am. Chem. Soc.* **2008**, *130*, 16858–16860.

[44] M. Hatano, K. Ishihara. *Asian J. Org. Chem.* **2014**, *3*, 352–365.

[45] (a) P. García-García, F. Lay, P. García-García, C. Rabalakos, B. List. *Angew. Chem. Int. Ed.* **2009**, *48*, 4363–4366; (b) M. Treskow, J. Neudörfl, R. Giernoth. *Eur. J. Org. Chem.* **2009**, *2009*, 3693–3697.

[46] M. C. Benda, S. France. *Org. Biomol. Chem.* **2020**, *18*, 7485–7513.

[47] S. Prévost, N. Dupré, M. Leutzsch, Q. Wang, V. Wakchaure, B. List. *Angew. Chem. Int. Ed.* **2014**, *53*, 8770–8773.

[48] L. Ratjen, M. van Gemmeren, F. Pesciaioli, B. List. *Angew. Chem. Int. Ed.* **2014**, *53*, 8765–8769.

[49] A. Berkessel, P. Christ, N. Leconte, J.-M. Neudörfl, M. Schäfer. *Eur. J. Org. Chem.* **2010**, *2010*, 5165–5170.

[50] H. Y. Bae, D. Höfler, P. S. J. Kaib, P. Kasaplar, C. K. De, A. Döhring, S. Lee, K. Kaupmees, I. Leito, B. List. *Nat. Chem.* **2018**, *10*, 888–894.

[51] (a) S. Ni, V. Ramesh Naidu, J. Franzén. *Eur. J. Org. Chem.* **2016**, *2016*, 1708–1713; (b) R. E. Shelton, S. Sezer, D. M. Hodgson. *Tetrahedron* **2020**, *76*.

[52] T. Gatzenmeier, M. van Gemmeren, Y. Xie, D. Höfler, M. Leutzsch, B. List. *Science* **2016**, *351*, 949–952.

[53] C. D. Gheewala, B. E. Collins, T. H. Lambert. *Science* **2016**, *351*, 961–965.

[54] S. Hoffmann, A. M. Seayad, B. List. *Angew. Chem. Int. Ed.* **2005**, *44*, 7424–7427.

[55] I. Čorić, B. List. *Nature* **2012**, *483*, 315–319.

[56] Z. Sun, G. A. Winschel, A. Borovika, P. Nagorny. *J. Am. Chem. Soc.* **2012**, *134*, 8074–8077.

[57] (a) S. Liao, I. Čorić, Q. Wang, B. List. *J. Am. Chem. Soc.* **2012**, *134*, 10765–10768; (b) J. H. Kim, I. Čorić, S. Vellalath, B. List. *Angew. Chem. Int. Ed.* **2013**, *52*, 4474–4477; (c) G. C. Tsui, L. Liu, B. List. *Angew. Chem. Int. Ed.* **2015**, *54*, 7703–7706; (d) Y. Xie, G.-J. Cheng, S. Lee, P. S. J. Kaib, W. Thiel, B. List. *J. Am. Chem. Soc.* **2016**, *138*, 14538–14541.

[58] S. Das, L. Liu, Y. Zheng, M. W. Alachraf, W. Thiel, C. K. De, B. List. *J. Am. Chem. Soc.* **2016**, *138*, 9429–9432.

[59] L. Liu, P. S. J. Kaib, A. Tap, B. List. *J. Am. Chem. Soc.* **2016**, *138*, 10822–10825.

[60] P. S. Kaib, L. Schreyer, S. Lee, R. Properzi, B. List. *Angew. Chem. Int. Ed.* **2016**, *55*, 13200–13203.

[61] (a) N. Tsuji, J. L. Kennemur, T. Buyck, S. Lee, S. Prévost, P. S. J. Kaib, D. Bykov, C. Farès, B. List. *Science* **2018**, *359*, 1501–1505; (b) P. Zhang, N. Tsuji, J. Ouyang, B. List. *J. Am. Chem. Soc.* **2021**, *143*, 675–680.

[62] L. Schreyer, P. S. J. Kaib, V. N. Wakchaure, C. Obradors, R. Properzi, S. Lee, B. List. *Science* **2018**, *362*, 216–219.

[63] S. A. Schwengers, C. K. De, O. Grossmann, J. A. A. Grimm, N. R. Sadlowski, G. G. Gerosa, B. List. *J. Am. Chem. Soc.* **2021**, *143*, 14835–14844.

[64] D. Blanco-Ania, F. P. J. T. Rutjes. *Beilstein J. Org. Chem.* **2018**, *14*, 2568–2571.

[65] C. Laurence, J.-F. Gal, Thermodynamic and Spectroscopic Scales of Hydrogen-Bond Basicity and Affinity. In *Lewis Basicity and Affinity Scales: Data and Measurement*, John Wiley & Sons: Chichester, UK, 2010; pp 111–227.

[66] (a) H. Mayr, M. Patz. *Angew. Chem. Int. Ed.* **1994**, *33*, 938–957; (b) T. B. Phan, M. Breugst, H. Mayr. *Angew. Chem. Int. Ed.* **2006**, *45*, 3869–3874; (c) H. Mayr, A. R. Ofial. *J. Phys. Org. Chem.* **2008**, *21*, 584–595.

[67] M. Xie, L. Lin, X. Feng. *Chem. Rec.* **2017**, *17*, 1184–1202.

[68] (a) K. Juhl, K. A. Jørgensen. *Angew. Chem. Int. Ed.* **2003**, *42*, 1498–1501; (b) Ł. Albrecht, G. Dickmeiss, C. F. Weise, C. Rodríguez-Escrich, K. A. Jørgensen. *Angew. Chem. Int. Ed.* **2012**, *51*, 13109–13113.

[69] Y.-C. Zhang, Q.-N. Zhu, X. Yang, L.-J. Zhou, F. Shi. *J. Org. Chem.* **2016**, *81*, 1681–1688.

[70] M. G. Vinogradov, O. V. Turova, S. G. Zlotin. *Adv. Synth. Catal.* **2021**, *363*, 1466–1526.

[71] B. Han, J.-L. Li, C. Ma, S.-J. Zhang, Y.-C. Chen. *Angew. Chem. Int. Ed.* **2008**, *47*, 9971–9974.

[72] X.-R. Ren, J.-B. Lin, X.-Q. Hu, P.-F. Xu. *Org. Chem. Front.* **2019**, *6*, 2280–2283.

[73] L.-Z. Li, C.-S. Wang, W.-F. Guo, G.-J. Mei, F. Shi. *J. Org. Chem.* **2018**, *83*, 614–623.

[74] H.-H. Liao, C.-C. Hsiao, I. Atodiresei, M. Rueping. *Chem.-Eur. J.* **2018**, *24*, 7718–7723.

[75] M. Fochi, L. Caruana, L. Bernardi. *Synthesis* **2013**, *46*, 135–157.

[76] L. He, M. Bekkaye, P. Retailleau, G. Masson. *Org. Lett.* **2012**, *14*, 3158–3161.

[77] F. Shi, G.-J. Xing, Z.-L. Tao, S.-W. Luo, S.-J. Tu, L.-Z. Gong. *J. Org. Chem.* **2012**, *77*, 6970–6979.

[78] M. Balha, C. Parida, S. C. Pan. *Asian J. Org. Chem.* **2021**, *10*, 2440–2453.

[79] M. L. Clarke, C. E. S. Jones, M. B. France. *Beilstein J. Org. Chem.* **2007**, *3*, 24.

[80] M. Rueping, T. Theissmann, A. Kuenkel, R. M. Koenigs. *Angew. Chem. Int. Ed.* **2008**, *47*, 6798–6801.

[81] (a) J. Kikuchi, H. Aramaki, H. Okamoto, M. Terada. *Chem. Sci.* **2019**, *10*, 1426–1433; (b) J. Kikuchi, Y. Aizawa, M. Terada. *Org. Chem. Front.* **2020**, *7*, 1383–1387.

[82] N. Momiyama, H. Okamoto, J. Kikuchi, T. Korenaga, M. Terada. *ACS Catal.* **2016**, *6*, 1198–1204.

[83] Q.-X. Zhang, Y. Li, J. Wang, C. Yang, C.-J. Liu, X. Li, J.-P. Cheng. *Angew. Chem. Int. Ed.* **2020**, *59*, 4550–4556.

[84] (a) J. R. Ludwig, P. M. Zimmerman, J. B. Gianino, C. S. Schindler. *Nature* **2016**, *533*, 374–379; (b) J. R. Ludwig, R. B. Watson, D. J. Nasrallah, J. B. Gianino, P. M. Zimmerman, R. A. Wiscons, C. S. Schindler. *Science* **2018**, *361*, 1363–1369.

[85] H. Albright, A. J. Davis, J. L. Gomez-Lopez, H. L. Vonesh, P. K. Quach, T. H. Lambert, C. S. Schindler. *Chem. Rev.* **2021**, *121*, 9359–9406.

[86] (a) A. K. Griffith, C. M. Vanos, T. H. Lambert. *J. Am. Chem. Soc.* **2012**, *134*, 18581–18584; (b) Y. Zhang, J. Jermaks, S. N. MacMillan, T. H. Lambert. *ACS Catal.* **2019**, *9*, 9259–9264; (c) Y. Zhang, J. H. Sim, S. N. MacMillan, T. H. Lambert. *Org. Lett.* **2020**, *22*, 6026–6030; (d) J. Jermaks, P. K. Quach, Z. M. Seibel, J. Pomarole, T. H. Lambert. *Chem. Sci.* **2020**, *11*, 7884–7895.

[87] V. R. Naidu, J. Bah, J. Franzén. *Eur. J. Org. Chem.* **2015**, *2015*, 1834–1839.

[88] U. P. N. Tran, G. Oss, D. P. Pace, J. Ho, T. V. Nguyen. *Chem. Sci.* **2018**, *9*, 5145–5151.

[89] L. Catti, K. Tiefenbacher. *Angew. Chem. Int. Ed.* **2018**, *57*, 14589–14592.

[90] U. P. N. Tran, G. Oss, M. Breugst, E. Detmar, D. P. Pace, K. Liyanto, T. V. Nguyen. *ACS Catal.* **2018**, *9*, 912–919.

[91] W. Xieqing, X. Chaogang, L. Zaiting, Z. Genquan, Catalytic Processes for Light Olefin Production. In *Practical Advances in Petroleum Processing*, 2006; pp 149–168.

[92] C. Perego, P. Pollesel, Advances in Aromatics Processing Using Zeolite Catalysts. In *Advances in Nanoporous Materials*, S. Ernst, Ed. 2010; Vol. 1, pp 97–149.

[93] (a) B. A. Vaughan, M. S. Webster-Gardiner, T. R. Cundari, T. B. Gunnoe. *Science* **2015**, *348*, 421–424; (b) X. Jia, A. M. Foley, C. Liu, B. A. Vaughan, B. A. McKeown, S. Zhang, T. B. Gunnoe. *Organometallics* **2019**, *38*, 3532–3541.

[94] J. A. Ragan, Addition to Carbon–Carbon Multiple Bonds. In *Practical Synthetic Organic Chemistry: Reactions, Principles, and Techniques*, S. Caron, Ed. 2020; pp 169–230.

[95] (a) E. Bernoud, C. Lepori, M. Mellah, E. Schulz, J. Hannedouche. *Catal. Sci. Technol.* **2015**, *5*, 2017–2037; (b) J.-S. Lin, P. Yu, L. Huang, P. Zhang, B. Tan, X.-Y. Liu. *Angew. Chem. Int. Ed.* **2015**, *54*, 7847–7851.

[96] G. L. Hamilton, E. J. Kang, M. Mba, F. D. Toste. *Science* **2007**, *317*, 496–499.

[97] R. Properzi, P. S. J. Kaib, M. Leutzsch, G. Pupo, R. Mitra, C. K. De, L. Song, P. R. Schreiner, B. List. *Nat. Chem.* **2020**, *12*, 1174–1179.

[98] W. Li, X.-F. Wu. *Adv. Synth. Catal.* **2015**, *357*, 3393–3418.

[99] S. Meninno, A. Lattanzi. *Chem. Rec.* **2016**, *16*, 2016–2030.

[100] (a) N. C. Wickramasinghe. *Astrophys. Space Sci.* **1999**, *268*, 111–114; (b) L. E. Snyder, D. Buhl, B. Zuckerman, P. Palmer. *Phys. Rev. Lett.* **1969**, *22*, 679–681.

[101] (a) J. P. Pinto, G. R. Gladstone, Y. L. Yung. *Science* **1980**, *210*, 183–185; (b) M. P. Kalapos. *Exp. Mol. Med.* **1999**, *31*, 1–4.

[102] A. W. Franz, H. Kronemayer, D. Pfeiffer, R. D. Pilz, G. Reuss, W. Disteldorf, A. O. Gamer, A. Hilt, Formaldehyde. In *Ullmann's Encyclopedia of Industrial Chemistry*, 7th ed.; 2016; pp 1–34.

[103] (a) *The 12 Molecular Orbitals of Formaldehyde (from Yale University -Organic Chemistry, Chemistry 220)*. http://ursula.chem.yale.edu/~chem220/chem220js/STUDYAIDS/MO-HTMLs/formaldehyde12mo-2-log.html (accessed 2021-10-18); (b) *Molecular Orbitals of Formaldehyde (from TU Darmstadt)*. http://csi.chemie.tu-darmstadt.de/ak/immel/tutorials/orbitals/molecular/formaldehyde.html (accessed 2021-10-18).

[104] N.-Y. Fu, Y.-F. Yuan, Z. Cao, S.-W. Wang, J.-T. Wang, C. Peppe. *Tetrahedron* **2002**, *58*, 4801–4807.

[105] S. Marcaccini, T. Torroba. *Nat. Protoc.* **2007**, *2*, 632–639.

[106] F. C. Whitmore, A. Ginsburg, W. Rueggeberg, I. Tharp, H. Nottorf, M. Cannon, F. Carnahan, D. Cryder, G. Fleming, G. Goldberg, H. Haggard, C. Herr, T. Hoover, H. Lovell, R. Mraz, C. Noll, T. Oakwood, H. Patterson, R. Van Strien, R. Walter, H. Zook, R. Wagner, C. Weisgerber, J. Wilkins. *Ind. Eng. Chem.* **1946**, *38*, 478–485.

[107] C. Liu, W. Huang, J. Zhang, Z. Rao, Y. Gu, F. Jérôme. *Green Chem.* **2021**, *23*, 1447–1465.

[108] M. H. Fischer. *J. Exp. Med.* **1905**, *6*, 487–518.

[109] A. Duong, C. Steinmaus, C. M. McHale, C. P. Vaughan, L. Zhang. *Mutat. Res.-Rev. Mutat.* **2011**, *728*, 118–138.

[110] R. J. Hopkinson, P. S. Barlow, C. J. Schofield, T. D. W. Claridge. *Org. Biomol. Chem.* **2010**, *8*, 4915–4920.

[111] H. He, E. Noor, P. A. Ramos-Parra, L. E. García-Valencia, J. A. Patterson, R. I. Díaz de la Garza, A. D. Hanson, A. Bar-Even. *Metabolites* **2020**, *10*, 65.

[112] H.-G. Schecker, G. Schulz. *Z. Phys. Chem.* **1969**, *65*, 221–224.

[113] W. G. Hughes, S. Weiss, J. Lambiris. PROCESS FOR THE PRODUCTION OF PARAFORMALDEHYDE. Patent US 3,446,854, 1969.

[114] J. G. Atkinson, D. W. Cillis, C. E. Frosst. DEUTERATED PARAFORMALDEHYDE PROCESS. Patent US 3,737,464, 1973.

[115] H. Staudinger, W. Kern. *Ber. Dtsch. Chem. Ges.* **1933**, *66*, 1863–1866.

[116] C. E. Schweitzer, R. N. MacDonald, J. O. Punderson. *J. Appl. Polym. Sci.* **1959**, *1*, 158–163.

[117] M. Haubs, K. Kurz, G. Sextro, Polyoxymethylenes. In *Ullmann's Encyclopedia of Industrial Chemistry*, 2012.

[118] R. Gronner, K.-F. Mück, H. Roeschert, S. Verma, M. Yearwood. Process for the preparation of thermally stable polyoxymethylene copolymers. Patent EP 1 186 620 A1, 2002.

[119] M. Arvidson, M. E. Fakley, M. S. Spencer. *J. Mol. Catal.* **1987**, *41*, 391–393.

[120] B. Lumpp, D. Rothe, C. Pastötter, R. Lämmermann, E. Jacob. *MTZ Worldw.* **2011**, *72*, 34–38.

[121] (a) M. Schlosser, D. Coffinet. *Synthesis* **1971**, *1971*, 380–381; (b) M. Schlosser, T. Jenny, Y. Guggisberg. *Synlett* **1990**, *1990*, 704–704.

[122] K. Maruoka, A. B. Concepcion, N. Murase, M. Oishi, N. Hirayama, H. Yamamoto. *J. Am. Chem. Soc.* **1993**, *115*, 3943–3949.

[123] T. Okachi, M. Onaka. *J. Am. Chem. Soc.* **2004**, *126*, 2306–2307.

[124] (a) A. T. Blomquist, J. Wolinsky. *J. Am. Chem. Soc.* **1957**, *79*, 6025–6030; (b) S. Olsen, H. Padberg. *Z. Naturforsch. A* **1946**, *1*, 448–458.

[125] O. Kriewitz. *Ber. Dtsch. Chem. Ges.* **1899**, *32*, 57–60.

[126] (a) H. J. Prins. *Chem. Weekblad* **1919**, *16*, 1072–1073; (b) H. J. Prins. *Chem. Weekblad* **1919**, *16*, 1510–1526; (c) H. J. Prins In *On the Condensation of Formaldehyde with some Unsaturated Compounds*, Proc. Acad. Sci. Amsterdam, J. Böeseken, Ed. 1919; p 51.

[127] E. Forneau, G. Benoit, R. Firmenich. *B. Soc. Chim. Fr.* **1930**, *47*, 858–885.

[128] E. Arundale, L. A. Mikeska. *Chem. Rev.* **1952**, *51*, 505–555.

[129] (a) N. C. Yang, D. D. H. Yang, C. B. Ross. *J. Am. Chem. Soc.* **1959**, *81*, 133–136; (b) L. J. Dolby. *J. Org. Chem.* **1962**, *27*, 2971–2975; (c) L. J. Dolby, C. N. Lieske, D. R. Rosencrantz, M. J. Schwarz. *J. Am. Chem. Soc.* **1963**, *85*, 47–52; (d) L. J. Dolby, M. J. Schwarz. *J. Org. Chem.* **1963**, *28*, 1456–1458; (e) L. J. Dolby, M. J. Schwarz. *J. Org. Chem.* **1963**, *30*, 3581–3586; (f) E. E. Smissman, R. A. Schnettler, P. S. Portoghese. *J. Org. Chem.* **1965**, *30*, 797–801; (g) L. J. Dolby, C. Wilkins, T. G. Frey. *J. Org. Chem.* **1966**, *31*, 1110–1116; (h) L. J. Dolby, F. A. Meneghini, T. Koizumi. *J. Org. Chem.* **1968**, *33*, 3060–3066; (i) L. J. Dolby, C. L. Wilkins, R. M. Rodia. *J. Org. Chem.* **1968**, *33*, 4155–4158; (j) K. B. Schowen, E. E. Smissman, R. L. Schowen. *J. Org. Chem.* **1968**, *33*, 1873–1876; (k) C. L. Wilkins, R. S. Marianelli. *Tetrahedron* **1970**, *26*, 4131–4138.

[130] (a) B. B. Snider, 2.1 The Prins and Carbonyl Ene Reactions. In *Comprehensive Organic Synthesis*, B. M. Trost, I. Fleming, Eds. Elsevier Ltd.: 1991; pp 527–561; (b) B. B. Snider, 2.03 Prins Reactions and Carbonyl, Imine, and Thiocarbonyl Ene Reactions. In *Comprehensive Organic Synthesis II*, P. Knochel, Ed. Elsevier Ltd.: 2014; pp 148–191; (c) I. M. Pastor, M. Yus. *Curr. Org. Chem.* **2012**, *16*, 1277–1312.

[131] F. Cohen, D. W. MacMillan, L. E. Overman, A. Romero. *Org. Lett.* **2001**, *3*, 1225–1228.

[132] J. S. Yadav, B. V. Subba Reddy, G. G. K. S. N. Kumar, G. M. Reddy. *Tetrahedron Lett.* **2007**, *48*, 4903–4906.

[133] J. J. Ritter. CYCLIC DIETHERS. Patent US 2,362,307, 1944.

[134] D. R. Adams, S. P. Bhatnagar. *Synthesis* **1977**, *1977*, 661–672.

[135] G. Foster, P. Johnson. PRODUCTION OF ISOPRENE. Patent GB1205397A, 1970.

[136] Y. Du, F. Tian. *Catal. Commun.* **2007**, *8*, 2012–2016.

[137] J. Zhang, L. Hua, F. Li, X. Wu, S. Tian, J. Yang. *Synthetic Commun.* **2011**, *42*, 1234–1242.

[138] (a) P. R. Stapp. *J. Org. Chem.* **1969**, *34*, 479–485; (b) A. Onopchenko, R. Seekircher. *J. Chem. Eng. Data* **1970**, *15*, 164–166.

[139] H. A. A. Almohseni, M. A. H. Stent, D. M. Hodgson. *Chem. Heterocycl. Comp.* **2018**, *54*, 474–477.

[140] P. R. Stapp. *J. Org. Chem.* **1970**, *35*, 2419–2420.

[141] G. Li, Y. Gu, Y. Ding, H. Zhang, J. Wang, Q. Gao, L. Yan, J. Suo. *J. Mol. Catal. A-Chem.* **2004**, *218*, 147–152.

[142] T. Bach, J. Lobel. *Synthesis* **2002**, *17*, 2521–2526.

[143] J. S. Yadav, B. V. S. Reddy, G. Bhaishya. *Green Chem.* **2003**, *5*, 264–266.

[144] (a) X. Hao, N. Hoshi. *Chem. Lett.* **2006**, *35*, 1102–1103; (b) B. Sreedhar, V. Swapna, C. Sridhar, D. Saileela, A. Sunitha. *Synthetic Commun.* **2005**, *35*, 1177–1182.

[145] J. S. Yadav, B. V. Subba Reddy, A. V. Hara Gopal, G. G. K. S. Narayana Kumar, C. Madavi, A. C. Kunwar. *Tetrahedron Lett.* **2008**, *49*, 4420–4423.

[146] (a) L. Chen, F. Mo, H. Cheng, Z. Qi. *Chem. Lett.* **2021**, *50*, 1194–1197; (b) Y. Gu, C. Ogawa, S. Kobayashi. *Chem. Lett.* **2006**, *35*, 1176–1177; (c) R. G. Kalkhambkar, Y. T. Jeong. *Synthetic Commun.* **2014**, *44*, 762–771.

[147] S. P. Bedenko, K. I. Dement'ev, V. F. Tret'yakov, A. L. Maksimov. *Petrol. Chem.* **2020**, *60*, 723–730.

[148] (a) R. El Gharbi, Y. L. Bigot, M. Delmas, A. Gaset. *Biomass* **1985**, *6*, 211–221; (b) R. El Gharbi, M. Delmas, A. Gaset. *Synthesis* **1981**, *1981*, 361–362; (c) R. El Gharbi, M. Delmas, A. Gaset. *Tetrahedron* **1983**, *39*, 2953–2963; (d) R. El Gharbi, M. Delmas, A. Gaset. *Tetrahedron* **1983**, *39*, 613–621.

[149] S. Chandrasekhar, B. V. Subba Reddy. *Synlett* **1998**, *1998*, 851–852.

[150] (a) K. J. Borah, M. Phukan, R. Borah. *Synthetic Commun.* **2008**, *38*, 3082–3087; (b) Y. Gu, A. Karam, F. Jérôme, J. Barrault. *Org. Lett.* **2007**, *9*, 3145–3148.

[151] (a) M. A. Aramendía, V. Borau, C. Jiménez, J. M. Marinas, F. J. Romero, F. J. Urbano. *Catal. Lett.* **2001**, *73*, 203–206; (b) M. Selvaraj, M. A. Assiri, H. Singh, J. N. Appaturi, C. Subrahmanyam, C.-S. Ha. *Dalton T.* **2021**, *50*, 1672–1682; (c) J.-i. Tateiwa, K. Hashimoto, T. Yamauchi, S. Uemura. *B. Chem. Soc. Jpn.* **1996**, *69*, 2361–2368; (d) T. Yashima, Y. Katoh, T. Komatsu. *Stud. Surf. Sci. Catal.* **1999**, *125*, 507–514.

[152] E. J. Corey, N. M. Weinshenker, T. K. Schaaf, W. Huber. *J. Am. Chem. Soc.* **1969**, *91*, 5675–5677.

[153] R. Peel, J. K. Sutherland. *J. Chem. Soc. Chem. Comm.* **1974**, *4*, 151–153.

[154] I. Tömösközi, L. Gruber, G. Kovács, I. Székely, V. Simonidesz. *Tetrahedron Lett.* **1976**, *17*, 4639–4642.

[155] I. Tömösközi, L. Gruber, E. Baitz-Gács. *Tetrahedron* **1992**, *48*, 10345–10352.

[156] K. Ishihara, H. Nakamura, H. Yamamoto. *Synlett* **2000**, *2000*, 1245–1248.

[157] W. Harnying, J. M. Neudörfl, A. Berkessel. *Synthesis* **2017**, *49*, 269–274.

[158] (a) E. Brenna, C. Fuganti, S. Serra. *Tetrahedron-Asymmetry* **2003**, *14*, 1–42; (b) A. Abate, E. Brenna, C. Fuganti, S. Serra. *Flavour Frag. J.* **2004**, *19*, 382–393.

[159] (a) Y. Li, X. Wang, Y. Guo, Z. Zhu, Y. Wu, Y. Gong. *Chem. Commun.* **2016**, *52*, 796–799; (b) X. Wang, Y. Li, Y. Guo, Z. Zhu, Y. Wu, W. Cao. *Org. Chem. Front.* **2016**, *3*, 304–308.

[160] X.-H. Liu, J. Leng, S.-J. Jia, J.-H. Hao, F. Zhang, H.-L. Qin, C.-P. Zhang. *J. Fluorine Chem.* **2016**, *189*, 59–67.

[161] T. Maegawa, Y. Koutani, K. Otake, H. Fujioka. *J. Org. Chem.* **2013**, *78*, 3384–3390.

[162] M. F. Andreasen, A.-K. Landbo, L. P. Christensen, Å. Hansen, A. S. Meyer. *J. Agr. Food Chem.* **2001**, *49*, 4090–4096.

[163] (a) G. D. Y. Sogah, D. J. Cram. *J. Am. Chem. Soc.* **2002**, *101*, 3035–3042; (b) D. Mosca, A. Stopin, J. Wouters, N. Demitri, D. Bonifazi. *Chem.-Eur. J.* **2017**, *23*, 15348–15354.

[164] (a) J. Yang, S. Wu, F.-X. Chen. *Synlett* **2010**, *2010*, 2725–2728; (b) Y.-M. Wang, J. Wu, C. Hoong, V. Rauniyar, F. D. Toste. *J. Am. Chem. Soc.* **2012**, *134*, 12928–12931.

[165] J. C. Ostrowski, J. R. A. Hudack, M. R. Robinson, S. Wang, G. C. Bazan. *Chem.-Eur. J.* **2001**, *7*, 4500–4511.

[166] S. K. Nimmagadda, M. Liu, M. K. Karunananda, D. W. Gao, O. Apolinar, J. S. Chen, P. Liu, K. M. Engle. *Angew. Chem. Int. Ed.* **2019**, *58*, 3923–3927.

[167] D. Verga, C. Percivalle, F. Doria, A. Porta, M. Freccero. *J. Org. Chem.* **2011**, *76*, 2319–2323.

[168] S. Kobayashi, J. Kobayashi, H. Ishiani, M. Ueno. *Chem.-Eur. J.* **2002**, *8*, 4185–4190.

[169] (a) H. Danjo, K. Hirata, S. Yoshigai, I. Azumaya, K. Yamaguchi. *J. Am. Chem. Soc.* **2009**, *131*, 1638–1639; (b) Y. He, Z. Bian, C. Kang, L. Gao. *Chem. Commun.* **2010**, *46*, 5695–5697.

[170] (a) J. P. Vigneron, M. Dhaenens, A. Horeau. *Tetrahedron* **1973**, *29*, 1055–1059; (b) A. M. Harned. *Tetrahedron* **2018**, *74*, 3797–3841.

[171] (a) *indoletal*. http://www.thegoodscentscompany.com/data/rw1033251.html (accessed 2021/11/01); (b) *Indoflor® Cryst.* https://www.symrise.com/fileadmin/symrise/Marketing/Scent_and_care/Aroma_molecules/Ingredient_finder/SYM_PC_Datenblaetter/SYM_PC-Indoflor-Cryst.pdf (accessed 2021/11/01); (c) A. M. Api, D. Belsito, D. Botelho, M. Bruze, G. A. Burton, Jr., J. Buschmann, M. L. Dagli, M. Date, W. Dekant, C. Deodhar, M. Francis, A. D. Fryer, L. Jones, K. Joshi, S. La Cava, A. Lapczynski, D. C. Liebler, D. O'Brien, A. Patel, T. M. Penning, G. Ritacco, J. Romine, N. Sadekar, D. Salvito, T. W. Schultz, I. G. Sipes, G. Sullivan, Y. Thakkar, Y. Tokura, S. Tsang. *Food Chem. Toxicol.* **2019**, *134*, 110725.

[172] (a) A. Heslinga. *Recl. Trav. Chim. Pay-B.* **1959**, *78*, 473–479; (b) W. F. Bailey, A. D. Rivera. *J. Org. Chem.* **1984**, *49*, 4958–4964.

[173] E. Francotte, R. M. Wolf. *Chirality* **1990**, *2*, 16–31.

[174] H. Fujioka, K. Senami, O. Kubo, K. Yahata, Y. Minamitsuji, T. Maegawa. *Org. Lett.* **2009**, *11*, 5138–5141.

[175] H. Fujioka, K. Senami, O. Kubo, K. Yahata, Y. Minamitsuji, T. Maegawa. *Chem. Pharm. Bull.* **2010**, *58*, 426–428.

[176] Y. Gao, K. B. Sharpless. *J. Org. Chem.* **1988**, *53*, 4081–4084.

[177] G. L. Khatik, R. Sharma, V. Kumar, M. Chouhan, V. A. Nair. *Tetrahedron Lett.* **2013**, *54*, 5991–5993.

[178] J. Yadav, M. Reddy, P. Rao, A. Prasad. *Synthesis* **2006**, *2006*, 4005–4012.

[179] (a) V. Ratovelomanana-Vidal, C. Girard, R. Touati, J. P. Tranchier, B. B. Hassine, J. P. Genêt. *Adv. Synth. Catal.* **2003**, *345*, 261–274; (b) R. Chênevert, G. Fortier, R. B. Rhlid. *Tetrahedron* **1992**, *48*, 6769–6776.

[180] H. E. Master, R. V. Newadkar, R. A. Rane, A. Kumar. *Tetrahedron Lett.* **1996**, *37*, 9253–9254.

[181] (a) T. Pirali, M. Serafini, S. Cargnin, A. A. Genazzani. *J. Med. Chem.* **2019**, *62*, 5276–5297; (b) A. E. Mutlib. *Chem. Res. Toxicol.* **2008**, *21*, 1672–1689; (c) T. G. Gant. *J. Med. Chem.* **2014**, *57*, 3595–3611.

[182] D. G. Kohler, S. N. Gockel, J. L. Kennemur, P. J. Waller, K. L. Hull. *Nat. Chem.* **2018**, *10*, 333–340.

[183] S. Yamabe, T. Fukuda, S. Yamazaki. *Beilstein J. Org. Chem.* **2013**, *9*, 476–485.

[184] K. Z. Gaca, J. A. Parkinson, L. Lue, J. Sefcik. *Ind. Eng. Chem. Res.* **2014**, *53*, 9262–9271.

[185] G. C. Lloyd-Jones, M. P. Muñoz. *J. Labelled Compd. Rad.* **2007**, *50*, 1072–1087.

[186] F. M. Bickelhaupt, K. N. Houk. *Angew. Chem. Int. Ed.* **2017**, *56*, 10070–10086.

[187] W. L. F. Armarego, *Purification of laboratory chemicals*. 8th ed.; Butterworth-Heinemann: Woburn, MA, 2003.

[188] J. Brecher. *Pure Appl. Chem.* **2006**, *78*, 1897–1970.

[189] R. K. Harris, E. D. Becker, S. M. Cabral de Menezes, P. Granger, R. E. Hoffman, K. W. Zilm. *Pure Appl. Chem.* **2008**, *80*, 59–84.

[190] F. Neese. *WIREs Comput. Mol. Sci.* **2011**, *2*, 73–78.

[191] Y. Zhang, W. Yang. *Phys. Rev. Lett.* **1998**, *80*, 890–890.

[192] (a) S. Grimme, J. Antony, S. Ehrlich, H. Krieg. *J. Chem. Phys.* **2010**, *132*, 154104; (b) S. Grimme, S. Ehrlich, L. Goerigk. *J. Comput. Chem.* **2011**, *32*, 1456–1465.

[193] F. Weigend, R. Ahlrichs. *Phys. Chem. Chem. Phys.* **2005**, *7*, 3297–3305.

[194] V. Barone, M. Cossi. *J. Phys. Chem. A.* **1998**, *102*, 1995–2001.

[195] Y. Zhao, D. G. Truhlar. *Theor. Chem. Acc.* **2007**, *120*, 215–241.

[196] C. Y. Legault: CYLview, 1.0b; Université de Sherbrooke, 2009 (http://www.cylview.org).

[197] W. Humphrey, A. Dalke, K. Schulten. *J. Mol. Graphics* **1996**, *14*, 33–38.

[198] X.-Y. Dong, Y.-F. Zhang, C.-L. Ma, Q.-S. Gu, F.-L. Wang, Z.-L. Li, S.-P. Jiang, X.-Y. Liu. *Nat. Chem.* **2019**, *11*, 1158–1166.

[199] L. Jiménez-González, S. García-Muñoz, M. Álvarez-Corral, M. Muñoz-Dorado, I. Rodríguez-García. *Chem-Eur. J.* **2007**, *13*, 557–568.

[200] Y. Gao, Y. Ou, L. J. Gooßen. *Chem.-Eur. J.* **2019**, *25*, 8709–8712.

[201] B. J. Al-Hourani, J. P. Bravo-Vasquez, L. R. H. High, H. Fenniri. *Tetrahedron Lett.* **2007**, *48*, 9144–9147.

[202] D. Caprioglio, S. Torretta, M. Ferrari, C. Travelli, A. A. Grolla, F. Condorelli, A. A. Genazzani, A. Minassi. *Bioorgan. Med. Chem.* **2016**, *24*, 140–152.

[203] M. Tang, S. Han, S. Huang, S. Huang, L.-G. Xie. *Org. Lett.* **2020**, *22*, 9729–9734.

[204] J. Gui, H. Xie, F. Chen, Z. Liu, X. Zhang, F. Jiang, W. Zeng. *Org. Biomol. Chem.* **2020**, *18*, 956–963.

[205] F.-T. Luo, C. Xue, S.-L. Ko, Y.-D. Shao, C.-J. Wu, Y.-M. Kuo. *Tetrahedron* **2005**, *61*, 6040–6045.

[206] E. Alacid, C. Nájera. *J. Org. Chem.* **2009**, *74*, 2321–2327.

[207] P. Yu, B. Morandi. *Angew. Chem. Int. Ed.* **2017**, *56*, 15693–15697.

[208] W. Jian, L. Ge, Y. Jiao, B. Qian, H. Bao. *Angew. Chem. Int. Ed.* **2017**, *56*, 3650–3654.

[209] R. Chen, X. Zhang, T. E. Hogen-Esch. *Macromolecules* **2003**, *36*, 7477–7483.

[210] X. Li, B. Fu, Q. Zhang, X. Yuan, Q. Zhang, T. Xiong, Q. Zhang. *Angew. Chem. Int. Ed.* **2020**, *59*, 23056–23060.

[211] Y. Kayaki, T. Koda, T. Ikariya. *Eur. J. Org. Chem.* **2004**, *2004*, 4989–4993.

[212] J. F. Cívicos, D. A. Alonso, C. Nájera. *Adv. Synth. Catal.* **2011**, *353*, 1683–1687.

[213] J. Waser, B. Gaspar, H. Nambu, E. M. Carreira. *J. Am. Chem. Soc.* **2006**, *128*, 11693–11712.

[214] S. Gandhi, B. Baire. *J. Org. Chem.* **2019**, *84*, 3904–3918.

[215] S. Yu, A. Noble, R. B. Bedford, V. K. Aggarwal. *J. Am. Chem. Soc.* **2019**, *141*, 20325–20334.

[216] J. Y. Park, S.-w. Jang, H. Lee. Preparation of imidazolopyrimidine compounds for organic electroluminescent device. Patent 2017126059, November 16, 2017.

[217] M. Kong, Y. Tan, X. Zhao, B. Qiao, C. H. Tan, S. Cao, Z. Jiang. *J. Am. Chem. Soc.* **2021**, *143*, 4024–4031.

[218] J. Xiao, Q. Li, R. Shen, S. Shimada, L. B. Han. *Adv. Synth. Catal.* **2019**, *361*, 5715–5720.

[219] D. Kapeller, R. Barth, K. Mereiter, F. Hammerschmidt. *J. Am. Chem. Soc.* **2007**, *129*, 914–923.

[220] W. D. King, D. J. Stanonis. *J. Appl. Polym. Sci.* **1974**, *18*, 547–554.

[221] G. Z. Raskil'dina, Y. G. Borisova, L. V. Spirikhin, S. S. Zlotskii. *Russ. Chem. B* **2019**, *68*, 2092–2097.

[222] D. E. Sood, S. Champion, D. M. Dawson, S. Chabbra, B. E. Bode, A. Sutherland, A. J. B. Watson. *Angew. Chem. Int. Ed.* **2020**, *59*, 8460–8463.

[223] J.-M. Adam, J. Aebi, A. Binggeli, L. Green, G. Hartmann, H. P. Maerki, P. Mattei, F. Ricklin, O. Roche. NOVEL HETEROCYCLYL COMPOUNDS. Patent US 2010/0022518 A1, January 28, 2010.

[224] S. Trofymchuk, M. Y. Bugera, A. A. Klipkov, B. Razhyk, S. Semenov, K. Tarasenko, V. S. Starova, O. A. Zaporozhets, O. Y. Tananaiko, A. N. Alekseenko, Y. Pustovit, O. Kiriakov, Gerus, I. I., A. A. Tolmachev, P. K. Mykhailiuk. *J. Org. Chem.* **2020**, *85*, 3110–3124.

[225] G. Garg, L. K. Forsberg, H. Zhao, B. S. J. Blagg. *Chem-Eur. J.* **2017**, *23*, 16574–16585.

[226] H. Ishitani, M. Ueno, S. Kobayashi. *J. Am. Chem. Soc.* **2000**, *122*, 8180–8186.

[227] Y. Yue, M. Turlington, X. Q. Yu, L. Pu. *J. Org. Chem.* **2009**, *74*, 8681–8689.

[228] I. Ahmed, D. A. Clark. *Org. Lett.* **2014**, *16*, 4332–4335.

[229] S. Lee, P. S. J. Kaib, B. List. *Synlett* **2017**, *28*, 1478–1480.

[230] O. Y. Kupova, I. V. Vakulin, R. F. Talipov, N. D. Morozkin, G. R. Talipova. *React. Kinet. Mech. Cat.* **2013**, *110*, 41–52.

A. Appendix

a. Erklärung/Declaration

Hiermit versichere ich an Eides statt, dass ich die vorliegende Dissertation selbstständig und ohne die Benutzung anderer als der angegebenen Hilfsmittel und Literatur angefertigt habe. Alle Stellen, die wörtlich oder sinngemäß aus veröffentlichten und nicht veröffentlichten Werken dem Wortlaut oder dem Sinn nach entnommen wurden, sind als solche kenntlich gemacht. Ich versichere an Eides statt, dass diese Dissertation noch keiner anderen Fakultät oder Universität zur Prüfung vorgelegen hat; dass sie noch nicht veröffentlicht worden ist sowie, dass ich eine Veröffentlichung der Dissertation vor Abschluss der Promotion nicht ohne Genehmigung des Promotionsausschusses vornehmen werde. Die Bestimmungen dieser Ordnung sind mir bekannt. Darüber hinaus erkläre ich hiermit, dass ich die Ordnung zur Sicherung guter wissenschaftlicher Praxis und zum Umgang mit wissenschaftlichem Fehlverhalten der Universität zu Köln gelesen und sie bei der Durchführung der Dissertation zugrundeliegenden Arbeiten und der schriftlich verfassten Dissertation beachtet habe und verpflichte mich hiermit, die dort genannten Vorgaben bei allen wissenschaftlichen Tätigkeiten zu beachten und umzusetzen. Ich versichere, dass die eingereichte elektronische Fassung der eingereichten Druckfassung vollständig entspricht.

Mülheim an der Ruhr, 15.11.2021
(Christian David Díaz-Oviedo)

Bisher sind folgende Teilpublikationen veröffentlicht worden:

“The Catalytic Asymmetric Intermolecular Prins Reaction“, C. D. Díaz-Oviedo, R. Maji, B. List, *J. Am. Chem. Soc.* **2021**, *143 (49)*, 20598–20604.
“Chiral Phosphoric Acid-Catalyzed Conversion of Epoxides to Thiiranes: Mechanism, Stereochemical Model, and New Catalyst Design”, M. Duan,† C. D. Díaz-Oviedo,† Y. Zhou, X. Chen, P. Yu, B. List, K. N. Houk, Y. Lan, *Angew. Chem., Int. Ed.* **2022**, 61, e202113204. (†Equal contribution)

b. Lebenslauf/CV

Christian David Díaz-Oviedo

Geboren am 01. April 1990 in Fusagasugá (Kolumbien)

Staatsangehörigkeit: kolumbianisch

Akademischer Werdegang

Promotion

02.2017–01.2022	Dissertation im Arbeitskreis von Prof. Dr. Benjamin List Max-Planck-Institut für Kohlenforschung, Mülheim an der Ruhr Titel: „The Catalytic Asymmetric Intermolecular Prins Reaction“

Hochschulstudium

02.2013–03.2015	Studium Master of Science – Chemie. Masterarbeit im Arbeitskreis von Prof. Dr. Rodolfo Quevedo Universidad Nacional de Colombia, Bogotá D.C. (Kolumbien) Titel: „Study of the reaction between β-(4-hydroxyphenyl)ethylamines and non-enolizable aldehydes“
01.2007–03.2012	Studium Bachelor of Science – Chemie. Bachelorarbeit im Arbeitskreis von Prof. Dr. Rodolfo Quevedo Universidad Nacional de Colombia, Bogotá D.C. (Kolumbien) Titel: „Study of the reaction of a 1,3-benzoxazinephane with sodium borohydride“

Schulbildung

01.2001–12.2006	Instituto Técnico Industrial “Francisco José de Caldas” (Sekundarschule), Bogotá D.C. (Kolumbien)